METACHROMATIC LEUKODYSTROPHY

IMPROVED DIAGNOSIS AND PROGNOSIS

by

Mohd Adi Firdaus TAN

B.Biomedical Sc. (Hons)

Department of Paediatrics

The University of Adelaide

Adelaide, South Australia

This thesis is submitted for the degree of Doctor of Philosophy

Date submitted: 28 March 2006

THESIS SUMMARY

Metachromatic leukodystrophy (MLD) is one of the more prevalent lysosomal storage disorders with a reported incidence of 1 in 92,000 births in Australia. The major cause of this disease is the deficiency of arylsulphatase A (ASA); this lysosomal enzyme, together with an activator protein, saposin B, is needed for the catabolism of sulphatide. The subsequent accumulation of sulphatides in the central nervous system results in progressive demyelination that leads to severe impairment of neurological function with a fatal outcome for the more severely affected infantile and juvenile patients.

Bone marrow transplantation has been carried out in MLD patients for more than 25 years. However, successful treatment of this disorder is often difficult and remains a challenge because patients are usually diagnosed after the onset of neurological symptoms. At present, MLD is diagnosed by measurement of ASA activity in peripheral blood leucocytes and cultured skin fibroblasts. However, a definitive diagnosis is usually only obtained after extensive testing with an array of auxiliary laboratory tests. The need for auxiliary tests is due to the presence of the ASA pseudo-deficiency (ASA-PD) mutation or ASA-PD/MLD, which leads to clinically normal individuals who have low ASA enzyme activity. These patients cannot be distinguished from MLD patients by conventional enzyme analysis; furthermore, normal enzyme activity cannot rule out MLD since saposin B deficiency is also known to cause the disorder.

In this study, immune-based ASA activity and protein assays, and a simple skin fibroblast sulphatide-loading protocol, were developed. In addition, a sulphatide quantification assay using mass spectrometry was established. The immune-based assays were shown to be highly specific. The immune-quantification ASA protein assay was sensitive and clearly distinguished unaffected, ASA-PD and MLD individuals in blood spots and skin fibroblast samples. However, ASA enzyme activity was not detected in either ASA-PD or MLD individuals in blood spots using the immune-capture ASA activity assay, a finding attributed to the instability of ASA activity in dried blood spots that had been stored at room temperature. The combination of these two assays has enabled determination of specific activity of the enzyme in different patients, thereby providing information on the effect of the mutation on protein stability and activity as well as an additional parameter with which to distinguish phenotypes.

To further develop the capacity to predict phenotype, induced accumulation of sulphatide in skin fibroblast cultures was performed; the resultant cells were quantified for accumulated sulphatide and other lipids using electrospray ionisation tandem mass spectrometry. A strong correlation was observed between residual enzyme activity and the amount of accumulated sulphatide: four out of five late-infantile MLD patients could be clearly distinguished from the juvenile and adult patients, although no difference was observed in the amount of accumulated sulphatide in the latter two groups. However, a clear difference was observed between attenuated adult-onset patients and ASA-PD/MLD compound heterozygotes. Analysis of urine for sulphatide and a range of other lipids from a cohort of unaffected controls, ASA-PD and MLD patients showed that, in addition to elevated sulphatide, MLD patients also showed alterations in some phosphatidylglycerol/ lysobisphosphatidic acid species, a finding that was also observed in the sulphatide-loaded skin fibroblasts. This observation enabled unequivocal discrimination of the late-infantile MLD phenotype.

The immune-based ASA activity and protein assays will simplify the procedures for collection, handling and storage protocols for MLD testing. This will be particularly important for countries where sample collection and transport services are not well established or where transport overseas is required. The combination of residual ASA protein and activity, urinary sulphatide and other lipids, and sulphatide accumulation in cultured skin fibroblasts, provides a detailed picture of patient biochemistry and has the potential to provide predictive assessment of phenotype where patients are identified asymptomatically.

CANDIDATE'S DECLARATION

This work contains no material which has been accepted for the award of any other degree or diploma in any university or other tertiary institution and, to the best of my knowledge and belief, contains no material previously published or written by another person, except where due reference has been made in the text.

I hereby give consent to this copy of my thesis, when deposited in the university library, being available for loan and photocopying.

ADI TAN
Date: March, 2006

ACKNOWLEDGMENTS

Numerous people have contributed to the successful completion of this project and I would like to thank them all most sincerely.

Firstly, I would like to thank my supervisors, Dr Peter Meikle and Prof. John Hopwood, for their encouragement and guidance throughout this project. I am most grateful to them for the precious time they spent in the weekly meetings that kept me constantly on my toes. Their superb guidance and interest in the project proved to be most valuable throughout the tenure of this project. I would also like to thank Prof. Zabidi (Field supervisor) for his support, and the Universiti Sains Malaysia for granting me the scholarships necessary for me to come to Adelaide to undertake this study.

I am most grateful to Assoc. Prof. Douglas Brooks, Dr. Peter Clements, Dr. Maria Fuller, Dr Michael Bawden, Dr Emma Parkinson, Dr Caroline Dean, Dr David Johnson, Dr Melissa Chang, Peter Sharp, Christine Boulter, Dr Litsa Karageorgos, Elaine Ravenscroft, Tina Rozaklis and Minh Trinh for their expertise and contributions over the years.

I would also like to thank Melanie Lovejoy, Michelle Bockmann, Timothy Nielsen, Christopher Turner, Debbie Zimmerman, Kerryn Mason and Sophie Lazenkas for their help and wonderful friendship that I will continue to cherish throughout my life. I also wish to thank Dr. Rowani Mohd Rawi, who is also undertaking her PhD studies in Adelaide in the area of lysosomal storage disorders; together, we hope to build up the laboratory back in Malaysia.

Special thanks to David Blacklock for his great companionship. I will always remember those wonderful fishing and crabbing trips in his 'Tinnie', and the grand 40th birthday we celebrated together.

Many thanks to all the staff in the Department of Genetic Medicine at the Women's and Children's Hospital in North Adelaide, for their kind assistance rendered to me during my work in the Department.

From the bottom of my heart, I would like to thank and dedicate this work to my lovely wife, Sabariah, and my children, Alif, Asyraf, Sabrina, Syazana and Sadrina, for their understanding and the sacrifices they made during my absence. Without their love and

encouragement, I doubt I would have made it. I love you all; no words can describe the extent of my love for all of you.

Finally, a special dedication to my beloved mother. I know she is beaming with pride at my achievement; sadly, her untimely demise during my study has changed the celebration we had planned. May God bless her soul.

"May God bless us all. Together, we can make this world a better place"

LIST OF ABBREVIATIONS

4-MUS	4-methylumbelliferyl sulphate
ABTS	2, 2'-azino-bis (3-ethylbenzo-thiazoline-6-sulphonic acid) diammonium salt
AEC	anion exchange chromatography
ASA	arylsulphatase A
ASA-PD	arylsulphatase pseudo-deficiency
BBB	blood-brain barrier
BCA	bicinchoninic acid
BME	Basal Eagle media
BMT	bone marrow transplantation
BSA	bovine serum albumin
CAD	collisionally activated dissociation
CAPS	3-[cyclohexylamino]-1-propanesulphonic acid
cDNA	complementary DNA
CE	collision energy
Cer	ceramide
CHAPS	3-{(3-cholamidopropyl)-dimethylammonio}-1-propanesulfonate
CHO-K1	Chinese hamster ovary $DHFR^-$ cell line
cm; mm; μm; nm	centimetre(s); millimetre(s); micrometre(s); nanometre(s)
CNS	central nervous system
CR	creatinine
CSF	cerebrospinal fluir
CTH	ceramide trihexoside
CUR	curtain gas setting
CV	coefficient of variance
CXP	collision cell exit potential
DELFIA	dissociation-enhanced lanthanide fluorescence immunoassay
dhSulp	dihexosyl sulphatide
DMEM	dodecyl modified Eagles medium
DMSO	dimethylsulphoxide
DNA	deoxyribonucleic acid
DP	declustering potential
EDTA	ethylenediaminetetraacetic acid

ELISA	enzyme-linked immunosorbent assay
EP	exit potential
ER	endoplasmic reticulum
ERT	enzyme replacement therapy
ESI-MS/MS	electrospray ionisation tandem mass spectrometry
Eu^{3+}	europium
FA-amide	fatty acid amide
FCS	foetal calf serum
FP	focusing potential
FPLC	fast protein liquid chromatography
g; mg; μg; ng	gram(s); milligram(s); microgram(s); nanogram(s)
G418	gentamycin
GC	glucosylceramide
GSD	glycophingolipidoses
GSL	glycosphingolipids
HAT	hypoxanthine, aminopterin and thymidine
HEPES	N-(2-hydroxyethyl) piperazine-N'-(2-ethanesulfonic acid)
hFA	α-hydroxy fatty acid
HIFCS	heat-inactivated foetal calf serum
HPLC	high pressure liquid chromatography
hr(s); min(s)	hour(s); minute(s)
HRP	horse radish peroxidase
hSulp	hydroxyl sulphatide
HT	hypoxanthine and thymidine
IS	ion spray voltage
ISTD	internal standards
kDa	kilo-daltons
L; mL; μL	litre(s); millilitre(s); microlitre(s)
LAMP	lysosome-associated membrane protein
LB	Luria broth
LC	lactosylceramide
LIMPs	lysosomal integral membrane proteins
LPBA	lysobisphosphatidic acid
LSD	lysosomal storage disorder(s)
m/z	mass-to-charge ratio

M6PR	mannose-6-phosphate receptor
MAL	myelin and lymphocyte protein
MEM	minimum essential medium
MLD	metachromatic leukodystrophy
mM; nM	millimoles per litre; nanomoles per litre
mmol, μmol, nmol, pmol	millimoles, micomoles, nanomoles, picomoles
MPS	mucopolysaccharidosis
MPSs	mucopolysaccharidoses
MRM	multiple reaction monitoring
MS	mass spectrometry
ms	millisecond(s)
Mw	molecular weight
M-WU	Mann-Whitney U test
NBS	newborn screening
NEB	neubuliser gas setting
NP-40	nonylphenoxy polyethoxy ethanol
N350S ASA	N350S arylsulphatase A enzyme
OD	optical density
PBS	phosphate buffered saline
PC	phosphatidylcholine
PCR	polymerase chain reaction
PG	phosphatidylglycerol
pI	isoelectric point
PI	phosphatidylinositol
p-NCS	p-nitrocatechol sulphate
PS	penicillin/streptomycin
PVDF	polyvinylidene difluoride
QBT buffer	equilibration buffer from Qiagen midi kit
RER	rough endoplasmic reticulum
RIA	radioimmunoassay
RP-HPLC	reverse phase-high *performance* liquid chromatography
RPMI	Roswell Park Memorial Institute medium
RT	room temperature
SDS	sodium dodecyl sulphate
SDS-PAGE	sodium dodecyl sulphate polyacrylamide gel electrophoresis
SEC	size exclusion chromatography

SF	skin fibroblast
SM	sphingomyelinase
Sulp	sulphatide
TBE	tris/borate-buffered ethylene diamine tetra acetic acid
TCA	trichloroacetic acid
TE buffer	tris-EDTA
TLC	thin layer chromatography
Tris	tris (hydroxymethyl) aminomethane
Tween-20	polyoxyethylenesorbitan monolaurate
UV	ultraviolet
V	volt(s)
w/v; v/v	weight per volume; volume per volume
Wt	wild type
Wt ASA	wild type arylsulphatase A enzyme
x g	times gravity force

TABLE OF CONTENTS

Chapter 2: Materials and methods

Chapter 3:
Expression, purification and characterisation of Wt ASA and N350 ASA enzymes

Chapter 5
Establishment of a sulphatide quantification method using electrospray ionisation-tandem mass spectrometry and development of a sulphatide-loading protocol

Chapter 6
Prediction of clinical severity in metachromatic leukodystrophy

CHAPTER ONE

Introduction

Chapter one reviews the literature to enable a full appreciation of the project's initial aims. This review starts with an overview of the lysosome, describing its protein composition and the mechanisms involved in its function and biogenesis. Two classes of lysosomal proteins, the sulphatases and saposins, are further elaborated upon due to their pathological role in metachromatic leukodystrophy (MLD). The trafficking mechanisms of lysosomal proteins are also discussed, since alterations to these mechanisms contribute to pathogenicity in MLD. The involvement of 'lipid rafts' in MLD pathogenesis is also briefly discussed.

In general, this thesis is concerned with establishing a holistic approach to the laboratory detection and characterisation of MLD by developing methodology that will allow accurate assignment of phenotype in the simplest way possible based on the biochemistry of the disorder. An array of assays, including those developed during this study and those previously developed in the Department of Genetic Medicine by others, were employed to facilitate this study. This chapter reviews current laboratory diagnostic methods for MLD, as well as factors that contribute to the problems encountered in the diagnosis of this genetically, clinically and biochemically heterogenous disease.

At the end of this review, two important gaps in our knowledge are identified and translated into six specific aims; corresponding experimental approaches are also presented.

1. Introduction

The first description of the lysosome by De Duve *et al.* (1955) started the quest for other researchers to study and understand a group of heterogeneous diseases now known as lysosomal storage disorders (LSD). Beginning with Hers, who, in 1963, demonstrated that the absence of α-glucosidase caused Pompe disease, a flurry of findings over the next 40-years has added significant knowledge to the overall understanding of these diseases. However, due to their complex nature, some questions remain unanswered.

1.1. The lysosome and its function

The lysosome was first identified as an intracellular organelle through sub-cellular fractionation experiments combined with enzyme activity determination. The lysosome is a

membrane-bound cytoplasmic organelle, dense in cell fractionation experiments, that contains various mature forms of lysosomal proteins and is a terminal compartment in the endocytic pathway (Storrie, 1988)

The lysosome is the major digestive organelle in eukaryotic cells that degrades a variety of macromolecules. These macromolecules can be delivered to lysosomes via the endocytic trafficking route through three major pathways: 1) clathrin-mediated endocytosis; 2) phagocytosis; and 3) autophagy, as shown in Figure 1.1 (Kornfeld, 1986). Endocytosis is the process whereby molecules are taken into the cell via the plasma membrane. This can be achieved by receptor-mediated uptake in which the intended molecule is bound to a specific receptor on the plasma membrane before being endocytosed (Wattiaux *et al.*, 1995). Alternatively, this process can take place in a fluid phase (adsorptive endocytosis) through non-specific binding to the plasma membrane before being taken-up (Wattiaux *et al.*, 2000). Once internalised, these molecules are rapidly delivered to early endosomes and then delivered to lysosomes for degradation, while most of the membrane-bound proteins are redirected to the plasma membrane for recycling (van Kerkhof *et al.*, 2001).

Phagocytosis is the cellular uptake of particulate material through engulfment. Firstly, cytoplasmic extensions formed on the plasma membrane engulf the particle; the membrane then pinches free to produce a phagosome, which will ultimately fuse with the lysosome for digestion (Beron *et al.*, 1995). A classic example of this process is the engulfment of micro-organisms by macrophages as part of the body's defence mechanism. The process of autophagy is the central mechanism by which the cell recycles its own cytosolic molecules and organelles (Knowles and Ballard, 1976). Intracellular material, such as the cytoplasm, is segregated by a membrane cisterna, which forms an autophagic vacuole known as an autophagosome. Autophagosomes are presumed to fuse with lysosomes before their contents are degraded by lysosomal enzymes (Mortimore and Schworer, 1977).

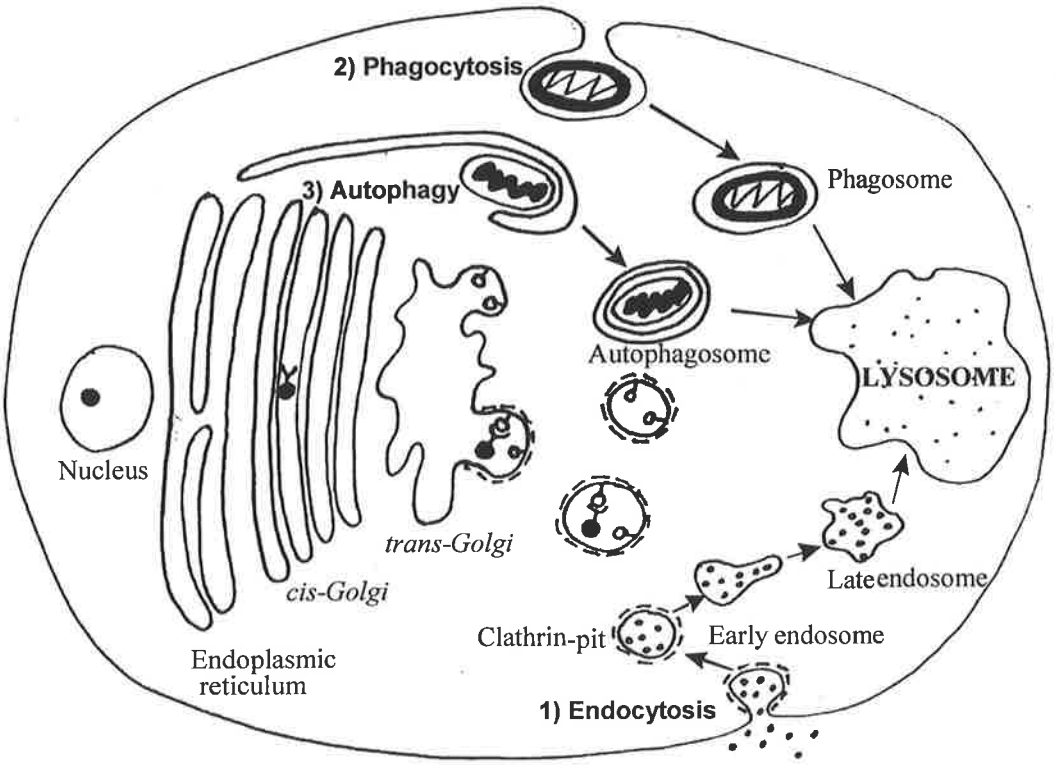

Figure 1.1 Delivery of macromolecules to the lysosome

Macromolecules enter the cell via: 1) endocytosis: extracellular molecules are endocytosed into the cell via clathrin-coated pits, which are then transported to the lysosome for degradation via endosome vesicles; 2) phagocytosis: products of ingestion (e.g. bacterium, food) are engulfed by the cell and the products are delivered to the lysosome in a vacuole called the phagosome; and 3) autophagy: worn-out organelles (e.g. mitochondria) are wrapped in a portion of the rough endoplasmic reticulum to form an autophagosome, which is then delivered to the lysosome.

1.2. Lysosomal proteins

Lysosomal proteins, which total more than 80, work in a cohesive manner to ensure the normal functioning of the lysosome (Hopwood and Brooks, 1997). These proteins are categorised into two groups based on their origin in the lysosome: (1) *lysosomal membrane proteins* are located in the membrane; and (2) *lysosomal luminal proteins* are located in the organelle milieu.

1.2.1. Lysosomal membrane proteins

Lysosomal membrane proteins consist of structural proteins, proton ATPases and various transporters. The structural proteins, also known as lysosomal membrane glycoproteins, play a vital role in containing the acidic content of the lysosome (Granger *et al.*, 1990). This acidic environment is maintained through the generation of electrical and chemical gradients across the organelle membrane with the help of the vacuolar proton ATPases (van Dyke, 1996).

Lysosomal membrane proteins that have been identified and sequenced were found to be heavily glycosylated. These polypeptides are the main structural constituent of the lysosomal membrane and found to have molecular weights (Mw) between 90 and 110 kDa (Peters and von Figura, 1994). Of the unsequenced membrane proteins, most have been functionally characterised as transporters for small molecules such as amino acids, calcium, sulphate, phosphate and monosaccharides (Hopwood and Brooks, 1997).

1.2.2. Lysosomal luminal proteins

This diverse group of acid hydrolases is found within the lumen of the lysosome and is responsible for the lysosomal degradation of macromolecules. The known acid hydrolases include proteases, glycosidases, sulphatases, phosphatases and lipases (Hopwood and Brooks, 1997). The sulphatases, together with another group of luminal proteins known as activator proteins, are discussed further in this chapter since both proteins are directly involved in the pathogenesis of MLD.

1.2.2.1. The sulphatases

The sulphatases are a group of enzymes that share a high degree of structural and functional homology. Twelve sulphatases have been identified (Table 1.1), eight of which are found in the lysosome; they act by desulphating glycosaminoglycans, glycolipids and glycoproteins. The other four sulphatases are associated with the microsomal fraction and

act on sulphated hydroxysteriods in the neutral milieu of the vacuolar network. Six sulphatases, known as arylsulphatases A to F (ASA, ASB, ASC, ASD, ASE and ASF), are known to act on artificial substrates such as p-nitrocatechol sulphate (p-NCS) and 4-methylumbelliferyl sulphate (4-MUS) in addition to their natural substrates (Parenti *et al.*, 1997). Due to this ability, these synthetic substrates are widely used in laboratory assays for the determination of sulphatase activities. The catalytic properties of some of these sulphatases towards both the artificial 4-MUS substrate and their natural substrates have been determined by Hopwood and colleagues, and are listed in Table 1.2 (Hopwood and Ballabio, 2001).

The cDNA of ASA and ASB was successfully sequenced and cloned by Stein *et al.* (1989) and Peters and co-workers (1989), respectively. Their work provided opportunities for others to study the consequences arising from mutations via *in-vitro* mutagenesis studies. A further important finding was the identification of the active site of these enzymes, which provided a major breakthrough in understanding their catalytic function. Schmidt *et al.* (1995) identified the active sites for ASA and ASB as cysteine at positions 69 and 91, respectively, through structural analysis of trypsin-digested ASA and ASB protein by reverse-phase high performance liquid chromatography (RP-HPLC) and mass spectrometry (MS). These active sites were later confirmed with the three-dimensional structure of crystallised ASB by Bond *et al.* (1997) and ASA by Lukatela *et al.* (1998). Crystallographic analysis also revealed the presence of α-formylglycine (2-amino-3-oxopropionic acid) instead of cysteine at the active sites of catalytically active ASA and ASB, which suggested that these two proteins undergo post-translational modification before becoming catalytically active. Schmidt *et al.* (1995) reported the isolation of a peptide in the trypsin digest of ASA that contained a 2-amino-3-oxopropanoic acid residue in place of the cysteine residue at position 69, as predicted by the genetic code of ASA. The modification of this active site cysteine is catalysed by the action of the multiple sulphatase gene (Cosma *et al.*, 2003).

In addition, the metal coordination sites are conserved between these two enzymes, with Ca^{2+} and Mg^{2+} being proposed as the metal ions involved in the catalytic mechanisms for ASB and ASA, respectively. However, analysis of the crystal structure of ASA in human placenta revealed that the metal ion present in the active site is Ca^{2+} rather than Mg^{2+}, as found in the recombinant enzyme (Chruszcz *et al.*, 2003). The active sites conserved between ASA and ASB and their proposed functions are listed in Table 1.3.

In an experiment by Waldow *et al.* (1999), who analysed the role of these active sites to determine the catalytic function of human ASA, the following putative sites were substituted with alanine: Asp^{29}, Asp^{30}, Asp^{281}, Asn^{282}, His^{125}, His^{229}, Lys^{123}, Lys^{302} and Ser^{150}. In addition, Asp^{29}, Asp^{30}, Asp^{281} and Asn^{282} residues that are known to be involved in the metal coordination of Mg^{2+} were substituted with either asparagine or aspartate. Results from these experiments showed that the V_{max} was lower in all mutants (between 1 to 26%), while the K_m was 10-fold higher for K123A and K302A and up to five-fold higher for other mutants when compared to wild type (Wt) ASA activity. It was thus concluded that all of these residues are vital for catalytic activity of ASA.

It has long been established that the deficiency of individual sulphatases causes various types of mucopolysaccharidoses (MPSs), with the exceptions of: ASA, which is associated with MLD; ASE, which is linked to chondrodysplasia punctata (Franco *et al.*, 1995); and ASC, which leads to X-linked ichthyosis (Robledo *et al.*, 1995); another LSD, multiple sulphatase deficiency, is caused by inactive sulphatases due to the failure of post-translational modification of cysteine (Schmidt *et al.*, 1995; Dierks *et al.*, 2003).

In addition to these, variants of LSD are known to exist as a consequence of sphingolipid activator protein (saposin) deficiency. The sulphatases, in hydrolysing glycosphingolipids (GSL) with more than six carbons in the acyl chain, require the aid of saposins to extract and solubilise the substrates before presenting the complex to the enzymes for hydrolysation (Vogel *et al.*, 1991). The saposins, and their relationship to MLD, are further discussed in section 1.2.2.2.

Table 1.1 Human sulphatases

Enzyme[a]	Localisation[b]	Substrate	Disease[c]
ASA	Lysosome	Sulphatide	MLD, MSD
ASB	Lysosome	Dermatan sulphate	MPS VI, MSD
ASC	Microsome	Sulphated steroid	XLI, MSD
ASD	ER	unknown	not established
ASE	Golgi apparatus	unknown	CP, MSD
ASF	ER	unknown	not established
I2S	Lysosome	Dermatan sulphate Heparan sulphate	MPS II, MSD
Gal6S	Lysosome	Keratan sulphate Chondroitin sulphate	MPS IVA, MSD
GlcN6S	Lysosome	Heparan sulphate	MPS IIID, MSD
GAS	Lysosome	Heparan sulphate	not established
GlcN3S	Lysosome	Heparan sulphate	not established
GlcNS	Lysosome	Heparan sulphate	MPS IIIA, MSD

Table modified from Parenti *et al.*, 1997; Hopwood and Ballabio, 2001.

[a] ASA = arylsulphatase A; ASB = arylsulphatase B; ASC = arylsulphatase C; ASD = arylsulphatase D; ASE = arylsulphatase E; ASF = arylsulphatase F; I2S = iduronate-2-sulphatase; Gal6S = N-acetylgalactosamine-6-sulphatase; GlcN6S = glucosamine-6-sulphatase; GAS = glucoronate-2-sulphatase; GlcN3S = glucosamine-3-sulphatase; GlcNS = sulphamidase;

[b] ER = endoplasmic reticulum;

[c] MLD = metachromatic leukodystrophy; MSD = multiple sulphatase deficiency; XLI = X-linked ichthyosis; MPS = mucopolysaccharidosis; CP = chondrodysplasia punctata

Table 1.2 Catalytic properties of a number of specific sulphatases toward the artificial substrate 4-methylumbelliferyl sulphate (A) and the natural substrate (B)

(A)

Enzyme	K_m (mM)	V_{max} (nmol/min/mg)	pH optimum
GlcNS	4.8	114	5.4
GlcN6S	5.8	10	5.2
I2S	12.4	300	5.6
Gal6S	4.4	120	4.7
ASB	1.2	48485	5.6

(B)

Enzyme[a]	K_m (μ/M)	V_{max} (μmol/min/mg)	pH optimum
GlcNS	10.7	0.8	5.2
GlcN6S	48.2	0.049	6.0
I2S	3.0	3.4	4.5
Gal6S	12.5	1.5	4.7
ASB	60.0	20.0	5.6
GAS	0.3	12.8	3.2

Tables reproduced from Hopwood and Ballabio, 2001.

[a] GlcNS = sulphamidase; GlcN6S = glucosamine-6-sulphatase; I2S = iduronate-2-sulphatase; Gal6S = N-acetylgalactosamine-6-sulphatase; ASB = arylsulphatase B; GAS = glucuronate-2-sulphatase

Table 1.3 Active site residues conserved between ASA and ASB

	Position		
Residue	**ASA**	**ASB**	**Proposed Function**
Aspartic acid	29	53	metal coordination
Aspartic acid	30	54	metal coordination
Aspartic acid	281	300	metal coordination
Asparagine	282	301	metal coordination
Cysteine	69	91	α-formylglycine
Arginine	73	95	catalytic mechanism
Lysine	123	145	catalytic mechanism
Histidine	125	147	catalytic mechanism
Histidine	229	242	catalytic mechanism
Lysine	302	318	catalytic mechanism

Table reproduced from Hopwood and Ballabio, 2001.

1.2.2.2. Saposins

In 1964, Mehl and Jatzkewitz discovered the first of these small non-enzymatic proteins and named it "activator of the cerebroside sulphatase"; it is now known as saposin B. There are five saposins: the four saposin homologues (A, B, C and D) and the monosialoganglioside (G_{M2}) activator protein (O'Brien and Kishimoto, 1991). With the exception of the G_{M2} activator protein, all saposins are derived from a common precursor protein called prosaposin (O'Brien *et al.*, 1988), are structurally similar and share a high degree of homology in their amino acid sequence (Kishimoto *et al.*, 1992)

Through kinetic and binding experiments, it was found that saposin B acts by extracting the lipid from the plasma membrane, solubilising it into a protein/lipid complex and then presenting the complex to the lysosomal enzymes for degradation (Fischer and Jatzkewitz, 1977). The crystallographic study of saposin B in dimer form has shown that the solubilisation mechanism is achieved through a conformational change in the protein, resulting in a large hydrophobic cavity used for sulphatide extraction from the membrane and its subsequent presentation to ASA for catalytic action (Ahn *et al.*, 2003).

Variants of LSD are known to arise from saposin deficiency (section 1.2.2.1): saposin C deficiency is associated with a variant form of Gaucher disease (Christomanou *et al.*, 1986), and a deficiency of saposin B is known to cause the variant in MLD (Kretz *et al.*, 1990). To date, six cases of MLD have been reported to result from a deficiency of saposin B, four of which are due to mutations at the glycosylation site that result in the loss of its carbohydrate moiety (Kretz *et al.*, 1990; Rafi *et al.*, 1990; Regis *et al.*, 1999; Wrobe *et al.*, 2000).

Therefore, patients with these LSD variants may not be diagnosed because their respective primary enzyme activity may be normal. Hence, it is imperative that both the clinician and laboratory personnel dealing with the diagnosis of LSD are aware of the existence of these variants. Diagnosis can be achieved through mutation analysis or by the determination of saposins by measuring their ability to accelerate the hydrolysis of glycolipids (Conzelmann and Sandhoff, 1979).

1.2.3. Endocytic trafficking

Protein trafficking pathways within the cell involve the plasma membrane and all elements of the vacuolar network, with the exceptions of mitochondria, peroxisomes and chloroplasts, which, as non-secretory organelles, have mechanically different protein trafficking processes (Grivell, 1988). The trafficking processes of the lysosomal luminal and membrane proteins will now be briefly discussed.

1.2.3.1. Targeting of the lysosomal luminal proteins

The synthesis of lysosomal luminal proteins occurs on the ribosome associated with the endoplasmic reticulum (ER). The proteins produced at this stage are precursor forms, which are then trafficked across the ER. During this process, co-translational modification, including proteolysis and glycosylation, takes place before these proteins are trafficked to the Golgi apparatus (Kornfeld, 1986).

Soluble enzymes that are destined for the lysosome undergo further post-translational modification with the acquisition of phosphomannosyl residues in the cis-Golgi (Finean *et al.*, 1984). This is essential for recognition of the enzyme by the mannose-6-phosphate receptor (M6PR) and its subsequent translocation to the endosomal-lysosomal network (von Figura and Hasilik, 1986). On reaching the endosome, these enzymes dissociate from their receptors and continue their journey to the lysosome while the M6PR is redirected back to trans-Golgi network for re-utilisation (Duncan and Kornfeld, 1988).

1.2.3.2. Targeting of lysosomal membrane proteins

While most of the trafficking processes associated with lysosomal luminal proteins were characterised in the mid- to late-1970s, the study of membrane protein trafficking only began in the early-1980s. The first significant study of the biosynthesis and trafficking of lysosomal membrane proteins was by Barriocanal *et al.* (1986): through kinetic studies of three lysosomal integral membrane proteins (LIMPs) they revealed that the translocation of LIMPs to lysosomes was via a N-linked carbohydrate-independent mechanism, hence the conclusion that lysosomal membrane proteins do not need the mannose-6-phosphate tag for translocation to the lysosome. This finding concurred in part with earlier work by von Figura *et al.* (1979), who showed that two LIMPs without their carbohydrate moiety could still be transported to the lysosome.

More recent studies have shown that the targeting of LIMPs to the lysosome depends upon a targeting signal near the C-terminal of the cytoplasmic tail (Hunziker and Geuze, 1996). In general, two types of targeting signals have been characterised: (i) the 'tyrosine-based signal' is found in the lysosome-associated membrane proteins Lamp-1, Lamp-2 and Lamp-3 and is composed of the amino acid sequence of tyrosine followed by any two amino acids and a hydrophobic residue (YXXØ) (Guarnieri *et al.*, 1993); and (ii) the 'dileucine-based signal', which has a pairing of two leucine residues as the targeting signal (Honing *et al.*, 1998), is found in cation-dependent M6PR. An alternative lysosomal targeting signal has also been described involving the peptide motif of leucine-isoleucine, which can be found in Limp II (Ogata and Fukuda, 1994).

1.3. Lysosomal storage disorders

LSD are a group of more than 45 distinct heritable disorders caused by functional deficiencies in lysosomal acid hydrolases, resulting in the accumulation of corresponding substrates in the lysosomes. Excessive accumulation of these substrates will lead to an increase in the number and size of lysosomes in affected cells (Hopwood and Brooks, 1997), as depicted in the electron micrograph in Figure 1.2.

LSD patients can present with a variety of clinical features. Clinical presentation is progressive and chronic depending on the severity and nature of the disease. The site of substrate storage also dictates the clinical presentation of these patients, which can be either somatic or affect the central nervous system (CNS) or both (Hopwood and Brooks, 1997). Some of the clinical features associated with somatic storage are facial dysmorphia, dysostosis multiplex and hepatosplenomegaly, while storage in the CNS results in cognitive deficits, behavioural abnormalities and delayed developmental milestones (Clarke, 1997).

The continued interest in and increased understanding of LSD has led to the identification and characterisation of several new disorders in recent years, including infantile neuronal ceroid lipofuscinosis (NCL), also known as Santavuori disease (Vesa *et al.*, 1995), pycnodysostosis (Gelb *et al.*, 1996), and classical late-infantile NCL, also known as Jansky-Bielschowshky disease (Sleat *et al.*, 1997). With improvements in our knowledge about the nature of LSD, it is inevitable that the list will continue to expand.

Most LSD are autosomally recessively inherited, with the exceptions of Fabry disease (Desnick *et al.*, 2001), Hunter syndrome (MPS type II) (Muenzer *et al.*, 2002) and Danon

disease (Nishino *et al.*, 2000), which are inherited in an X-linked manner. LSD can be grouped on the basis of enzyme deficiency and accumulating substrates. The types of LSD, their enzyme deficiencies, prevalence, stored substrates and the types of diagnostic investigations available for each disorder are listed in Table 1.4 (Meikle *et al.*, 2004a).

1.3.1. The incidence of lysosomal storage disorders

The incidence of LSD in Australia ranges from about 1 in 57 000 live births for Gaucher disease, to 1 in 2.1 million live births for aspartylglucosaminuria (Meikle *et al.*, 1999). In Australia the combined incidence of LSD has been estimated to be approximately 1 in 7 700 live births (Meikle *et al.*, 1999), however, incidence can vary substantially based on ethnicity and geography. For example, Gaucher disease, the most prevalent LSD, was reported to occur in 1 in 855 live births in the Ashkenazic Jewish population (Beutler and Grabowski, 1995) as opposed to 1 in 57 000 live births in Australia (Meikle *et al.*, 1999); this also holds true for late-infantile MLD, which was found to be extraordinarily high in Habbanite Jews in Israel, with a reported incidence of 1 in 75 live births (Zlotogora *et al.*, 1980) compared to 1 in 92,000 in the Australian population (Meikle *et al.*, 1999).

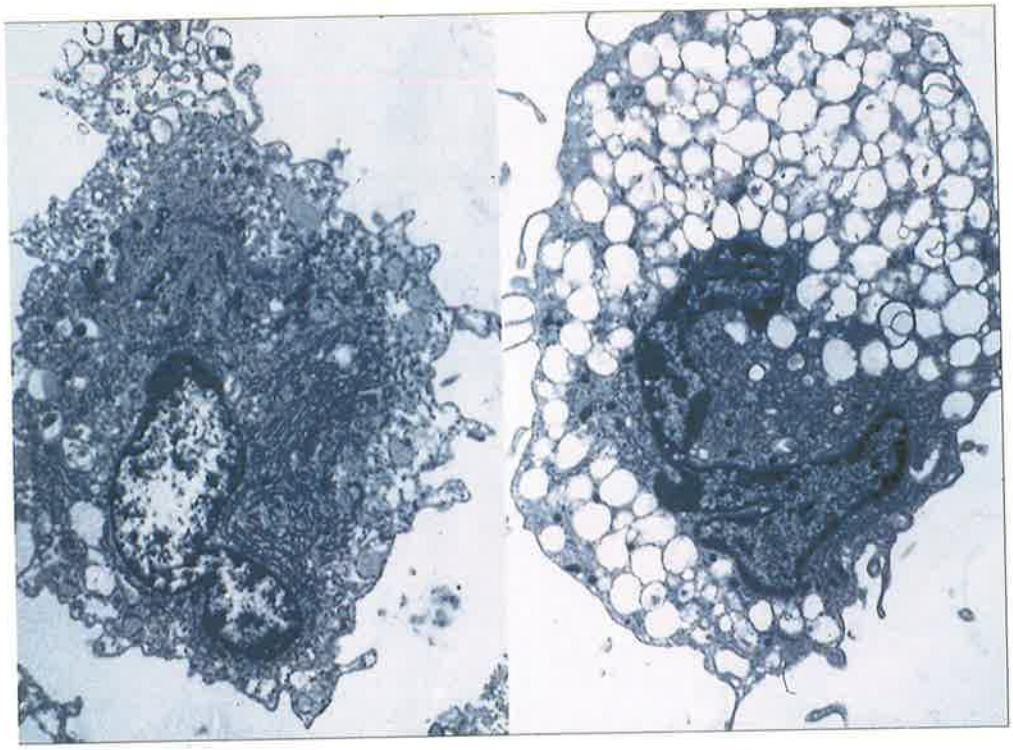

Control LSD

Figure 1.2 Substrate storage in skin fibroblasts

Electron micrographs of skin fibroblasts (SF) from an unaffected individual (left) and a LSD patient (right). The enlargement and accumulation of acidic vacuoles due to substrate storage is a characteristic biochemical feature of LSD cells. (Micrographs reproduced with courtesy from Professor John Hopwood).

Table 1.4 Diagnosis of lysosomal storage disorders

Disease	Clinical Phenotype	OMIM No.	Enzyme Deficiency	Australian Prevalence[a]	Storage Substrates	Screen[b]	Biochemical Analysis[c]	Molecular analysis	Prenatal diagnosis[c]
α-N-Acetylgalactosaminidase deficiency	Schindler disease; Kanzaki disease[d]	104170	α-N-Acetylgalactosaminidase		Oligosaccharides	urine oligo	E	yes	E[e]
Acid lipase deficiency	Cholesterol ester storage disease; Wolman disease	278000	Acid lipase	1:528,000	Cholesterol esters		E	yes	E
Aspartylglucosaminuria		208400	Aspartylglucosaminidase	1:2,111,000	Glycopeptides	urine oligo	E	yes	E
Ceroid lipofuscinosis neuronal 1, infantile; CLN1	Santavuori disease	256730	Palmitoyl-protein thioesterase 1		Protein, lipofuscin, lipids		E	yes	E
Ceroid lipofuscinosis neuronal 2, late-infantile; CLN2	Jansky-Bielschowsky disease	204500	Tripeptidyl peptidase I		Protein, lipofuscin, lipids		E	yes	E
Ceroid lipofuscinosis neuronal 3, juvenile; CLN3	Batten disease	204200	CLN3p (function unknown)		Protein, lipofuscin, lipids			yes	M
Ceroid lipofuscinosis neuronal 5; CLN5	Finnish variant late-infantile NCL	256731	CLN5p (function unknown)		Protein, lipofuscin, lipids			yes	M
Ceroid lipofuscinosis neuronal 6; CLN6	Variant late-infantile NCL	601780	CLN6p (function unknown)		Protein, lipofuscin, lipids			yes	M
Ceroid lipofuscinosis neuronal 8; CLN8	Northern epilepsy	600143	CLN8p (function unknown)		Protein, lipofuscin, lipids			yes	M
Cystinosis		219800	Cystine transporter	1:192,000	Cystine		F, S	yes	F, S
Danon disease		300257	LAMP-2		Glycogen			yes	M
Fabry disease	Fabry disease	301500	α-Galactosidase A	1:117,000	Trihexosyl ceramide		E, S	yes	E
Farber lipogranulomatosis	Farber disease	228000	Acid ceramidase		Ceramide		E	yes	E

Table 1.4 Continued

Disease	Clinical Phenotype	OMIM No.	Enzyme Deficiency	Australian Prevalence[a]	Storage Substrates	Screen[b]	Biochemical Analysis[c]	Molecular analysis	Prenatal diagnosis[c]
Fucosidosis		230000	α-L-Fucosidase	>1:2,000,000	Glycopeptides, oligosaccharides	Urine oligo	E	yes	E
Galactosialidosis types I / II		256540	Protective protein		Oligosaccharides	Urine oligo	E[f]	yes	E[f]
Gaucher disease types I / II / III	Gaucher disease	230800 230900 231000	β-Glucocerebrosidase	1:57,000	Glucosyl ceramide		E	yes	E
Gaucher disease		see 176801	Saposin C		Glucosyl ceramide		S, F		M
Globoid cell leukodystrophy	Krabbe disease	245200	β-Galactocerebrosidase	1:201,000	Galactosyl ceramide		E	yes	E
Glycogen storage disease II	Pompe disease	232300	α-Glucosidase	1:146,000	Glycogen, oligosaccharides	Urine oligo	E	yes	E
G_{M1}-Gangliosidosis types I/II/III		230500	β-Galactosidase	1:384,000	Oligosaccharides, gangliosides		E	yes	E
G_{M2}-Gangliosidosis, type AB		272750	G_{M2}-activator deficiency		Oligosaccharides, gangliosides		F	yes	M
G_{M2}-Gangliosidosis type I (B variant)	Tay Sachs disease	272800	β-Hexosaminidase A	1:201,000	Oligosaccharides, gangliosides		E	yes	E
G_{M2}-Gangliosidosis type II (O variant)	Sandhoff disease	268800	β-Hexosaminidase A & B	1:384,000	Oligosaccharides, gangliosides	Urine oligo	E	yes	E
α-Mannosidosis types I / II		248500	α-D-Mannosidase	1:1,056,000	Oligosaccharides	Urine oligo	E	yes	E, S
β-Mannosidosis		248510	β-D-Mannosidase		Oligosaccharides	Urine oligo	E	yes	E
Metachromatic leukodystrophy		250100	Arylsulphatase A	1:92,000	Sulphatide		E	yes	E
Metachromatic leukodystrophy		249900	Saposin B		Sulphatide		S, F	yes	M
Mucolipidosis type I	Sialidosis types I / II	256550	Neuraminidase		Oligosaccharides		E	yes	E

Table 1.4 Continued

Disease	Clinical Phenotype	OMIM No.	Enzyme Deficiency	Australian Prevalence[a]	Storage Substrates	Screen[b]	Biochemical Analysis[c]	Molecular analysis	Prenatal diagnosis[c]
Mucolipidosis types II / III	I-cell disease; pseudo-Hurler polydystrophy	252500 252600	N-Acetylglucosamine-1-phosphotransferase	1:325,000	Oligosaccharides, glycolipids	Urine oligo	ME	yes	ME[g]
Mucolipidosis type IIIC	Pseudo-Hurler polydystrophy	252605	N-Acetylglucosamine-1-phosphotransferase γ-subunit		Oligosaccharides, glycolipids		ME	yes	ME[g]
Mucolipidosis type IV		252650	Mucolipin 1					yes	M
Mucopolysaccharidosis type I	Hurler/Scheie syndrome	607014 607015 607016	α-L-Iduronidase	1:88,000	DS, HS, oligosaccharides	Urine GAG	E	yes	E
Mucopolysaccharidosis type II	Hunter syndrome	309900	Iduronate-2-sulphatase	1:136,000	DS, HS, oligosaccharides	Urine GAG	E	yes	E
Mucopolysaccharidosis type IIIA	Sanfilippo syndrome	252900	Heparan-N-sulphatase	1:114,000	HS, oligosaccharides	Urine GAG	E	yes	E
Mucopolysaccharidosis type IIIB	Sanfilippo syndrome	252920	α-N-Acetylglucosaminidase	1:211,000	HS, oligosaccharides	Urine GAG	E	yes	E
Mucopolysaccharidosis type IIIC	Sanfilippo syndrome	252930	AcetylCoA:glucosamine-N-acetyltransferase	1:1,407,000	HS, oligosaccharides	Urine GAG	E	no	E
Mucopolysaccharidosis type IIID	Sanfilippo syndrome	252940	N-Acetylglucosamine-6-sulphatase	1:1,056,000	HS, oligosaccharides	Urine GAG	E	yes	E
Mucopolysaccharidosis type IVA	Morquio syndrome	253000	N-Acetylgalactosamine-6-sulphatase	1:169,000	DS, oligosaccharides	Urine GAG	E	yes	E
Mucopolysaccharidosis type IVB	Morquio syndrome	253010	β-Galactosidase		DS, oligosaccharides	Urine GAG	E	yes	E
Mucopolysaccharidosis type VI	Maroteaux-Lamy syndrome	253200	N-Acetylgalactosamine-4-sulphatase	1:235,000	DS, oligosaccharides	Urine GAG	E	yes	E

Table 1.4 Continued

Disease	Clinical Phenotype	OMIM No.	Enzyme Deficiency	Australian Prevalence[a]	Storage Substrates	Screen[b]	Biochemical Analysis[c]	Molecular analysis	Prenatal diagnosis[c]
Mucopolysaccharidosis type VII	Sly syndrome	253220	β-Glucuronidase	1:2,111,000	DS, oligosaccharides	Urine GAG	E	yes	E
Mucopolysaccharidosis type IX		601492	Hyaluronidase 1		Hyaluronan		E	yes	none
Multiple sulphatase deficiency		272200	Formylglycine generating enzyme	1:1,407,000	HS, DS, CS, oligosaccharides	Urine GAG	ME	yes	E, ME[g]
Niemann-Pick disease type A / B	Niemann-Pick disease	257200 607616	Acid sphingomyelinase	1:248,000	Sphingomyelin		E	yes	E
Niemann-Pick disease type C1	Niemann-Pick disease	257220	NPC1 protein (involved in cholesterol trafficking)	1:211,000	Cholesterol		S, F	yes	S, F
Niemann-Pick disease type C2	Niemann-Pick disease	607625	NPC2 protein (involved in cholesterol trafficking)		Cholesterol		S, F	yes	S, F
Prosaposin deficiency		176801						yes	M
Pycnodysostosis		265800	Cathepsin K				E	yes	
Sialic acid storage disease	Infantile free sialic acid storage disease (ISSD); salla disease	269920 604369	Sialin (Sialic acid transporter)	1:528,000	Sialic acid, uronic acid	Urine oligo	S	yes	S
Sialuria		269921	UDP-N-acetylglucosamine 2-epimerase		Sialic acid	Urine oligo	S, E	yes	M

[a] Meikle *et al.*, 1999; [b] urine oligo = urine thin layer chromatography; urine GAG = urine high resolution electrophoresis;

[c] E = enzyme analysis; S = substrate determination; F = functional assay; ME = multiple enzyme analysis; M = molecular analysis (note that molecular analysis can be used for prenatal diagnosis for all disorders where the gene has been isolated); [d] Bakker *et al.* 2001 [91], indicate that classic infantile Schindler disease is not due to α-N-acetylgalactosaminidase deficiency; [e] presumed that enzyme activity would be deficient in chorionic villus cells and amniocytes; [f] analysis of neuraminidase activity should be used in cultured cells;

[g] prenatal diagnosis by lysosomal enzyme analysis can only be performed in families with clear enzyme deficiencies in cultured cells.

Table reproduced from Meikle *et al.* (2004a).

1.4. Metachromatic leukodystrophy

MLD is a neurodegenerative disease that is inherited in an autosomal recessive manner. The primary defect results from the decreased catalytic action of ASA on galactosyl-3-sulphate (sulphatide), resulting in its accumulation in the lysosomal compartment of cells in several peripheral organs, notably the CNS. Whilst there is no pathophysiological effect from this accumulation in most peripheral tissues, the CNS exhibits progressive demyelination that leads to severe impairment of neurological function with a fatal outcome (Kolodny and Fluharty, 1995).

1.4.1. Classification of MLD

MLD is classified into four clinical sub-types based on the age of onset, as shown in Table 1.5 (von Figura *et al.*, 2001). The most severe sub-type is the late-infantile form, in which death ensues one- to seven-years after diagnosis. The juvenile type has a more protracted clinical course with the majority of patients dying before reaching the age of 20-years, although some patients have survived into their late-20s (Kolodny and Fluharty, 1995); some juvenile cases have presented at a very young age (four- to six-years), which has led to further sub-categorisation into 'early-juvenile' and 'late-juvenile' (Kolodny and Fluharty, 1995). The adult form is the mildest, with patients reported to survive well into their sixth-decade (Hageman *et al.*, 1995; Duyff and Weinstein, 1996). The reported incidence for the late-infantile and juvenile forms is equally divided, with the adult form reported to be 25% of all cases (von Figura *et al.*, 2001).

1.4.2. Clinical manifestations

The presenting clinical features differ in each of the four types of MLD even though they share the same pathophysiological defect in the CNS; these are summarised in Table 1.5. In 1963, Hagberg further sub-divided the late-infantile form into four stages that correspond to clinical deterioration as a result of disease progression (section 1.4.2.1; reproduced from von Figura *et al.*, 2001). The clinical onset of late-infantile MLD can be as early as six-months to four-years of age.

1.4.2.1. Late-infantile MLD

Clinical stage I. Most patients have hypotonia of the legs or of all four limbs. The gait therefore becomes unsteady and the child requires support to stand or walk. The deep tendon reflexes may be diminished or absent secondary to a progressive polyneuropathy. This stage lasts for a few months to more than one-year.

Clinical stage II. In this stage the patient can no longer stand and shows mental regression. Speech deteriorates as a result of dysarthria and aphasia. Nystagmus is observed, as well as optic atrophy and a greyish discoloration of the macula. The neuropathy may be painful (intermittent pain in arms and legs). Ataxia and truncal titubation become obvious, and muscle tone is increased in the legs. This stage lasts only a few months.

Clinical stage III. Gradually, involvement of the pyramidal system causes the flaccid paresis to be superseded by spastic tetraplegia with pathologic reflexes such as extensor planter reflexes, and the child becomes bedridden. Bulbar and pseudobulbar palsies occur, causing feeding difficulties and airway obstruction. Epileptic seizures occur in about 25% of the children. Although their mental state and speech further deteriorate, these children may still be able to smile and respond.

Clinical stage IV. In this final stage, patients lose all contact with their surroundings, as they are blind and in a decerebrate state, without purposeful movements. They have to be fed through a nasogastric or gastrostomy tube. This stage may last for several years. Death usually occurs about five-years after the onset of clinical symptoms.

1.4.2.2. Juvenile MLD

Juvenile MLD can be sub-divided into early- and late-onset forms based on the age at clinical presentation. The early juvenile form will have a clinical onset between the ages of four- to six-years with signs of abnormal gait and postural problems; at this stage the reflexes will still be normal. Behavioural and emotional changes are also associated with this group, which tend to precede the onset of neurological symptoms. The deteriorating neurological tract will lead to optic atrophy and spastic quadriparesis. In contrast, the presenting age of late-juvenile patients can be between the ages of six- and 16-years; clinical signs are mostly associated with behavioural problems, poor school performance and language regression; neurological problems follow the onset of CNS involvement (Manowitz *et al.*, 1978).

Table 1.5 Characteristics of late-infantile, juvenile and adult forms of MLD

Type	Age at onset (years)	Main clinical manifestations	Spinal fluid protein	Nerve conduction velocity	Urinary sulphatide excretion
Infantile	0.5 - 4	Gait disturbance, decreased tendon reflexes, mental regression, loss of speech, optic atrophy, ataxia, progressive spastic, quadriparesis	Elevated	Slowed	Elevated
Early juvenile	4 – 6	Gait and postural abnormalities, emotional and behavioural disturbances, optic atrophy, progressive spastic quadriparesis	Elevated	Slowed	Elevated
Late juvenile	6-16	Behavioural abnormalities, poor school performance, language regression, gait disturbance, slowly progressive spastic tetraparesis	Elevated	Slowed	Elevated
Adult	>16	Mental regression, psychiatric symptoms, incontinence, slowly progressive spastic tetraparesis	Normal or elevated	Normal or slowed	Elevated

Table reproduced from von Figura *et al.* (2001).

1.4.2.3. Adult MLD

Patients with adult MLD can present clinically as early as the late-teens or as late as the fourth decade. The presenting clinical symptoms are mostly associated with psychological disorders such as schizophrenia-like psychosis and dementia, with neurological signs appearing very late in the course of the disease (Baquis *et al.*, 1991). Baumann *et al.* (2002) further sub-divided adult MLD into a neurological form and a psychiatric form based on the presenting signs at the onset of disease. Other profound symptoms include incontinence and a slow but progressive spastic quadriparesis.

1.4.3. Biochemical changes in MLD

The biochemical changes in MLD arise from the deficiency of ASA that leads to the accumulation of sulphatide in several visceral organs, notably the CNS. Morphological changes resulting from accumulating sulphatide include demyelination and deposits of metachromatic granules in the central and peripheral nervous systems. Analysis of the metachromatic granules has shown a sulphatide content of 39% of the total lipid content; other major lipid components in these metachromatic granules are cholesterol and phosphatides (Suzuki and Chen, 1967).

1.4.3.1. Arylsulphatase A (E.C.3.1.6.1)

A deficiency in ASA activity is the major cause of MLD. Except for the form of MLD caused by saposin B deficiency, all forms of MLD are due to allelic mutations in the ASA gene, which has been mapped to distal chromosome 22 band q13 (Phelan *et al.*, 1992). The full-length cDNA of ASA spans 3.2 kb with eight exons that encode a 62 kDa protein with three N-glycosylation sites (Kreysing *et al.*, 1990) but various Mw have been reported depending on the origin of the ASA. The ASA cDNA transcribes three different mRNA species of 2.1, 3.7 and 4.4 kb in length, which produce identical polypeptides but in different amounts. The shorter mRNA accounts for about 90% of the polypeptides and the two longer transcripts account for the rest (Gieselmann *et al.*, 1989).

The ASA mRNA is translated into a precursor protein of 507 amino acids in the rough ER. After translocation to the ER, the nascent ASA is transformed into a mature protein of 489 amino acids with the putative signal peptide of 18 amino acids cleaved off (Lukatela *et al.*, 1998); within the ER it also undergoes glycosylation, receiving three N-linked oligosaccharides on Asn 158, Asn 184 and Asn 350 (Sommerlade *et al.*, 1994).

The protein is then trafficked through the Golgi apparatus where further modification to the carbohydrate side chains occurs and the M6PR residues are incorporated into Asn 158 and Asn 350. Prior to leaving the ER, the ASA forms dimers and maintains this form until reaching the lysosome where octamerisation occurs (Sommerlade *et al.*, 1994). Crystallographic analysis of ASA suggests that octamerisation of ASA is due to the protonation of glutamic acid at position 426 located at the interface between the dimers that formed the octamer (Lukatela *et al.*, 1998). Figure 1.3 shows the tertiary structure of ASA from human cDNA sequence reported by Stein *et al.* (1989). Figure 1.4 shows the ASA structure in octamer form (A) and an enlargement of the contact site showing Glu 426 involvement in the octamerisation process (B) (reproduced from von Bulow *et al.*, 2002).

1.4.3.1.1. Biochemical characteristics

The Mw of ASA by sodium dodecylsulphate-polyacrylamide gel electrophoresis (SDS-PAGE) has been reported to be either 62 kDa or 59.5 kDa and can exist in both forms. The difference in Mw has been attributed to the number of N-linked oligosaccharides present on the polypeptide (Waheed *et al.*, 1983). In neutral or alkaline pH media, ASA is known to exist as a dimer and associates to become an octamer at acidic pH (Nicholls and Roy, 1971). Both forms of ASA have been reported to be equally catalytically active with the same specific activities (Roy, 1976).

ASA is also known to be non-specific in its catalytic action; it cleaves a variety of synthetic sulphate esters at a higher rate than its physiological substrates and has a pH optimum between five and six (Nicholls and Roy, 1971; Waheed and van Etten, 1980). Apart from sulphatide, other physiological substrates hydrolysed by ASA include lactosylceramide 3-sulphate and seminolipids (von Figura *et al.*, 2001).

ASA is also known to have anomalous kinetic behaviour with the artificial substrate p-NCS. It has been suggested that this phenomenon is due to the loss of its secondary structure as a result of the interaction between enzyme and substrate (Waheed and van Etten, 1980); this anomaly is not observed with the use of the fluorogenic substrate 4-MUS (Christomanou and Sandhoff, 1977). ASA can be inactivated by the presence of ferrate ions, structural analogues of orthophosphate and oxidising agents (Laidler, 1991). Heavy metals such as lead have been used to inhibit the activity of ASA to differentiate it from the activity of ASB (Christomanou and Sandhoff, 1977).

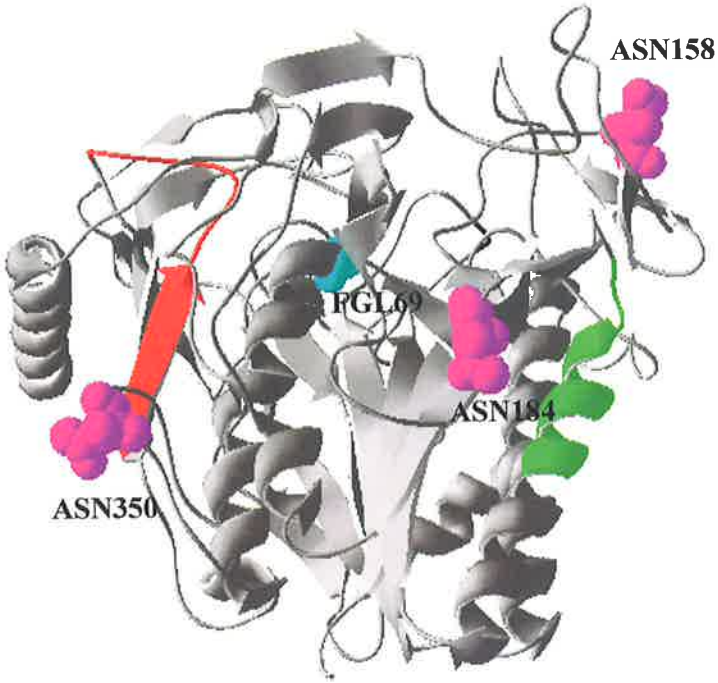

Figure 1.3 Secondary structure of ASA

The ASA enzyme is moulded around 10 α-helices and 18 β-strands with six disulphide bonds; the three glycosylation sites are labelled at their respective positions as ASN 158, ASN 184 and ASN 350, with the active site labelled as FGL 69 (Lukatela *et al.*, 1998). The figure is drawn with Mol script based on human cDNA sequence by Stein *et al.* (1989).

(A)

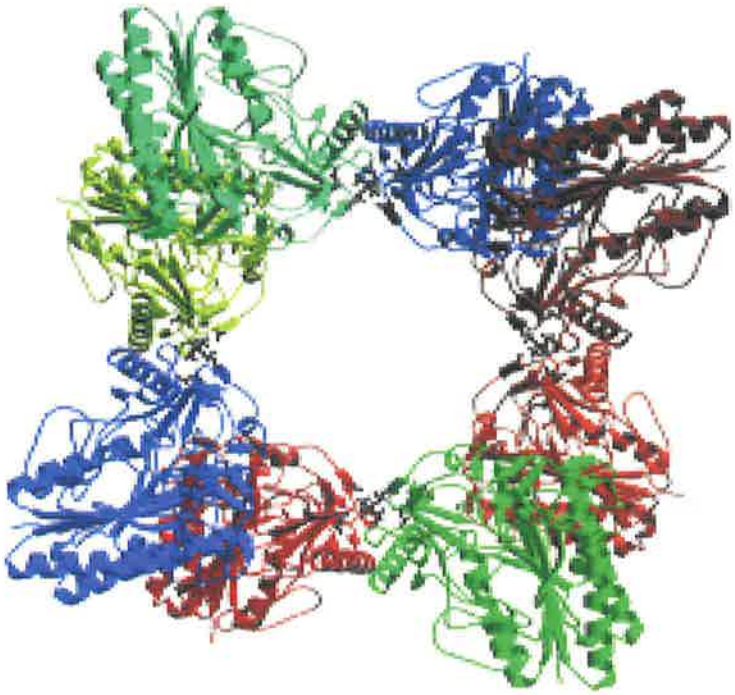

(B)

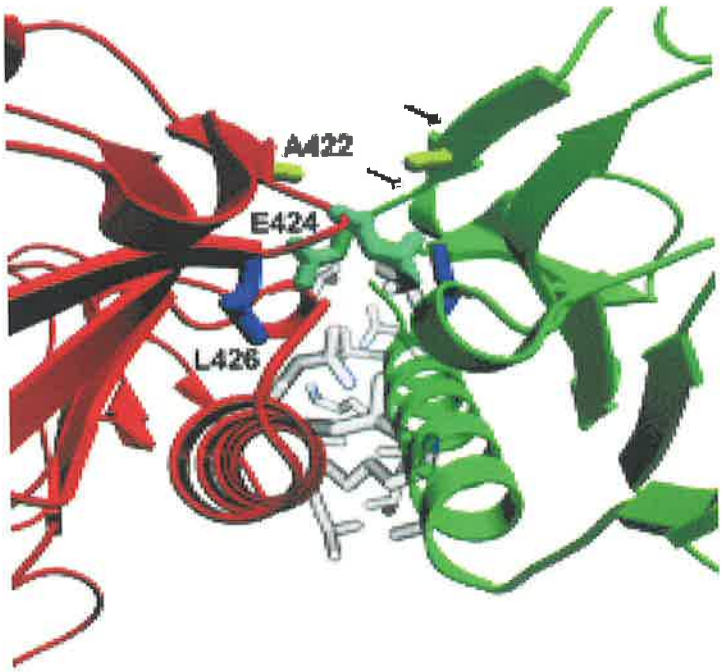

Figure 1.4 Quaternary structure of ASA

The ASA structure in octamer form, consisting of four homodimers held together by hydrogen bonds surrounding Glu 426 (A), and a close-up of the contact points involving amino acids between two homodimers (B). Figures are from von Bulow *et al.* (2002).

1.4.3.2. Sulphatide

Sulphatide, or galactosylceramide 3-sulphate (shown in Figure 1.5), is a major component of the myelin sheath. Sulphatide is known to play an important role in insulating the myelin membrane bilayer (Bosio *et al.*, 1996). In MLD patients, sulphatide is known to accumulate not only in the CNS but also in other organs such as the kidney, gall bladder, liver, pancreas, adrenal cortex and sweat glands; sulphatide is also excreted in the urine in all types of MLD (von Figura *et al.*, 2001).

Analysis of sulphatide from human brain and kidney shows that these two organs share the same species of fatty acids but in different proportions: kidney sulphatides have 10-times more behenic acid (22:0); the kidney also has a higher proportion of lignoceric acid (24:0) than nervonic acid (24:1) compared to the brain (Malone *et al.*, 1966). In addition, dihexosyl sulphatide has been detected in human urine (Whitfield *et al.*, 2001a) but not in the human brain. These differences, together with the normal amount of sulphatide in MLD serum (Svennerholm and Svennerholm, 1962), has led to the suggestion that the sulphatide excreted in the urine of MLD patients originates from the kidney rather than the brain or from any other organs (von Figura *et al.*, 2001).

1.4.3.2.1. Biosynthesis and degradation

Sulphatide is an essential component of myelin membranes with the site of synthesis located almost exclusively in the oligodendrocytes of the CNS (Vos *et al.*, 1994). Sulphatide is synthesised through the action of ceramide galactosyltransferase on ceramide to attach the galactose moiety, forming galactosylceramide (also known as galactocerebroside). The subsequent sulphation of galactocerebroside by the action of galactocerebroside sulphotransferase (3'-phosphoadenosine-5'-phosphosulphate) (Hauser, 1964) results in sulphatide. The degradation of sulphatide is mediated by saposin B for the catalytic action of ASA (Fischer and Jatzkewitz, 1977). This is followed by the catalytic action of galactosylceramidase on galactocerebroside, producing ceramide and galactose.

1.4.3.2.2. Pathophysiology from accumulating sulphatides

In MLD, sulphatide accumulates in a number of organs in the body (section 1.4.3.2). Except for the pathological effect on the CNS, which leads to demyelination, other organs are not affected by this accumulation even though investigations have shown that sulphatide accumulation in some organs can be up to 100-fold higher than normal (von Figura *et al.*, 2001). Accumulation of sulphatide in the gall bladder has been reported to

lead to progressive functional impairment of the organ but this impairment does not contribute to the fatality of the disease (Heier *et al.*, 1983; Burgess *et al.*, 1985; Clarke *et al.*, 1989; Simanovsky *et al.*, 1998).

In normal myelin, sulphatide constitutes about 3.5 to 4% of total lipids; in MLD patients this level is grossly elevated (seven-fold) and an increase in the sulphatide-to-cerebroside ratio has also been noted (Norton and Poduslo, 1982). It has been suggested that demyelination in MLD results from the changes brought about by sulphatide accumulation in the cells involved in myelin maintenance. This was supported by the finding of subcellular changes in the cells of MLD patients long before any morphologic abnormalities are found in the myelin sheath (von Figura *et al.*, 2001). A number of hypothetical explanations about the cause of myelin breakdown have been put forward, including:

a) the loss of integrity in the myelin sheath due to defective resorption of sulphatide in the sheath's innermost layer. It has been proposed that catabolism of this layer is required for cross-sectional diameter growth of the axon, which, in the absence of functional ASA in the catalytic process, leads to structural impairment of the sheath (Austin, 1973);

b) the cytotoxic effect from lysosulphatide. Toda *et al.* (1990) reported that lysosulphatide is markedly increased in the white matter, spinal cord and sciatic nerve of MLD patients. Lysosulphatide is known to inhibit the activity of cytochrome kinase and protein kinase C in the cell metabolism cycle;

c) unstable myelin due to altered lipid composition found in the myelin sheath in MLD patients. This form of myelin has been found to be unstable at physiological temperature leading to earlier than usual break-down (Ginsberg and Gershfeld, 1991).

In addition, other possible pathogenic effects resulting from sulphatide accumulation include the failure in signal transduction and protein sorting in oligodendrocytes (Saravanan *et al.*, 2004). Furthermore, the involvement of lipid rafts in the pathogenesis of this disease cannot be ruled out as these domains are reportedly enriched in sphingolipids and cholesterol (Munro, 2003). The accumulation of cholesterol in the endosomes and lysosomes of MLD fibroblasts has been reported (Chen *et al.*, 1999) to result in altered cholesterol homeostasis in these cells (Puri *et al.*, 1999). These events are known to

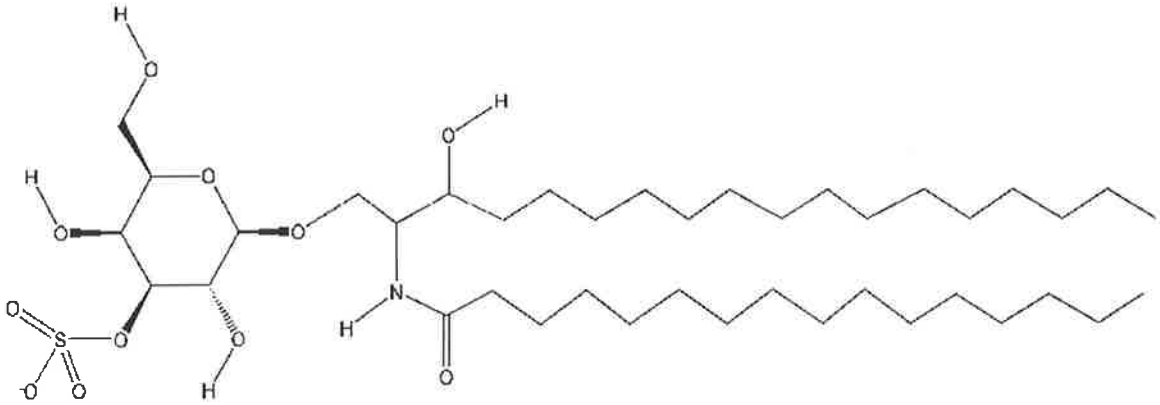

Figure 1.5 Structure of sulphatide

The molecule consists of sphingosine, fatty acids and galactose; the sulphate moiety is joined by an ester linkage to the C-3 hydroxyl of galactose.

have detrimental effects on the cell that lead to the impairment of functions such as signalling, protein sorting and cholesterol transport, hence contributing to the clinical phenotype of this disease.

1.4.3.2.3. Lipid rafts in the pathogenesis of MLD

Lipid rafts are plasma membrane microdomains that are highly enriched in sphingolipids, cholesterol and associated proteins. Simons and Ikonen (1997) described lipid rafts as simply "the dynamic clustering of the sphingolipids and cholesterol to form rafts that move within the fluid bilayer". The functional roles of these rafts in the membrane trafficking of proteins and membrane signaling have recently been reviewed by Simons and Gruenberg, (2000), who suggest that the disturbed homeostasis in these rafts in relation to their function(s) plays a major role in the pathogenesis in several disorders including the glycosphingolipidoses (GSD).

A variety of cellular processes have been proposed to occur in these microdomains, including signal transduction (Parpal *et al.*, 1995), cholesterol transport (Oram and Yokoyama, 1996; Smart *et al.*, 1996), calcium homeostasis (Isshiki and Anderson, 1999) and protein sorting (Simons and Ikonen, 1997). Each of these four processes has been implicated in LSD pathogenesis. It has been suggested that heterogeneity in LSD depends on accumulating GSL and their effect on a range of cellular pathways and processes (Raas-Rothschild *et al.*, 2004).

Recently, Saravanan *et al.* (2004) demonstrated that sulphatide in the MLD mouse model is elevated in both the lysosome and myelin membranes. An important finding from this study was the derangement in targeting of a lipid raft-associated protein known as myelin and lymphocyte protein (MAL), resulting in a reduction of this protein. MAL is known to organise and stabilise GSL in lipid rafts and is assumed to have some involvement in the regulation of myelin turnover and stability; diminished MAL may therefore contribute to the pathogenic mechanisms in MLD (Saravanan *et al.*, 2004). This is the first description of the involvement of lipid rafts in the pathogenesis of MLD.

1.4.4. Molecular pathology in MLD

The genetic heterogeneity of MLD is reflected in the high number of mutations detected in the ASA gene. Most of these mutations are caused by either point mutations or small

insertions and deletions (Gieselmann *et al.*, 1998). Two common mutations, each accounting for approximately 25% of MLD alleles, have been detected within the ASA gene: the first mutation, which alters the first base of intron 2 (459+1 G>A), affects a splice donor site; the second mutation is a C to T transition at nucleotide 1277 of the cDNA, which causes the substitution of proline at position 426 for a leucine (P426L) (Polten *et al.*, 1991). Another mutation, a substitution of isoleucine at position 179 for a serine (I179S), accounts for an additional 12% of total mutations (Berger *et al.*, 1997); the I179S mutation was only found in late-onset MLD individuals and is therefore expected to retain some residual ASA activity (Lugowska *et al.*, 2002).

The permutations arising from the first two mutations lead to the three major forms of MLD: individuals who are homozygous for the 459+1 G>A mutation will develop the late-infantile form of MLD, as no functional ASA enzyme is produced due to the effect of the splicing of a donor site; P426L homozygotes will develop the adult form of MLD; and compound heterozygotes (459+1 G>A/P426L) will present with the juvenile form of the disorder (Polten *et al.*, 1991).

Other, less frequently occurring mutations have often been associated with a particular ethnicity: for example, the T274M mutation is common in patients of Lebanese origin (Harvey *et al.*, 1993); P377L homozygotes have been found in all affected Habbanite Jews in Israel (Zlotogora *et al.*, 1995); and the 848+1G>A single splice donor site mutation is common in patients of Alaskan Eskimo and Navajo Indian origin (Pastor-Soler *et al.*, 1995). The majority of the remaining mutations reported thus far are single amino acid substitutions. The deleterious effects of these mutations are likely to result in the instability and abnormal intracellular sorting of ASA. The least frequent mutation is the small deletion which leads to either a frame-shift or frame-loss with no ASA protein detected in patient fibroblasts (von Figura *et al.*, 2001).

1.4.5. Incidence of MLD

MLD is thought to occur pan-ethnically, with a high incidence observed in populations that are segregated and involved in intra-tribal or consanguineous marriages (Zlotogora *et al.*, 1980; Heinisch *et al.*, 1995; Ozkara and Topcu, 2004). The reported incidence varies greatly between countries, as cited in the literature: a figure of 1:40 000 has been quoted by Gustavson and Hagberg (1971), Gieselmann *et al.* (1989), Hess *et al.* (1996), Berger *et al.* (1997) and Eng *et al.* (2003) but this number is believed to be attributed to the earlier report

made by Gustavson and Hagberg (1971) from their survey in a restricted locality of Northern Sweden; in Australia, an occurrence of 1:92 000 live births has been reported (Meikle *et al.*, 1999); Portugal has a reported incidence of 1:55 000 (Pinto *et al.*, 2004); The Netherlands (Poorthuis *et al.*, 1999) and Turkey (Ozkara and Topcu, 2004) have the same incidence of approximately 1:70 000; Germany has a much lower incidence of about 1:170 000 live births (Heim *et al.*, 1997).

1.4.6. Pseudo-deficiency in MLD

Enzyme pseudo-deficiencies are known to occur in many LSD, including MLD. The first case of ASA pseudo-deficiency (ASA-PD) was reported by Dubois and co-workers in 1975, when they discovered the absence of ASA activity in a healthy father of a MLD patient (Dubois *et al.*, 1975). The absence of activity mentioned in that report could be due to the low sensitivity of the analytical method employed, as it is now widely accepted that the range of ASA activity in ASA-PD individuals is between 5-15% of normal. In general, ASA-PD individuals are clinically normal, as the residual ASA activity *in-vivo* is assumed to be sufficient to degrade sulphatide.

Even though ASA-PD has been perceived to have no clinical consequence, it has been acknowledged that the high occurrence of these individuals - estimated to be 1-2% in Europeans - causes diagnostic problems. Baldinger *et al.* (1987) proposed that ASA-PD individuals can be either ASA-PD/ASA-PD homozygotes or ASA-PD/MLD compound heterozygotes. The problem encountered in diagnosis is the inability to differentiate these individuals from adult-onset MLD patients based on the measurement of enzyme activity alone (Kihara *et al.*, 1980).

Difficulties can also arise in genetic counselling of ASA-PD/MLD compound heterozygotes who have a MLD carrier partner, as their offspring can be either unaffected or affected. Speculation has arisen about the potential clinical implications for ASA-PD/MLD compound heterozygotes (Hohenschultz *et al.* 1988). However, this remains a subject for on-going research, as a study by Penzien *et al.* (1993) on 16 individuals with this genotype did not show progressive neurological symptoms that resemble those of MLD, thus ruling out the possible clinical implications suggested by Hohenschultz *et al.* (1988).

1.4.6.1. ASA pseudo-deficiency at the molecular level

Langenbeck *et al.* (1977) were the first to propose that the gene encoding ASA-PD was allelic to the ASA gene. This proposal was supported by the finding of Chang and Davidson (1983), who used somatic cell hybrids from MLD and ASA-PD patient fibroblasts to demonstrate that, even in diploid and tetraploid clones, these cells failed to restore ASA activity. Gieselmann *et al.* (1989) found that the mutations in ASA-PD were associated with two A to G transitions: the first resulted in the amino acid substitution of asparagine at position 350 with serine (N350S) in exon 6 that led to the loss of a N-glycosylation site; and the second resulted in the loss of a polyadenylation signal in exon 8 at the 3' end of the ASA gene. The loss of the oligosaccharide side chain explains the reduced Mw (Fluharty *et al.*, 1983; Kihara *et al.*, 1986) and different isoelectric point (pI) (Chang *et al.*, 1984).

The reduced ASA activity seen in ASA-PD individuals has been attributed to the second A to G change that alters the sequence of the major 2.1 kb polyadenylation signal from A**A**TAAC to A**G**TAAC. Northern blot analysis showed that this 2.1 kb mRNA species was translated to produce about 90% of the total ASA mRNA in unaffected individuals and that this transcript was absent in ASA-PD homozygotes. In addition, the amount of enzyme activity expressed in baby hamster kidney cells or SF transfected with the cDNA of a N350S mutant was comparable to normal. With these findings, it has been suggested that the low ASA activity observed in ASA-PD individuals is due to reduced synthesis of ASA rather than an effect of the N350S mutation (Gieselmann *et al.*, 1989).

The results of earlier studies that examined the kinetics and biochemical characteristics of the ASA-PD and Wt ASA enzymes showed no significant difference between the two except the pI value (Chang *et al.*, 1984; Herz and Bach, 1984). However, the ASA-PD enzyme was found to have a higher affinity for the p-NCS substrate and was more susceptible to heat-inactivation compared to the Wt ASA enzyme (Qu *et al.*, 1997/98).

The assumption that the N350S mutation has no effect on enzyme activity in the mutant enzyme has also been proven incorrect by a number of researchers. Shen *et al.* (1993) reported that N350S/MLD compound heterozygotes without the polyadenylation defect have lower ASA activity compared to obligate MLD carriers: they estimated that the N350S mutation results in ASA activity that is 12 to 21% of normal and suggested that the reduced activity is due to the instability of the mutant protein that shortens the half-life of

the enzyme. In a separate study, Harvey *et al.* (1998) found that the combined effect of the N350S mutation and the loss of the polyadenylation signal reduced ASA activity to approximately 8% of normal, as opposed to the estimated value of 10% due to the loss of the polyadenylation signal alone, as reported by Gieselmann *et al.* (1989). Harvey *et al.* (1998) attributed the further reduction in activity to the aberrant targeting of the mutant enzyme to the lysosome.

It has now been established that both the N350S and the polyadenylation defect can exist independently: while most ASA-PD individuals are known to have both the N350S and the polyadenylation defect mutations, individuals with either one or the other mutation have also been reported (Nelson *et al.*, 1991; Barth *et al.*, 1994; Ricketts *et al.*, 1996).

1.4.6.2. Incidence of ASA-pseudodeficiency

ASA-PD is transmitted as a simple Mendelian trait in affected families (Langenbeck *et al.*, 1977). It has been estimated that 1-2% of the European population is homozygous for ASA-PD based on the reported ASA-PD carrier frequencies of 7.3% to 26% (von Figura *et al.*, 2001).

1.4.7. Genotype-to-phenotype correlation

Due to the heterogenic nature of MLD, direct genotype-to-phenotype correlation does not always hold, with the exceptions of those clinical phenotypes resulting from the 459+1 G>A and P426L mutations, as mentioned in section 1.4.4. Poor correlation between genotype and presenting phenotype was often observed in compound heterozygotes who had a non-functional allele together with a mutant allele that produced some residual enzyme activity, and cases of siblings with the same genotype but marked differences in the age of clinical onset and severity have also been reported (Clarke *et al.*, 1989; Arbour *et al.*, 2000).

The finding of a late-infantile patient with the P426L mutation was more puzzling and further complicated direct genotype-to-phenotype correlation (Barth *et al.*, 1993). Moreover, the majority of mutations identified thus far are due to single amino acid changes unique to each family. To date, a number of these single amino acid mutations have been studied through site-directed mutagenesis, expression studies or biosynthesis studies. This is discussed in section 1.4.7.1, below.

1.4.7.1. Enzyme activity and phenotype correlation

A correlation between residual enzyme activity, measured as catalytic capacity, and disease severity has been demonstrated for some LSD (Ashton *et al.*, 1992; Bunge *et al.*, 1998): a high amount of residual enzyme activity suggests attenuated disease progression; conversely, the absence of enzyme would suggest severe onset. It has been predicted that a threshold exists between disease and normal, and that 'normal' is just a fraction of the normal activity of the enzyme (Neufeld, 1991).

With the exception of three permutations arising from the 459+1 G>A and P426L mutations, which show good correlation between enzyme activity and clinical phenotype, the same does not apply to other combinations of mutations in MLD. It has been acknowledged that correlations between genotype and enzyme activity do not enable the accurate prediction of clinical severity for most LSD (Wegrzyn *et al.*, 2004). In MLD, most mutations have been found to cause altered intracellular sorting that leads to the retention of the mutant enzymes in the ER. Mutations reported to have this effect include: G154D and P167R (Kappler *et al.*, 1994); T274M and D335V (Hess *et al.*, 1996); P426L, which is known to produce unstable enzyme despite correct targeting to the lysosome (von Figura *et al.*, 1983); and G309S (Kreysing *et al.*, 1993), which is also known to produce unstable enzyme with degradation occurring in the post-Golgi compartment.

In cases where the defect is due to altered trafficking or lysosomal instability, it is anticipated that a reasonable amount of enzyme activity can be detected *in-vitro* but the actual catalytic capacity *in-vivo* is altered. In these cases, as well as those where residual enzyme activity is very low, there is a need to perform additional assays, such as sulphatide-loading in SF, to determine the *'in-situ'* activity of the enzyme. The use of the sulphatide-loading assay and other auxiliary assays to distinguish between normal, ASA-PD and MLD individuals will be discussed in section 1.4.8.1.1.

1.4.8. Laboratory diagnosis of MLD

Biochemical diagnosis of MLD is usually achieved through the measurement of ASA activity in peripheral blood leucocytes and/or cultured SF. Prior to the introduction of enzymatic assays, laboratory diagnosis was mostly confined to histological methods for the detection of metachromatic staining material on either autopsy or biopsy tissues. Due to the complexity in the interpretation of results, a definitive diagnosis was usually only obtained after extensive testing with an array of supplementary laboratory assays. The analytical

methods employed to resolve these ambiguities include enzymatic assay, sulphatide-loading tests, electrophoresis and polymerase chain reaction (PCR).

1.4.8.1. Enzymatic assays

The first enzymatic assay for the determination of ASA activity was developed in 1959 using p-NCS as substrate (Baum *et al.*, 1959). p-NCS and 4-MUS are two artificial substrates that are widely used in enzymatic assays, as mentioned in section 1.2.2.1; the structural formula of these substrates is shown in Figure 1.6. These substrates can be cleaved by other sulphatases, leading some laboratories to use the natural substrate, sulphatide (radio-labelled), in the presence of detergent to obtain a more selective measurement of ASA activity.

The radio-labelled natural substrate is more cumbersome and expensive to use than the artificial substrates. Consequently, methods modified from the original protocol of Baum *et al.* (1959) are now used for the determination of ASA activity in various biological samples. In 1976, Kolodny and Mumford reported the successful utilisation of 4-MUS in the determination of ASA and ASB activity in MLD and MPS VI, respectively. This was achieved with prior physical separation of the arylsulphatases using ion exchange chromatography. To increase specificity, the assay conditions were performed using the differential thermal stabilities and heavy metal inhibition properties of these enzymes.

The assay used by Kolodny and Mumford (1976) was reported to be more sensitive and have a higher selectivity when compared to the p-NCS substrate used by Baum. Another modification of Baum's method that is widely used in laboratories derives from Lee-Vaupel and Conzelmann (1987), who used p-NCS as the substrate with the catalytic action of ASA measured at 0°C; at this temperature ASB was found to be almost inactive while ASA retained 24% of its activity measured at 37°C. Technically, this method sacrifices three-quarters of its sensitivity to achieve a respectable specificity.

The loss of assay sensitivity inherent in these modifications and the low amount of enzyme activity present in ASA-PD individuals makes enzyme analysis alone inadequate for differentiating MLD from ASA-PD individuals, and has prompted the need for additional methods to distinguish the two groups.

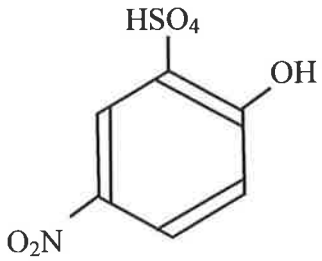

p-nitrocatechol sulphate

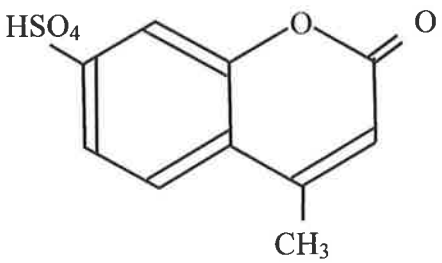

4-methylumbelliferyl sulphate

Figure 1.6 **Structures of artificial substrates used for the determination of ASA activity**

Figure reproduced from von Figura *et al.*, 2001

1.4.8.1.1. Auxiliary methods used in the diagnosis of MLD

MLD, ASA-PD and ASA-PD/MLD individuals can now be distinguished using a number of methods, the most reliable of which is the sulphatide-loading test (Fluharty *et al.*, 1978). However, this assay is laborious, primarily because the radioactive substrates are not available commercially and must be prepared in the laboratory. In addition, SF or amniotic cells are required for this assay, which is technically demanding (Gieselmann, 1991). Other methods utilise electrophoretic techniques, using either cellogel or isoelectric focusing to separate the enzymes based on their physical properties: Chang *et al.* (1984) reported that residual ASA activity can be detected in ASA-PD individuals, while MLD patients have no detectable enzyme activity in fibroblast extracts. However, these methods are also laborious, offer low sensitivity and are regarded as semi-quantitative analyses.

A simple method by Gieselmann (1991) employing 3'-mis-match PCR is also used in a number of laboratories to screen for the two A to G transitions simultaneously. However, a weakness of this method is its inability to identify a MLD mutation on the ASA-PD allele (Gieselmann *et al.*, 1991) and the ASA-PD variant with only the N350S mutation (Shen *et al.*, 1993).

A further auxiliary parameter that is considered useful in differentiating MLD from ASA-PD is the detection of urinary sulphatide. This is based on the fact that normal and ASA-PD individuals excrete very little sulphatide in their urine while a large amount of sulphatide can be detected in the urine of MLD patients (Kolodny and Fluharty, 1995). A number of methods have been successfully employed to detect sulphatide in urine, including thin layer chromatography (TLC) (Molzer *et al.*, 1992; Lugowska *et al.*, 1997), high performance liquid chromatography (HPLC) (Strasberg *et al.*, 1985; Natowicz *et al.*, 1996) and, more recently, electrospray ionisation-tandem mass spectrometry (ESI-MS/MS) (Whitfield *et al.*, 2001a).

Lugowska *et al.* (1997) reported increased excretion of urinary sulphatide in ASA-PD/MLD compound heterozygotes using TLC separation followed by densitometry measurement. Another interesting finding was made by Whitfield *et al.* (2001a) who reported higher than expected urinary sulphatide excretion in ASA-PD individuals when the calculation of total sulphatide was adjusted to urinary phosphatidylcholine instead of creatinine, which is normally used; sulphatide quantification was achieved using ESI-

MS/MS. These two findings point to possible clinical complications later in life for these individuals, as speculated by some researchers (see section 1.4.6).

1.4.8.2. Immune-based assays

Immune-based approaches to differentiate the allelic variants of ASA present in individuals with suspected MLD have been used: in 1971, Stumpf *et al.* reported an immuno-precipitation method to determine the presence of residual ASA in the urine of MLD patients using a mono-specific antibody produced against human liver ASA; Neuwelt *et al.* (1971) also reported the successful identification of residual ASA in MLD patients; Shapira and Nadler (1975) used the Ouchterlony precipitation method to prove that the residual activity detected with Baum's method in three liver homogenates from MLD patients derived from ASB, and concluded that the enzyme activity assay was not suitable for use in studies of the nature of residual ASA and ASB.

A quantitative immune-based assay using a radioimmunoassay (RIA) technique was developed by Laidler *et al.* (1985a) to measure ASA in sera and urine from patients with colon cancer; the method was later reported to be suitable for use as a diagnostic tool for lung and CNS cancer, in which ASA is elevated compared to controls (Laidler, 1991). However, no quantitative immune-based assay for the determination of ASA in MLD has been described. The intrinsic ability of the antibody, such as specificity and strong binding capacity, can be exploited to provide the specificity and sensitivity required for a reliable assay. The major challenges faced in the development of immune-based assays are the availability of proteins (antigen) required to produce antibody and the production of specific antibodies with appropriate affinities.

1.4.8.3. Problems in laboratory diagnosis

MLD or ASA-PD? This question arose from complications caused by the presence of ASA-PD individuals who are known to have low ASA activity. Differentiating these individuals from MLD patients by determination of ASA activity alone is not possible and is further compounded by the presence of the 'MLD variant', which is caused by a deficiency of saposin B. Thus, low ASA activity does not necessarily mean MLD, and normal ASA activity does not unequivocally exclude MLD (von Figura *et al.*, 2001).

From the methods described in sections 1.4.8.1 and 1.4.8.1.1, there is no single assay that can be used independently with high reliability to diagnose MLD. This led Penzien *et al.*

(1993) to make this concluding remark about the best approach to the diagnosis of MLD: "A proper diagnosis can only be achieved by combined determination of enzyme activities and sulphatide excretion, cerebroside sulphate-loading assays and molecular genetic techniques".

A diagnostic protocol proposed by Li *et al.* (1992) is shown in Figure 1.7, which demonstrates the difficult and laborious nature of testing for ASA-PD, ASA-PD/MLD and MLD status. The number of assays involved and the degree of difficulty in establishing those assays is not achievable by many laboratories; not surprisingly, delays in diagnosis and mis-diagnosis are still common, even in developed countries.

1.4.9. Therapy for MLD

Several strategies have been evaluated in the development of therapy for MLD, the earliest being the restricted dietary intake of sulphur (Moser *et al.*, 1967) and vitamin A (Warner, 1975). These regimens were carried out with the aim of slowing down the synthesis and accumulation of sulphatide in the lysosome, as sulphur and vitamin A are required for sulphatide synthesis; however, the outcome was disappointing. Therapeutic strategies based on *in-vitro* findings such as the use of chemicals to stabilise the mutant enzyme, as proposed by von Figura *et al.* (1983), and enzyme replacement therapy (ERT) by direct infusion have also been unsuccessful (Kolodny and Fluharty, 1995). However, recent ERT experiments in MLD knock-out mice have shown promising results: after single intravenous administration, ASA was detected in several organs, including the brain albeit at very low levels; the half-life of the enzyme was estimated to be four-days. More importantly, prolonged high-dose treatment (20 mg/kg once weekly for four-weeks) showed a reduction of sulphatide in several organs including the brain and spinal cord (Matzner *et al.*, 2005). However, further assessments are required to substantiate these results, as intravenously administered enzymes are thought to be ineffective due to their inability to permeate the blood-brain barrier (BBB).

To date, the only effective therapy for MLD has been bone marrow transplantation (BMT). Bayever *et al.* (1985) reported the first positive outcome from allogeneic BMT. Since that report, BMT has been carried out in a number of MLD patients by various groups, with results showing a slowing down of disease progression; stabilisation of symptoms was also noted after full engraftment (Kidd *et al.*, 1998). The best outcomes have been reported in the adult and juvenile forms of MLD following successful engraftment, while the outcome

in the majority of the late-infantile types has been disappointing (Krivit, 2004). The reason for this is that both the juvenile and adult forms of MLD retain residual enzyme activity, hence only a small amount of enzyme is required from BMT to alter the course of the disease (Polten *et al.*, 1991). Results from these treatments showed that the highest efficacy was obtained when BMT was carried out before the onset of clinical symptoms. It has been acknowledged that the pathophysiological state of the CNS is not reversible once symptoms are apparent (Navarro *et al.*, 1996; Kapaun *et al.*, 1999; Krivit *et al.*, 1999).

On the same note, Bayever *et al.* (1985) suggested that BMT should be carried out soon after birth. One way of achieving this is to unambiguously diagnose and treat the presymptomatic sibling of an affected child (Krivit *et al.*, 1990). However, in the absence of an affected sibling, clinical diagnosis before the appearance of symptoms is not currently possible. The only practical way to diagnose an asymptomatic child is by newborn screening (NBS). This might become a reality in the near future, as a group of researchers led by Professor Hopwood in Australia has started the process of establishing NBS for LSD (Krivit, 2004).

In conclusion, two factors are crucial in ensuring a better prognosis for MLD patients: 1) early detection; and 2) successful BMT with full engraftment. However, with presymptomatic detection, the decision about the most appropriate form of treatment and when to initiate it will depend on the accurate prediction of clinical severity in an asymptomatic individual. The accurate prediction of severity in MLD is not possible through genotype/phenotype or enzyme activity/phenotype correlations, as discussed in sections 1.4.7 and 1.4.7.1. In view of this, the development of a method to predict clinical phenotype has been identified as one aim of this present study.

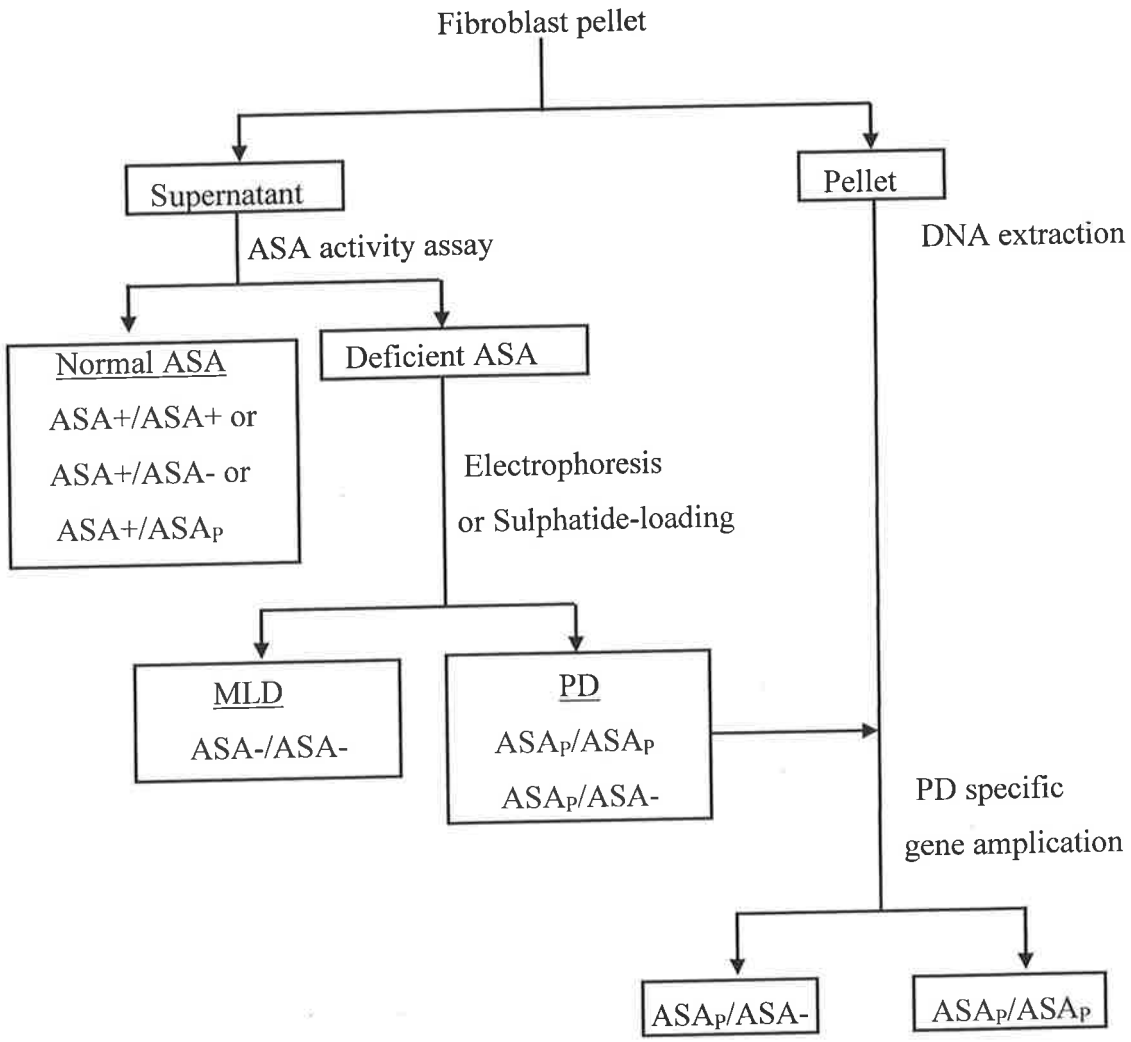

Figure 1.7 Diagnostic protocols for differentiating ASA-PD, ASA-PD/MLD and MLD

The diagnostic protocol proposed by Li *et al.* (1992). The analytical work involves the extraction of DNA and supernatant from SF. The supernatant is used to assay ASA activity; further analysis by electrophoresis or sulphatide-loading is used to distinguish MLD from ASA-PD individuals. ASA-PD individuals can be genotyped using the ASA-PD-specific gene amplification method to distinguish ASA-PD/ASA-PD homozygotes from ASA-PD/MLD compound heterozygotes.

1.4.10. Newborn screening

Currently, NBS is available for a number of inherited disorders in most developed countries, including Australia. NBS is used to reduce the morbidity and mortality associated with these disorders (Farrell *et al.*, 1994) and as a preventative medicine (Wilcken, 2003). The disorders for which screening is available in Australia include primary congenital hypothyroidism, cystic fibrosis, phenylketonuria and galactosaemia. In addition, some screening centres in Australia also screen for biotinidase deficiency, congenital adrenal hyperplasia and the haemoglobinopathies; recently, the NBS programme has been expanded to include more than 30 disorders of amino acid, organic acid and fatty acid metabolism (Human Genetics Society of Australasia–Royal Australasian College of Physicians, NBS Policy, 2004).

1.4.10.1. Newborn screening for LSD

In general, for a disorder to be incorporated into a NBS programme, the following criteria must be met: (i) there should be a benefit to the infant from early diagnosis; (ii) there must be suitable and cost-effective tests; and (iii) treatment and follow-up services must be available. The high incidence of LSD as a group, together with their devastating effects on patients and families, and the impact on the health system in general, make LSD a probable candidate for inclusion into NBS programmes. NBS would enable presymptomatic detection and, where available, treatment before the onset of otherwise irreversible symptoms, particularly for those LSD with CNS involvement, such as MLD (see section 1.4.9). However, screening for LSD remains a contentious issue, partly because of the current lack of effective treatments for every disorder. Nevertheless, early detection would provide families with appropriate genetic counselling and reproductive options in subsequent pregnancies (Meikle *et al.*, 1997).

To successfully incorporate LSD into a NBS programme, a single procedure is required for the detection of all, or at least the majority of LSD. One way to achieve this is to use diagnostic markers that are altered in multiple LSD, such as LAMP-1 (Meikle *et al.,* 1997), LAMP-2 (Hua *et al.*, 1998) and saposins (Chang *et al.*, 2000). Alternatively, ESI-MS/MS or multiplexing technology can be employed for the measurement of multiple analytes or substrates and the quantification of specific protein markers, respectively (Meikle *et al.*, 2004b). These technologies have the potential to provide rapid, reproducible and cost-effective screening procedures.

1.4.11. Monitoring of therapy in MLD

Post-BMT monitoring is a complex process, requiring long-term clinical and laboratory investigations. Weitzner *et al.* (1999) have shown that continuous monitoring increases the patient's emotional distress at all stages of the process. The period of laboratory monitoring can take many years, as the engraftment progress is slow with only incremental changes expected over a long period of time; clinical evaluations can take up to 20-years before conclusions can be drawn about the treatment's effectiveness (von Figura *et al.*, 2001).

In the case of MLD, the main laboratory parameters that are deemed crucial and indicative of successful engraftment are: (i) leucocyte enzyme activity; (ii) urinary sulphatide; and (iii) karyotyping of the marrow cells and CSF leucocytes to determine the origin of the cells (Bayever *et al.*, 1985). Methods are currently available by which to monitor these changes, however there is a need for more sensitive methods that provide more definitive measurement and allow accurate monitoring of therapy in presymptomatic individuals.

1.5. DELFIA technology for immune-based assays

Dissociation-enhanced lanthanide fluorescence immunoassay (DELFIA) is a technology based on time-resolved fluorometry. DELFIA has been reported to be more sensitive and specific in a number of applications when compared to RIA (Menjivar *et al.*, 1993) and enzyme-linked immunosorbent assay (ELISA) (Smith *et al.*, 2001). It has also been reported to be suitable for use in high-throughput screening in the diagnostic industry (Wilson and Howell, 2002).

The higher sensitivity, precision and ability to detect over a wide dynamic range was achieved by using lanthanide metal such as europium (Eu^{3+}) as the fluorescent label (Ryall *et al.*, 1993); measurement of Eu^{3+} concentration as low as 10^{-14} M has been reported (Hemmila *et al.* 1984). A further advantage of using Eu^{3+}as the fluorescence label is its long-lived fluorescence emission after excitation; this characteristic has been utilised to reduce the background reading of other contributing fluorescence from sera, solvents, cuvettes and reagents, which have a shorter half-life, by delaying the measurement of the fluorescence emission (Diamandis *et al.*, 1988).

In the commercial kit manufactured by Wallac, Eu^{3+} is chelated to a polycarboxylic acid, N^1-(p-isothiocyanatobenzyl)-diethylenetriamine-N^1, N^2, N^3, N^4-tetraacetic acid. This

Eu^{3+}chelate is bound to the target substance (i.e. antibody, antigen, hapten) and used in immune-based assays as the detecting reagent. The Eu^{3+} dissociates from the chelate after lowering of the pH and is subsequently chelated with the 2-napthoyltrifluoroacetone and tri-N-octylphosphine oxide present in the enhancement solution to emit highly intense fluorescence (Diamandis *et al.*, 1988).

Its high sensitivity, wide dynamic range, non-isotopic nature and the availability of commercial kits has made DELFIA technology the preferred method for many clinical biochemistry measurements.

1.6. Electrospray-tandem mass spectrometry for the quantification of lipids

MS is a powerful and highly sensitive analytical technique that can be used for structural characterisation of unknown biomolecules and for the quantification of known materials. The analysis of organic compounds by MS involves the following events: (i) ionisation of the compound in the ion source; (ii) separation of the ions based on their mass-to-charge (*m/z*) ratio in the mass analyser; and (iii) determination of the abundance of the separated ions by the detector (Niwa, 1995).

Electrospray ionisation (ESI) was developed by Dole and co-workers almost 40-years ago (Dole *et al.*, 1968). Unlike other soft ionisation methods, ESI can produce multiple charged molecular ions if the analyte has multiple sites in which protonation or deprotonation can occur. This property has allowed ESI/MS to be used in the analysis of protein molecules in the range of 10^5 Da with a measurement error of 0.01% (Meng *et al.*, 1988).

Early work in the study of lipids and their sub-classes was achieved with the use of HPLC (Cooper and Anders, 1975). The use of MS technology in the analysis of endogenous lipids such as sphingolipids (Kerwin *et al.*, 1994) and ceramides (Gu *et al.*, 1997; Liebisch *et al.*, 1999) started in the mid-1990s and it has since gained prominence in the field of lipidomics.

The use of ESI/MS was reported to enable rapid and comprehensive quantitation of all lipid sub-classes and individual molecular species without prior chromatographic separation or derivatisation when the samples were appropriately prepared (Han and Gross, 2003); this method was also found to have a better signal-to-noise ratio, a wider dynamic range with an experimental error of less than 5%, and excellent reproducibility of sample measurement.

Figure 1.8 illustrates a general approach to the analysis of lipids from different biological sources without prior chromatographic separation. According to Han and Gross (2003), ESI//MS is preferred over ESI-MS/MS because the latter may yield different fragment ion patterns in individual molecular species with various acyl components under different collision energies.

However, the use of ESI-MS/MS techniques to quantify lipid species in various biological samples has also been reported, including the quantification of ceramide species (Liebisch *et al.*, 1999; Han, 2002), glucosylceramide and lactosylceramide (Whitfield *et al.*, 2002), sulphatides and phosphatidylcholine (Whitfield *et al.*, 2001a), and galactosylsphingosine or psychosine (Whitfield *et al.*, 2001b). More recently, the simultaneous analysis of 29 individual lipid species, including ceramide, glucosylceramide, lactosylceramide and ceramide trihexoside, was reported using the same technology (Fuller *et al.*, 2005a). With the exception of the quantitation of ceramide species by Liebisch *et al.* (1999) and Han (2002), quantitation of the lipid species mentioned above was achieved using the multiple reaction monitoring (MRM) mode.

MRM enables the simultaneous identification of multiple analytes in a single analysis. This mode is highly specific, in which the first (Q1) and third (Q3) quadrupoles of the instrument are set to identify specific *m/z* values of an analyte. The specific *m/z* values of the analyte can be obtained from Q1 and product ion scanning using MS/MS.

The application of this technology to lipidomics has opened up another frontier in science after genomics and proteomics. This exciting development will improve our understanding of the effects of lipid alteration and their potential role in disease pathogenesis, diagnostics and therapeutics (Han and Gross, 2005).

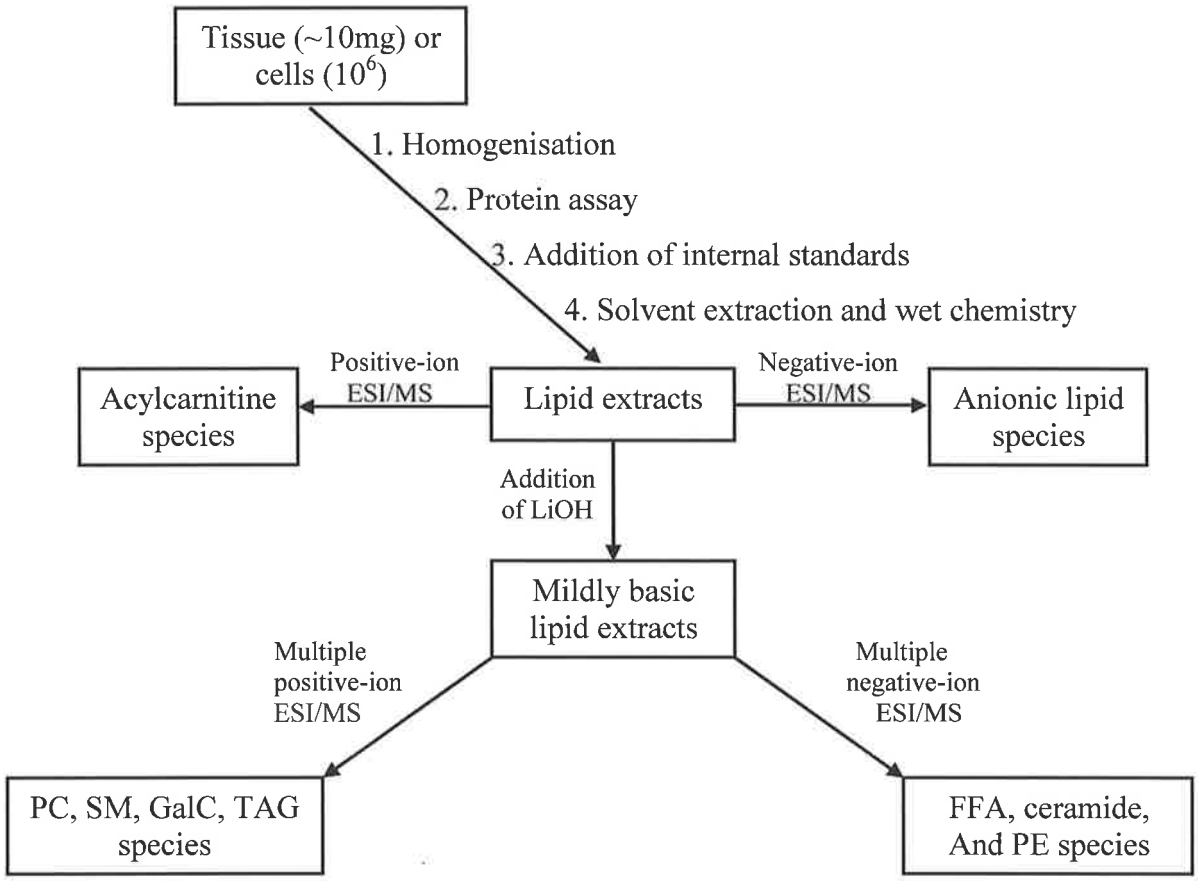

Figure 1.8 **Schematic diagram of the experimental approach of Han and Gross for the analysis of cellular lipids using crude extracts of biological samples**

Figure reproduced from Han and Gross, 2003.

Abbreviations:

PC = choline glycerophospholipids;

SM = sphingomyelin(s);

GalC = galactosylcerebroside(s);

TAG = triacylglycerol(s);

FFA = free fatty acids;

PE = ethanolamine glycerophospholipids.

1.7. Aims and objectives

The two major goals of this study were to develop laboratory-based methods that would enable (1) improved diagnosis of MLD; and (2) accurate prognosis in asymptomatic individuals. The difficulties associated with the diagnosis of MLD have been discussed in section 1.4.8.3. To overcome these difficulties, the development of immune-based assays using DELFIA technology was proposed: the immune-based assay system was preferred since the intrinsic specificity and strong binding capacity of antibodies would provide the necessary assay specificity, and the use of DELFIA technology would enhance assay sensitivity; furthermore, combining these technologies would result in assays that are rapid, amenable to high throughput, easy to use and cost-effective.

Three immune-based assays will be developed in this study: (i) an immune-capture ASA activity assay that measures activity from the catalytic action of antibody-captured ASA towards the synthetic 4-MUS substrate; (ii) an immune-quantification ASA protein assay that uses a sandwich immune assay to combine antibody-captured ASA protein with a secondary antibody labelled with Eu^{3+}; and (iii) an immune-quantification assay for the mutant N350S ASA protein that uses a sandwich immune assay to combine antibody-captured N350S ASA protein with a secondary antibody labelled with Eu^{3+}.

In common with most LSD, the prognosis for MLD patients is poor because diagnosis is usually made after the onset of clinical symptoms. However, if treatment can be initiated before symptoms are apparent, improved clinical outcome is expected. In the near future, presymptomatic detection of MLD may be possible through a NBS programme. In this scenario, the clinician will rely on the laboratory to provide accurate information about a patient's expected clinical phenotype before making a decision about the most appropriate form of therapy and when it should commence.

Thus, the second major aim of this study was to develop methods that can be used to predict the clinical phenotype of MLD patients in asymptomatic individuals. To achieve this, biochemical profiling utilising a combination of approaches, including the determination of residual enzyme protein/activity using the immune-based assays and metabolite profiling using ESI-MS/MS, has been proposed. A cohort of urine and SF samples representing the clinical spectrum of MLD plus unaffected controls will be used in the study.

The specific aims of this project are to:

1. develop an immune-capture activity assay for ASA;
2. develop an immune-quantification assay for ASA protein;
3. develop an immune assay for the detection of ASA-PD individuals;
4. improve an existing sulphatide quantification assay using ESI-MS/MS;
5. validate these methods to enable the prediction of clinical severity of MLD; and
6. evaluate the suitability of these methods towards the diagnosis of MLD

1.8. Further organisation of this thesis

This thesis is organised into six additional chapters:

Chapter 2:	Materials and methods;
Chapter 3:	Expression, purification and characterisation of Wt ASA and N350S ASA enzymes;
Chapter 4:	Production and purification of antibodies, and development and validation of immune-based assays;
Chapter 5:	Establishment of a sulphatide quantification method using ESI/MS-MS and development of a sulphatide-loading protocol;
Chapter 6:	Prediction of clinical severity in MLD;
Chapter 7:	Concluding remarks.

CHAPTER TWO

Materials and Methods

2.1. Materials

2.1.1. Solvents and chemicals

All solvents and chemicals used in this study were of analytical grade unless otherwise specified.

Acetic acid	Ajax Chemical Ltd., Auburn, NSW, Australia
Ammonium persulphate	Bio-Rad Laboratories, Richmond, VA, USA
2, 2'-Azino-bis (3-ethylbenzo-thiazoline-6-sulphonic acid) diammonium salt (ABTS)	Sigma Chemical Co., St. Louis, MO, USA
Boric acid	BDH Chemicals Pty. Ltd., Kilsyth, Vic, Australia
β-Mercaptoethanol	Sigma Chemical Co., St. Louis, MO, USA
Calcium chloride tissue culture grade	Sigma Chemical Co., St. Louis, MO, USA
Chloroform (HPLC grade)	BDH Chemicals Pty. Ltd., Kilsyth, Vic, Australia
Chloroform with 1% (v/v) ethanol (HPLC grade)	BDH AnalaR®, Merck Pty. Ltd., Kilsyth, Vic, Australia
4-Chloro-1-naphthol	Sigma Chemical Co., St. Louis, MO, USA
3-[Cyclohexylamino]-1-propanesulphonic acid (CAPS)	Sigma Chemical Co., St. Louis, MO, USA
Dimethyl sulphoxide (DMSO)	Sigma Chemical Co., St. Louis, MO, USA
Ethanol	BDH Chemicals Pty. Ltd., Kilsyth, Vic, Australia
Ethidium bromide	Boehringer Mannheim, Sandhofer Strasse, Mannheim, Germany
Formaldehyde	Sigma Chemical Co., St. Louis, MO, USA
Formic acid	Ajax Chemical Ltd., Auburn, NSW, Australia
Glutaraldehyde	Sigma Chemical Co., St. Louis, MO, USA
Glycine	BDH Chemicals Pty. Ltd., Kilsyth, Vic, Australia
Glycerol	Biolab Scientific., Clayton, Vic, Australia
Hydrogen peroxide 30%	Univar, Asia Pacific Specialty Chemical Ltd., Seven Hills, NSW, Australia

Hydrochloric acid	BDH Chemicals Pty. Ltd., Kilsyth, Vic, Australia
1-[2-Hydroxyethyl]-1-piperazinethansulphonasaure (HEPES)	Roche Diagnostics Corp., Indianapolis, IN, USA
Isopropanol	Ajax Chemicals Ltd., Auburn, NSW, Australia
Methanol (HPLC grade)	Unichrom, Ajax Finechem, Auburn, NSW, Australia
Mineral oil	Sigma Chemical Co., St. Louis, MO, USA
Nonidet P-40	Sigma Chemical Co., St. Louis, MO, USA
Orthophosphoric acid	M & B Australia, West Footscray, Vic, Australia
Phenol	Sigma Chemical Co., St. Louis, MO, USA
Potassium chloride	Ajax Chemicals Ltd., Auburn, NSW, Australia
Sodium acetate	BDH Chemicals Pty. Ltd., Kilsyth, Vic, Australia
Sodium azide	Sigma Chemical Co., St. Louis, MO, USA
Sodium chloride	Ajax Chemicals Ltd., Auburn, NSW, Australia
Sodium carbonate anhydrous	Ajax Chemicals Ltd., Auburn, NSW, Australia
Sodium di-hydrogen orthophosphate monohydrate	BDH Chemicals Pty. Ltd., Kilsyth, Vic, Australia
Sodium citrate	Ajax Chemicals Ltd., Auburn, NSW, Australia
Sodium dodecylsulphate (SDS)	Sigma Chemical Co., St. Louis, MO, USA
Sodium hydrogen carbonate	Ajax Chemicals Ltd., Auburn, NSW, Australia
Sodium hydroxide	Ajax Chemicals Ltd., Auburn, NSW, Australia
Silver nitrate	Calbiochem-Novabiochem Corp., La Jolla, CA, USA
Sodium thiosulphate	Ajax Chemicals Ltd., Auburn, NSW, Australia
Tris [hydroxymethylaminomethane] (Tris)	Roche Diagnostics Corp., Indianapolis, IN, USA
Tween 20	BDH Chemicals Pty. Ltd., Kilsyth, Vic, Australia
N, N, N^1, N^1-Tetramethylethylenediamine (TEMED)	Bio-Rad Laboratories, Richmond, VA, USA
Thiourea	Sigma Chemical Co., St. Louis, MO, USA
Urea	Sigma Chemical Co., St. Louis, MO, USA

2.1.2. Antibodies

Donkey anti-sheep HRP conjugated antibody	Chemicon Pty. Ltd., Boronia, Vic, Australia
Sheep anti-mouse HRP conjugated antibody	Chemicon Pty. Ltd., Boronia, Vic, Australia
Anti-ASA polyclonal antibody	Generated in this study
Anti-N350S peptide conjugate polyclonal antibody	Generated in this study

2.1.3. Cells and Vectors

CHO-K1 cells	CSL Ltd., Melbourne, Vic, Australia
N350S ASA CHO-K1 cell line	Dept. of Genetic Medicine, Women's and Children's Hospital, Adelaide, SA, Australia
All SF cell lines used in this study	Dept. of Genetic Medicine, Women's and Children's Hospital, Adelaide, SA, Australia
E. coli Top 10 strain	Invitrogen New Zealand Ltd., Penrose, Auckland, New Zealand
P3-653 murine myeloma cells (NS-1 variant)	American Type Culture Collection (ATCC), Manassas, VA, USA
ASA cDNA in pRSVN.07 vector	Dept. of Genetic Medicine, Women's and Children's, Adelaide, SA, Australia

2.1.4. Monoclonal antibody production reagents

Freund's adjuvant (Complete)	Gibco® Laboratories, Life Technology Inc., Grand Island, NY, USA
Freund's adjuvant (Incomplete)	Sigma Chemical Co., St. Louis, MO, USA
Hypoxanthine, aminopterin and thymidine (HAT)	Gibco® Laboratories, Life Technology Inc., Grand Island, NY, USA
Hypoxanthine and thymidine (HT)	Gibco® Laboratories, Life Technology Inc., Grand Island, NY, USA
ImmuneEasy™ mouse adjuvant	QIAGEN Pty Ltd., Clifton Hill, Vic, Australia
IsoStrip mouse monoclonal isotyping kit	Roche Diagnostics Corp., Indianapolis, IN, USA
Polyethylene glycol 1500 (PEG 1500)	Roche Diagnostics GmbH, Sandhofer Strasse, Mannheim, Germany

2.1.5. Peptide conjugates for the production of antibodies

All peptide conjugates were manufactured by MIMOTOPES Pty. Ltd., Clayton, Vic, Australia

H-CAGAPLPSVTLDG-NH_2

H-LPGLEARYMAFAC-OH

H-GFDLSPLLLGTGC-OH

H-LFFYPSYPDEVRC-OH

All peptides were conjugated to diphtheria toxoid with maleimidocaproyl-N-hydroxy-succinimide (MCS) as a linker.

2.1.6. Enzymes, enzymatic substrates and standards

Wt ASA enzyme	Generated in this study
N350S ASA enzyme	Generated in this study
4-Methylumbelliferyl sulphate (4-MUS)	Sigma Chemical Co., St. Louis, MO, USA
4-Methylumbelliferone (4-MU)	Koch-Light Laboratories Ltd., Colnbrook, UK

2.1.7. Tissue culture reagents

Ampicillin	Boehringer Mannheim, Sandhofer Strasse, Mannheim, Germany
Bacto-agar	Difco Laboratories, Detroit, MI, USA
Dulbecco's modified eagle media (DMEM)	Gibco BRL, Life Technology Inc., Grand Island, NY, USA
Foetal calf serum (FCS)	CSL Biosciences, CSL Ltd., Melbourne, Vic, Australia
G 418	Boehringer Mannheim, Sandhofer Strasse, Mannheim, Germany
HAM'S F 12 media	MP Biomedicals Ltd., Aurora, Ohio, USA
Penicillin/Streptomycin sulphate	CSL Biosciences, CSL Ltd., Melbourne, Vic, Australia
Dulbecco's phosphate buffered saline (PBS)	CSL Biosciences, CSL Ltd., Melbourne, Vic, Australia
RPMI 1640 media	ICN Biomedicals Inc., Aurora, WI, USA
Trypsin-versene	CSL Biosciences, CSL Ltd., Melbourne, Vic, Australia

2.1.8. Custom PCR primers for ASA plasmid DNA sequencing

All custom PCR primers were manufactured by Invitrogen™ Life Technologies, Invitrogen New Zealand Ltd., Penrose, Auckland, New Zealand.

CTG GAC CTG CTG CCT ACC

AGC AAA AAC CCC ACG GAC

CAG CTC TCT GAC TGC TCA

AGG TCA CAG CTG CGT CTA

TCC AGG TTG GGA GTG GTA

CAT TGC CCA GAT CCC CAT

TCC CTC CTC CTG GCC CTG G

GAT GGG CAT GTA CCC TGG

ATG GGG GGG CAG GAA GGC

TTG CGA CGG TGG CTG TGA CC

ACA GGA AGA AGG GGC GAT

CTG ATG GAG CTG GAT GCA

GTC GTT CCC TTT CCA CAC

TTT TTT CAG ATG TGC AAG

Sequences are listed from 5' to 3'end.

2.1.9. Standards for mass spectrometry analysis

Ceramide (Cer17:0)	Matreya Inc., Pleasant Gap, PA, USA
Glucocerebroside deuterated (GC16:0-*d3*)	Matreya Inc., Pleasant Gap, PA, USA
Monosialogangliosides (G_{M2}22:1 and 24:1)	Matreya Inc., Pleasant Gap, PA, USA
Lactosylceramide, deuterated (LC16:0-*d3*)	Matreya Inc., Pleasant Gap, PA, USA
Palmitoyl sulphatide (sulp16:0)	Matreya Inc., Pleasant Gap, PA, USA
Phosphatidylcholine (PC28:0)	Sigma Chemical Co., St. Louis, MO, USA
Phosphatidylglycerol (PG28:0)	Avanti Polar Lipids, Inc., Alabaster, AL, USA
Phosphatidylinositol (PI32:0)	Avanti Polar Lipids, Inc., Alabaster, AL, USA
Sulphatide (bovine brain)	Sigma Chemical Co., St. Louis, MO, USA

2.1.10. Commercial kits

DELFIA® assay buffer	Wallac, North Ryde, NSW, Australia
DELFIA® enhancement solution	Wallac, North Ryde, NSW, Australia
DELFIA® Eu-labelling kit 1244-302	Wallac, North Ryde, NSW, Australia
DELFIA® wash buffer	Wallac, North Ryde, NSW, Australia
Micro BCA™ protein assay reagent kit	PIERCE Chemical Co., Rockford, IL USA

QIAGEN plasmid midi/maxi kit	QIAGEN Pty Ltd., Clifton Hill, Vic, Australia

2.1.11. Equipment and software

Analyst version 1.1 software	PE Sciex, Foster City, CA, USA
Agilent 1100 binary HPLC	Agilent Technologies, Inc., Palo Alto, CA, USA
Beckman JA-20 centrifuge	Beckman Instruments, Inc., Palo Alto, CA, USA
Megafuge 1.0R centrifuge	Heraeus Sepatech Instruments, Radiometer Pacific, Adelaide, SA, Australia
Biofuge 13 centrifuge	Heraeus Sepatech Instruments, Radiometer Pacific, Adelaide, SA, Australia
BioLogic DuoFlow system	Bio-Rad Laboratories, Hercules, CA, USA
Ceres 900 HDI plate reader	Bio Teck Instruments, Inc., Vinooski, VT, USA
BTX electrocell manipulator ECM 395	BTX Pty. Ltd., San Diego, CA, USA
ChemoView NT version 1.2	PE Sciex, Foster City, CA, USA
DELFIA 1234 research fluorometer	Wallac, North Ryde, NSW, Australia
DELFIA® plate shaker	Wallac, North Ryde, NSW, Australia
DELFIA® plate washer	Wallac, North Ryde, NSW, Australia
Dry block heater	Ratek Instruments Pty Ltd., Melbourne, Vic Australia
Electrophoresis power supply EPS 600	Amersham Pharmacia Biotech, Inc., Uppsala, Sweden
Gilson 233 autosampler	Gilson, Inc., Middleton, WI, USA
Hoefer Mighty Small II electrophoresis unit	Hoefer Scientific Instruments, San Francisco, CA, USA
Horizontal gel electrophoresis tanks	Eastman Kodak Co., New Haven, CT, USA
LKB Biochrom Ultrospec II spectrophotometer	BIOCHROM, Cambridge Science Park, Cambridge, England
Luminescence spectrometer LS 50 B with autosampler AS 91	Perkin-Elmer Ltd., Beaconsfield, Bucks, UK
Microtitration plate shaker	ADIL Instruments, Strasbourg, Schil Tigheim, France
Microtitration plate washer	ADIL Instruments, Strasbourg, Schil Tigheim, France
Perkin-Elmer 1420 multilabel counter	Perkin-Elmer Ltd., Norwalk, CT, USA
Reactivap™ evaporating unit with reacti-therm heating unit	Pierce Chemical Co., Rockford, IL, USA

SEQMAN program software	DNA Star, Madison, WI, USA
TE Series transphor transfer unit	Hoefer Scientific Instruments, San Francisco, CA, USA
Triple-quadrupole mass spectrometer (PE Sciex API-3000)	Perkin-Elmer Sciex, Foster City, CA, USA
UVItec-gel documentation system	UVItec Ltd., Union Lane, Cambridge, England

2.1.12. Miscellaneous

Affi-Gel 10	Bio-Rad Laboratories, Hercules, CA, USA
BenchMark™ prestained protein ladder	GibcoBRL® Life Technologies, San Diego, CA, USA
BenchMark™ protein ladder	Invitrogen™ Life Technologies, San Diego, CA, USA
Bovine serum albumin (BSA)	Sigma Chemical Co., St. Louis, MO, USA
Brilliant blue G-colloidal stain	Sigma Chemical Co., St. Louis, MO, USA
BTX electroporation cuvette plus (model #610, 1 mm gap)	BTX Pty. Ltd., San Diego, CA, USA
Corning® 25 cm^2, 75 cm^2, 175 cm^2 tissue culture flasks	Corning Costar Corp., Cambridge, MA, USA
Corning® 96, 24, 12 and 6 well tissue culture plates	Corning Costar Corp., Cambridge, MA, USA
Corning® 100 mm tissue culture dishes	Corning Costar Corp., Cambridge, MA, USA
Costar® 96-well vinyl assay plate	Costar®, Cambridge, MA, USA
Diaflo YM 30 and YM 10 ultrafiltration membranes	Amicon®, Beverly, MA, USA
Pharmacia K9/15 column	Amersham Pharmacia Biotech, Inc., Uppsala, Sweden
HiTrap affinity column (1.0 mL)	Amersham Pharmacia Biotech, Inc., Uppsala, Sweden
HiTrap IgM purification HP (1.0 mL)	Amersham Pharmacia Biotech, Inc., Uppsala, Sweden
Hitrap™ protein G column (1.0 mL)	Amersham Pharmacia Biotech, Inc., Uppsala, Sweden
Immunlon® 4HBX Removawell® strips and holder	Dynatech Laboratories, Inc., Chantilly, VA, USA
ISOLUTE-96 C18 column (25 mg)	International Sorbent Technology Ltd., Mid Glamorgan, UK
Linbro® plate sealer	ICN Biomedicals Inc., Aurora, WI, USA

Microtitre plate, 96 wells, V-shape	Greiner Bio-One GmbH, Maybachstrasse, Frickenhausen, Germany
Ministart® single use syringe filter (0.2 µm)	Sartorius, Weender Lanstr, Göttingen, Germany
Minicon filter cartridge	Sartorius, Weender Lanstr, Göttingen, Germany
Multipin™ peptides	Chiron Mimotopes Pty. Ltd., Clayton, Vic, Australia
Mw standards	Pharmacia Biotech, Uppsala, Sweden
Neubauer hemocytometer	Superior, Bad Mergentheim, Germany
Nunc 1264 cm^2 2-tray cell factory	Nalge Nunc International, Rochester, NY, USA
PolyScreen® PVDF transfer membrane	NEN™ Life Science Products, Boston, MA, USA
Prep/scale™-TFF concentrator	Milipore Corporation, Bedford, MA, USA
Pyrex® culture tube (size 16 x 100 mm)	Corning Inc., New York, USA
Self Pack™ POROS® 20 R1 media	PerSeptive Biosystems, Inc., Framingham, MA, USA
SGE Hamilton syringe (100 µL)	Sigma Aldrich Pty. Ltd., Castle Hill, NSW, Australia
Stirred-cell ultrafiltration unit (10 mL and 250 mL)	Amicon®, Beverly, MA, USA
Superose 6 HR 30 FPLC column (1.0 x 30 cm)	Amersham Pharmacia Biotech, Inc., Uppsala, Sweden
Superose 12 HR 30 FPLC column (1.0 x 30 cm)	Amersham Pharmacia Biotech, Inc., Uppsala, Sweden
Supelco Visiprep™ 24	Sigma Aldrich Pty. Ltd., Castle Hill, NSW, Australia
Tris glycine-SDS gels (12%)	Gradipore Ltd., Pyrmont, NSW, Australia
UNO™ Q1 anion exchange column	BIO-RAD Laboratories, Hercules, CA, USA
UV trans-illuminator model 44-16	Polaroid Ltd., Cambridge, MA, USA
Vibron sonicator	Galsonic Pty. Ltd., Valley View, SA, Australia
YSTROM sonicator	Technic International Inc., Westwood, NJ, USA

2.1.13. Buffers, solutions and cell culture media

All buffers and solutions were prepared in Milli-Q® water. Cell culture media was prepared in sterilised distilled water and sterilised by filtration (0.2 µm).

2.1.13.1. Buffers and solutions

10x acetic acid	0.2 M CH_3COOH
1% agarose gel	1x TBE buffer, 1% (w/v) agarose
Buffer A	20 mM sodium acetate/acetic acid buffer, pH 5.0
Buffer B	20 mM sodium acetate/acetic acid buffer, 1.0 M NaCl, pH 5.0
2x HEPES buffered saline	0.28 M NaCl, 0.05 M HEPES, 1.5 mM Na_2HPO_4/NaOH, pH 7.05
10 x loading buffer (agarose gel electrophoresis)	92.5% (v/v) formamide, 20 mM EDTA, 0.1% (w/v) xylene cyanol, 0.1% (w/v) bromophenol blue
2x loading buffer (SDS-PAGE)	125 mM Tris/HCl, pH 6.8, 4% (w/v) SDS, 20% (v/v) glycerol, 10% (v/v) 2-mercaptoethanol
Phosphate buffered saline (PBS)	10 mM H_3PO_4/NaOH, pH 7.4, 0.15 M NaCl
10 x PBS, pH 7.2	1.37 M NaCl, 26 mM KCl, 81 mM Na_2HPO_4, 14 mM KH_2PO_4
10x PBS (for pin plate disruption)	2.5 M NaCl, 28 mM Na_2HPO_4, 75 mM Na_2HPO_4
10x sodium acetate	0.2 M $CH_3COONa.\ 3H_2O$
Sodium hydrogen carbonate buffer	0.1 M $NaHCO_3$
10 x SDS-PAGE running buffer	0.25 M Tris, 1.92 M glycine, 1% (w/v) SDS
TE buffer	10mM Tris/HCl, pH 8.0, 1mM EDTA
5x TBE buffer	45 mM Tris/borate, pH 8.0, 1 mM EDTA
10x Tris-NaCl	0.2 M Tris/HCL, pH 7.2, 2.5 M NaCl

2.1.13.2. Cell culture media

Basal media eagle (BME) 10% FCS	commercially prepared BME, 10% FCS
COON's media	DMEM 15.5 g/L
COON's media, 10% FCS	DMEM 15.5 g/L, 10% FCS
LB-agar	LB broth, 1.5% (w/v) Bacto agar
LB-amp	LB agar, 100 mg/L ampicillin
LB-broth	1% (w/v) Bacto tryptone, 0.5% (w/v) Bacto yeast extract, 1% (w/v) NaCl, NaOH, pH 7.5
HAT media	RPMI 1640 10.4 g/L, 10% FCS, 1x HAT, 1% PS
HT media	RPMI 1640 10.4 g/L, 10% FCS, 1x HT, 1% PS
Selection media	F12 10.6 g/L, 10% FCS, G 418 750 µg/mL
F12 media 10% FCS	BME 9.19 g/L, 10% FCS

2.2. Methods

2.2.1. Expression of full-length ASA

The full-length ASA expression vector was constructed by Dr J Harvey (Department of Genetic Medicine, Women's and Children's Hospital, Adelaide, SA, Australia). The full-length ASA cDNA clone in HT 14/CP 8 pBluescript® vector (Stein *et al.*, 1989) was provided by Professor Volkmar Gieselmann (Biochemisches Institut, Christian-Albrecht-Universitat, Kiel, Germany). The full length ASA cDNA was excised from the pBluescript® vector with restriction endonucleases *Nco I* and *Not I*. The excised ASA cDNA, together with 5' untranslated rat preproinsulin sequences (synthesised and annealed from oligonucleotides encoding the rat preproinsulin 5' untranslated sequences containing a 5' *Hind III* and a 3' *Nco I* sticky end sites), were ligated in a single reaction into the *Hind III*- and *Not I*-restricted pRSVN.07 expression vector. The final yield of ASA cDNA 5' untranslated sequence was achieved by mixing equal molar amounts of each oligonucleotide, heating the mixture to 70°C and allowing it to cool to room temperature (Harvey, PhD Thesis, 1996).

2.2.1.1. Agarose gel electrophoresis

Electrophoresis of DNA for analytical purposes was performed on 1% agarose gels in a horizontal gel electrophoresis tank (Eastman Kodak Co., New Haven, CT, USA). Samples were prepared by mixing the DNA with H_2O and 3x agarose gel loading buffer. The gel was electrophoresed (40-60 mV) in 1x Tris/borate-buffered ethylene diamine tetra-acetic acid (TBE) running buffer until the bromophenol blue dye indicator had migrated a distance sufficient to ensure adequate separation of the DNA fragments. The gel was stained in ethidium bromide (10 μg/mL) for 10 min and destained with running water (5-10 min). The DNA was then visualised on an UV trans-illuminator, model 44-16 (Polaroid Ltd., Cambridge, MA, USA). An image of the gel was then recorded using the UVItec-gel documentation system (UVItec Ltd., Union Lane, Cambridge, UK).

2.2.1.2. Purification of plasmid cDNA

Purification of the plasmid cDNA was performed using a QIAGEN plasmid midi/maxi kit, following the manufacturer's instructions. Briefly, recombinant *E. coli* cells from an overnight culture (100 mL) were harvested by centrifugation in a Beckmann JA-20 centrifuge (6 000 x g, 4°C, 15 min) then resuspended in Buffer P1 (4.0 mL) containing RNase A (100 μg/mL). This was followed by the addition of Buffer P2 (4.0 mL), mixed by

gentle inversion (4-6x) and left at room temperature (RT) for 5 min. Buffer P3 (4.0 mL) was then added, mixed by inversion and incubated on ice for 20 min. The mixture was then centrifuged (20 000 x g, 4°C, 30 min) and the supernatant containing plasmid DNA retained. The supernatant was centrifuged again (20 000 x g, 4°C, 15 min) before being applied to a QIAGEN-tip 100 that had been pre-equilibrated with 4.0 mL of QBT buffer. The QIAGEN-tip was washed twice with 10 mL of Buffer QC before elution of the plasmid DNA with 5.0 mL of Buffer QF. The eluted DNA was precipitated with 3.5 mL of isopropanol and pelleted by centrifugation (≥ 15 000 x g, 4°C, 30 min). The resulting pellet was washed with 2.0 mL of 70% (v/v) ethanol, air-dried, then redissolved in 100 µL of TE buffer, pH 8.0.

2.2.1.3. Quantification of DNA

DNA purified by the QIAGEN plasmid midi/maxi kit was quantified by diluting in water (1:500) and measuring the absorbance at 260 nm. The formula of Sambrook *et al.* (1989) was used to calculate the DNA concentration:

OD_{260} = 1.0 for 50 µg/mL solution of DNA

or amount of DNA = OD_{260} x dilution factor x 50

2.2.1.4. Sequencing of plasmid DNA

The plasmid was sequenced directly using Big Dye Termination (version 3). Cycle sequencing and analysis was performed by the Institute of Medical and Veterinary Science Sequencing Centre, Molecular Pathology Department, Adelaide, SA, Australia. Fourteen custom PCR primers listed in section 2.1.8 were used as the sequencing primers. Sequencing results were analysed using the SEQMAN program software.

2.2.1.5. Electroporation of E. coli cells with plasmid DNA

Plasmid DNA was transferred into electrocompetent *E. coli* strain Top 10 (Invitrogen New Zealand Ltd., Penrose, Auckland, New Zealand) by electroporation using the following protocol: 25 µL of electrocompetent *E. coli* was added to 2.0 µL of plasmid DNA in a sterile Eppendorf tube and mixed gently before transfer to an ice-cooled, sterile BTX electroporation cuvette plus (model #610, 1 mm gap). Electroporation was carried out using a BTX electrocell manipulator ECM 395 set at HV mode, 1.5 kV (BTX Pty. Ltd., San Diego, CA, USA). After electroporation, 500 µL of LB-broth was added and the cells were then transferred to a new sterile Eppendorf tube and incubated at 37°C for 30 min. Cells were then pelleted by centrifugation (740 x g, 5 min); 90% of the supernatant was removed

and the pellet was resuspended before plating onto a LB-amp agar supplemented with 100 μg/mL ampicillin and incubation overnight at 37°C.

2.2.1.6. Transfection of a Chinese hamster ovary-K1 (CHO-K1) cell line

Plasmid DNA samples for transfection (5.0 μg in a final volume of 100 μL) were precipitated by the addition of 10 μL of 3 M sodium acetate/acetic acid, pH 5.2, and 200 μL of 70% (v/v) ethanol (cooled at -20°C) followed by incubation (-80°C, 30 min). The precipitate was pelleted by centrifugation (13 800 x g, 4°C, 20 min). The pellet was washed with 200 μL of 70% (v/v) ethanol and the plasmid DNA was pelleted by centrifugation (13 800 x g, 4°C, 10 min). The pellet was then resuspended in sterile water (450 μL) and 50 μL of 2.5 M $CaCl_2$ was added. The DNA/$CaCl^{2-}$complex solution (500 μL) was added drop-wise to a tube containing 500 μL of 2x HEPES-buffered saline with continuous vortexing. The mixture was vortexed for a further 30 sec, then left at 20°C for 60 sec. The DNA mixture was then added drop-wise to the culture dish grown with CHO-K1 cells for transfection. After an overnight incubation in a 37°C, 5% CO_2 humidified incubator, the media from the cell lines was replaced with fresh media and the cells were further incubated for 48 hrs.

After 72 hrs, dishes containing confluent transfected cell lines were harvested by removing the media followed by washing with Dulbecco's PBS (1x, 5.0 mL) (CSL Biosciences, CSL Ltd., Melbourne, Vic, Australia), then adding 10% (v/v) trypsin-versene solution (3.0 mL) (CSL Biosciences, CSL Ltd., Melbourne, Vic, Australia). The dishes were left at RT for 5 min before cells were dislodged by pipetting gently several times. Cells transfected with DNA were split 1:3, whereas control cells without DNA were split 1:50, in duplicate, into 75 mL culture flasks containing selection media (F 12, 10% FCS with 750 μg/mL G 418). Cells were then incubated at 37°C in a 5% CO_2 humidified incubator for seven-days with media changes every three-days. On day eight, transfected cells were harvested and resuspended in new flasks with fresh selection media. The transfected cells were harvested and resuspended again (in duplicate) on day 14.

2.2.1.7. Cloning of recombinant cells

Cloning of recombinant cells was carried out using a serial dilution method. Briefly, cells were counted using a Neubauer hemocytometer (Superior, Bad Mergentheim, Germany) and diluted to a solution containing 80 cells/mL in a sterile 10 mL polyethylene tube containing 6.0 mL of selection media. Serial dilutions were then carried out to obtain

concentrations of 40 cells/mL, 20 cells/mL and 10 cells/mL. Each cell dilution was pipetted into a 96-well plate (100 µL/well) in the following positions: rows A and B, 80 cells/mL; rows C and D, 40 cells/mL; rows E and F, 20 cells/mL; and rows G and H, 10 cells/mL. A further 100 µL of F 12 with 10% FCS was added to each well before incubation at 37°C in a 5% CO_2 humidified incubator for seven- to 10-days; 50 µL media/well was subsequently added within that period and the number of clones in each well were counted before the media was analysed for ASA activity as described below.

2.2.1.8. Enzymatic assay for ASA (free assay)

ASA enzyme activity was assayed in wells of Immunlon® 4HBX Removawell® strips, (Dynatech Laboratories, Chantilly, VA, USA). Samples (50 µL, in duplicate) or blanks (50 µL H_2O, in duplicate) were incubated (37°C, 2 hrs) with 4-MUS substrate (40 mmol/L, 50 µL) prepared in 0.1 M sodium acetate/acetic acid buffer, heat-treated 0.1% BSA, pH 5.6. After incubation, 4-methylumbelliferone standard (0.142 mmol/L, Koch-Light Laboratories Ltd., Colnbrook, UK) was diluted 1 in 20 before 100 µL was pipetted into three empty wells (100 µL/well). The enzyme reaction was stopped by the addition of 0.2 mol/L glycine/NaOH buffer, pH 10.7 (100 µL/well). For the glycine blank, 0.2 mol/L glycine/NaOH buffer, pH 10.7, was pipetted into three empty wells (200 µL/well). The fluorescence was read on a Perkin-Elmer 1420 multilabel counter (Perkin-Elmer Ltd., Norwalk, CT, USA). The reading from wells with H_2O was used as the substrate blank. Enzyme activity was calculated according to the following formula:

$$\textbf{Enzyme activity (pmol/min/mL)} = \frac{(\text{FU test} - \text{FU of substrate blank}) \times 710 \times 1000}{(\text{FU of standard} - \text{FU of glycine blank}) \times 120 \times \text{vol. of sample (µL)}}$$

FU = fluorescence unit

vol. = volume

2.2.1.9. Enzymatic assay for ASA (free assay, tube method)

ASA activity was assayed using two Wt ASA calibrators with concentrations of 250 and 500 ng/mL. Briefly, each Wt ASA calibrator (5.0 µL, in duplicate) and H_2O (5.0 µL, in duplicate) was added to tubes containing 4-MUS substrate (5.0 mmol/L) prepared in 0.1 M sodium acetate/acetic acid buffer, heat-treated 0.1% BSA, pH 5.0 (100 µL/tube). In addition, two tubes were used as standards (0.142 mmol/L 4-methylumbelliferone, 20 µL/tube). The tubes were then incubated at 37°C for 60 min in a water bath.

The enzyme reaction was stopped by the addition of glycine/NaOH buffer, pH 10.7 (0.2 mol/L; 1.6 mL/tube); two additional tubes were used as glycine buffer blanks with the addition of the same amount of glycine buffer. Fluorescence was read on a Luminescence spectrometer LS 50 B with autosampler AS 91 (Perkin-Elmer Ltd., Beaconsfield, Bucks., UK). The instrument settings for excitation and emission wavelengths/slit widths were set at 366/15 nm and 446 nm/15 nm, respectively. The reading from the tubes with H_2O was used as the substrate blank. Enzyme activity was calculated according to the following formula:

$$\textbf{Enzyme activity (pmol/min/mL)} = \frac{\text{(FU test-FU of substrate blank) x 710 x 1000}}{\text{(FU of standard-FU of glycine blank) x 60 x vol. of sample (µL)}}$$

FU = fluorescence unit

Vol. = volume

2.2.1.10. Freezing-down of cells

Cells that were to be stored frozen were grown to confluence in 75 cm^2 flasks. Each flask was harvested by removing the media, followed by washing with Dulbecco's PBS (1x, 5.0 mL). Trypsinisation was carried out by the addition of 10% (v/v) trypsin-versene solution (3.0 mL). The flasks were incubated at RT for 5 min, after which the cells were dislodged from the flask by pipetting gently several times. The cells were then transferred to sterile polypropylene tubes containing PBS (7.0 mL), mixed and centrifuged (415 x g, 5 min) before the supernatant was carefully discarded. This washing process was repeated once before the pellet was resuspended gently in selection media containing 10% (v/v) DMSO (1.0 mL). The cells were then pipetted into freezing vials, snap frozen and stored in liquid nitrogen.

2.2.2. Production of conditioned media for purification

CHO-K1 cells expressing the recombinant enzyme (Wt ASA or N350S ASA) were grown to confluence in Nunc 1264 cm^2 2-tray cell factories (Nalge Nunc International, Rochester, NY, USA) in COON's media with 10% FCS (250 mL). Cells were then conditioned with FCS-free media (200 mL) for four- to five-days, after which media was collected, centrifuged (970 x g, 10 min), pooled and kept at 4°C. The first collection immediately following the change from 10% FCS to FCS-free media was not used for protein purification. Media was pooled until a volume of 6.0 to 8.0 L was reached, before it was concentrated and purified. After three- to four collections of FCS-free media (depending

on the condition of the cells), cells were cycled back with COON's containing 5% FCS and the process of conditioning and collection of media was repeated.

2.2.2.1. Concentration of conditioned media

The conditioned media from the Wt ASA or N350S ASA CHO-K1 cell expression systems was pooled and kept at 4°C in a sterile condition. Media with a volume of less than 1.0 L, was clarified by centrifugation (970 x g, 10 min) and concentrated using a 250 mL stirred-cell ultrafiltration unit with either a Diaflo YM 30 or YM 10 ultrafiltration membrane (Amicon®, Beverly, MA, USA).

Media with a volume of more than 1.0 L was clarified by centrifugation (970 x g, 10 min) before concentration in a Prep-Scale™-TFF concentrator (Millipore Corp., Bedford, MA, USA) using the protocol specified by the manufacturer. Concentrated media from this step was further concentrated in a 250 mL stirred-cell ultrafiltration unit using either a Diaflo YM 30 or YM 10 ultrafiltration membrane.

2.2.3. Purification of Wt ASA and N350S ASA from conditioned media

The method used to purify Wt ASA and N350S ASA was developed during this study (developmental work discussed in section 3.3). Briefly, the concentrated media (section 2.2.2.1) was dialysed overnight at 4°C against 20 mM sodium acetate/acetic acid buffer, pH 5.0 (Buffer A), and clarified by centrifugation (970 x g, 4°C, 10 min). The supernatant was filtered with a Ministart® single use syringe filter (0.2 μm) before loading onto an anion exchange column (Self Pack™ POROS® 20 R1 media in a Pharmacia K9/15 column) connected to a BioLogic DuoFlow system (Bio-Rad Laboratories, Hercules, CA, USA) using Buffer A as loading buffer. The flow rate was set at 2.0 mL/min with the fraction collector set to collect 1.0 mL/fraction.

A combination of isocratic and linear gradients between Buffer A and 20 mM sodium acetate/acetic acid buffer, 1.0 M NaCl, pH 5.0 (Buffer B), was used in the elution protocol. Before loading, the column was equilibrated with Buffer A (60 mL). After sample loading, the column was washed with Buffer A (15 mL), then eluted with a linear gradient from 0 to 7% of Buffer B (4.0 mL), followed by an isocratic flow (35 mL) and a second linear gradient from 7 to 12% of Buffer B (7.5 mL); a further isocratic flow followed (15 mL) before a final gradient from 12 to 100% of Buffer B (4.0 mL). This final concentration was maintained (4.0 mL) before returning the column to its starting condition with a gradient from 100 to 0% Buffer B (4.0 mL).

The third purification step was performed using size exclusion chromatography (SEC). A Superose 6 HR 30 column (1.0 x 30 cm) was connected to a BioLogic DuoFlow system with the flow rate set at 0.5 mL/min and the fraction collector set at 0.5 mL/fraction. The column was equilibrated with 20 mM sodium acetate/acetic acid buffer with 0.15 M NaCl (30 mL) before loading the sample. Fractions containing enzyme from anion exchange chromatography (AEC) were pooled and concentrated to 250 µL using a 10 mL stirrer-cell ultrafiltration unit with either a Diaflo YM 30 or YM 10 ultrafiltration membrane. The enzyme concentrate was then loaded and run on the SEC column using 20 mM sodium acetate/acetic acid buffer with 0.15 M NaCl as elution buffer (26 mL). Fractions containing the enzyme were collected and analysed by SDS-PAGE (12% Tris-glycine-SDS gels) using the method of Laemmli (1970), as described in section 2.2.4, to determine enzyme purity. The enzyme concentration in these fractions was determined with bicinchoninic acid (BCA), as described in section 2.2.5.

2.2.4. Sodium dodecylsulphate-polyacrylamide gel electrophoresis

SDS-PAGE was performed according to the method of Laemmli (1970) on 12% Tris-glycine-SDS gels (Gradipore Ltd., Pyrmont, NSW, Australia). Samples were mixed with SDS loading buffer containing 5% (v/v) β-mercaptoethanol and heated (95°C, 10 min). The polyacrylamide gels were run at a constant voltage (180 V) in a Hoefer Mighty Small II electrophoresis unit (Hoefer Scientific Instruments, San Francisco, CA, USA). The Mw of the proteins was determined using semi-log plot comparison of the bands in the BenchMark™ protein ladder (Invitrogen™ Life Technologies, San Diego, CA, USA) versus the migration distance travelled. Visualisation of the bands was made possible by either Coomassie staining (see section 2.2.4.1) or silver staining (see section 2.2.4.2).

2.2.4.1. Coomassie staining of the SDS-PAGE gel

SDS-PAGE gels were fixed with fixing solution (7% glacial acetic acid in 40% methanol [v/v]) for 1 hr. The brilliant blue G-colloidal stain (Sigma Chemical Co., St. Louis, MO, USA) was prepared according to the manufacturer's instructions. The gel was then placed in the staining solution (overnight, with shaking), followed by destaining with 10% acetic acid in 25% ethanol [v/v] (60 sec, with shaking) and rinsing with 25% methanol before further destaining with 25% methanol until a clear background was obtained. An image of the gel was then recorded using the UVItec-gel documentation system.

2.2.4.2. *Silver staining of SDS-PAGE gels*

Silver staining of SDS-PAGE gels was performed according to the method of Chataway and Barritt (1994), with minor modifications. Briefly, each gel was fixed for 60 min (40% (v/v) ethanol, 10% (v/v) acetic acid), then incubated in periodic acid solution (25 mM periodic acid, 25% (v/v) ethanol, 5% (v/v) acetic acid) (5 min) and washed with water (3 x 10 min). The gel was then placed in incubation solution (0.5 M sodium acetate, 13 mM sodium thiosulphate, 0.13% (v/v) glutaraldehyde, 33% (v/v) ethanol) overnight, washed in water (3 x 10 min), then incubated in silver nitrate solution (12 mM silver nitrate, 0.05% (v/v) formaldehyde) for 1 hr. Following a brief rinse with water (2 min), the gel was developed in developing solution (0.24 M sodium carbonate, 0.05% (v/v) formaldehyde) until the protein bands reached the desired intensity; development was stopped by placing the gel in stopping solution (40 mM EDTA) for 10 min. Each gel was then washed in water (2 x 5 min) and incubated in preserving solution (10% (v/v) glycerol) for 30 min and air-dried between cellophane sheets at RT.

2.2.4.3. *Western blotting*

Following SDS-PAGE, each gel was rinsed (3x) in transfer buffer (10 mM CAPS, pH 11.0, 10% MeOH [v/v]) before transfer to a PolyScreen® PVDF transfer membrane (NEN™ Life Science Products Inc., Boston, MA, USA) using the TE Series transphor transfer unit (Hoefer Scientific Instruments, San Francisco, CA, USA). Transfer was performed in transfer buffer at a constant current (250 mA) for 70 min. On completion, the transfer membrane was rinsed with wash solution (1x, 20 mM Tris/HCl, 250 mM NaCl, 1% (w/v) BSA, pH 7.0), then incubated in blocking buffer (20 mM Tris/HCl, 5% (w/v) BSA, 0.05% (v/v) Tween 20, pH 7.0) for 1 hr. The membrane was then washed (3 x 10 min) in 100 mL wash solution and probed with sheep polyclonal antibody diluted (1:1 000) in wash solution or monoclonal antibody from culture media (10 mL) at 4°C, overnight. Each membrane was then washed (3 x 10 min) with the wash solution and incubated with a HRP-conjugated secondary antibody (sheep anti-mouse HRP-conjugated or donkey anti-sheep HRP-conjugated) at a dilution of 1:1 000 (RT, 1 hr, with shaking). The membrane was washed in the wash solution (3 x 10 min), then in PBS (1 x 10 min).

For visualisation, the membrane was developed by incubation in 4-chloro-1-naphthol substrate (60 mg) dissolved in ice-cold MeOH (20 mL), added to 100 mL of 20 mM Tris/HCl, 250 mM NaCl, pH 7.0, and 60 µL H_2O_2. Colour development was stopped by placing the membrane in water. Mw was estimated by semi-log plot comparison of the

bands in the BenchMark™ prestained protein ladder (GibcoBRL® Life Technologies, San Diego, CA, USA).

2.2.5. Protein determination

Protein determination was performed using the micro assay, BCA method of Smith *et al.* (1985). Assays were performed in Costar® 96-well vinyl assay plates with the use of a Micro BCA™ protein assay reagent kit according to the protocol recommended by the manufacturer. BSA was used as the assay calibrator at a concentration of 10 to 200 µg/mL. Plates were read on a Ceres 900 HDI plate reader (Bio Teck Instruments Inc., Vinooski, VT, USA).

2.2.6. Production of polyclonal antibodies

Two polyclonal antibodies were generated in sheep for this study by the Veterinary Division of the Institute of Medical and Veterinary Science, Adelaide, SA, Australia. The first polyclonal antibody was raised against a 13-mers peptide, H-CAGAPLP**S**VTLDG-NH_2, conjugated to diphtheria toxoid at a ratio of 4.2 mg peptide to 30.3 mg diphtheria toxoid, with maleimidocaproyl-N-hydroxysuccinimide as a linker; this peptide conjugate will hereafter be referred to as the N350S peptide conjugate and the polyclonal antibody raised against it will be referred to as the anti-N350S peptide conjugate polyclonal antibody. The second polyclonal antibody was raised against the N350S ASA enzyme and will be henceforth referred to as the anti-ASA polyclonal antibody. The immunisation protocol used to produce the polyclonal antibodies was as follows: a pre-bleed sample was taken before the primary inoculation (2.0 mg peptide conjugate or 1.0 mg N350S ASA) was administered at week zero, followed by three booster doses of the same amount of antigen given at three-week intervals. A test bleed was taken at 7.5–weeks; the sheep was bled-out at week 10.5.

2.2.7. Purification of polyclonal antibodies

Sheep sera was subjected to ammonium sulphate precipitation, by adding an equal volume of saturated ammonium sulphate (761 g/L ammonium sulphate) to sheep sera drop-wise with continual mixing followed by overnight incubation (4°C, with stirring). The mixture was then centrifuged (1 162 x g, 3 min) and the supernatant discarded. The pellet was resuspended in PBS and dialysed against PBS (4°C, overnight), then filtered with a Ministart® single use syringe filter (0.2 µm). The immunoglobulin (IgG) fraction from sheep sera raised against the N350S ASA enzyme was then affinity-purified on a HiTrap

affinity column (1.0 mL) (Amersham Pharmacia Biotech Inc., Uppsala, Sweden) coupled to 2.0 mg N350S ASA. The IgG fraction from sheep sera raised against the N350S peptide conjugate was affinity-purified using thiopropyl-sepharose 6B gel (3.0 mL) (MIMOTOPES Pty. Ltd., Clayton, Vic, Australia) covalently coupled to the same peptide used for immunisation.

Antibody was loaded onto the affinity column at a flow rate of 1.0 mL/min. After loading, unbound proteins were removed by washing with PBS (10 mL). The polyclonal antibody was eluted with 0.1 M H_3PO_4/NaOH, pH 2.5, at 1 mL/min; 0.5 mL fractions were collected. To neutralise the acidic eluant, 200 µL of 1.0 M Na_2HPO_4, pH 9.0, was added to each fraction. Eluted antibody was immediately dialysed against PBS (4°C, overnight).

2.2.8. Production of monoclonal antibodies

Several methods were used to produce monoclonal antibodies in this study, which will be elaborated upon in Chapter 3; in general, however, the monoclonal antibody production strategy was based on that of Zola and Brooks (1982), as described below.

2.2.8.1. Immunisation regime for mice using Freund's adjuvant

Briefly, the immunisation regime used was as follows: antigen was administered either via subcutaneous or intra-peritoneal injection with a 26 G needle. The first inoculation consisted of antigen in PBS mixed with complete Freund's adjuvant in a 1:1 mixture (100 µL/mouse); the second and third booster inoculations were given with antigen in PBS mixed with incomplete Freund's adjuvant in a 1:1 mixture (100 µL/mouse); the last booster was given with antigen in PBS (100 µL/mouse). Inoculations were administered three-weeks apart, with the last inoculation given four-days before fusion. Each inoculation contained between 35 to 100 µg N350S ASA or Wt ASA in a final volume of 100 µL, while the amount of peptide conjugate used was 100 µg/100 µL.

2.2.8.2. Immunisation regime for mice using ImmuneEasy™ mouse adjuvant

The immunisation regime for mice using ImmuneEasy™ mouse adjuvant was carried out as recommended by the manufacturer. The amount of antigen used for each inoculation was between 5 to 25 µg/mouse. A total of three inoculations (100 µL/mouse, subcutaneously) were administered at two-week intervals, with the last inoculation given three-days before the fusion was performed.

2.2.8.3. Fusion protocol

A standard fusion protocol was used to generate monoclonal antibodies, as described by Clements *et al.* (1985). Briefly, the mouse was killed by CO_2 asphyxiation. The mouse spleen was removed and placed in a Petri dish containing Dulbecco's PBS (5.0 mL); blood was collected by puncturing the heart with a Pasteur pipette.

The connective and fatty tissues were trimmed and discarded before injecting Dulbecco's PBS (5.0 mL) into the spleen using a 21 G needle to expel the plasma cells. The spleen was then teased apart into very fine shreds with another needle. The shredded tissues were transferred to a 50 mL centrifuge tube; the dish was rinsed with Dulbecco's PBS (10 mL) and the slurry transferred to the centrifuge tube. The tube was left to stand at RT for 5 min, after which it was decanted into a new 50 mL centrifuge tube and left to stand for a further 5 min (RT) before being decanted into a 50 mL centrifuge tube containing 10^7 murine myeloma cells.

The mixed cells were pelleted by centrifugation (415 x g, 5 min) before pre-warmed (37°C) 42% PEG 1500 (1.0 mL, [v/v] in 75 mM HEPES, pH 8.0) was added drop-wise over 1 min, with shaking. This was followed by the addition of RPMI (10 mL) drop-wise, with shaking, over 5 min before further addition of RPMI (40 mL). The fusing cells were then centrifuged (415 x g, 5 min) and pelleted. The cell pellet was resuspended in 10 mL RPMI containing 10% FCS, 1x HAT, 1% penicillin/streptomycin sulphate and 2.0 mL of feeder lavage that had been prepared earlier (section 2.2.8.3.1), and mixed. The volume was made up to 200 mL with the same media, before plating into eight Corning® 24-well tissue culture plates (1.0 mL/well). Plates were labelled and incubated (5% CO^2, 37°C). Hybridomas were examined microscopically with colonies marked and counted after incubation for one-week; hybridoma screening was performed after two-weeks (after two changes of media) using the protocol described in section 2.2.8.5.

2.2.8.3.1. Feeder lavage

Feeder lavage was obtained from a non-immunised mouse on the same day as the fusion. Briefly, the mouse was killed by CO_2 asphyxiation. Dulbecco's PBS (5.0 mL) was injected into the peritoneal cavity using a syringe with a 21 G needle, with the bevel of the needle facing downward to avoid the organs. Once the Dulbecco's PBS was fully injected, at least 2.0 mL of clear liquid (lavage) was withdrawn using the same syringe; the lavage was added to 200 mL of RPMI containing 10% FCS, 1x HAT and 1% penicillin/streptomycin sulphate. The media was kept incubated at 37°C until use.

2.2.8.4. Determination of antibody titres

Determination of antibody titres was carried out by ELISA using a secondary HRP detection system. Briefly, samples (100 µL/well) consisting of sheep sera or mouse sera (1:1 000 dilution in 1% (w/v) BSA, 20 mM Tris/HCl, 0.25 M NaCl, pH 7.2) were serially diluted 1:2 across the wells in a Costar® 96-well vinyl assay plate coated with the antigen or BSA (2.0 µg/mL). The plate was shaken (10 min, speed 4) on a DELFIA® plate shaker (Wallac, North Ryde, NSW, Australia) before incubation at RT for 2 hrs. The plate was then washed (6x) with 20 mM Tris/HCl, 0.25 M NaCl, pH 7.2, on a microtitration plate washer (ADIL Instruments, Strasbourg, Schil Tigheim, France).

Depending on the sample being tested, either donkey anti-sheep HRP-conjugated antibody or sheep anti-mouse HRP-conjugated antibody (1:1 000 dilution in 1% (w/v) BSA, 20 mM Tris/HCl, 0.25 M NaCl, pH 7.2) was added (100 µL/well) before incubation at RT for 1 hr. This was followed by washing (6x) with 20 mM Tris/HCl, 0.25 M NaCl, pH 7.2, before freshly prepared ABTS substrate (see section 2.2.8.4.1) was added (100 µL/well). Colour development was aided by shaking (speed 4, 20 min) on a DELFIA® plate shaker before the OD (410 nm) was read on a Ceres 900 HDI plate reader. Antibody titre was determined as the lowest dilution of sera at which the OD was greater than two standard deviations above background reading.

2.2.8.4.1. Preparation of 2, 2'-azino-bis (3-ethylbenzo-thiazoline-6-sulphonic acid) diammonium salt (ABTS) for ELISA

ABTS (10 mg) was dissolved in H_2O (0.6 mL) before the addition of 0.2 mL to 0.05 M citric acid/NaOH, pH 4.0 (10 mL). Just before use, 30% H_2O_2 (10 µL) was added to the solution. The solution was kept away from light until use.

2.2.8.5. *Screening of hybridoma clones*

Hybridoma clones were screened for the production of monoclonal antibodies against the corresponding antigen used to raise the antibodies by ELISA with a sheep anti-mouse HRP-conjugated antibody detection system. A non-related peptide conjugate and BSA were used as false-positive and negative controls, respectively. Briefly, hybridoma clone media (50 µL) and 1% BSA in 20 mM Tris/HCl, 0.25 M NaCl, pH 7.2 (50 µL), was added to the wells in Costar® 96-well vinyl plates pre-coated with the corresponding antigen, non-related peptide conjugate and BSA (5.0 µg/mL, 100 µL/well) diluted in 0.1 M $NaHCO_3$ and incubated (RT, 2 hours). Plates were washed (6x, 20 mM Tris/HCl, 0.25 M NaCl, pH 7.2) in a microtitration plate washer before sheep anti-mouse HRP-conjugated antibody (100 µL of 1:1 000 dilution in 1% BSA in 20 mM Tris/HCl, 0.25 M NaCl, pH 7.2) was added to each well and incubated (RT, 1 hour). After incubation, the plates were washed and freshly prepared ABTS (section 2.2.8.4.1) was added (100 µL). The plates were then incubated on a DELFIA® plate shaker for 20 min (at speed 4) for colour development before the OD (410 nm) was read on a Ceres 900 HDI plate reader.

2.2.8.6. *Isotyping, cloning and freezing-down of hybridomas*

Hybridomas testing positive were expanded to T25 flasks in RPMI media (RPMI 1640 10.4 g/L, 10% FCS, 1x HT, 1% PS) until day 30. At that time, the media was changed to RPMI media with 10% FCS. Monoclonal antibodies were isotyped using an IsoStrip mouse monoclonal isotyping kit (Roche Diagnostics Corp., Indianapolis, IN, USA). Hybridomas deemed useful were cloned using the procedure described in section 2.2.1.7. Hybridomas were frozen-down using the protocol described in section 2.2.1.10.

2.2.8.7. *Purification of anti-N350 peptide conjugate monoclonal antibody*

Media from hybridomas was pooled and clarified by centrifugation (970 x g, 4°C, 10 min). The supernatant was filtered with a Ministart® single use syringe filter (0.2 µm) before loading onto a Hitrap™ protein G column (1.0 mL) (Amersham Pharmacia Biotech Inc., Uppsala, Sweden) connected to a BioLogic DuoFlow system using PBS, pH 7.2, as loading buffer. The flow rate was set at 0.5 mL/min with the fraction collector set to collect eluate in 0.5 mL fractions. All unbound proteins were removed by further washing with PBS (25 mL). The monoclonal antibody was then eluted with 0.1 M H_3PO_4/NaOH, pH 2.5, at 1.0 mL/min. The eluates were neutralised with Na_2HPO_4, pH 9.0 (200 µL/fraction). Eluted antibody was immediately dialysed against PBS, pH 7.2 (4°C, overnight).

2.2.8.8. *Quantification of antibodies*

Antibodies were quantified based on their absorbance at 280 nm using the formula of Harlow and Lane (1988):

$$OD_{280} = 1.4 \text{ for } 1.0 \text{ mg/mL protein}$$

2.2.8.9. *Europium labelling of anti-ASA polyclonal antibody*

Purified anti-ASA polyclonal antibody was labelled with Eu^{3+} chelate using the DELFIA® Eu-labelling kit 1244-302 (Wallac, North Ryde, NSW, Australia) according to the manufacturer's instructions. Labelled antibodies were purified on a Superose 12 HR 30 fast protein liquid chromatography (FPLC) column (1.0 x 30 cm, Amersham Pharmacia Biotech Inc., Uppsala, Sweden) connected to a BioLogic DuoFlow system. The column was equilibrated with 50 mM Tris/HCl, pH 7.8, 0.9% (w/v) NaCl (elution buffer) (30 mL). The sample (200 µL) was applied at a flow rate of 0.5 mL/min and eluted with elution buffer; 1.0 mL fractions were collected. The fractions with the labelled antibody were pooled and the concentration determined (section 2.2.8.8). BSA was added to purified labelled antibodies to a final concentration of 0.1% and stored in aliquots of 20 µL/tube at -20°C.

2.2.9. Epitope mapping of antibodies

Epitope mapping of antibodies was performed using Multipin™ peptide plates (Chiron Mimotopes Pty. Ltd., Clayton, Vic, Australia). The method used to synthesise peptides for epitope mapping was as described in Rodda and Tribbick (1996). A total of 84 peptides were synthesised. Each peptide was 12 amino acids in length and had an overlap of six amino acids with the previous peptide. The peptide represented the entire amino acid sequence of ASA. Six extra peptides were made, three each across the amino acid asparagine (N) at position 350, with N positioned at the first quarter, middle and last quarter of the peptide, respectively; three additional peptides were also made across the same position with serine (S) substituting N. The protocols used were those recommended by the manufacturer, and the processing steps involved are described below.

2.2.9.1. *Peptide pin plate cleaning*

The peptide pin plate was washed by sonication (15 min) in a Vibron sonicator (Galsonic Pty. Ltd., Valley View, SA, Australia) with preheated (60°C) disruption buffer (650 mL 10x PBS, 20 mL 10% SDS, 750 µL β-mercaptoethanol). The plate was then rinsed with preheated (60°C) Milli-Q water (2 x 30 sec) followed by a wash with preheated (60°C)

Milli-Q water (30 min). The peptide pin plate was then placed in preheated (60°C) MeOH for 30 sec. The entire cleaning process was carried out at least twice before proceeding to conjugate testing, as follows.

2.2.9.2. Peptide pin plate conjugate testing

The peptide pin plate was washed with PBS (10 min) before being placed into a Costar® 96-well vinyl assay plate containing 200 µL/well of blocking solution (PBS with 1% BSA and 0.1% Tween 20). This was then placed on a microtitration plate shaker (speed 5) at RT for 60 min. After washing with PBS (10 min, with shaking), the peptide pin plate was incubated in a new Costar® 96-well vinyl assay plate containing 200 µL/well of HRP-conjugated secondary antibody (1:1 000 dilution with PBS containing 1% BSA and 0.1% Tween 20 (v/v)) and incubated at RT (1 hr, with shaking, speed 5). The peptide pin plate was then washed with PBS (4 x 10 min) before incubation (20 min, with shaking, speed 5) in the same Costar® 96-well vinyl assay plate containing 200 µL/well of freshly made ABTS substrate (section 2.2.8.4.1). The OD was then measured at 410 nm; an OD reading of 0.3 or lower was required for each pin before epitope mapping was performed.

2.2.9.3. Preparation of primary antibody

Antibody for epitope mapping was pre-absorbed by incubation with ovalbumin/BSA coupled to Affi-Gel 10 (Bio-Rad Laboratories, Hercules, CA, USA) by incubation at 4°C, overnight. Albumin-absorbed antibody was then diluted to 1:1 000 in PBS with 1% BSA and 0.1% Tween 20 (v/v), pH 7.2, before being used in epitope mapping, as described below.

2.2.9.4. Primary antibody testing

To epitope map antibodies, the peptide pin plate was placed in a Costar® 96-well vinyl assay plate containing 200 µL/well of blocking solution (PBS with 1% BSA and 0.1% Tween 20, pH 7.2) for 1 hr, with shaking, on a microtitration plate shaker (RT, speed 5). The pin plate was washed with PBS containing 0.1% Tween 20 (v/v) before incubation (4°C, overnight) in a new Costar® 96-well vinyl assay plate containing 200 µL/well of primary antibody (1:1 000 dilution in PBS with 1% BSA and 0.1% Tween 20 (v/v), pH 7.2). The pin plate was then washed with PBS (1 hr, with shaking, speed 5) before incubation (1 hr, with shaking, RT) with 200 µL/well of secondary antibody (HRP-conjugated sheep anti-mouse or donkey anti-sheep [albumin-absorbed], 1:1 000 dilutions in PBS with 1% BSA and 0.1% Tween 20 (v/v), pH 7.2). The pin plate was washed with PBS

(3 x 10 min) before being placed in a new Costar® 96-well vinyl assay plate containing 200 µL/well of freshly prepared ABTS solution (section 2.2.8.4.1) for colour development on a microtitration plate shaker (with shaking, speed 5). The OD (410 nm) was read on a Ceres HDI plate reader after 10 min and 20 min of incubation.

2.2.10. Determination of ASA with immune-based assays

Two immune-based assays have been developed in this study and utilised to determine ASA activity and protein in biological samples. The protocols for carrying out the assays are described below.

2.2.10.1. Immune-capture of ASA activity in dried blood spots and skin fibroblast lysates

ASA enzyme activity in dried blood spots was determined by eluting two blood spots (3.0 mm in diameter) in pre-coated (anti-ASA polyclonal antibody, 5.0 µg/mL) wells of Immunlon® 4HBX Removawell® strips. The blood spots were eluted in 0.1 M sodium acetate/acetic acid buffer, 0.1% heat-treated BSA, pH 5.0 (200 µL) for 1 hr, with shaking, on a microtitration plate shaker (RT, speed 4) before incubation (4°C, overnight). After incubation, the plate was shaken (speed 4, 30 min) and the filter papers removed. The plate was then washed (6x) with 20 mM sodium acetate/acetic acid buffer, pH 5.0, using a microtitration plate washer.

Depending on the cell line assayed, ASA activity in SF lysates was determined with different quantities of lysate. The quantity of sample used in the assay was as follows: 2 to 5 µL for unaffected SF lysate; 25 µL for ASA-PD SF lysate; and 40 µL for MLD SF lysate. Briefly, up to 40 µL sample was placed in pre-coated wells (anti-ASA polyclonal antibody, 5.0 µg/mL) of Immunlon® 4HBX Removawell® strips. The volume in the wells was then made up to 100 µL by the addition of 0.1 M Tris/HCl, 0.25 M NaCl buffer, pH 7.2, containing 0.1% heat-treated BSA, and the plates were incubated at 4°C overnight. After incubation, the plate was washed (6x) with buffer (0.1 M Tris/HCl, 0.25 M NaCl, pH 7.2) on a microtitration plate washer.

Immune-captured ASA activity in dried blood spots and SF lysates was determined by adding 5.0 mM 4-MUS, 0.1 M sodium acetate/acetic acid, 0.1% heat-treated BSA, pH 5.0 (100 µL) to each well. The plate was then sealed with Linbro® plate sealer (ICN Biomedicals Inc., Aurora, WI, USA), placed in a plastic zip-bag, sealed to prevent

evaporation, and incubated at 37°C for 24 hrs. The enzyme reaction was stopped by the addition of 0.2 M glycine/NaOH buffer, pH 10.7 (100 µL/well), and the fluorescence read on a Perkin-Elmer 1420 multilabel counter. Wt ASA (40 ng/mL) was used to generate the calibration curve by a 1:2 serial dilution across the wells, with a final concentration ranging from 2.0 ng/well to 2.0 pg/well. The specific activity of the calibrator was determined on the same day using the free assay tube method, as described in section 2.2.1.9.

2.2.10.2. Immune-quantification of ASA protein in dried blood spots and skin fibroblast lysates

ASA protein was quantified from single dried spots (3.0 mm in diameter) eluted in pre-coated (anti-ASA polyclonal antibody, 5.0 µg/mL) wells of Immunlon® 4HBX Removawell® strips. The blood spot was eluted in DELFIA® assay buffer (Wallac, North Ryde, NSW, Australia) (100 µL), with shaking, on a microtitration plate shaker (RT, speed 4, 1 hr) before incubation at 4°C, overnight. After incubation, the plate was shaken (RT, speed 4, 30 min) and the filter papers removed. The plate was then washed (6x) with DELFIA® wash buffer (Wallac, North Ryde, NSW, Australia) on a DELFIA® plate washer (Wallac, North Ryde, NSW, Australia).

The quantity of SF lysate used in the ASA protein assay was as follows: 2.0 to 5.0 µL for unaffected controls; 25 µL for ASA-PD individuals; and 40 µL for MLD patients. Briefly, up to 40 µL sample was placed in pre-coated (anti-ASA polyclonal antibody, 5.0 µg/mL) wells of Immunlon® 4HBX Removawell® strips. The volume in the wells was then made up to 100 µL by the addition of DELFIA® assay buffer and the plate was incubated at 4°C, overnight. The plate was washed (6x) with DELFIA® wash buffer on a DELFIA® plate washer.

The amount of immune-captured ASA protein in the dried blood spots and SF lysates was determined by the addition of DELFIA® assay buffer (100 µL) containing 0.2 µg/mL of Eu^{3+}-labelled anti-ASA polyclonal antibody to each well followed by incubation at 4°C, overnight. The plate was washed (6x) with DELFIA® wash buffer on a DELFIA® plate washer before DELFIA® enhancement solution (Wallac, North Ryde, NSW, Australia) was added (200 µL/well). The plate was shaken (15 min) before fluorescence was read on a DELFIA 1234 research fluorometer (Wallac, North Ryde, NSW, Australia). Wt ASA calibrator (40 ng/mL) was used to generate the calibration curve by serial dilution of 1:2 across the wells, with a final concentration ranging from 2.0 ng/well to 2.0 pg/well.

2.2.11. Preparation of the calibrator for immune-based assays

The concentration of the Wt ASA used as a calibrator for the immune assays was determined using the protein determination method described in section 2.2.5. The enzyme was then diluted to 1.0 μg/mL with DELFIA® assay buffer for the immune-quantification protein assay, and 0.1 M sodium acetate/acetic acid buffer, 0.1% heat-treated BSA, pH 5.0, for the immune-capture activity assay. The diluted Wt ASA calibrator was stored at -20°C in aliquots of 60 μL/tube until use.

2.2.12. Skin fibroblast culture

Human SF were established from primary skin biopsies. SF cell lines were cultured in Basal Media Eagle (BME) (10 mL) containing 10% (v/v) FCS in 75 cm^2 culture flasks, with incubation in a humidified atmosphere (5% CO^2, 37°C) and media changed every four-days.

2.2.13. Harvesting of skin fibroblasts

SF were harvested using neat trypsin-versene. Briefly, SF were washed with Dulbecco's PBS (3 x 10 mL) before neat trypsin-versene (2.0 mL) was added and left to stand (RT, 3 min). The flask was gently tapped to dislodge the cells, which were then transferred to a 10 mL sterile tube containing 8.0 mL of Dulbecco's PBS with 1% FCS. The tube was then centrifuged (700 x g, 5 min) and the supernatant discarded. The cell pellet was washed with Dulbecco's PBS (10 mL), centrifuged (700 x g, 5 min) and the supernatant discarded. The cells were washed two more times and the cell pellet was stored at -20°C.

2.2.14. Preparation of sulphatide stock and its incorporation in culture media

Bovine brain sulphatide was prepared to a stock solution (20 mM) in chloroform/methanol (2:1 [v/v]). To prepare 25 mL of SF culture media containing 64 μM of sulphatide, 80 μL of stock solution (20 mM) was added to 25 mL of pre-warmed (37°C) BME containing 5% heat-inactivated FCS and 1% penicillin/streptomycin in a sterile 50 mL Falcon centrifuge tube, and mixed gently by inverting the tube for at least 5 min. This preparation was used immediately or maintained at 37°C until use.

2.2.15. Sulphatide-loading for cultured skin fibroblasts

SF were cultured as described in section 2.2.12. At one-week post-confluence the cells were washed with Dulbecco's PBS (3 x 10 mL) and BME (8.0 mL) with 5% heat-

inactivated FCS (HIFCS), 1% penicillin/streptomycin; 64 μM bovine brain sulphatide (Matreya Inc., Pleasant Gap, PA, USA) was added and the cells were incubated (5% CO_2, 37°C) for up to eight-days. Cells were then harvested as described in section 2.2.13, and the pellets stored at -20°C until use.

2.2.16. Preparation of skin fibroblast lysate

Cell pellets were resuspended in either Tris-NaCl + 0.1% NP 40 (for enzyme assays) or in sterile water for mass spectrometry experiments (200 μL/75 cm^2 culture flask) and transferred to Eppendorf tubes. The tubes were placed in a container filled with crushed ice to keep the temperature low for the suspension. Sonication was carried out using a Ystrom sonicator (Technic International Inc., Westwood, NJ, USA) for 20 sec, with the power set at 8 and tune set at 3.5. After sonication, the cell suspension was centrifuged (13 800 x g, 5 min, 4°C) and the supernatant stored at -20°C until use.

2.2.17. Sample preparation for mass spectrometry experiments

Urine and SF lysates were used in the mass spectrometry experiments: urine was subjected to lipid extraction using the method of Bligh and Dyer (1959), and SF lysates were subjected to lipid extraction using the method of Folch *et al.* (1957) with some modification. The protocols for both extraction methods are briefly outlined below.

2.2.17.1. Sample extraction using the method of Bligh and Dyer

Urine (1.5 mL) was added to screw-cap Pyrex® culture tubes (size 16 x 100 mm; Corning Inc., New York, USA) containing chloroform/methanol (1:2 [v/v], 5.6 mL). Internal standards (ISTD) consisting of Sulp16:0 (2.5 nmol) and a mixture of Cer17:0, GC16:0-*d3*, G_{M2}, LC16:0-*d3*, PC28:0, PG28:0 and PI32:0 (400 pmol/each) were then added to each tube. The tubes were shaken (150 rpm, 10 min) and left to stand (RT, 1 hour). Phase partitioning was promoted by the addition of chloroform (1.9 mL) and Milli-Q® water (1.9 mL). The tubes were shaken again (150 rpm, 10 min) before centrifugation (830 x g, 2 min). The upper phase was gently transferred to a new tube and kept aside for ganglioside extraction (see section 2.2.17.3); the lower phase was washed by the addition (0.5 mL) of synthetic upper phase, vortexed and centrifuged (830 x g, 2 min) before the upper phase was removed and discarded. The samples were dried under N_2 flow at 40°C on a Reactivap™ evaporating unit with a reacti-therm heating unit (Pierce Chemical Co., Rockford, IL, USA). The dried lipid extract was then resuspended in 200 μL of methanol containing 10 mM ammonium formate prior to analysis by ESI-MS/MS.

2.2.17.2. Sample extraction using the method of Folch

SF lysates (100 µL) were added to screw-cap Pyrex® culture tubes containing chloroform/methanol (2:1 [v/v], 2.0 mL). ISTD consisting of Sulp16:0 (2.5 nmol) and a mixture of Cer17:0, GC16:0-*d3*, GM2, LC16:0-*d3*, PC28:0, PG28:0 and PI32:0 (400 pmol/each) were then added to each tube. Tubes were shaken (150 rpm, 10 min) and left to stand (RT, 1 hour). Phase partitioning was promoted by the addition of Milli-Q® water (0.4 mL). Tubes were shaken again (150 rpm, 2 min) before centrifugation (1 108 x g, 10 min). The upper phase was gently transferred to a new tube and set aside for ganglioside extraction (section 2.2.17.3); the lower phase was washed by the addition (0.5 mL) of synthetic upper phase, vortexed and centrifuged (830 x g, 2 min) before the upper phase was removed and discarded. The lower phase was dried under N_2 flow at 40°C on a Reactivap™ evaporating unit and a reacti-therm heating unit. The dried lipid extract was resuspended in 200 µL methanol containing 10 mM ammonium formate prior to analysis by ESI-MS/MS.

2.2.17.3. Ganglioside extraction

The upper phase from either the Bligh and Dyer or Folch extraction methods (sections 2.2.17.1 and 2.2.17.2) was loaded onto a primed (3 x 1.0 mL methanol followed by 3 x 1.0 mL Milli-Q® water) ISOLUTE-96 C18 column (25 mg; International Sorbent Technology Ltd., Mid Glamorgan, UK) and placed on a Supelco Visiprep™ 24-position extraction tank (Sigma Aldrich Pty. Ltd., Castle Hill, NSW, Australia). After the upper phase had completely entered the solid phase, the column was washed with Milli-Q® water (3 x 1.0 mL). The gangliosides were eluted (2 x 1.0 mL methanol) and collected into a clean glass tube and dried under N_2 flow at 40°C on a Reactivap™ evaporating unit and a reacti-therm heating unit. The dried lipid extract was resuspended in 200 µL methanol containing 10 mM ammonium formate prior to analysis by ESI-MS/MS.

2.2.18. Mass spectrometry

All mass spectrometric analyses were performed on a PE Sciex API-3000 triple-quadrupole mass spectrometer (Perkin-Elmer Sciex, Foster City, CA, USA) equipped with a turbo-electrospray ion source. All samples (20 µL) were injected into the turbo-electrospray ion source (200°C) using a Gilson 233 autosampler (Gilson Inc., Middleton, WI, USA) at a flow rate of 80 µL/min using an Agilent 1100 binary HPLC system. Where necessary, samples were infused manually, as described in section 2.2.18.5. Nitrogen was used as the

collision gas at a pressure of 4 x 10^{-5} Torr; air was used as the nebuliser gas. Neat methanol was used as the carrier solvent for all analytes. Quantification of analytes was performed using MRM mode. For each quantitative measurement ions were monitored for 100 milliseconds (ms) each over the injection period and the consecutive scans were averaged. The ions monitored for each lipid type are detailed in the following sections. The ratio of the signal intensity for each ion to the respective ISTD was used to calculate concentrations, assuming an equal response. Thus, the ratio of the signal intensity from GC16:0 to GC16:0-*d3* was used to calculate the concentration of GC16:0. Analysis of mass spectrometric data was performed using a combination of Analyst version 1.1 software with ChemoView NT version 1.2 software (Perkin-Elmer Sciex, Foster City, CA, USA).

2.2.18.1. Determination of sulphatide by ESI-MS/MS

Urine extracts (140 µL/well; section 2.2.17.1) or SF extracts (140 µL/well; section 2.2.17.2) were pipetted into a 96-well V-shape microtitre plate (Greiner Bio-One GmbH, Frickenhausen, Germany) and covered with aluminium foil before analysis. Sulphatide analysis was carried out on these samples in negative ion mode using MRM mode with ion pairs as shown in Table 2.1. A total of 19 molecular species were monitored, representing 18 prominent species of sulphatide and Sulp16:0 (ISTD).

The MS settings for sulphatide analysis were as follows: declustering potential (DP) = -100; focusing potential (FP) = -310; collision energy (CE) = -120V; collision cell exit potential (CXP) = -15.00; exit potential (EP) = -10.00; ion spray voltage (IS) = -4 500; nebuliser gas setting (NEB) = 3.00; curtain gas setting (CUR) = 10.00; and collision cell gas (CAD) = 4.00. Other instrument settings were as specified in section 2.2.18.

2.2.18.2. Determination of phospholipids by ESI-MS/MS

Phospholipid analysis was carried out on the same samples used for sulphatide analysis (section 2.2.18.1). Analysis was carried out in negative ion mode using MRM mode with ion pairs as shown in Table 2.2. The MRM method used to determine the phospholipid species measured both phosphatidylglycerol (PG) and lysobisphosphatidic acid (LBPA), both of which are structurally similar (Matsuzawa and Hostetler, 1979), hence the amount measured using the ion pairs for MRM can represent both or either species. LBPA is also referred to in the literature as bismonoacylglycerophosphate (BMP). A total of 13 PG/LBPA species and 10 phosphatidylinositol (PI) species were monitored; PG28:0 and PI32:0 were used as ISTD.

The MS settings for phospholipid analysis were as follows: DP = -80; FP = -330; CXP = -10.00; EP = -10.00; IS = -4 200; NEB = 5.00; CUR = 10.00; CAD = 2.00. Other instrument settings were as specified in section 2.2.18.

2.2.18.3. Determination of glycolipids, sphingomyelin and phosphatidylcholine by ESI-MS/MS

Prior to the determination of urinary glycolipids, sphingomyelin and phosphatidylcholine, the 96-well, V-shape microtitre plate used for the analysis of sulphatide and phospholipids (sections 2.2.18.1 and 2.2.18.2, respectively) was removed and the samples were dried under a gentle flow of N_2 on a dry-block heater (Ratek Instruments Pty. Ltd., Vic., Australia). The samples were then resuspended with the addition of methanol containing 10 mM ammonium formate (100 µL/well). The plate was covered with aluminium foil before analysis was carried out in positive ion mode using MRM mode with ion pairs as shown in Table 2.3. Seven ceramide (Cer) species, six glucosylceramide (GC) species, six lactosyl ceramide (LC), six ceramide trihexoside (CTH) species, seven phosphatidylcholine (PC) species and three sphingomyelin (SM) species were monitored; Cer17:0, GC16:0-*d3*, LC16:0-*d3* and PC28:0 were used as ISTD.

The MS settings for DP and FP in Cer, GC, LC, and CTH species analysis are shown in Table 2.4. All of these glycolipid species have the same value for the following: CXP = 12.00; EP = -10.00; IS = 5 000 NEB = 6.00; CUR = 8.00; and CAD = 2.00. The MS setting for SM and PC species analysis was as follows: DP = 96; FP = 230; CXP = 12.00; EP = 10.00; IS = 5 000; NEB = 6.00; CUR = 8.00; and CAD = 2.00. Other instrument settings were as specified in section 2.2.18.

2.2.18.4. Determination of gangliosides by ESI-MS/MS

Urine or SF samples extracted for ganglioside analysis (section 2.2.17.3) were pipetted into a 96-well, V-shape microtitre plate (100 µL/well) and covered with aluminium foil before analysis. Determination of gangliosides in these samples was carried out in negative ion mode using MRM mode with ion pairs as shown in Table 2.5. Four G_{M3} species were monitored; G_{M2}22:1 and G_{M2}24:1 were used as ISTD.

The MS settings for DP, FP, CE and CXP for the ganglioside species analysis are listed in Table 2.6. All ganglioside species have the same values for the following parameters; EP =

-10.00; IS = -4 200; NEB = 10.00; CUR = 6.00; and CAD = 4.00. Other instrument settings were as specified in section 2.2.18.

2.2.18.5. Infusion method

Infusion of samples into the mass spectrometer was carried out with samples diluted in a mixture of chloroform/methanol (1:4) using a SGE Hamilton 100 µL syringe (Sigma Aldrich Pty. Ltd., Castle Hill, NSW, Australia) with a Harvard apparatus syringe pump (5.0 µL /min). Other instrument settings were as specified in section 2.2.18.

Table 2.1 Sulphatide species and ion pairs used for MRM analysis

Sulphatide species[a]	Ion pair[b]
Sulp16:0[c]	778.8/97.0
hSulp16:0	794.8/97.0
Sulp18:0	806.7/97.0
hSulp18:0	822.8/97.0
Sulp20:0	834.7/97.0
hSulp20:1	848.8/97.0
hSulp20:0	850.8/97.0
Sulp22:0	862.7/97.0
Sulp23:0	876.9/97.0
hSulp22:0	878.9/97.0
Sulp24:1	888.7/97.0
Sulp24:0	890.7/97.0
hSulp23:0	892.8/97.0
hSulp24:1	904.8/97.0
hSulp24:0	906.8/97.0
hSulp25:1	918.8/97.0
hSulp25:0	920.8/97.0
dhSulp22:0	1024.7/97.0
dhSulp24:0	1052.7/97.0

[a] Sulp = sulphatide; hSulp = hydroxy sulphatide; dhSulp = dihexoxyl sulphatide;

[b] Ion pairs indicate Q1/Q3 settings

[c] ISTD

Table 2.2 Phospholipid species and ion pairs used for MRM analysis

Analytes[a]	Ion pair[b]	CE[c]
PG28:0[d]	665.5/227.2	-50
PG/LBPA16:0/22:6	793.5/255.2	-50
PG/LBPA16:1/20:4	767.5/253.3	-54
PG/LBPA18:1/18:0	775.6/281.3	-50
PG/LBPA18:1/18:1	773.5/281.3	-54
PG/LBPA18:1/18:2	771.5/281.3	-54
PG/LBPA18:1/20:4	795.5/303.2	-48
PG/LBPA18:1/22:5	821.6/281.3	-60
PG/LBPA18:1/22:6	819.5/281.3	-54
PG/LBPA18:2/22:6	817.5/279.2	-50
PG/LBPA20:4/22:6	841.5/303.2	-50
PG/LBPA22:5/22:5	869.5/329.3	-55
PG/LBPA22:6/22:5	867.5/329.3	-48
PG/LBPA22:6/22:6	865.6/327.3	-50
PI32:0[d]	809.5/255.2	-66
PI16:0/18:0	835.6/283.2	-61
PI16:0/20:4	857.5/255.2	-61
PI18:0/18:1	863.6/283.3	-67
PI18:0/18:1	865.6/283.3	-48
PI18:0/20:3	887.6/283.3	-73
PI18:0/20:4	885.6/283.3	-70
PI18:0/22:5	911.6/283.3	-73
PI18:1/18:1	861.6/281.3	-60
PI18:1/20:4	883.5/281.3	-70

[a] PG/LBPA = phosphatidylglycerol/lysobisphosphatidic acid; PI = phosphatidylinositol

[b] ion pairs indicate Q1/Q3 settings;

[c] collision energy used in analysis, unit in volts;

[d] ISTD.

Table 2.3 Glycolipid, sphingomyelin and phosphatidylcholine species and ion pairs used in MRM analysis

Analytes[a]	Ion pair[b]	CE[c]
Cer17:0[d]	552.7/264.4	37
Cer16:0	538.7/264.4	37
Cer20:0	592.7/264.4	37
Cer20:1	590.7/264.4	37
Cer23:0	636.7/264.4	37
Cer23:1	634.8/264.4	37
Cer24:0	650.7/264.4	37
Cer24:1	648.7/264.4	37
GC16:0-*d3*[d]	703.8/264.4	47
GC16:0	700.6/264.4	47
GC18:0	728.6/264.4	47
GC20:0	756.8/264.4	47
GC22:0	784.7/264.4	53
GC24:0	812.7/264.4	59
GC24:1	810.8/264.4	59
LC16:0-*d3*[d]	865.4/264.4	59
LC16:0	862.4/264.4	59
LC20:0	918.7/264.4	59
LC22:0	946.7/264.4	59
LC22:0-OH	962.7/264.4	59
LC24:0	974.8/264.4	59
LC24:1	972.8/264.4	59
CTH16:0	1024.8/264.4	75
CTH18:0	1052.7/264.4	75
CTH20:0	1080.9/264.4	75
CTH22:0	1108.9/264.4	75
CTH24:0	1136.9/264.4	75
CTH24:1	1134.9/264.4	75
PC28:0[d]	678.5/184.1	41
PC32:0	734.7/184.1	41
PC32:1	732.7/184.1	41
PC34:1	760.6/184.1	41
PC34:2	758.5/184.1	41
PC36:2	786.6/184.1	41
PC36:4	782.6/184.1	41
PC38:4	810.8/184.1	41
SM16:0	703.9/184.1	41
SM 22:0	787.8/184.1	41
SM 24:0	815.8/184.1	41

[a] Cer = ceramide; GC = glucosylceramide; LC = lactosyl ceramide; CTH = ceramide trihexoside; PC = phosphotidylcholine; SM = sphingomyelin;

[b] ion pairs indicate Q1/Q3 settings;

[c] collision energy used in analysis, unit in volts;

[d] ISTD

Table 2.4 Declustering potential and focusing potential values for glycolipid species

Analytes[a]	DP (volts)	FP (volts)
Cer	36	180
GC	56	270
LC	51	250
CTH	81	360

[a] Cer = ceramide; GC = glucosylceramide; LC = lactosyl ceramide; CTH = ceramide trihexoside;

Table 2.5 Ganglioside species and ion pairs used in MRM analysis

Ganglioside species[a]	Ion pair[b]
G_{M2}22:1[c]	1383.0/290.0
G_{M2}24:1[c]	1410.8/290.0
G_{M3}16:0	1151.9/290.0
G_{M3}22:0	1235.9/290.0
G_{M3}24:0	1263.1/290.0
G_{M3}24:1	1261.6/290.0

[a] G_{M2} and G_{M3} = monosialogangliosides;

[b] ion pairs indicate Q1/Q3 settings;

[c] ISTD

Table 2.6 Declustering potential (DP), focusing potential (FP), collision energy (CE) and collision cell exit potential (CXP) values for ganglioside species

Analytes[a]	DP (volts)	FP (volts)	CE (volts)	CXP (volts)
G_{M2}22:1	-66	-330	-82	-19
G_{M2}24:1	-71	-350	-84	-19
G_{M3}16:0	-91	-350	-64	-21
G_{M3}22:0	-101	-350	-74	-19
G_{M3}24:0	-96	-350	-74	-19
G_{M3}24:1	-81	-320	-70	-13

[a] G_{M2} and G_{M3} = monosialogangliosides

CHAPTER THREE

Expression, Purification and Characterisation of Wt ASA and N350S ASA Enzymes

3. Introduction and aims

One aim of this study was to improve the diagnostic procedures for MLD by the development of immune-based assays. To do so, ASA enzyme from a continuous and viable source was required for both the production of antibodies and ongoing developmental work. Thus, the two aims of this section of the study were, firstly, to obtain purified Wt ASA and N350S ASA enzymes from a viable source and, secondly, to characterise these enzymes before utilising them for the production of antibodies. The antibodies were subsequently used for the establishment of the immune-based assays (Chapter 4).

ASA is constitutively expressed and can be found in most tissues. ASA has been purified from a number of biological sources such as urine (Stevens *et al.*, 1975; Laidler *et al.*, 1985b), liver (James and Austin, 1979) and placenta (Gniot and Dzialoszynski, 1964). ASA has also been purified from a baby hamster kidney cell expression system by immuno-affinity purification of the culture media (Schmidt *et al.*, 1995; Lukatela *et al.*, 1998).

In this study, Wt ASA was generated using a CHO-K1 cell expression system. In addition to this, a mutant enzyme associated with ASA-PD (N350S ASA) was also generated using the same expression system. The N350S ASA CHO-K1 cell line was previously established by Harvey *et al.* (1998) in the Department of Genetic Medicine at the Women's and Children's Hospital, Adelaide, SA, Australia. CHO-K1 cells were used to express both enzymes, as this expression system had been successfully used for a number of other lysosomal enzymes such as α-glucosidase (Fuller *et al.*, 1995), sulphamidase (Bielicki *et al.*, 1998; Perkins *et al.*, 1999) and α-mannosidase (Berg *et al.*, 2001).

3.1. Expression of ASA in CHO-K1 cells

To establish the Wt ASA CHO-K1 cell expression system, the ASA cDNA in the pRSVN.07 expression vector (section 2.1.3) was transfected into CHO-K1 cells. The original full-length ASA cDNA in the HT 14/CP 8 pBluecript® vector was provided by Professor Volkmar Gieselmann (Biochemisches Institut, Christian-Albrecht-Universitat,

Kiel, Germany), and the reconstruction of the full-length ASA in the pRSVN.07 expression vector was performed by Dr J Harvey, as described in section 2.2.1.

3.1.1. Plasmid purification and transfection into CHO-K1 cells

Prior to transfection, the plasmid containing the ASA cDNA in the pRSVN.07 vector, designated as ASAp RSVN.07, was electroporated into competent *E. coli* cells using the method described in section 2.2.1.5, and purified using a QIAGEN plasmid midi/maxi kit (section 2.2.1.2). The purified plasmids were quantified (section 2.2.1.3) and the ASA cDNA was sequenced (section 2.2.1.4).

Transfection of CHO-K1 cells with the ASAp RSVN.07 vector was performed using the calcium phosphate transfection method described in section 2.2.1.6. As a negative control, the pRSVN.07 vector (5 μg/100 μL) was transfected into CHO-K1 cells under the same conditions, and a further two flasks of CHO-K1 cells were also grown using the same media and conditions (untransfected controls). Colonies that were G 418-resistant were evident after one-week in selection media; the untransfected CHO-K1 cells had died during this period.

3.1.2. Demonstration of successfully transfected CHO-K1 cells

To demonstrate successful transfection or otherwise, 50 μL media from each mass culture flask was assayed for ASA activity using the free assay method described in section 2.2.1.8. Figure 3.1 shows the enzyme activity detected in the culture media: media from the ASAp RSVN.07-transfected cells was approximately 100-times higher than the media from the cells transfected with the pRSVN vector and the control CHO-K1 cells, both of which had negligible ASA activity.

3.1.2.1. Cloning and selection of CHO-K1 cells expressing the highest level of ASA enzyme

The cloning of successfully transfected cells was carried out on day 21 using the protocol described in section 2.2.1.7. The first round of selection was performed on day 14 post-cloning; 22 clones were selected from a total of 56 wells that had colonies, based on the amount of enzyme activity detected in the culture media. These clones were expanded using Corning® 24-well tissue culture plates. A second round of selection was carried out one-week later and the six highest-expressing clones were selected, expanded and frozen (section 2.2.1.10). ASA activity detected in the culture media of these six clones, designated Wt 1 through to Wt 6, ranged from 205 to 387 pmol/min/mL. The highest-

expressing clone, designated Wt 3, was re-cloned, expanded and used to produce the Wt ASA enzyme.

3.2. CHO-K1 expression system for N350S ASA

A CHO-K1 cell line producing N350S ASA was previously established by Dr J Harvey at the Women's and Children's Hospital, Adelaide, SA, Australia. Construction of mutant N350S ASA cDNA, its incorporation into a CHO-K1 cell line and its characterisation have been reported previously (Harvey *et al.* 1998). This cell line was expanded and cloned (section 2.2.1.7) before being used to produce N350S ASA.

3.2.1. Optimisation of culture conditions for ASA enzyme expression

CHO-K1 cells expressing Wt ASA and N350S ASA (seven flasks each) were grown to confluence in F 12 with 10% FCS. The media in each flask was changed to F 12; MEM; COON'S; F 12 with 10% FCS; COON'S with 1% FCS; COON'S with 10% FCS; and COON'S with 10% FCS plus 1.0% DMSO, respectively. Media was conditioned for three-days and sampled for the determination of enzyme activity (section 2.2.1.8).

The amount of enzyme activity detected in the media from each flask is summarised in Table 3.1: both the Wt ASA- and N350S ASA CHO-K1-expressing cells had the highest enzyme activity when cultured in COON'S media, at 599 pmol/min/mL and 737 pmol/min/mL, respectively. Based on these results, COON'S media without FCS supplement was used for the CHO-K1 cultures.

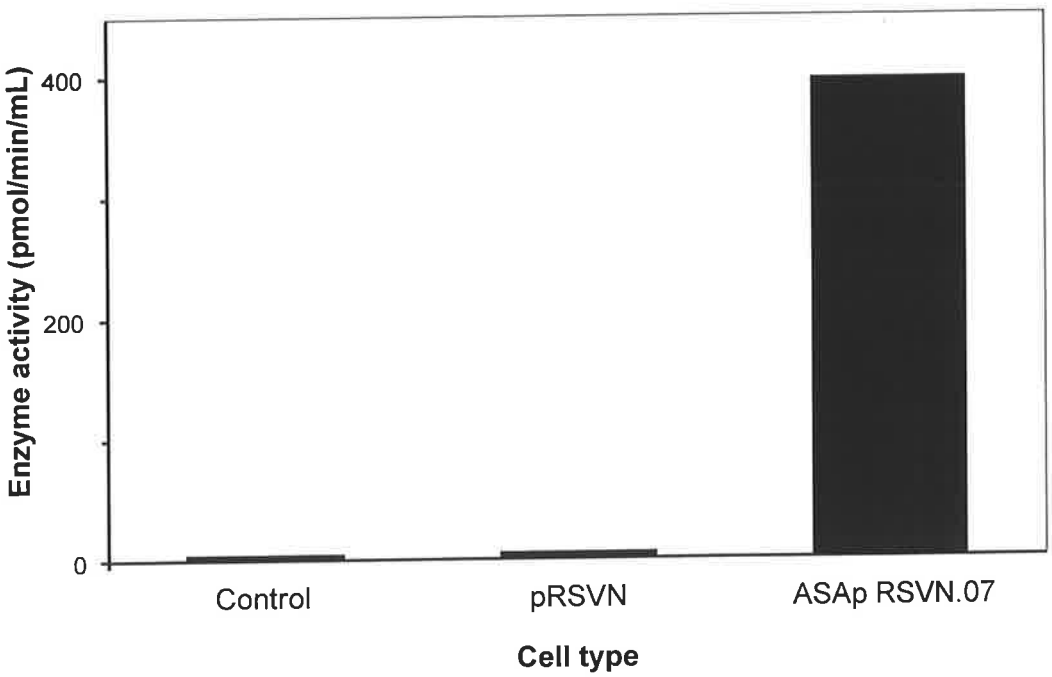

Figure 3.1 Enzyme activity detected in media from transfected and non-transfected cells

Transfected CHO-K1 cells (pRSVN vector and ASAp RSVN.07) were grown in F 12 supplemented with 10% FCS and G 418 (750 μg/mL). The control (CHO-K1 cells) was grown in the same media without G 418 and conditioned for the same period. The media was conditioned for six-days before 50 μL was used to determine enzyme activity using the free assay method (section 2.2.1.8).

Table 3.1 Expression of Wt ASA and N350S ASA in CHO-K1 cells

Culture media	Activity (pmol/min/mL)	
	Wt ASA	N350S ASA
F 12	256	252
MEM	389	327
COON'S	599	737
F 12, 10% FCS	298	348
COON'S, 1.0% FCS	345	585
COON'S, 10% FCS	157	71
COON'S, 10% FCS, 1.0% DMSO	68	121

Wt ASA and N350S cell lines (seven flasks each) were grown to confluence in F 12 with 10% FCS before being changed to the media listed in the table. Media was conditioned for three-days before 50 μL of each was used for the determination of ASA activity, as described in section 2.2.1.8.

3.3. Purification of ASA enzyme

The use of affinity chromatography to purify ASA from cell culture media has been previously reported (Schmidt *et al.*, 1995; Lukatela *et al.*, 1998) and is the ideal purification method. However, in this study, an antibody against the ASA enzyme was not available, hence a three-step purification protocol using two chromatography columns was developed to purify Wt ASA and N350S ASA using conditioned media from the CHO-K1 cell expression systems. The first step involved concentration of the conditioned media, followed by the use of AEC to partially purify the media; the final step involved the use of SEC. The development of the purification protocols is described below.

3.3.1. Anion exchange chromatography

The initial procedure using AEC to purify ASA enzyme was performed on a 1.0 mL UNO^{TM} Q1 anion exchange column (Bio-Rad Laboratories, Hercules, CA, USA) connected to a BioLogic DuoFlow system at a flow rate of 1.0 mL/min. Briefly, media from a Wt ASA CHO-K1 expression system was concentrated (section 2.2.2.1) and dialysed against Buffer A (4°C, overnight). Dialysed media (2.0 mL) was then applied to the column, followed by a wash with Buffer A (15 mL). Elution was carried out using a linear gradient (0-25%) from Buffer A to Buffer B (40 mL), followed by a second gradient of 25-100% Buffer B (5.0 mL). The final concentration (100% Buffer B) was maintained (5.0 mL) before a final gradient of 100-0% Buffer B (2.5 mL) was used to return the column to its starting condition. Fractions (1.0 mL) were collected and assayed for enzyme activity (section 2.2.1.8). Figure 3.2 (Panel A) shows the chromatogram of ASA separation, with absorbance (280 nm) plotted against enzyme activity.

3.3.1.1. Optimisation of ASA enzyme purification with anion exchange chromatography

ASA enzyme separation by AEC was further optimised using a combination of gradient and isocratic elution. In this experiment, pooled Wt ASA media was concentrated (section 2.2.2.1) and dialysed against Buffer A. Dialysed media (5.0 mL) was loaded onto the AEC column that had been equilibrated with Buffer A (20 mL), and washed with Buffer A (10 mL) before elution. The enzyme fractions were eluted with a linear gradient from 0 to 7% of Buffer B (5.0 mL), followed by an isocratic flow (15 mL). A second linear gradient from 7 to 12% of Buffer B (2.0 mL) was then applied, followed by another isocratic flow (18 mL), before the application of a final gradient from 12 to 100% of Buffer B (10 mL). This final concentration was maintained (5.0 mL) before the gradient was reduced to 0% Buffer B (2.0 mL) to return the column to its starting condition.

Fractions (1.0 mL) were collected and assayed for enzyme activity (section 2.2.1.8). Figure 3.2 (Panel B) shows the chromatogram of ASA separation, with absorbance (280 nm) plotted against the amount of enzyme activity detected. Compared with the linear gradient elution (section 3.3.1), this elution protocol resulted in a higher purification fold (>3) and the enzyme was eluted as a single peak in a total volume of 10 mL.

3.3.1.2. Scaling-up

The final elution protocol was later adapted to a larger volume AEC column using Self Pack™ POROS® 20 R1 media packed in a Pharmacia K9/15 column with the following modifications: the flow rate was set at 2.0 mL/min and 1.0 mL fractions were collected; the wash volume after sample loading was increased from 10 mL to 15 mL, followed by a steeper gradient of 0-7% Buffer B (4.0 mL); the isocratic flow was also increased (35 mL); the second isocratic flow was decreased from 18 mL to 7.5 mL; and the increase of the final gradient from 12 to 100% of Buffer B was also decreased from 5.0 to 4.0 mL. Figure 3.3 (Panel A) shows the chromatogram of the AEC using the finalised protocol. The use of the larger column enabled the run time to be reduced by 30 min. Scaling-up to a larger column was necessary to accommodate a higher level of protein load from larger volumes of media.

3.3.2. Size exclusion chromatography

The partially purified ASA enzyme fractions from AEC were pooled and concentrated (x10) using a 10 mL stirred-cell ultrafiltration unit with a Diaflo YM 10 ultrafiltration membrane before loading onto a Superose 6 HR 30 column connected to a BioLogic DuoFlow system at a flow rate of 0.5 mL/min; 20 mM sodium acetate/acetic acid buffer, 0.15 M NaCl, pH 5.0, was used as the loading buffer. Fractions (0.5 mL) were collected and assayed for enzyme activity (section 2.2.1.8). Figure 3.3 (Panel B) shows the chromatogram of ASA enzyme separation using SEC, with absorbance (280 nm) plotted against enzyme activity.

3.3.2.1. Polishing step using size exclusion chromatography

An additional polishing step was performed by pooling five fractions from eluates at 13 to 15 mL from the SEC run (Figure 3.3, Panel B). The eluates were concentrated to 250 µL using a Minicon filter cartridge (Sartorius, Weender Lanstr, Göttingen, Germany), and then reapplied to the SEC column using the protocol described in section 3.3.2. The resulting polishing effect is shown in Figure 3.3 (Panel C). By performing this step, the eluates at 13.5, 14.0 and 14.5 mL were found to have a purity of more than 95%.

3.3.3. Recovery of ASA enzyme from purification

The complete ASA enzyme purification process consisted of five steps. Media from each step was analysed for enzyme activity (section 2.2.1.8) and protein (section 2.2.5): Step 1, conditioned media (3.6 L) from the Wt ASA CHO-K1 expression system was concentrated (section 2.2.2.1) to approximately 250 mL with a three-fold purification achieved; Step 2, the media was further concentrated to 36 mL using a 250 mL stirred-cell ultrafiltration unit with a Diaflo YM 30 ultrafiltration membrane. The concentrated media was dialysed against Buffer A (4°C, overnight), clarified by centrifugation (970 x g, 10 min) and filtered through a Ministart® single use syringe filter (0.2 μm) to achieve a 25-fold purification; Step 3, the filtered media was loaded onto the AEC column and eluted as described in section 2.2.3. The eluate from 56 to 64 mL with enzyme activity was pooled (see Figure 3.3, Panel A) and a six-fold purification achieved; Step 4, the partially purified media was concentrated to approximately 250 μL using a 10 mL stirred-cell ultrafiltration unit with a Diaflo YM 10 ultrafiltration membrane, and a further 1.2-fold purification achieved; Step 5, the concentrated media was loaded onto a SEC column (section 2.2.3). The enzyme activity detected indicates that the enzyme was eluted between 12.5 and 15 mL, as shown in Panel B in Figure 3.3. Fractions at volumes 13.5 and 14.0 mL (1.0 mL) that contained the purified ASA were pooled and a further five-fold purification was achieved. Table 3.2 summarises the purification steps, recovery and the purification fold achieved for the Wt ASA enzyme. Enzyme with a specific activity of 2.2 μmol/min/mg protein was obtained through a 2,742-fold purification with 36.2% yield.

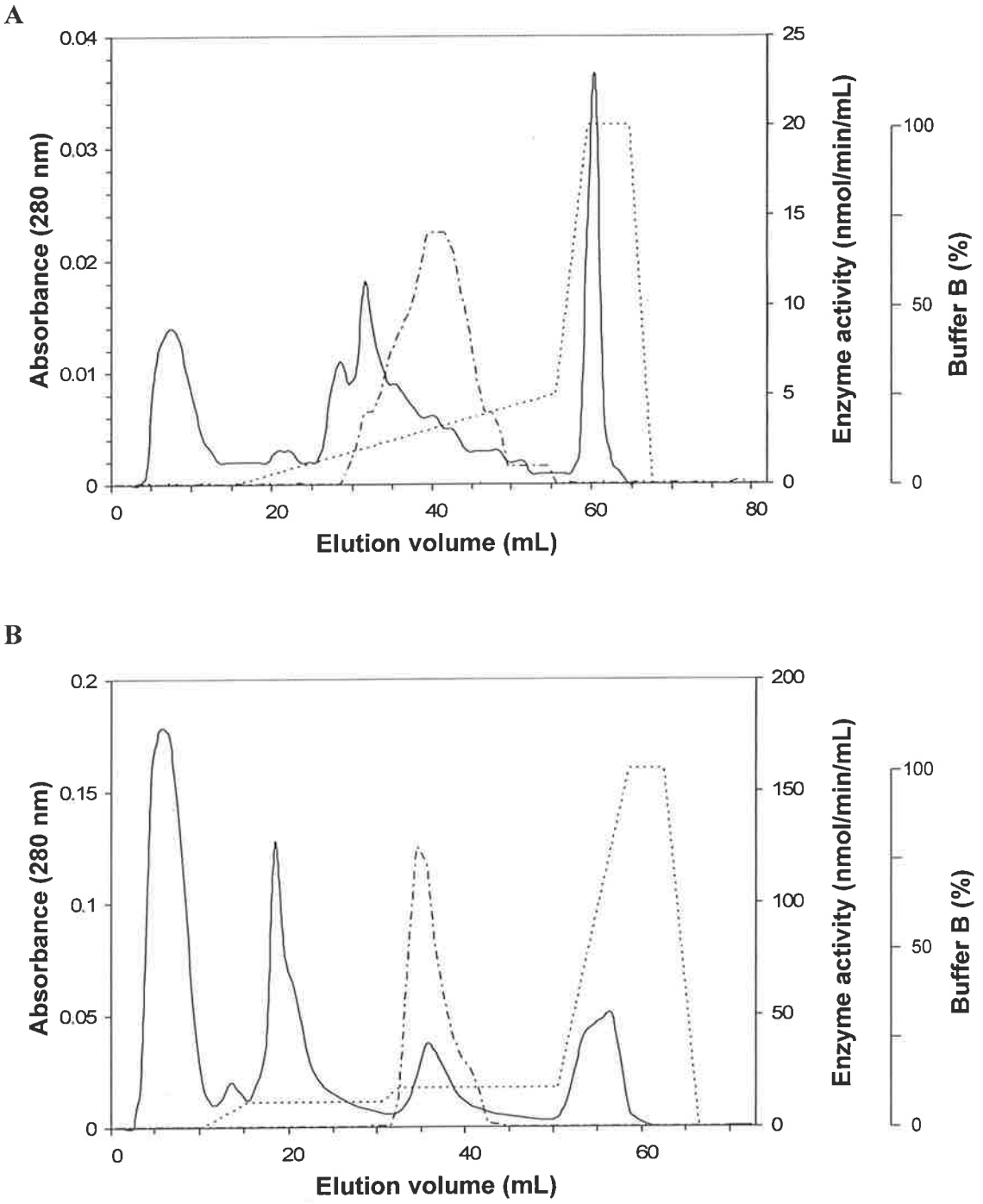

Figure 3.2 Anion exchange chromatography of ASA enzyme

Panel A shows the chromatogram of Wt ASA on a 1.0 mL UNO^{TM} Q1 anion exchange column. Dialysed Wt ASA media (2.0 mL) was loaded on the column and eluted with a linear gradient as described in section 3.3.1. Panel B shows the chromatogram of Wt ASA on the same column using a combination of gradient and isocratic elution, as described in section 3.3.1.1. The value of absorbance (280 nm) is represented by the solid line; enzyme activity is represented by the intermittent line; and the concentration of elution Buffer B is represented by the dotted line.

3.3.4. Determination of the purity of ASA enzyme

To determine the purity of the eluted enzyme from SEC, eluates at 13.5, 14.0 and 14.5 mL (Figure 3.3, Panel B) were subjected to SDS-PAGE (section 2.2.4). Visualisation of the gel was achieved by silver staining (section 2.2.4.2). Figure 3.4 shows the polyacrylamide gel image of purified Wt ASA: eluate at 13.5 mL (lane 1) showed one major polypeptide band at 58 kDa with a lesser band at 51 kDa, while eluate at 14.0 mL (lane 2) showed only one major band at 58 kDa; eluate at 14.5 mL showed one major polypeptide band at 58 kDa with two very faint bands at 64 kDa and 51 kDa; eluates at 13.5 and 14.0 mL were found to be of higher purity compared to eluate at 14.5 mL, based on the calculated specific activity of the enzyme.

3.4. Characterisation of the Wt ASA and N350S ASA enzymes

ASA was one of the first sulphatases to be identified and is the best known among all sulphatases (Roy, 1976). The physical and kinetic properties of this enzyme have been characterised from different tissues and biological sources. Depending on the origin of ASA, differences have been reported in its physical properties and kinetic values. Hence, structural and kinetic characterisation of the enzymes used in this study was performed to clarify the inconsistencies reported in the literature and to confirm the properties of the enzymes used for antibody generation and assay development.

3.4.1. Mw determination of the Wt ASA and N350S ASA enzymes by SDS-PAGE

To determine the Mw of these enzymes, purified Wt ASA and N350S ASA were run on SDS-PAGE under reducing conditions, as described in section 2.2.4. Visualisation of the gel was achieved by Coomassie staining (section 2.2.4.1). Figure 3.5 shows Wt ASA and N350S bands on the SDS-PAGE gel image captured using the UVItec-gel documentation system. The Mw of protein bands was determined using semi-log plots of the BenchMark™ protein ladder versus the migration distance travelled. The calculated Mw was 58 kDa for Wt ASA and 56 kDa for N350S ASA.

Figure 3.3 Anion exchange chromatography and size exclusion chromatography of ASA enzyme

Panel A shows the chromatogram of Wt ASA on a Pharmacia K9/15 column, packed with Self Pack™ POROS® 20 R1 media. Dialysed Wt ASA media (36 mL) was loaded onto the column and eluted with a combination of gradient and isocratic elution, as described in section 3.3.1.2. Eluate from 56 to 64 mL was pooled for further purification. Panel B shows the Wt ASA enzyme on the SEC column. Pooled and concentrated eluate from AEC was loaded onto the SEC column and eluted using the protocol described in section 3.3.2. Panel C shows the chromatogram of the Wt ASA enzyme obtained in the polishing step using the same SEC column. Eluate from 13 to 15 mL in the first SEC separation (Panel B) was pooled and concentrated using a Minicon filter cartridge before being loaded onto the same SEC column. The value of absorbance (280 nm) is represented by the solid line; enzyme activity is represented by the intermittent line; and the concentration of elution Buffer B is represented by the dotted line.

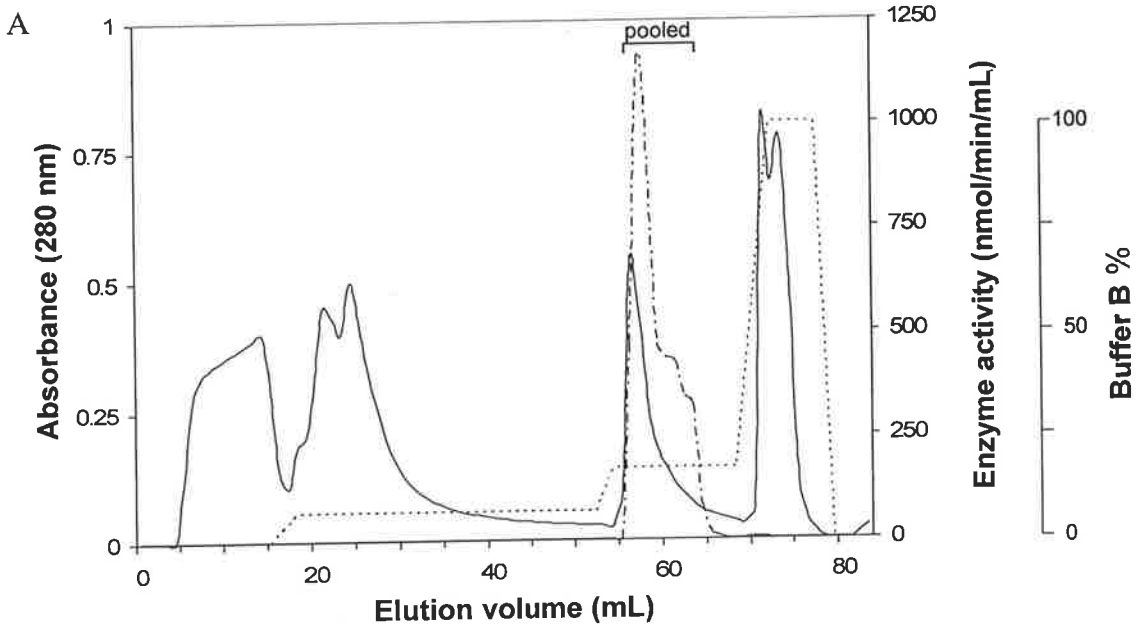
A
pooled
Absorbance (280 nm)
Enzyme activity (nmol/min/mL)
Buffer B %
Elution volume (mL)

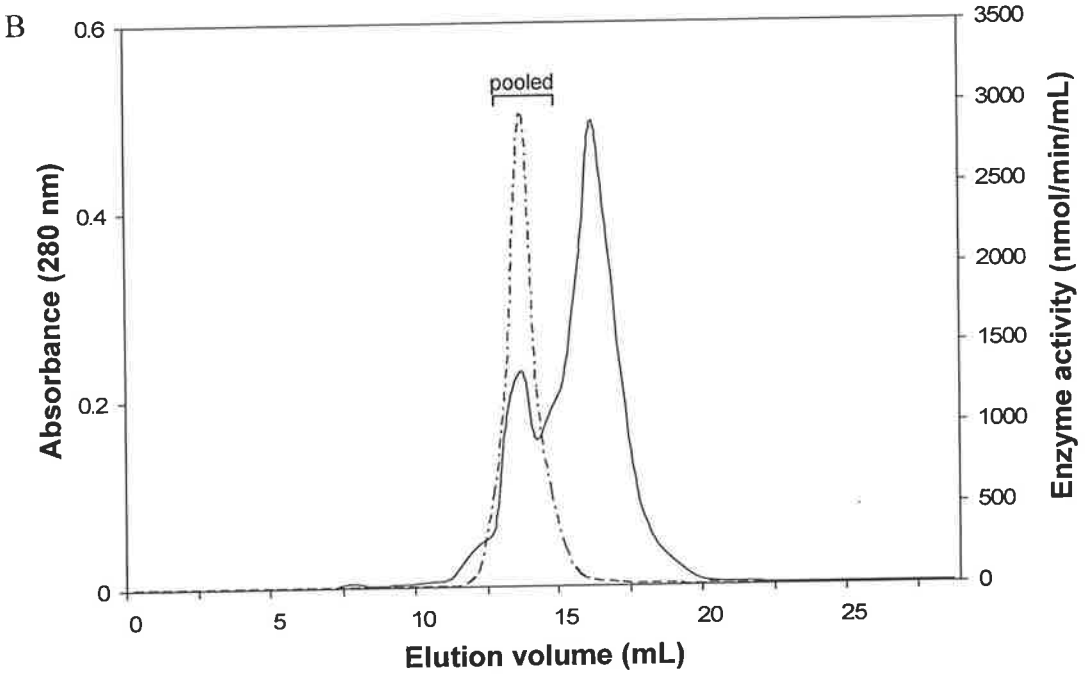
B
pooled
Absorbance (280 nm)
Enzyme activity (nmol/min/mL)
Elution volume (mL)

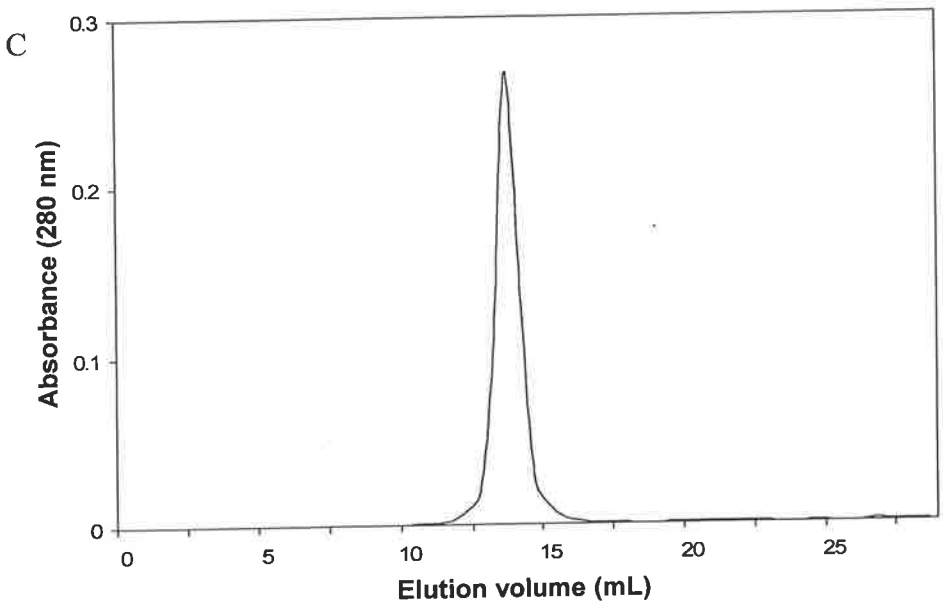
C
Absorbance (280 nm)
Elution volume (mL)

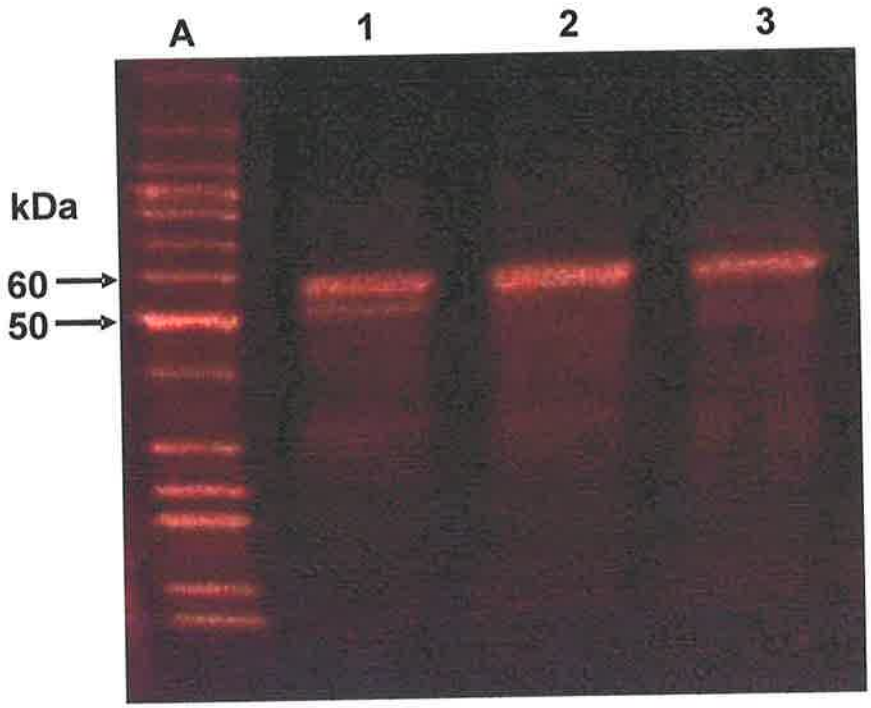

Figure 3.4 SDS-PAGE of Wt ASA

Eluate collected from SEC at 13.5 mL (lane 1), 14.0 mL (lane 2) and 14.5 mL (lane 3) was electrophoresed (1 μg/sample) on a 12% polyacrylamide gel at a constant voltage (180 V) using the method described in section 2.2.4. A BenchMark^{TM} protein ladder (5.0 μL) (A) was used to determine the Mw of the protein bands. The gel was stained with silver staining (section 2.2.4.2) and the image was captured using the UVItec-gel documentation system.

Table 3.2 Purification of Wt ASA[a]

Purification step	Volume (mL)	Protein (mg/mL)	Activity (nmol/min/mg)	Total activity (nmol/min)	Recovery (%)	Purification (Fold)
Crude media	3600	0.8	2	5952	100	1
After concentration 1	250	4.0	5	5431	91.3	x3
After concentration 2 and dialysis	36	0.9	150	5044	84.8	x25
Anion exchange column	9	0.5	943	3935	66.1	x6
After concentration 3	0.25	11.4	1078	3079	51.7	x1.2
Purified ASA after SEC	1	0.4	5510	2153	36.2	x5

[a] The ASA enzyme purification process consisted of five steps: in each step the volume was measured, and an aliquot of media was taken and analysed for enzyme activity (section 2.2.1.8) and protein (section 2.2.5).

3.4.2. Determination of ASA quaternary structure using size exclusion chromatography

To determine the quaternary structure of N350S ASA, SEC was performed on a Superose 6 HR 30 column using purified N350S ASA in buffers at pH 5.0 and pH 7.2. Prior to this experiment, the column was calibrated using commercial Mw standards (Pharmacia Biotech, Uppsala, Sweden), as described below.

3.4.2.1. Calibration of the Superose 6 HR 30 column

The Superose 6 HR 30 column was calibrated with the following Mw standards: thyroglobulin (669 kDa), ferritin (440 kDa), catalase (232 kDa), aldolase (158 kDa) and albumin (67 kDa). Each standard was dissolved in 20 mM sodium acetate/acetic acid buffer, pH 5.0, with 0.15 M NaCl (10 mg/mL). A solution containing 100 µg of each standard was prepared and made up to 250 µL with the same buffer. The standards were loaded onto the column using the same buffer at a flow rate of 0.5 mL/min. Figure 3.6 shows the chromatogram of the Mw standards from the Superose 6 HR 30 chromatography column.

3.4.2.2. Size exclusion chromatography of N350S ASA at pH 5.0 and pH 7.2

To determine the Mw of N350S ASA at pH 5.0, purified N350S ASA (34 ng/250 µL) in 20 mM sodium acetate/acetic acid buffer, 0.15 M NaCl, pH 5.0, was loaded onto the Superose 6 HR 30 column connected to a BioLogic DuoFlow system. Elution was performed using the same buffer at a flow rate of 0.5 mL/min. Figure 3.7 (Panel A) shows the SEC chromatogram with a single peak at volume 13.1 mL. The Mw of this peak was calculated to be 337 kDa (Panel C). To determine the Mw of the enzyme at pH 7.2, a further aliquot of the same enzyme (34 ng/250 µL) was dialysed in PBS, pH 7.2 (overnight, 4°C), before loading onto the Superose 6 HR 30 column and elution with PBS, pH 7.2. Figure 3.7 (Panel B) shows the SEC chromatogram with a small peak at volume 13.1 mL and a major peak at volume 15.6 mL; the Mw of the major peak was calculated to be 138 kDa (Panel C).

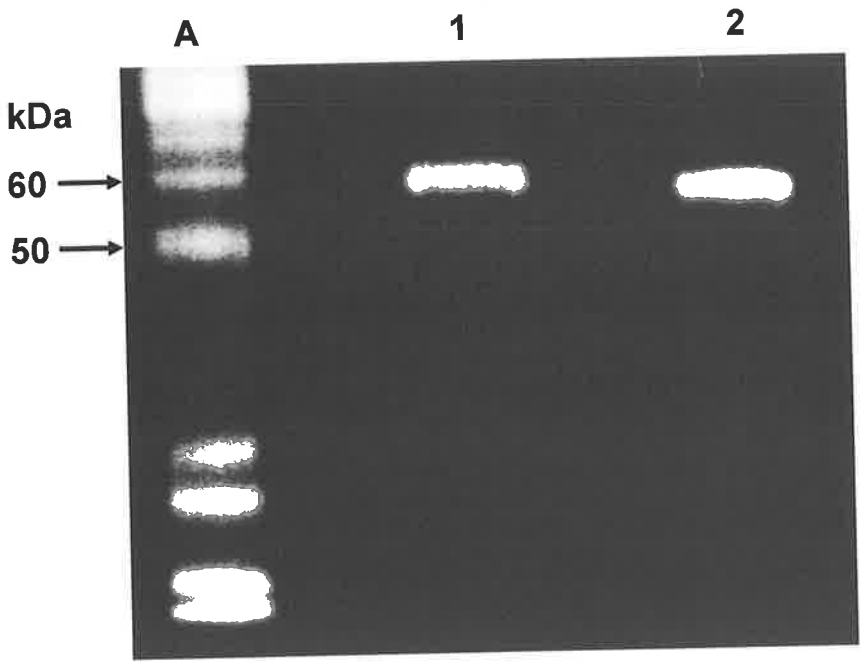

Figure 3.5 SDS-PAGE gel image of Wt ASA and N350S ASA

Gel image showing the Wt ASA band (lane 1) and the N350S ASA band (lane 2) with the BenchMark™ protein ladder (lane A).

3.4.3. The pH optima of Wt ASA and N350S ASA

To determine the pH optima for Wt ASA and N350S ASA, the activity of each enzyme was determined using the 4-MUS substrate (20 mM) prepared in 0.1 M sodium acetate/acetic acid buffer, heat-treated 0.1% BSA, with pH ranging from 4.0 to 6.5. The assays were performed using the protocol described in section 2.2.1.8. Figure 3.8 shows the pH profiles for Wt ASA and N350S ASA; both enzymes were found to have a pH optima of slightly less than pH 5.0.

3.4.4. Kinetic properties of Wt ASA and N350S ASA

The kinetic parameters, K_m and V_{max}, were determined for Wt ASA and N350S ASA. Each enzyme was assayed using 4-MUS substrate at concentrations ranging from 0.3125 to 20 mM prepared in 0.1 M sodium acetate/acetic acid buffer, 0.1% BSA, pH 5.6, using the assay conditions described in 2.2.1.8.

A Lineweaver-Burk plot was constructed, with K_m determined as the negative reciprocal of the x intercept, and V_{max} as the reciprocal of the y intercept (Figure 3.9). The K_m values for Wt ASA and N350S ASA were 7.3 and 8.5 mM, respectively, whilst the V_{max} values for Wt ASA and N350S ASA were 48.5 and 36.6 μmol/h/mg, respectively.

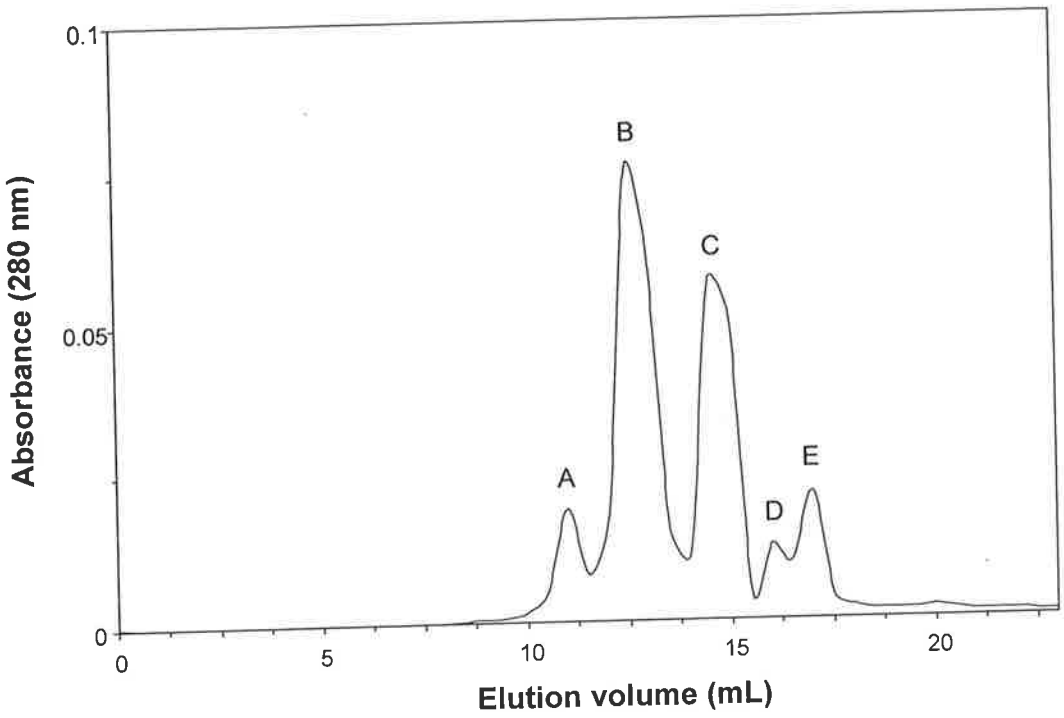

Figure 3.6 Elution profiles of Mw standards from a Superose 6 HR 30 chromatography column

Calibration standards (100 µg each) were prepared in 20 mM sodium acetate/acetic acid buffer, 0.15 M NaCl, pH 5.0 (250 µL), then applied to a Superose 6 HR 30 column and eluted with the same buffer at a flow rate of 0.5 mL/min. Eluted proteins were: A) thyroglobulin (669 kDa); B) ferritin (440 kDa); C) catalase (232 kDa); D) aldolase (158 kDa); and E) albumin (67 kDa)

Figure 3.7 Size exclusion chromatography of N350S ASA under different pH conditions

Panel A: chromatogram showing the peak from the separation of N350S ASA at pH 5.0 using the protocol described in section 3.3.2 (third step of purification process); Panel B: chromatogram showing the peak(s) from the same enzyme (after dialysis in PBS, pH 7.2) separated at pH 7.2; Panel C: the graph used to determine the Mw was plotted using the log value of the following standards: thyroglobulin (669 kDa); ferritin (440 kDa); catalase (232 kDa) and aldolase (158 kDa) on the y-axis, with the value of elution volume of each standard on the x-axis.

A

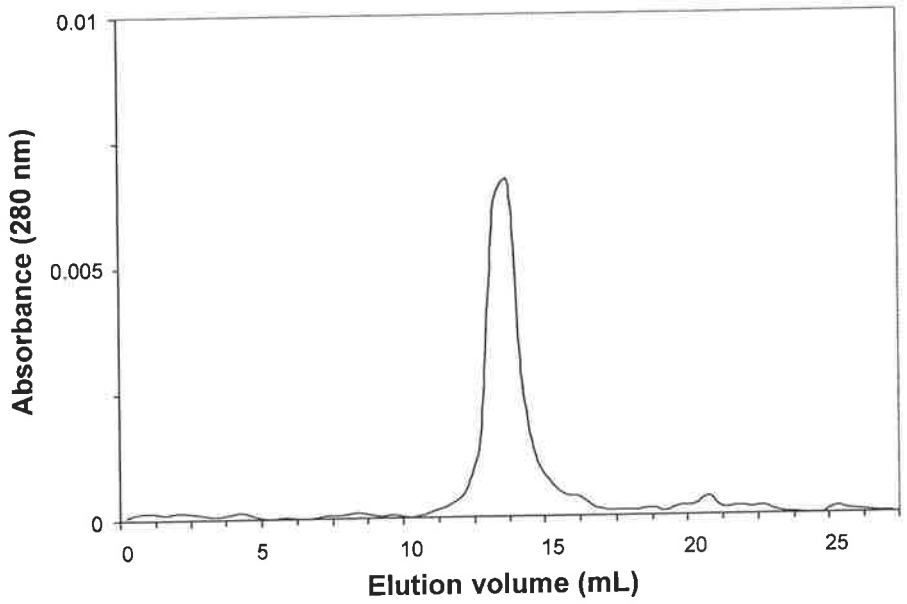
0.01
0.005
0
Absorbance (280 nm)
0
5
10
15
20
25
Elution volume (mL)

B

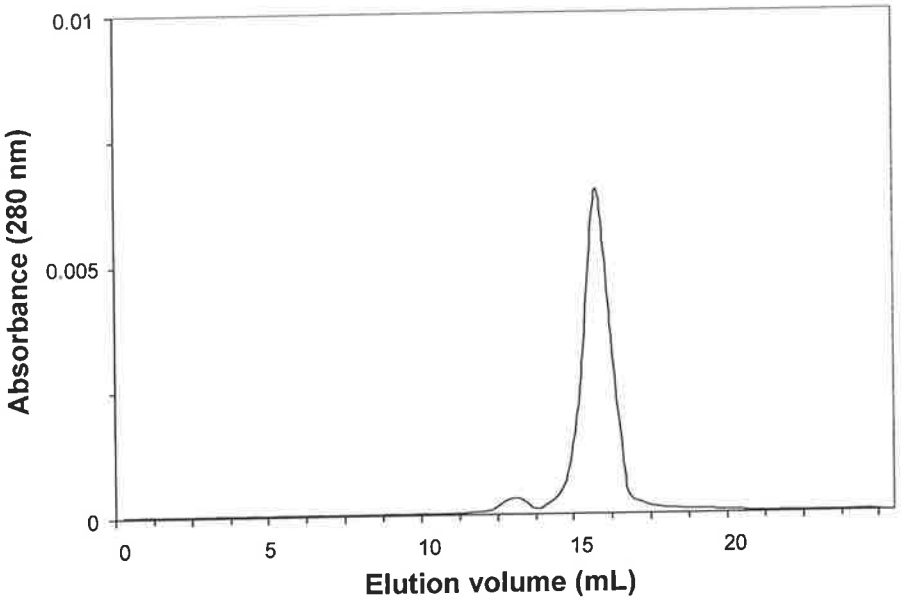
0.01
0.005
0
Absorbance (280 nm)
0
5
10
15
20
Elution volume (mL)

C

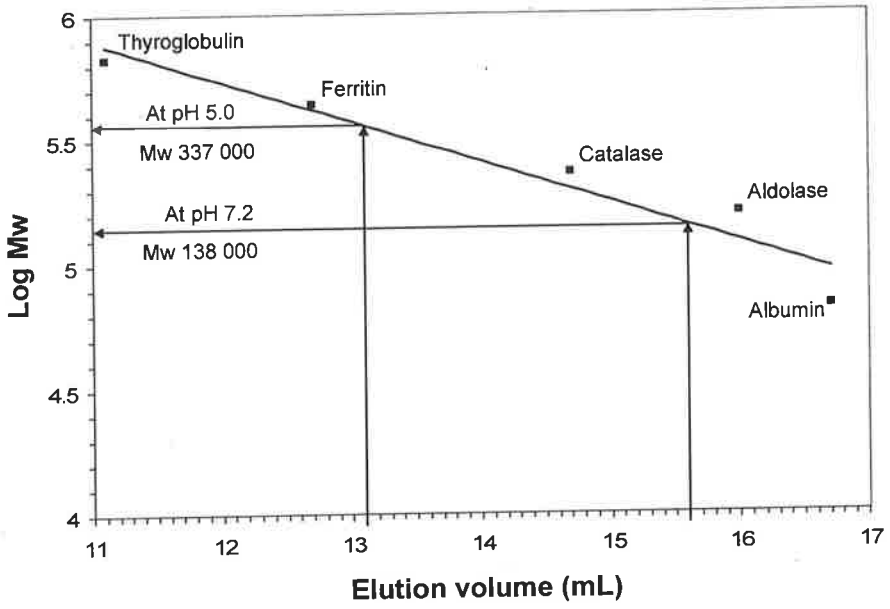
6
5.5
5
4.5
4
Log Mw
Thyroglobulin
Ferritin
At pH 5.0
Mw 337 000
Catalase
Aldolase
At pH 7.2
Mw 138 000
Albumin
11
12
13
14
15
16
17
Elution volume (mL)

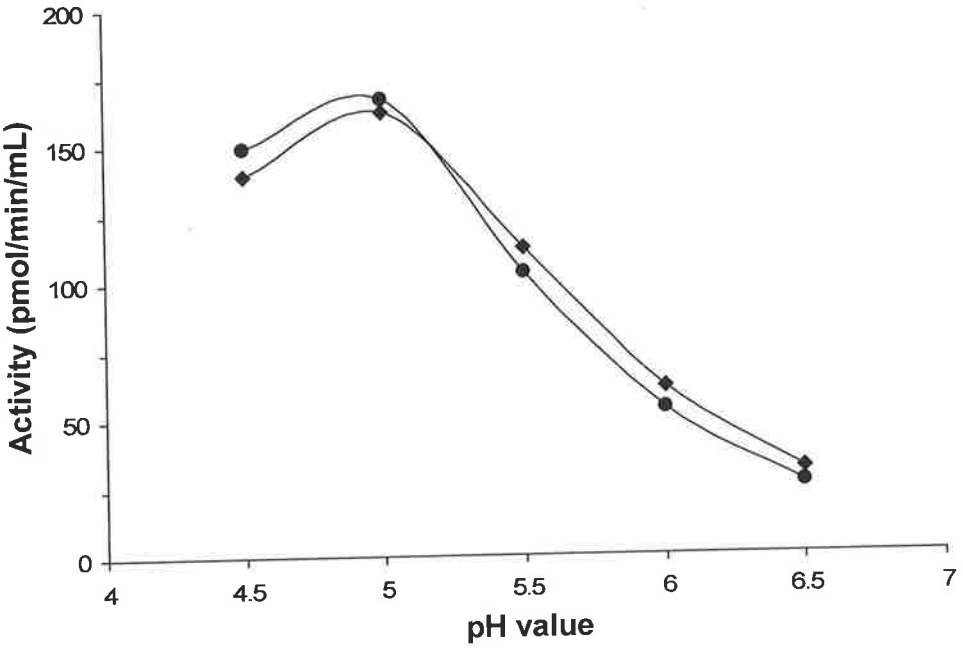

Figure 3.8 pH optima of Wt ASA and N350S ASA

The activity of Wt ASA (●) and N350S ASA (■) was determined using the assay protocol described in section 3.4.3. Enzyme activity was plotted against the pH value of each 4-MUS substrate used in the assay

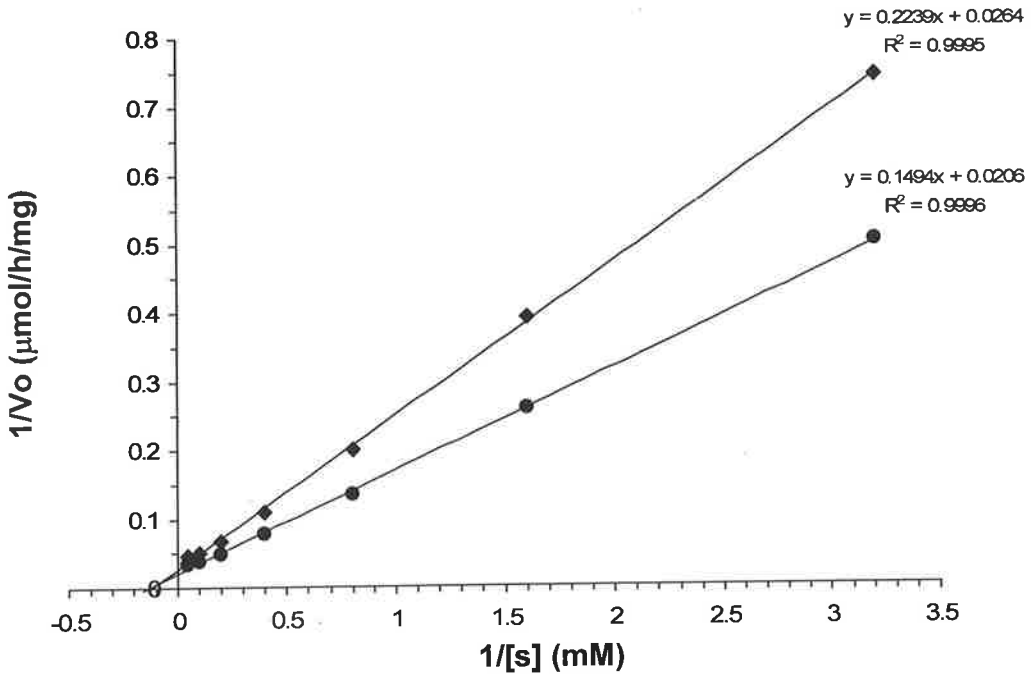

Figure 3.9 Lineweaver-Burk plots of Wt ASA and N350S ASA

The activity of Wt ASA (●) and N350S ASA (■)was determined using the assay protocol described in section 3.4.4. K_m was determined as the negative reciprocal of the x intercept, and V_{max} as the reciprocal of the y intercept.

3.5. Discussion

Expression of lysosomal enzymes using CHO-K1 cells has been performed successfully in this Department over many years (e.g. Fuller *et al.*, 1995; Bielicki *et al.*, 1998; Perkins *et al.*, 1999 and Berg *et al.*, 2001). The CHO-K1 cell expression system offers the advantages expected of a mammalian expression system: the intracellular processes of the CHO-K1 cell during post-translational modifications are known to retain most of the lysosomal enzyme characteristics such as activity, stability and the mannose-6-phosphate moieties necessary for correct trafficking. However, CHO-K1 cell expression systems can result in lower levels of expression when compared to non-mammalian expression systems (Berg *et al.*, 2001).

The amount of enzyme expressed by the Wt ASA and N350S ASA CHO-K1 cell lines used in this study was relatively low at 1.7 mg/L (0.4 mg^{-1} $L^{-1}day^{-1}$) and 2.4 mg/L (0.5 mg^{-1} $L^{-1}day^{-1}$), respectively. Attempts to increase the expression level of each cell line by the addition of 1% DMSO (v/v) in the culture media, as described by Berg *et al.* (2001), were unsuccessful: the addition of DMSO resulted in an increased number of dead cells (observed microscopically) and decreased enzyme activity (see Table 3.1). However, the CHO-K1 cells could be grown in serum-free media, which not only reduced the cost of enzyme production but also resulted in an enzyme preparation of higher specific activity that required less purification steps.

Purification of Wt ASA and N350S ASA was optimised to provide the highest yield and purity in the least steps possible. The use of the Prep-Scale™ concentrator (Mw cut-off 10,000) was not expected to have a significant effect, with only a three-fold purification achieved. However, lowering the pH to 5.0, followed by centrifugation and further concentration over a stirred-cell ultrafiltration unit with a Diaflo YM 30 ultrafiltration membrane (Mw cut-off of 30,000), removed more than 95% of the contaminating protein and was the most effective step, achieving a 25-fold purification. The high purification fold achieved in this step was thought to result from the precipitation effect due to the acidic pH on the protein during dialysis, as a large precipitate (pellet) was obtained after dialysis upon centrifugation.

The choice of AEC as the first step in ASA purification took advantage of the low pI of the enzyme, which was reported to be 4.0 (Qu *et al.*, 1997/98). Enzymes are known to bind adequately to the anion column when separated at 1 pH unit above their pI value, hence 20 mM sodium acetate/acetic acid buffer, pH 5.0 (Buffer A) was chosen as the loading buffer.

The acidic buffer system was not only effective in binding ASA to the column but, as discussed earlier, the concentrated media dialysed in this buffer removed more than 95% of the contaminating protein; furthermore, it was found that ASA was stable at pH 5.0. SEC was used in the subsequent purification step, since the ASA from the first purification step using AEC was expected to be in octamer form with a Mw of approximately 411 kDa in acidic pH (Roy, 1976). Therefore, the partially purified ASA could be loaded directly to the SEC column without additional steps, such as dialysis, and with minimal change to the buffer system.

In contrast to Wt ASA, the biochemical characteristics of N350S ASA have not been extensively cited in the literature. Most reports about this enzyme refer to SF studies in individuals who were either ASA-PD homozygotes or ASA-PD/MLD compound heterozygotes. Qu *et al.* (1997/98) found that the enzyme in the SF of an ASA-PD homozygote had a higher affinity towards the p-NCS substrate and was more susceptible to heat-inactivation compared to controls. This contrasted with earlier findings by both Chang and Davidson (1983) and Herz and Bach (1984), who reported no difference in the kinetic properties determined with 4-MUS substrate but a slight difference in the pI value of the residual enzyme obtained in the SF of ASA-PD/MLD compound heterozygotes.

In this study, Wt ASA and N350S ASA were obtained from a new expression system (CHO-K1 cells). Therefore, enzyme characterisation was performed to ensure that the enzymes produced were indeed ASA and also to evaluate their characteristics. The Mw of Wt ASA and N350S ASA determined using SDS-PAGE under reducing conditions was calculated to be approximately 58 and 56 kDa, respectively, and within the range reported thus far: Qu *et al.* (1997/98) reported that the Mw of ASA in SF from unaffected controls was 54 kDa, while ASA in SF from ASA-PD individuals was determined to be 51.5 kDa; in separate studies, Stevens (1974) reported a Mw of 55 kDa for controls, and Laidler *et al.* (1985b), who isolated ASA from urine under reducing conditions, found the Mw to be 63.5 kDa with a subunit at 54.5 kDa; it was also reported that, in cultured cells, the precursor form of ASA has a Mw of 62 kDa (von Figura *et al.*, 2001); the Mw of recombinant human ASA obtained from a CHO expression system similar to the one used in this study was recently confirmed to have a Mw of 57 kDa using SDS-PAGE and matrix-assisted laser desorption ionisation-time of flight mass spectrometry (Matzner *et al.* 2005).

The difference in Mw of 2 kDa between Wt ASA and N350S ASA observed in this study is consistent with earlier reports and is due to the loss of the carbohydrate moiety in the N350S ASA enzyme (Fluharty *et al.*, 1983; Kihara *et al.*, 1986).

The lack of available Wt ASA at the beginning of the project meant that only N350S ASA could be evaluated for its ability to octamerise under acidic pH using SEC. ASA is known to exist as a dimer at neutral pH and octamerises at acidic pH; octamerisation was attributed to the protonation of glutamic acid at position 426 located at the interface between the dimers that formed the octamer (Lukatela *et al.*, 1998). It has been reported that the quaternary structure of ASA is highly pH-dependent and some mutations, such as C300F and P425T, were reported to have altered octamerisation capacity that leads to a lowered catalytic property (Marcao *et. al.*, 2003).

Evaluation of the octamerised mutant N350S by SEC showed that it was eluted in a single peak at pH 5.0 with a calculated Mw of 337 kDa. After overnight incubation at pH 7.2 in PBS, the enzyme eluted with a major peak at 138 kDa and a small peak with a Mw of 337 kDa; the latter was from the enzyme that remained in octamer form. The Mw obtained from this experiment did not correspond exactly to the expected Mw of dimer and octamer forms, which was calculated to be 112 kDa and 448 kDa, respectively. This discrepancy, however, can be attributed to the limitations of SEC, a method that is known to be less accurate when used to estimate Mw.

In this study, the K_m for Wt ASA and N350S ASA was determined to be 7.25 mM and 8.16 mM, respectively. These values do not significantly differ from those reported in SF lysates by Chang and Davidson (1983), where K_m in unaffected cells (mean value, n=4) was 7.87 mM, and 11.6 mM in ASA-PD/MLD cells; Stevens *et al.* (1975) reported an almost similar K_m value for ASA purified from urine (8.0 mM); both experiments were performed using 4-MUS as substrate. The V_{max} values obtained from the Wt ASA and N350S ASA enzymes in this study showed no significant difference between the two, although Stevens *et al.* (1975) reported a V_{max} of 311 μmol/h/mg for ASA purified from urine, six-times higher than the value obtained in this study. The difference could be attributed to differences in the source of the ASA, storage conditions or the assay conditions. In terms of the pH optima, Stevens *et al.* (1975) reported pH 5.2 and Chang and Davidson (1983) reported pH 5.0 to 5.3; the finding from this study shows that the pH optima for both enzymes studied was around pH 4.9 (see Figure 3.7). Once again, the slight difference in these values could be due to differences in the source of the enzymes or

the assay conditions. The results of these characterisation studies showed that the enzymes were indeed ASA and that their characteristics did not significantly differ from earlier reported values.

In conclusion, the successful development of a purification protocol led to the procurement of purified Wt ASA and N350S ASA that enabled this study to proceed to the next phase - the production of the anti-ASA antibody - which is discussed in the following chapter.

CHAPTER FOUR

Production and Purification of Antibodies and Development and Validation of Immune-based Assays

4. Introduction and aims

The shortcomings associated with current laboratory diagnostic procedures for MLD have been discussed in section 1.4.8.3. To briefly reiterate, however, the diagnosis of MLD is often difficult and requires a complex array of laboratory assays to be performed on various biological samples. The high incidence of ASA-PD individuals further complicates diagnosis because conventional enzymatic assays employed in most laboratories are not sufficiently sensitive to distinguish between ASA-PD individuals and MLD patients, based on analysis of enzyme activity alone. The lack of specificity of enzymatic assays that use artificial fluorogenic substrates has also compounded the problem, since other sulphatases are known to also act on these substrates. Despite the availability of improvised assays that have increased specificity by suppressing the activity of other enzymes, the sensitivity of these assays tends to be compromised. The biochemical confirmation of an ASA-PD individual is usually achieved with auxiliary testing such as sulphatide-loading or genotyping. However, these methods are time-consuming and can only be carried out by experienced staff in specialised laboratories.

To improve the MLD detection system, Laidler *et al.* (1985a) suggested the use of immune-based methods for the measurement of ASA, reasoning that an antibody would provide the necessary specificity to resolve the interference of other sulphatases. However, the use of immune-based assays to quantify protein or determine enzyme activity was limited until recently. In 2001, an immune-based assay with 100% sensitivity and specificity was reported for the determination of α-glucosidase activity in dried blood spots, which has been used successfully to detect individuals affected by Pompe disease (Umapathysivam *et al.*, 2001). The advantages reported for this method augur well for the development of a NBS programme for LSD, and prompted the development of better, more rapid and definitive procedures for use in the diagnosis of MLD.

This chapter commences with a discussion of the experimental approach used to produce and purify the antibodies used in this study. In addition, details of the development and validation of the immune-based assays, as outlined at the end of Chapter 1, are also provided. The experimental work described in this chapter encompasses the first three aims of this study, which were to develop: (1) an immune-capture activity assay for ASA

enzyme; (2) an immune-quantification assay for ASA protein; and (3) assays similar to those in (1) and (2) for the detection of ASA-PD cases (without genotyping, for the N350S polymorphism). The experimental work relating to Aim 3 commenced simultaneously with most of the work described in Chapter 3. The discussion therefore commences with Aim 3, followed by a discussion of the work related to Aims 1 and 2.

4.1. Development of an immune-based assay for the detection of ASA-PD

ASA-PD is known to be associated with the polymorphism that causes the substitution of asparagine by serine at position 350 of the amino acid sequence. This results in the loss of the glycosylation site, leading to the loss of a carbohydrate moiety (section 1.4.6.1). The crystal structure of ASA reveals that the N350 site is well-exposed and could be a potential binding site for antibodies. This prompted the use of a synthetic peptide that spans the N350S sequence for the production of a polyclonal antibody.

4.1.1. Production of a polyclonal antibody against the N350S peptide conjugate

The immunisation of sheep was carried out at the Institute of Medical and Veterinary Science, Adelaide, SA, Australia, using the immunisation protocol described in section 2.2.6. The antigen used was the N350S peptide conjugated to diphtheria toxoid (4.2 mg peptide to 30.3 mg diphtheria toxoid; section 2.2.6). A pre-bleed (at week 0) and a test-bleed (at week 7.5) sample were taken and titrated against the N350S peptide conjugate (H-CAGAPLP**S**VTLDG-NH2-DT) and against an unrelated peptide also conjugated to diphtheria toxoid (H-CLUGRKRSHAGYQTI-OHNH2-DT; Mimotopes Pty. Ltd., Clayton, Vic, Australia). BSA (2.0 µg/mL) was used as a negative control in these antibody titrations. The protocol used for this assay is specified in section 2.2.8.4.

The pre-bleed sample had a titre of 1:1 000 (antibody titre was determined as the lowest dilution of sera at which the OD was greater than two standard deviations above background reading; section 2.2.8.4) against the peptide conjugate and the unrelated peptide conjugate. In the test-bleed sample a strong immune response was observed against the peptide conjugate, with a titre of 1:1 024 000, approximately three-fold greater than the titre obtained against the unrelated peptide conjugate, where the antibody reacted against diphtheria toxoid. This indicated that the antibody had a strong and specific reaction against the H-CAGAPLP**S**VTLDG-NH2 sequence.

4.1.1.1. *Purification of the sheep anti-N350S peptide conjugate polyclonal antibody*

From 100 mL sheep sera, 0.9 g of an ammonium sulphate-precipitated immunoglobulin fraction was obtained in 50 mL. After dialysis against PBS, pH 7.2 (4°C, overnight), 8.0 mL was applied to the peptide affinity column described in section 2.2.7; 14 mg of affinity-purified antibody was recovered.

4.1.1.2. *Western analysis of the Wt ASA and N350S ASA enzymes with sheep anti-N350S peptide conjugate polyclonal antibody*

Western analysis was performed in accordance with the protocol outlined in section 2.2.4.3, to assess the reactivity of the sheep anti-N350S peptide conjugate polyclonal antibody against the N350S peptide conjugate, Wt ASA and N350S ASA (1.0 μg). Figure 4.1 shows the PVDF membrane with the pre-stained marker on the left, the N350S peptide conjugate (1), N350S ASA (2) and Wt ASA (3). A single cross-reactive band at approximately 56 kDa (2), representing N350S ASA, was obvious; no cross-reactive band was apparent on the lane loaded with Wt ASA. This indicated that the polyclonal antibody produced against the peptide conjugate cross-reacted with N350S ASA but not Wt ASA.

4.1.1.3. *Attempts to develop an immune-capture activity assay using sheep anti-N350S peptide conjugate polyclonal antibody*

The polyclonal antibody was diluted in 0.1 M $NaHCO_3$ (5.0 μg/mL), coated onto wells of Immunlon® 4HBX Removawell® strips and incubated (4°C, overnight). After the plate was washed (6x, 0.1 M Tris/HCl, 0.25 M NaCl, pH 7.2), culture media from the Wt ASA and N350S ASA expression systems was diluted in 20 mM Tris/HCl, 0.25 M NaCl, pH 7.2 (80 μL in 1.0 mL), before 1:2 serial dilutions were performed across the plate (100 μL/well). Activity was determined by the addition of 20 mM 4-MUS substrate prepared in 0.1 M sodium acetate/acetic acid buffer, heat-treated 0.1% BSA, pH 5.8. As a control, the same media was diluted in 0.1 M sodium acetate/acetic acid buffer, heat-treated 0.1% BSA, pH 5.8 (160 μL in 1.0 mL), before 1:2 serial dilutions were performed across a plate with uncoated wells (50 μL/well). Fifty μL of 40 mM 4-MUS substrate in 0.1 M sodium acetate/acetic acid buffer, heat-treated 0.1% BSA, pH 5.8, was then added to each well and incubated at 37°C for 2 hrs. The enzyme reaction was stopped by the addition of 0.2 M glycine/NaOH buffer, pH 10.7 (100 μL/well), and fluorescence read on a Perkin-Elmer 1420 multilabel counter.

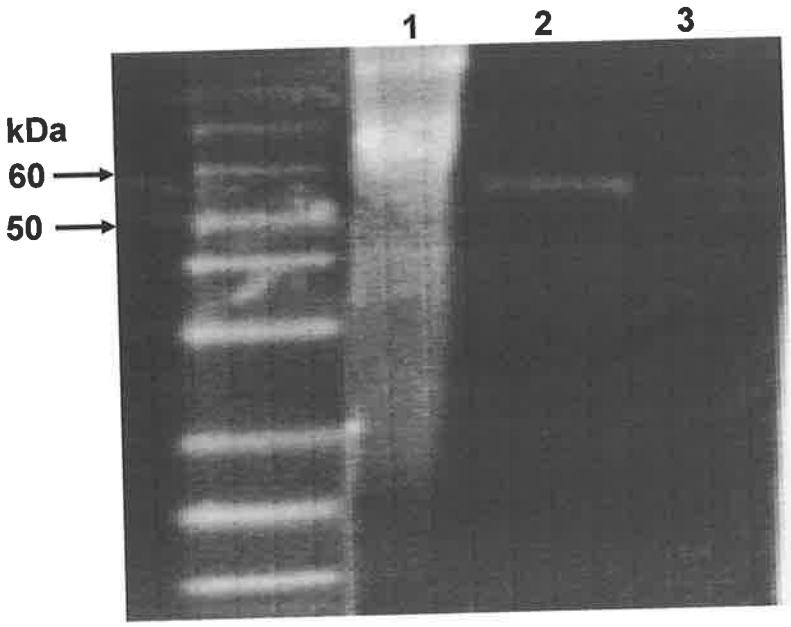

Figure 4.1 Western blot analysis of Wt ASA and N350S ASA with sheep anti-N350S peptide conjugate polyclonal antibody

Pre-stained marker (left) (5.0 µL), N350S peptide conjugate (1), N350S ASA (2) and Wt ASA (3) (1.0 µg/each) were electrophoresed on a 12% Tris-glycine-SDS gel at a constant voltage (180 V), as described in section 2.2.4, and transferred to a PVDF membrane at a constant current (250 mA), as described in section 2.2.4.3. The membrane was probed with sheep anti-N350S peptide conjugate polyclonal antibody (1.0 µg/mL) and reactive protein detected with donkey anti-sheep HRP-conjugate (1:1 000 dilution). The image of the PVDF membrane was recorded using the UVItec-gel documentation system.

No enzyme activity was detected in the immune-captured wells but the positive controls showed activity averaging 5.6 μmol/min/mL for the highest concentration of N350S ASA and 4.1 μmol/min/mL for Wt ASA. This indicated that the polyclonal antibody was either not capturing the enzymes or that the captured enzymes were inactive.

To define this, a separate experiment was carried out in which the amount of enzyme removed from the media during the capture step was measured: 50 μL of media from each well was transferred to new wells after the overnight incubation (capturing step) and assayed for activity using the protocol described above for the positive controls. The amount of activity detected was the same (after correction) as that detected in the positive controls, thus confirming the inability of the polyclonal antibody to capture both forms of the enzyme.

4.2. Production of an anti-ASA monoclonal antibody

In addition to the polyclonal antibody, the production of a monoclonal antibody was also proposed for use in the immune-based assays. Apart from offering defined specificity, a monoclonal antibody would also resolve the problem of lack of uniformity resulting from batch-to-batch variation that can be encountered with polyclonal antibodies, since the production of monoclonal antibodies can be maintained indefinitely through an immortal hybridoma cell line.

4.2.1. Immunisation, fusion and hybridoma screening of mice immunised with N350S ASA and Wt ASA

To produce a monoclonal antibody, three mice were immunised with N350S ASA (40 μg/dose) using Freund's adjuvant (section 2.2.8.1), and two mice were immunised with the same enzyme (one each at 20 μg/dose and 5.0 μg/dose) using ImmuneEasy™ mouse adjuvant (section 2.2.8.2). At the completion of the immunisation protocol the mouse spleens were removed and the plasma cells fused with myeloma cells, as described in section 2.2.8.3. Hybridoma screening was performed two-weeks post-fusion using the protocol described in section 2.2.8.5. Blood was collected from each mouse during fusion for assay of sera antibody titre (section 2.2.8.4).

Table 4.1 summarises the fusions performed on the five mice immunised with N350S ASA. Of the five, only three fusions were performed because the mice immunised with ImmuneEasy™ mouse adjuvant failed to respond to the immunisation: the antibody titre

was only 1:4 000, compared with 1:256 000 for the mice immunised using Freund's adjuvant.

Hybridoma screening identified two wells containing hybridomas that were positive, one each from fusion N350S 2 and N350S 3, with OD values against Wt ASA of >5.0 and 3.8 compared to BSA control values of 1.3 and 0.8, respectively. The hybridomas were cloned (section 2.2.1.7) and expanded, however, the antibody titre of the media from these two hybridomas dropped to background reading on subsequent testing during the expansion process.

Four additional mice were immunised with Wt ASA (40 μg/dose) using Freund's adjuvant (section 2.2.8.1) and had fusions performed (section 2.2.8.3). Hybridoma screening was performed two-weeks post-fusion using the protocol described in section 2.2.8.5. Blood was collected from the mice during fusions for assay of sera antibody titre (section 2.2.8.4).

Table 4.2 summarises the fusions carried out in mice immunised with Wt ASA. Hybridoma screening in the four fusions identified one well that contained hybridomas (fusion Wt 1) with an OD reading of >5.0 against Wt ASA and N350S ASA, while the OD reading for the BSA control was 0.6. The hybridomas were cloned (section 2.2.1.7), expanded and isotyped (section 2.2.8.6), and designated as MonoWt 1. The subclass of the monoclonal antibody was determined to be IgM.

4.2.1.1. Purification of IgM monoclonal antibody

Conditioned media (50 mL) from cloned hybridoma MonoWt 1 was collected and purified using affinity chromatography (Hi-Trap IgM purification HP, 1.0 mL; Amersham Pharmacia Biotech Inc., Uppsala, Sweden) according to the manufacturer's instructions. The yield of monoclonal antibody from 50 mL of media was 1.4 mg, corresponding to 28 μg/mL in the hybridoma supernatant. The purified monoclonal antibody was kept at -20°C in aliquots of 200 μL until use.

Table 4.1 Summary of fusions from mice immunised with N350S ASA

Fusion ID	Amount (µg/dose)	Number of doses of antigen	Adjuvant[a]	Sera titre	Wells with hybridoma (Total wells=192)	Positive hybridoma
N350 1	40	3 plus 1	Freund's complete/incomplete	1:256 000	164 (85%)	None
N350 2	40	3 plus 2[b]	Freund's complete/incomplete	1:256 000	147 (72%)	1
N350 3	40	3 plus 2[b]	Freund's complete/incomplete	1:256 000	172 (90%)	1
No fusion	20	3 plus 1	ImmuneEasy™ mouse adjuvant	1:4 000	NA[c]	None
No fusion	5	3 plus 1	ImmuneEasy™ mouse adjuvant	1:4 000	NA[c]	None

[a] Mice were immunised according to the protocol described in sections 2.2.8.1 and 2.2.8.2;

[b] extra booster dose was given three-days prior to fusion;

[c] NA = not available

Table 4.2 Summary of fusions from mice immunised with Wt ASA

Fusion ID	Amount (µg/dose)	Number of doses of antigen	Adjuvant[a]	Sera titre	Wells with hybridoma (Total wells=192)	Positive hybridoma
Wt 1	40	3 plus 1	Freund's complete/incomplete	1:256 000	158 (82%)	1
Wt 2	40	3 plus 1	Freund's complete/incomplete	1:512 000	144 (75%)	None
Wt 3	40	3 plus 2[b]	Freund's complete/incomplete	1:256 000	154 (80%)	None
Wt 4	40	3 plus 2[b]	Freund's complete/incomplete	1:256 000	129 (67%)	None

[a] Mice were immunised according to the protocol described in sections 2.2.8.1 and 2.2.8.2;

[b] extra booster dose was given three-days prior to fusion

4.2.1.2. *Attempts to develop an immune-quantification assay using IgM monoclonal antibody*

The IgM monoclonal antibody (MonoWt 1) was diluted in 0.1 M $NaHCO_3$, coated onto wells of Immunlon® 4HBX Removawell® strips (5 µg/mL) and incubated at 4°C, overnight. The coated strips were used to capture Wt ASA with concentrations ranging from 2 ng/mL to 2 pg/mL (100 µL/well). Sheep anti-ASA polyclonal antibody (5.0 µg/mL) was used as the secondary antibody with the HRP-conjugated donkey anti-sheep antibody (1:1 000 dilution); ABTS was used for colour development. The results indicated non-specific capturing/binding by the IgM monoclonal antibody as the OD was similar at different concentrations of enzyme in each well, ranging from 1.5 to 1.7. This experiment was repeated and similar results were obtained.

4.2.2. Epitope mapping of polyclonal antibody from sheep and mice

The low number of positive hybridomas obtained from a total of seven fusions in mice immunised with the native enzyme prompted a revised strategy for monoclonal antibody production. The use of peptides representing the specific sequence of ASA was proposed for mouse immunisations. The peptide sequences were determined by epitope mapping of the polyclonal antibodies (sheep and mouse sera) against the linearised ASA enzyme sequence using a Multipin™ peptide plate.

Epitope mapping of antibodies was performed using the protocols described in section 2.2.9.1 through to section 2.2.9.4. Figure 4.2 shows the epitope maps of the polyclonal antibodies from sheep and mouse sera: sera from sheep immunised with N350S ASA (Panel A) and the sheep anti-ASA polyclonal antibody (Panel B) show very similar reactivity patterns with 25% and 21% of high affinity epitopes (defined as an OD of greater than 2.5), respectively; mouse sera immunised with the same enzyme had 31% high affinity epitopes (Panel D); and the sera from mice immunised with Wt ASA (Panel C) had only four high affinity epitopes (5%). None of the four samples tested reacted to the N-linked glycosylation site at amino acid position 350 (peptide number 56, LAGAPLPNVTLD; and peptide number 57, PNVTLDGFDLSP), which is associated with the N350S mutation.

4.2.2.1. *Designing the ASA peptides*

The design of ASA peptides for immunisation was based on the results obtained from epitope mapping of the sheep anti-ASA polyclonal antibody, sera from sheep and mice immunised with N350S ASA, and sera from mice immunised with Wt ASA. All epitopes with an OD >2.5 (high affinity) toward the linear ASA sequence were compared to

sequences reported by Schierau *et al.* (1999), who reportedly produced eight monoclonal antibodies against the ASA enzyme. The selected sequences were then mapped onto the crystal structure of the ASA enzyme to evaluate their location.

Table 4.3 lists all epitopes with an OD reading of >2.5, their amino acid sequence and the hydrophobicity index; the amino acid sequences recognised by the anti-ASA monoclonal antibodies produced by Schierau *et al.* (1999) were added for comparative purposes. Three amino acid sequences were selected (bolded in Table) and mapped onto the crystal structure of the ASA enzyme, as shown in Figure 4.3. The sequences selected to construct the ASA peptides were: 1) peptide pin 33 (WLPGLEARYMAF); 2) peptide pin 60 (GFDLSPLLLGTG); and 3) peptide pin 63 (LFFYPSYPDEVR).

4.2.3. Generation of monoclonal antibodies against the ASA peptide conjugates

Three groups of mice (three/group) were immunised with ASA peptide conjugate 1 (H-WLPGLEARYMAF-OH/100 μg/dose), ASA peptide conjugate 2 (H-GFDLSPLLLGTG-OH/100 μg/dose) and ASA peptide conjugate 3 (H-LFFYPSYPDEVR-OH/100 μg/dose), respectively, using Freund's adjuvant (section 2.2.8.1). Antibody titre levels were determined following the second boost using the corresponding peptide conjugates and Wt ASA; an unrelated peptide conjugate was used as a control, according to the protocol described in section 2.2.8.4.

Table 4.4 summarises the titre levels of the mouse sera. All mice responded well to the immunisation regime with a minimum titre of 1:1 040 000 achieved towards the corresponding peptide conjugate; all mice showed strong cross-reactivity to the unrelated peptide conjugate (cross-reactivity against the diphtheria toxoid), although the titre was lower in some mice at approximately half the value observed for the specific peptide used for immunisation; and all mice had low titres against the ASA enzyme.

Fusions were carried out after the test-bleed, as described in section 2.2.8.3. Five fusions were performed: one mouse from group one (peptide 1) and two mice each from groups two (peptide 2) and three (peptide 3). Table 4.5 summarises the fusions performed on the five mice, together with the immunisation details, the number of hybridomas and the hybridomas that tested positive in each fusion.

A hybridoma from fusion 2b (designated P2P4B4), with an OD >5.0 against peptide 2, an OD of 1.3 against Wt ASA and an OD reading of <0.15 (background) for both diphtheria toxoid and BSA, was cloned and isotyped (section 2.2.8.6), which identified the monoclonal antibody as IgG_1 subclass with kappa light chain.

4.2.3.1 Purification of the P2P4B4 monoclonal antibody

Culture media (60 mL) from the P2P4B4 hybridoma culture was purified using the protocol described in section 2.2.8.7. The yield of monoclonal antibody from 60 mL of media was 1.8 mg, corresponding to 30 μg/mL in the hybridoma supernatant. The purified monoclonal antibody was kept at -20°C in aliquots of 200 μL until use.

4.2.3.2 Attempts to develop an immune-capture activity assay using the P2P4B4 monoclonal antibody

Purified P2P4B4 monoclonal antibody was diluted in 0.1 M $NaHCO_3$, coated onto wells of Immunlon® 4HBX Removawell® strips (5.0 μg/mL) and incubated (4°C, overnight). An immune-capture activity assay was performed using Wt ASA at concentrations ranging from 2.0 ng/mL to 2.0 pg/mL (section 2.2.10.1). As a control, Wt ASA with the same concentration was captured using strips coated with anti-ASA polyclonal antibody. The activity of the captured enzymes was determined by the addition of 20 mM 4-MUS substrate prepared in 0.1 M sodium acetate buffer, heat-treated 0.1% BSA, pH 5.8 (100 μL/well).

No activity was detected in the strips coated with the monoclonal antibody but the activity reading in the control strips was proportionate to the amount of enzyme in each well. These results indicated that either the monoclonal antibody was not capturing the enzymes or that the captured enzymes were inactive. This could result from the antibody binding to the active site or near the active site and limiting its access to the substrate.

The inability of the antibody to capture ASA was confirmed by an ASA activity assay of the capture solutions after incubation in the antibody-coated wells; no change in activity was observed before or after the capture step.

Figure 4.2 Epitope maps of polyclonal antibodies from sheep and mouse sera

Epitope mapping of antibodies was performed using a Multipin™ peptide plate and the protocol described in section 2.2.9.4. All samples were diluted in PBS with 1% BSA and 0.1% Tween 20 (v/v), pH 7.2 (1:1 000 dilution). Epitope maps were as follows: sera from sheep immunised with N350S ASA (Panel A); sheep anti-ASA polyclonal antibody (Panel B); sera from a mouse immunised with Wt ASA (Panel C); and sera from a mouse immunised with N350S ASA (Panel D).

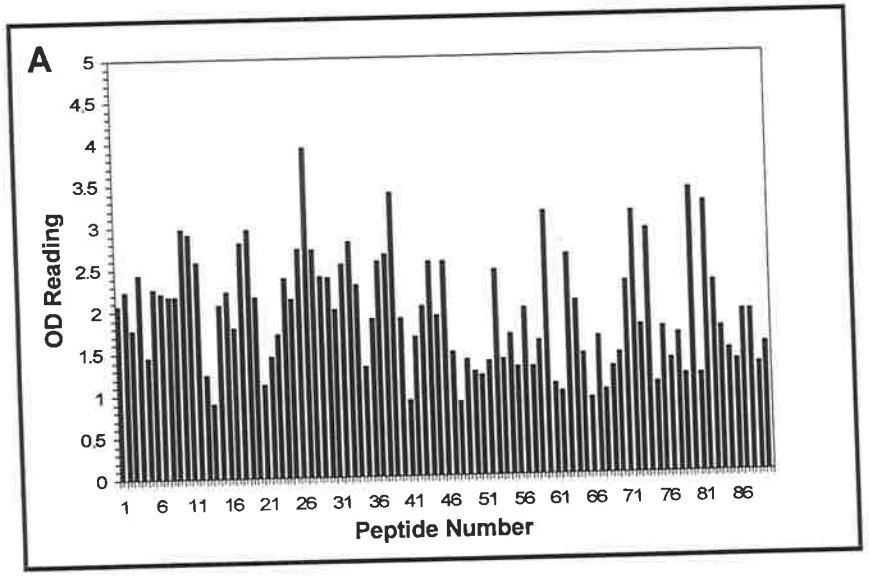
A
OD Reading
Peptide Number

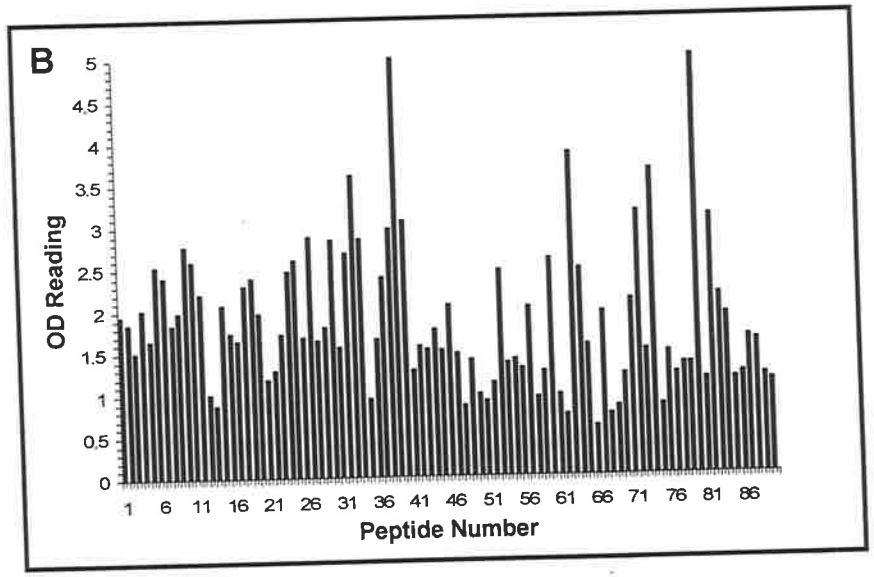
B
OD Reading
Peptide Number

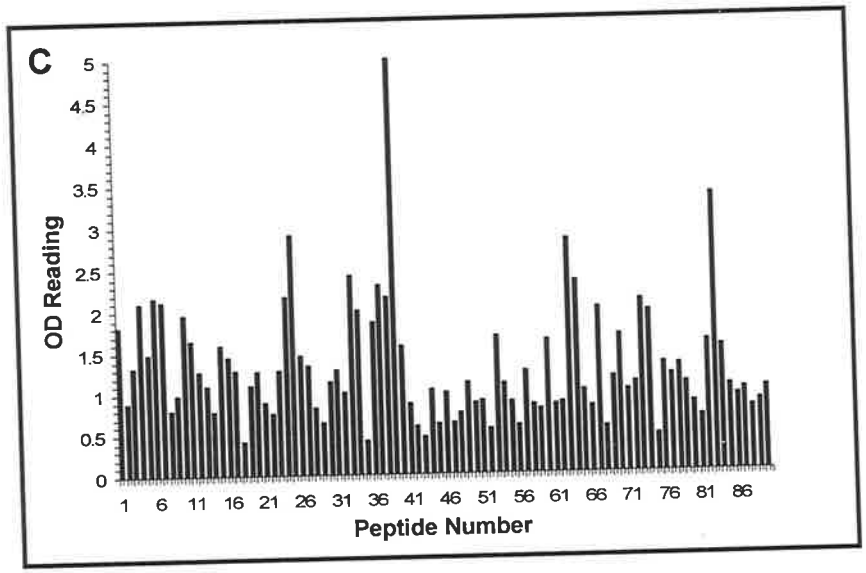
C
OD Reading
Peptide Number

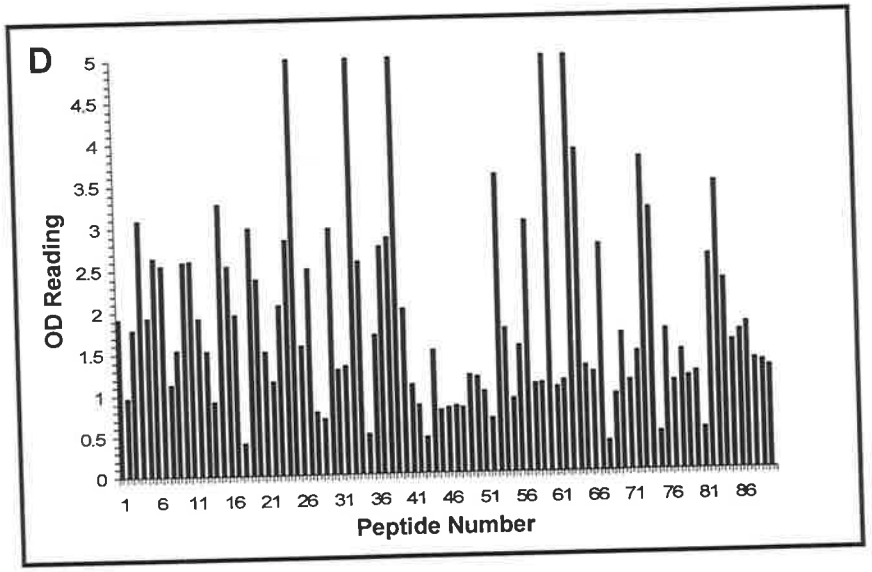
D
OD Reading
Peptide Number

Table 4.3 Alignment of high affinity epitopes with known anti-ASA monoclonal antibody sequence

	OD405 nM				Amino acids			Schierau *et al.*, 1999
Pin no.	Sheep sera	Sheep poly-Ab	Mouse N350S ASA	Mouse Wt ASA	Sequence	Position	Hydrophobicity index	Amino acids position
4			3.096		RPPNIVLIFADD	19-30	0.42	19
6		2.536	2.64		LGYGDLGCYGHP	31-42	0.43	
7			2.552		GCYGHPSSTTPN	37-48	0.21	
10	2.977	2.782	2.595		GGLRFTDFYVPV	55-66	0.49	
11	2.909	2.586	2.603		DFYVPVSLCTPS	61-72	0.59	
12	2.583				SLCTPSRAALLT	67-78	0.46	
15			3.281		MGMYPGVLVPSS	85-96	0.57	85-86
16			2.545		VLVPSSRGGLPL	91-102	0.49	93, 97
18	2.807				EEVTVAEVLAAR	103-114	0.19	
19	2.957		2.988		EVLAARGYLTGM	109-120	0.36	
24			2.842		QGFHRFLGIPYS	139-150	0.47	
25		2.605	>5.0	2.907	LGIPYSHDQGPC	145-156	0.4	
26	2.724				HDQGPCQNLTCF	151-162	0.35	
27	3.936	2.888			QNLTCFPPATPC	157-168	0.55	
28	2.706				PPATPCDGGCDQ	163-174	0.22	165-169
30		2.839	2.973		GLVPIPLLANLS	175-186	0.71	
32	2.542	2.686			VEAQPPWLPGLE	187-198	0.49	
33	**2.807**	**3.609**	**>5.0**		**WLPGLEARYMAF**	**193-204**	0.59	
34		2.859	2.585		ARYMAFAHDLMA	199-210	0.39	202-206
37	2.568		2.752		RPFFLYYASHHT	217-228	0.48	
38	2.642	2.979	2.858		YASHHTHYPQFS	223-234	0.29	
39	3.384	>5.0	>5.0	>5.0	HYPQFSGQSFAE	229-240	0.25	
40		3.067			GQSFAERSGRGP	235-246	-0.08	239-240
44	2.548				GTLMTAIGDLGL	259-270	0.51	256, 260
46	2.552				LEETLVIFTADN	271-282	0.39	
								287-459
53			3.581		PALAFWPGHIAP	313-324	0.7	
57			3.022		LPTLAALAGAPL	337-348	0.63	

Table 4.3 Continued

	OD value				Amino acids			Schierau *et al.*, 1999
Pin no.	Sheep sera	Sheep Poly-Ab	Mouse N350S ASA	Mouse Wt ASA	Sequence	Position	Hydrophobicity index	Amino acids position
60	**3.136**	**2.593**	**>5.0**		**GFDLSPLLLGTG**	**355-366**	0.56	
63	**2.617**	**3.851**	**>5.0**	**2.833**	**LFFYPSYPDEVR**	**373-384**	0.46	
64			3.866		YPDEVRGVFAVR	379-390	0.22	
67			2.731		HFFTQGSAHSDT	397-408	0.19	
72	3.112	3.148			LLYDLSKDPGEN	427-428	0.14	
73			3.763		KDPGENYNLLGG	433-444	0.04	
74	2.904	3.646	3.159		YNLLGGVAGATP	439-450	0.40	
								462-507
80	3.378	>5.0			SQVARGEDPALQ	475-486	0.03	
82	3.229	3.086	2.598		ICCHPGCTPRPA	487-498	0.52	
83			3.461	3.345	CTPRPACCHCPD	493-504	0.45	

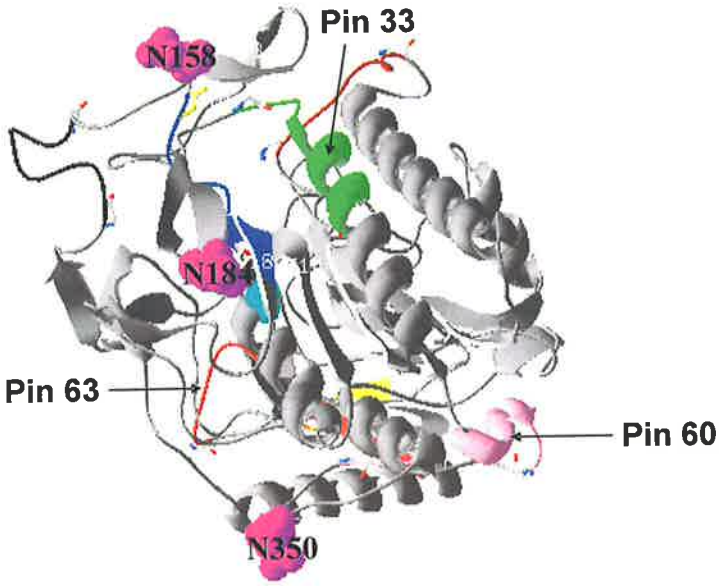

Figure 4.3 Mapping of high affinity epitopes onto the ASA crystal structure

Three epitopes of high affinity were identified: peptide pin 33 (WLPGLEARYMAF); peptide pin 60 (GFDLSPLLLGTG); and peptide pin 63 (LFFYPSYPDEVR). These epitopes were mapped onto the crystal structure of ASA (Lukatela *et al.*, 1998). The figure is drawn with Mol script software based on human cDNA sequence by Stein *et al.* (1989).

Table 4.4 Titre levels of mouse sera against the corresponding peptide conjugate, diphtheria toxoid and Wt ASA

Mouse[a]	Antigen		
Group 1	Peptide 1	Diphtheria toxoid	Wild type ASA
1a	1:1 040 000	1:1 040 000	1:3 200
1b	1:1 040 000	1:1 040 000	1:3 200

Mouse[b]	Antigen		
Group 2	Peptide 2	Diphtheria toxoid	Wild type ASA
2a	1:2 080 000	1:1 040 000	1:6 400
2b	1:1 040 000	1:512 000	1:3 200

Mouse	Antigen		
Group 3[c]	Peptide 3	Diphtheria toxoid	Wild type ASA
3a	1:1 040 000	1:1 040 000	1:3 200
3b	1:1 040 000	1:1 040 000	1:1 600
3c	1:1 040 000	1:512 000	1:1 600

[a] mice immunised with peptide conjugate 1 (H-LPGLEARYMAFAC-OH);
[b] mice immunised with peptide conjugate 2 (H-GFDLSPLLLGTGC-OH);
[c] mice immunised with peptide conjugate 3 (H-LFFYPSYPDEVRC-OH).

Table 4.5 Fusions and immunisations of mice immunised with conjugated peptides

Fusion ID[a]	Amount (µg/dose)	Number of doses	Wells with hybridomas (Total wells=192)	Type of peptide	Positive hybridoma
Pep 1a	100	3 plus 1 booster	146 (76%)	1	1
Pep 2a	100	3 plus 1 booster	145 (76%)	2	None
Pep 2b	100	3 plus 2 boosters[b]	141 (73%)	2	3
Pep 3a	100	3 plus 1 booster	187 (97%)	3	None
Pep 3b	100	3 plus 2 boosters	180 (94%)	3	None

[a] mouse 1a was immunised with peptide conjugate 1 (H-LPGLEARYMAFAC-OH); mice 2a and 2b were immunised with peptide conjugate 2 (H-GFDLSPLLLGTGC-OH); and mice 3a and 3b were immunised with peptide conjugate 3 (H-LFFYPSYPDEVRC-OH);

[b] an extra booster dose was given three-days prior to fusion

4.3. Development and validation of immune-based assays using the anti-ASA-polyclonal antibody

Two immune-based assays were developed in this study to determine captured ASA activity and to quantify the ASA protein in dried blood spots, SF lysates and culture media.

4.3.1. Production of anti-ASA polyclonal antibody

The production of an anti-ASA polyclonal antibody was carried out at the Veterinary Division of the Institute of Medical and Veterinary Science, Adelaide, SA, Australia, as described in section 2.2.6. Pre-bleed (at week 0) and test-bleed (at week 7.5) sera were titrated against Wt ASA and N350S ASA with BSA as a negative control using the protocol described in section 2.2.8.4. Pre-bleed sera had a titre of 1:2 000 with the three proteins tested; a strong immune response was observed against Wt ASA and N350S ASA in the test bleed sera, with a titre of 1:2 048 000.

4.3.1.1 Purification of sheep anti-ASA polyclonal antibody

Precipitation of sheep sera (250 mL) with ammonium sulphate (section 2.2.7) produced 2.7 g of Ig fraction in 150 mL of PBS, pH 7.2. This was dialysed against PBS, pH 7.2 (4°C, overnight), and 5.0 mL was further purified by affinity chromatography on the N350S ASA affinity column, as described in section 2.2.7. The eluate from the affinity column (Figure 4.4) contained 4.6 mg, an equivalent yield of 0.6 mg/mL of sera.

4.3.1.2 Western analysis of Wt ASA and N350S ASA with sheep anti-ASA polyclonal antibody

Using the protocol outlined in section 2.2.4.3, Western analysis was performed to determine the reactivity of the sheep anti-ASA polyclonal antibody against Wt ASA and N350S ASA (1.0 µg/enzyme). Figure 4.5 shows the PVDF membrane with the pre-stained marker on the left, Wt ASA (1) and N350S ASA (2). Single cross-reactive bands were detected at 58 kDa (1) and 56 kDa (2), representing Wt ASA and N350S ASA, respectively. This indicated that the polyclonal antibody produced against N350S ASA cross-reacted with both enzymes.

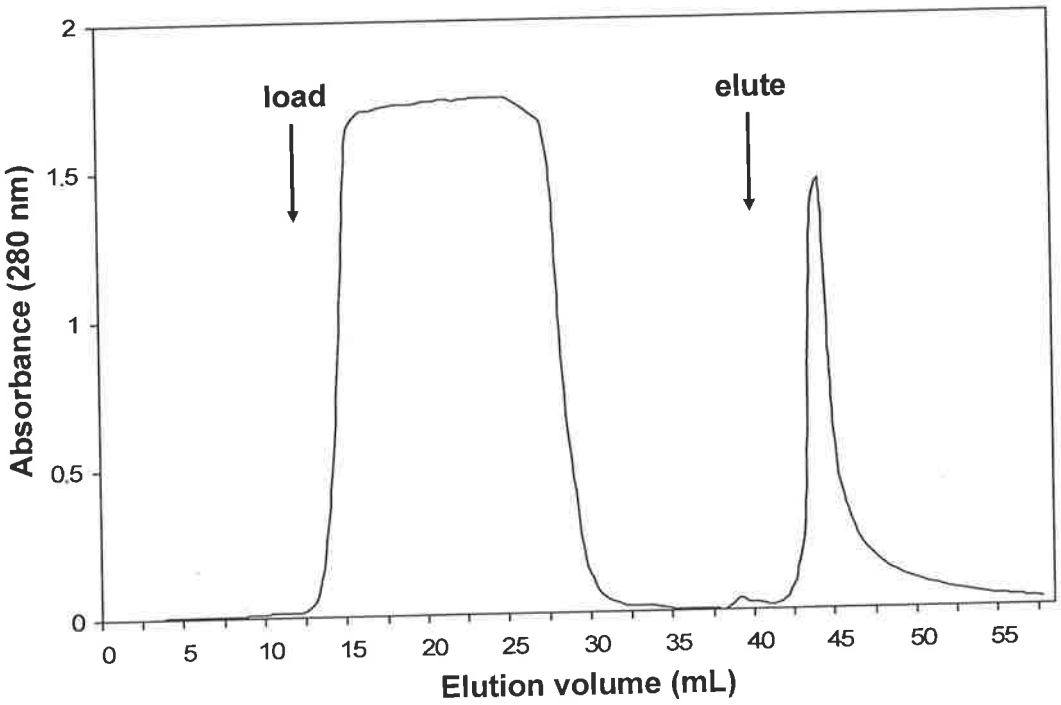

Figure 4.4 Loading and elution profile from the purification of sheep sera immunised with N350S ASA

Ammonium sulphate-precipitated Ig fraction (5.0 mL) was dialysed against PBS, pH 7.2 (4°C, overnight), and loaded onto the N350S ASA enzyme affinity column as described in section 2.2.7. Arrows indicate the point at which loading of the sample and its elution with 0.1 M H_3PO_4/NaOH, pH 2.5, commenced. Eluates (44 mL through to 46 mL) were pooled, dialysed and quantified (section 2.2.8.8).

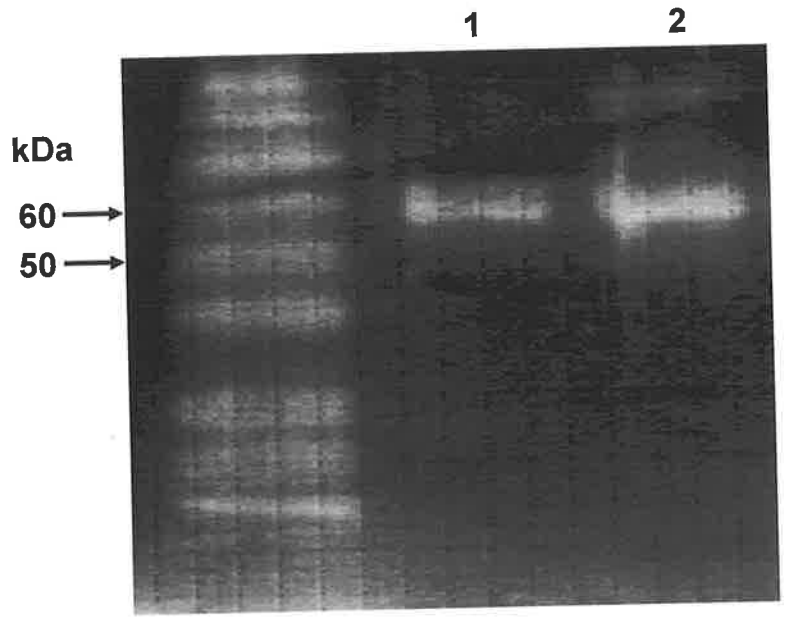

Figure 4.5 Western analysis of Wt ASA and N350S ASA with anti-ASA polyclonal antibody

Pre-stained marker (left) (5.0 μL), Wt ASA (1) and N350S ASA (2) were electrophoresed on a 12% Tris-glycine-SDS gel at a constant voltage (180 V), as described in section 2.2.4, and transferred to a PVDF membrane at a constant current (250 mA). The membrane was probed with sheep anti-ASA polyclonal antibody (1.0 μg/mL) and reactive proteins detected with donkey anti-sheep HRP-conjugate (1:1 000 dilution), as described in section 2.2.4.3. The image of the PVDF membrane was recorded using the UVItec-gel documentation system.

4.3.2. Preparation of reagents

The purification procedure for the sheep anti-ASA polyclonal antibody is described in section 2.2.7. The purified polyclonal antibody was stored in aliquots of 60 µL/tube at -20°C until use. Purified Wt ASA from the CHO-K1 cell expression system (section 2.2.11) was used as a calibrator for these assays.

4.3.2.1 Preparation of the europium-labelled anti-ASA polyclonal antibody

The Eu^{3+}–labelled anti-ASA polyclonal antibody was prepared by labelling the anti-ASA polyclonal antibody (1.0 mg/200 µL) with Eu^{3+} according to the manufacturer's instructions (section 2.2.8.9). Figure 4.6 shows the chromatogram of the Eu^{3+}-labelled anti-ASA polyclonal antibody on SEC (Superose 12 HR 30). The eluate containing the Eu^{3+}–labelled anti-ASA polyclonal antibody (24 through to 27 mL) was pooled and the concentration determined (section 2.2.8.8). The final yield of labelled anti-ASA polyclonal antibody was 0.7 mg in a volume of 3.0 mL. The labelling efficiency was within the range recommended by the manufacturer (7 Eu^{3+} atoms per antibody molecule).

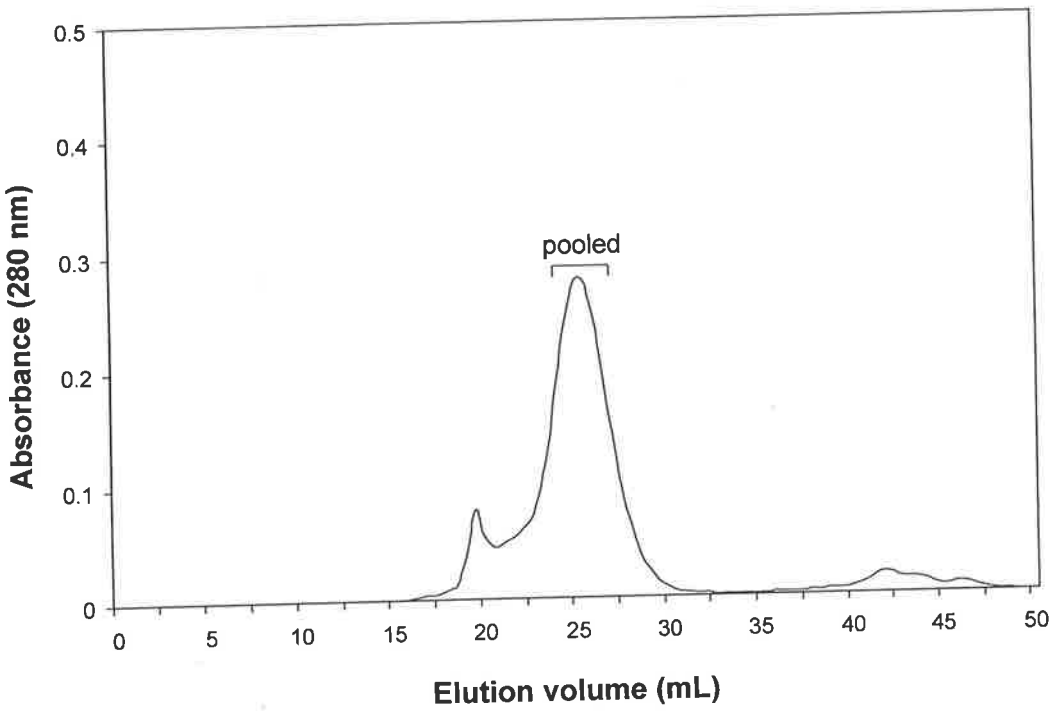

Figure 4.6 Size exclusion chromatography of the Eu^{3+}-labelled anti-ASA polyclonal antibody

Anti-ASA polyclonal antibody (1.0 mg/200 µL) was labelled with Eu^{3+} according to the manufacturer's instructions, and purified by SEC (Superose 12 HR 30) connected to a Biologic DuoFlow system using the protocol described in 2.2.8.9. Eluates 24 through to 27 mL were pooled and quantified.

4.3.3. Immune-capture activity assay

An immune-capture activity assay using the sheep anti-ASA polyclonal antibody was developed, optimised and validated. The experimental details involved in establishing this assay follow.

4.3.3.1. Optimising the concentration for primary antibody coating and incubation time

To determine the optimal coating concentration for the primary antibody (anti-ASA polyclonal antibody) and the optimum capturing period for the assay, Immunlon® 4HBX Removawell® strips (12 wells/strip) were coated with the primary antibody at concentrations of 10, 8, 4, 2 and 1 μg/mL (in duplicate), diluted in 0.1 M $NaHCO_3$ (100 μL/well) and incubated at 4°C, overnight. A total of 10 strips were coated, with two strips each (one blank and one test) designated for each incubation time. The strips were washed (6x) before Wt ASA (3.2 ng in 100 μL in 0.1 M sodium acetate/acetic acid buffer, 0.1% BSA, pH 5.6) was added to each test strip. The strips were incubated for 1, 2, 4 and 8 hrs at RT, and also for 8 and 16 hrs at 4°C. At the end of each incubation time, strips were washed (6x) before 20 mM 4-MUS substrate in 0.1 M acetate buffer, heat-treated 0.1% BSA, pH 5.6, was added (100 μL/well) and incubated at 37°C for 2 hrs. The reaction was stopped by the addition of 0.2 M glycine/NaOH buffer, pH 10.7 (100 μL/well), and fluorescence read on a Perkin-Elmer 1420 multilabel counter.

Figure 4.7 shows the fluorescence units plotted against the concentration of primary antibody used in coating. From these results, it was determined that a coating concentration of 5.0 μg/mL and an incubation time of 16 hrs at 4°C were optimum for the assay. These values were chosen as a compromise between assay sensitivity, consumption of reagents, convenience and consistency of assay performance.

4.3.3.2. Determination of substrate concentration

To determine the optimum substrate concentration for the assay, Wt ASA in 20 mM acetate buffer with 0.1% BSA, pH 5.5 (16 ng/well), was added to Immunlon® 4HBX Removawell® strips pre-coated with the primary polyclonal antibody (5.0 μg/mL) and incubated at 4°C, overnight. The strips were washed (6x) before the addition of 4-MUS substrate at concentrations of 2.5, 5, 10 and 20 mM prepared in 0.1 M sodium acetate/acetic acid buffer, heat-treated 0.1% BSA, pH 5.8 (100 μL, in duplicate), and incubated at 37°C for 2 hrs. Reactions were stopped by the addition of 0.2 M glycine/NaOH buffer, pH 10.7 (100

μL/well), and fluorescence read on a Perkin-Elmer 1420 multilabel counter. Figure 4.8 shows the fluorescence units plotted against the concentration of 4-MUS substrate used in the assay.

From these results, it was determined that 4-MUS substrate at a concentration of 10 mM gave the highest activity reading but, as a compromise between assay sensitivity due to background reading and consumption of reagents, it was decided to use 4-MUS substrate at a concentration of 5.0 mM. The lower background reading for 4-MUS substrate at 5.0 mM gave a higher signal-to-noise ratio, thus increasing the lower limit of detection in the assay.

4.3.3.3. Determination of optimum pH

To determine the optimum pH, Wt ASA (40 ng/mL) in 20 mM sodium acetate/acetic acid buffer, heat-treated 0.1% BSA, pH 5.5 (100 μL/well in duplicate), was added to Immunlon® 4HBX Removawell® strips pre-coated with the primary polyclonal antibody (5.0 μg/mL) and incubated (4°C, overnight). The plates were washed (6x) before 5 mM 4-MUS substrate in 0.1 M sodium acetate/acetic acid buffer, heat-treated 0.1% BSA, pH ranging from 4.5 to 7.0, was added (100 μL/well) and incubated at 37°C for 2 hrs. Reactions were stopped by the addition of 0.2 M glycine/NaOH buffer, pH 10.7 (100 μL/well), and fluorescence read on a Perkin-Elmer 1420 multilabel counter. Figure 4.9 shows the fluorescence units plotted against the pH. From this result, the pH optimum of the immune-capture assay was determined to be pH 5.0.

4.3.3.4. Immune-capture activity assay performance

The Wt ASA calibrator was serially diluted from 2.0 ng/well to 2.0 pg/well in 20 mM sodium acetate/acetic acid buffer, heat-treated 0.1% BSA, pH 5.5, in Immunlon® 4HBX Removawell® strips pre-coated with the primary polyclonal antibody (5.0 μg/mL), in duplicate. The plates were incubated at 37°C overnight and washed (6x) with 20 mM sodium acetate/acetic acid buffer, pH 5.0, before the addition of 5 mM 4-MUS substrate prepared in 20 mM sodium acetate/acetic acid buffer, heat-treated 0.1% BSA, pH 5.0 (100 μL/well). The plate was sealed with Linbro® plate sealer and incubated at 37°C for 24 hrs. Reactions were stopped by the addition of 0.2 M glycine/NaOH buffer, pH 10.7 (100 μL/well), and fluorescence read on a Perkin-Elmer 1420 multilabel counter. The specific activity of the Wt ASA calibrator used in the assay was determined using the tube method (section 2.2.1.9).

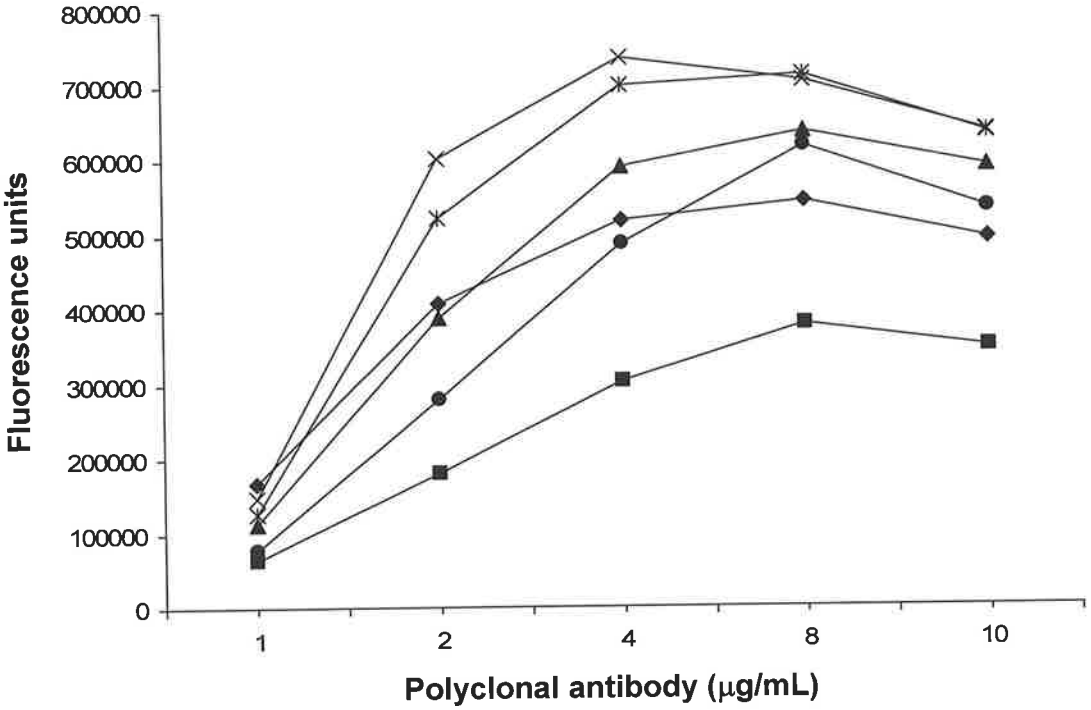

Figure 4.7 Immune capture activity assay of Wt ASA with varying concentrations of antibody coating and incubation times

Immunlon® 4HBX Removawell® strips were coated with the primary antibody at concentrations of 10, 8, 4, 2 and 1 μg/mL. Wt ASA (3.2 ng in 100 μL) was assayed as described in section 4.3.3.1, with incubations carried out for 1 hr (■), 2 hrs (◆), 4 hrs (▲) and 8 hrs (●) at RT, and 8 hrs (×) and 16 hrs (∗) at 4°C.

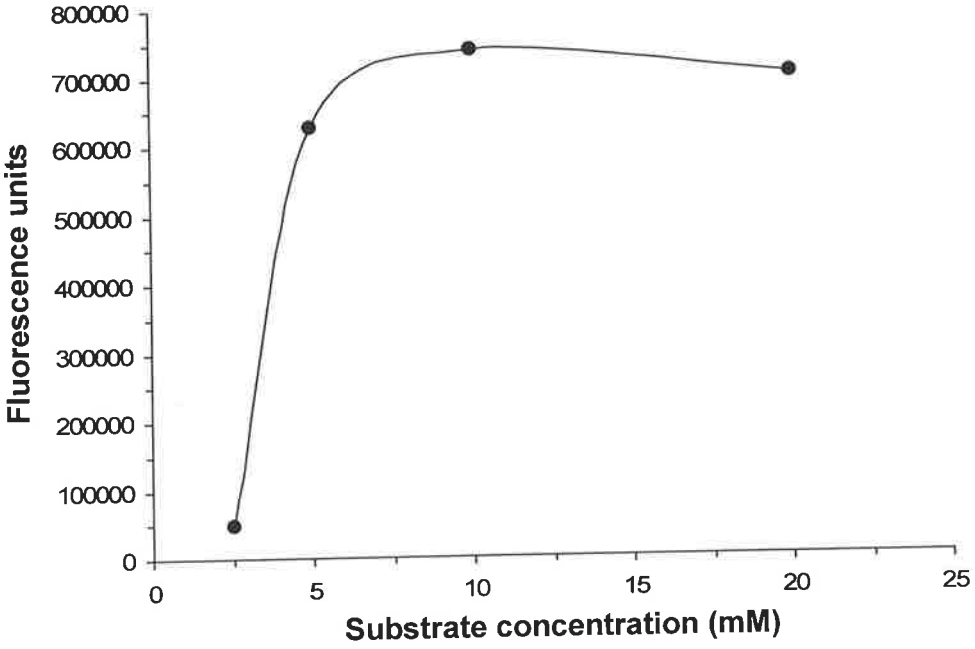

Figure 4.8 Immune capture activity assay of Wt ASA with varying substrate concentrations

Immunlon® 4HBX Removawell® strips were coated with primary polyclonal antibody (5 μg/mL) and incubated at 4°C, overnight. Wt ASA (16.0 ng/100 μL) was assayed as described in section 4.3.3.2.

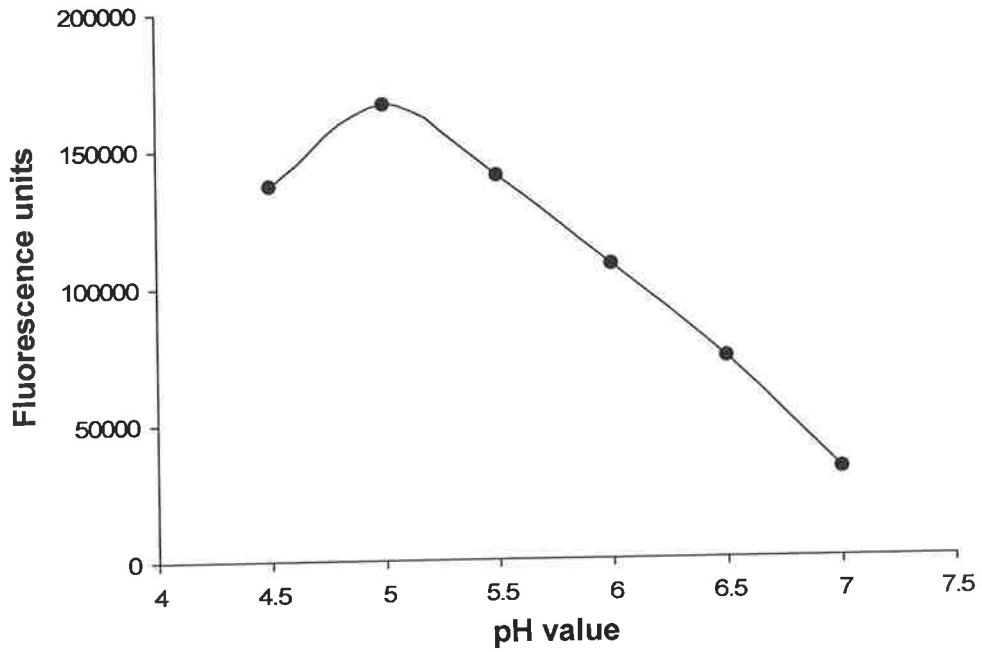

Figure 4.9 Immune capture activity assay of Wt ASA with varying pH

Immunlon® 4HBX Removawell® strips were coated with primary polyclonal antibody (5 μg/mL) and incubated at 4°C, overnight. Wt ASA (40 ng/mL) was assayed as described in section 4.3.3.3.

Figure 4.10 shows the calibration curve for the Wt ASA calibrator in the immune-capture activity assay. The assay showed a linear response over the range 3.0 to 780 pmol/h/well.

To monitor assay performance, three liquid quality control samples prepared from Wt ASA at concentrations of 0.2, 0.8 and 2.0 ng/mL in 20 mM sodium acetate/acetic acid buffer, 0.1% heat-treated BSA, pH 5.0, were used: intra-assay CV, based on 20 observations, was 18%, 14% and 6%, respectively. Two quality control samples prepared from Wt ASA, designated Low QC (0.4 ng/mL) and High QC (4.0 ng/mL), were included in each assay for the determination of inter-assay CV: based on six observations over 3.5 months, inter-assay CV was 19% and 13%, respectively.

The intra-assay CV was also determined for dried blood spot samples from an unaffected control, which, based on 20 observations, was found to be 7%. A second blood spot from another unaffected control was used as a quality control in each assay for the determination of inter-assay CV, which, based on six observations over 2.5 months, was 16%.

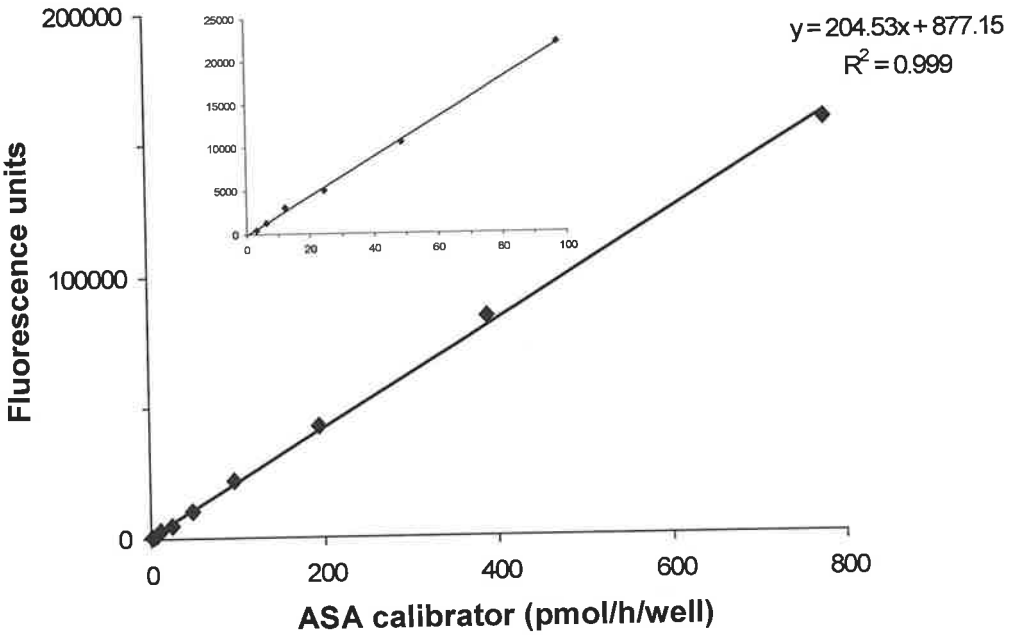

Figure 4.10 Calibration curve for ASA in the immune-capture activity assay

The ASA calibrator, at concentrations of 2.0 pg/well to 2.0 ng/well, was assayed using the immune-capture activity assay described in section 4.3.4.1. The specific activity of ASA was determined using the tube method described in section 2.2.1.9. The insert is an enlargement of the graph showing the values of the ASA calibrator between 0 to 100 pmol/h/well.

4.3.4. Immune-quantification protein assay

An immune-quantification assay using the sheep anti-ASA polyclonal antibody was developed, optimised and validated. The experimental work involved in establishing this assay is detailed below.

4.3.4.1. Optimising the concentration for antibody coating and the assay incubation time

To determine the optimum coating concentration for the primary antibody and the optimum capturing period for the assay, Immunlon® 4HBX Removawell® strips (12 wells/strip) were coated with the primary antibody at concentrations of 10, 8, 4, 2 and 1 μg/mL, diluted in 0.1 M $NaHCO_3$ across the strip in duplicate (100 μL/well) and incubated at 4°C, overnight. Ten strips were coated, with two strips each (one for blank) designated for each incubation time. The strips were washed (6x with DELFIA® wash buffer) on a DELFIA® plate washer before Wt ASA (2.0 ng in 100 μL) diluted in DELFIA® assay buffer was added to each. The strips were incubated for 1, 2, 4 and 8 hrs (RT), and a further two strips were incubated for 16 hrs (4°C). At the end of each incubation time, the strips were washed (6 x, DELFIA® wash buffer) on a DELFIA® plate washer. DELFIA® assay buffer (100 μL/well) containing 0.3 μg/mL of Eu^{3+}-labelled anti-ASA polyclonal antibody was added and the strips were incubated overnight at 4°C. The strips were then washed (6x, DELFIA® wash buffer) before the addition of 200 μL of DELFIA® enhancement solution to each well. The plate was shaken (15 min) and fluorescence measured on a DELFIA 1234 research fluorometer.

Figure 4.11 shows the fluorescence units plotted against the concentration of antibody coating. From these results, it was determined that a coating concentration of 5.0 μg/mL with an incubation time of 16 hrs at 4°C was optimum for the assay. These values were chosen as a compromise between assay sensitivity, consumption of reagents, convenience and consistency of assay performance.

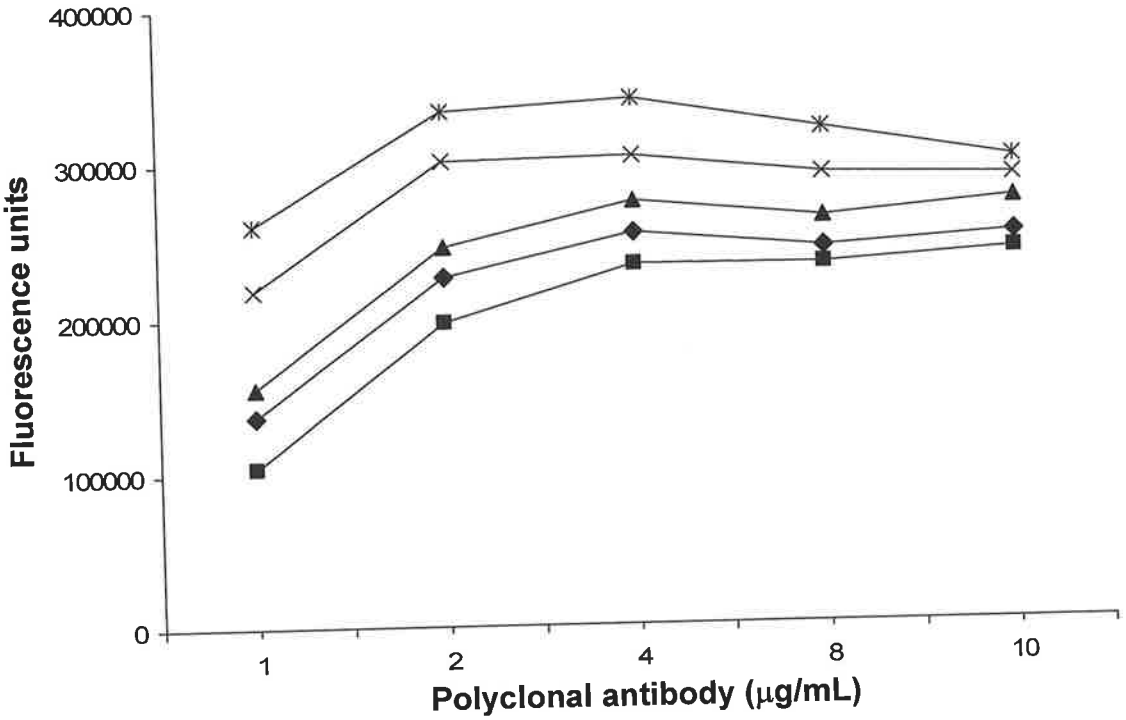

Figure 4.11 Immune-quantification of Wt ASA with varying primary antibody concentrations and incubation times

Immunlon® 4HBX Removawell® strips were coated with the primary antibody at concentrations of 10, 8, 4, 2, 1 and 0.5 µg/mL. Wt ASA (2.0 ng in 100 µL) was assayed (section 4.3.4.1) with incubations carried out for 1 hr (■), 2 hrs (◆), 4 hrs (▲) and 8 hrs (×) at RT, and 16 hrs (∗) at 4°C.

4.3.4.2 *Optimising the detection antibody concentration*

To determine the optimum concentration of the detection antibody (Eu^{3+}-labelled anti-ASA polyclonal antibody) for the immune-quantification assay, Wt ASA (40 ng/mL) prepared in DELFIA® assay buffer was serially diluted 1:2 (100 µL, in duplicate) in the pre-coated (primary polyclonal antibody, 5.0 µg/mL) wells of Immunlon® 4HBX Removawell® strips and incubated at 4°C, overnight. The strips were washed (6x, DELFIA® wash buffer), then DELFIA® assay buffer (100 µL) containing 0.1, 0.2 and 0.4 µg/mL of Eu^{3+}-labelled anti-ASA polyclonal antibody was added to each designated strip and incubated overnight at 4°C. The strips were then washed (6x, DELFIA® wash buffer) and 200 µL of DELFIA® enhancement solution was added to each well. The plate was shaken (15 min) and fluorescence measured on a DELFIA 1234 research fluorometer.

Figure 4.12 shows the fluorescence level plotted against different concentrations of detection antibody. From the results, it was determined that a detection antibody concentration of 0.2 µg/mL was the most suitable despite the fact that 0.4 µg/mL gave the highest reading. The decision was based on the background reading obtained from the concentrations tested at 0.1, 0.2 and 0.4 µg/mL, which were 3 577, 5 444 and 8 874 fluorescence units, respectively. The selection of 0.2 µg/mL for the assay was a compromise between assay sensitivity, consumption of reagents and consistency of assay performance.

4.3.4.3. *ASA immune-quantification assay performance*

Wt ASA was diluted to 40 ng/mL in DELFIA® assay buffer, serially diluted 1:2 (100 µL/well, in duplicate) in pre-coated (primary polyclonal antibody, 5.0 µg/mL) wells of Immunlon® 4HBX Removawell® strips and assayed in the final conditions described in section 2.2.10.2. Figure 4.13 shows the calibration curve for the Wt ASA calibrator in the immune-quantification assay. The results showed that the assay was linear in its response over the range 8.0 to 1 000 pg/well.

To monitor assay performance, three liquid quality control samples prepared from Wt ASA at concentrations of 0.2, 0.8 and 2.0 ng/mL in DELFIA® assay buffer were used: the intra-assay CV, based on 20 observations, was 18%, 14% and 9%, respectively. A further two samples prepared from Wt ASA, designated Low QC (0.4 ng/mL) and High QC (4.0 ng/mL), were also included in each assay as quality controls for the determination of inter-assay CV, which, from a total of seven observations over five-months, was found to be 10% for both samples.

Dried blood spot samples from an unaffected control were also used for intra-assay CV evaluation, which, based on 20 observations, was found to be 10%. A further blood spot from an unaffected control was used as a quality control in each assay for the determination of inter-assay CV, which, based on six observations over three-months, was 19%.

4.4. Additional parameters affecting assay performance

In addition to the assay optimisation process, other parameters that were considered to have an effect on the assay were also assessed.

4.4.1. Comparison of enzyme activity in the free and immune-captured activity assays

The specific activity of Wt ASA in the free and immune-captured activity assays was compared. The Wt ASA calibrator (2.0 ng/well to 2.0 pg/well) was immune-captured and activity determined using the protocol described in section 4.3.3.4. The free assay was performed using the same amount of Wt ASA calibrator in each well (50 µL in 20 mM sodium acetate/acetic acid buffer, heat-treated 0.1% BSA, pH 5.0), with 50 µL of 10 mM 4-MUS substrate prepared in 20 mM sodium acetate/acetic acid buffer, heat-treated 0.1% BSA, pH 5.0, assayed using uncoated Immunlon® 4HBX Removawell® strips, followed by incubation at 37°C for 24 hrs. Reactions were stopped by the addition of 0.2 M glycine/NaOH buffer, pH 10.7 (100 µL/well), and fluorescence read on a Perkin-Elmer 1420 multilabel counter. The specific activity of Wt ASA used in the assay was determined using the tube method (section 2.2.1.9).

Figure 4.14 shows the amount of ASA activity detected in the immune-capture activity assay and the free assay: on average, the amount of activity detected using the immune-captured assay was 47% of the level detected using the free assay.

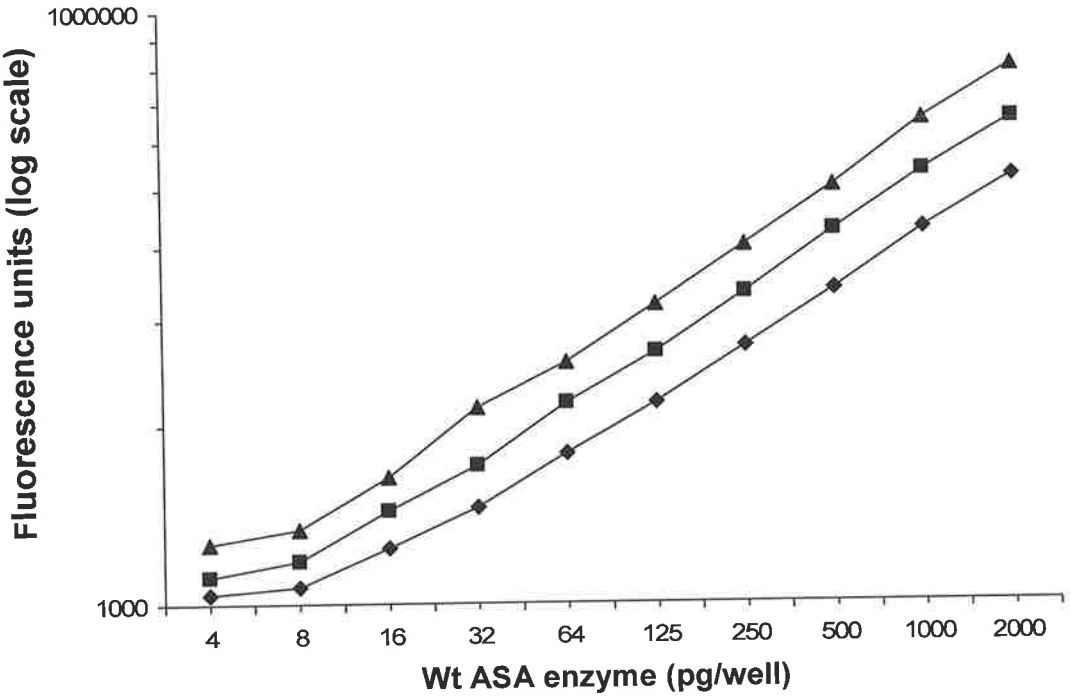

Figure 4.12 Immune-quantification of Wt ASA with varying concentrations of detection antibody

Wt ASA, at concentrations ranging from 4 pg/well to 2 000 pg/well, was assayed in pre-coated (primary polyclonal antibody, 5.0 µg/mL) wells of Immunlon® 4HBX Removawell® strips using the protocol described in section 4.3.4.2. In each test strip, fluorescence was determined by the addition of Eu^{3+}-labelled anti-ASA polyclonal antibody (detection antibody) at concentrations of 0.1 (◆), 0.2 (■) and 0.4 µg/mL (▲), respectively. Fluorescence was measured on a DELFIA 1234 research fluorometer.

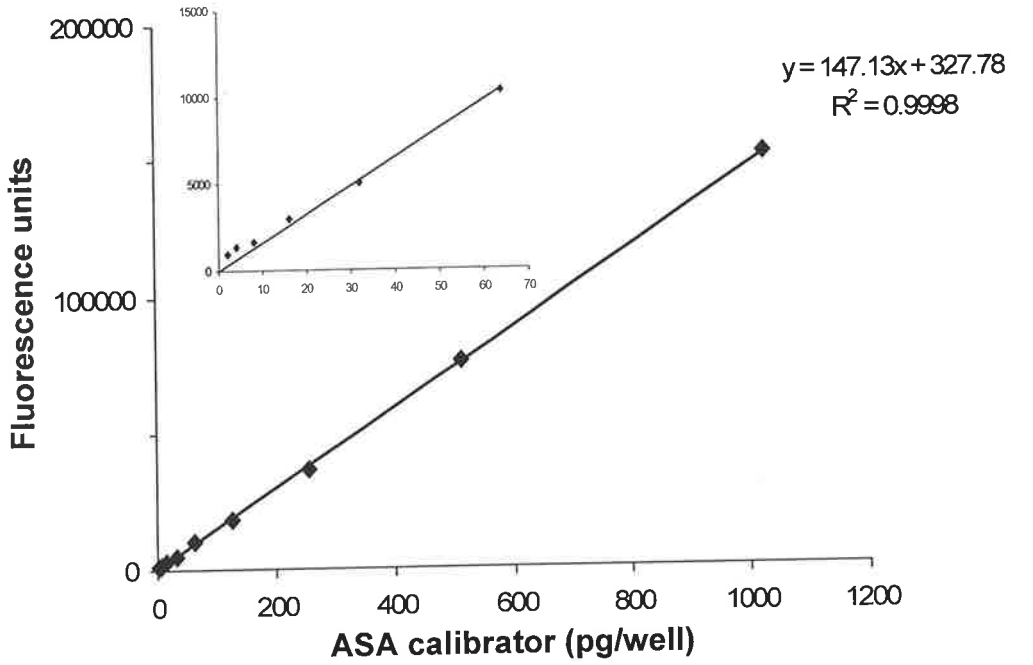

Figure 4.13 Calibration curve for Wt ASA in the immune-quantification assay

The Wt ASA calibrator, at concentrations of 2.0 pg/well to 2.0 ng/well, was assayed using the immune-quantification assay described in section 2.2.10.2. Fluorescence was determined by the addition of Eu^{3+}-labelled anti-ASA polyclonal antibody (0.2 μg/mL). Fluorescence was measured on a DELFIA 1234 research fluorometer. The insert is an enlargement of the graph showing the values of the Wt ASA calibrator between 0 to 70 pg/well.

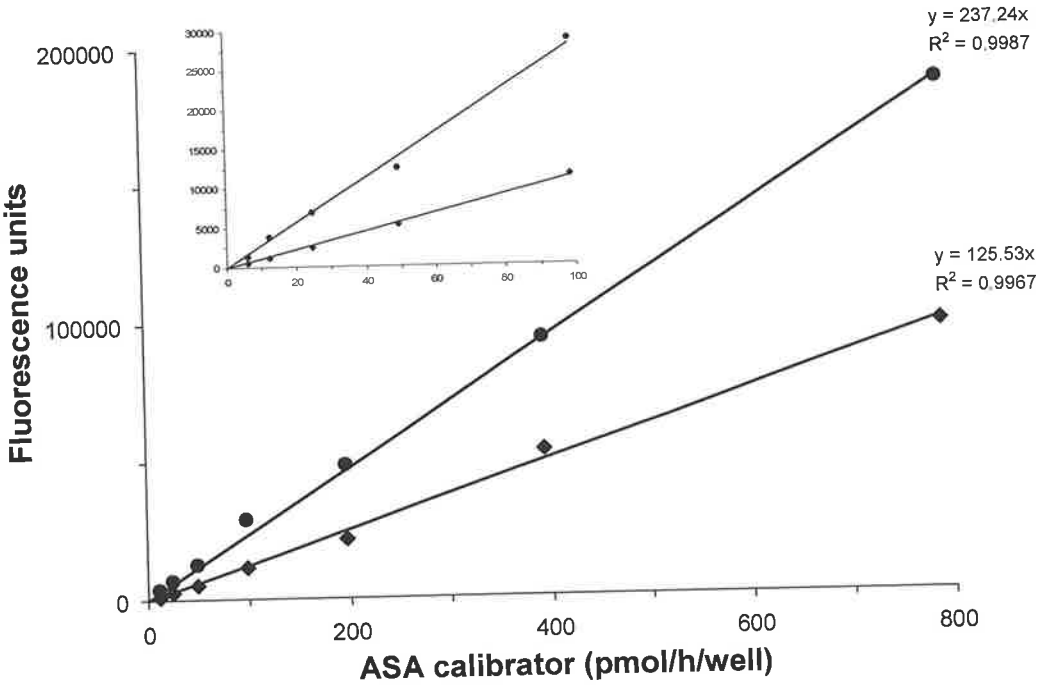

Figure 4.14 Calibration curves for Wt ASA in the free and immune-capture activity assays

Wt ASA calibrator, at concentrations of 2.0 pg/well to 2.0 ng/well, was assayed using the immune-capture activity assay (◆) described in section 4.3.3.4, and the free assay (●) described in section 4.4.1. ASA specific activity was determined using the tube method described in section 2.2.1.9. The insert is an enlargement of the graph showing the values of the ASA calibrator between 0 to 100 pmol/h/well.

4.4.2. Percentage of Wt ASA captured by the anti-ASA polyclonal antibody in the immune-capture activity assay

To determine the percentage of enzyme captured by the anti-ASA polyclonal antibody in the immune-capture activity assay, Wt ASA (4.0 ng in 100 µL diluted in 0.1 M sodium acetate/acetic acid buffer, heat-treated 0.1% BSA, pH 5.6) was captured in pre-coated (5.0 µg/mL anti-ASA polyclonal antibody) Immunlon® 4HBX Removawell® strips (in duplicate) by incubation at 4°C, overnight. After incubation, 50 µL was transferred to new uncoated wells of Immunlon® 4HBX Removawell® strips. The coated test strips were washed (6x) before the addition to each well of 100 µL of 20 mM 4-MUS substrate prepared in 20 mM sodium acetate/acetic acid buffer, heat-treated 0.1% BSA, pH 5.6; 50 µL of 40 mM 4-MUS substrate prepared in 20 mM sodium acetate/acetic acid buffer, heat-treated 0.1% BSA, pH 5.6, was added to each well of the uncoated strip. Both test strips were incubated at 37°C for 2 hrs. The reactions were stopped by the addition of 0.2 M glycine/NaOH buffer, pH 10.7 (100 µL/well), and fluorescence read on a Perkin-Elmer 1420 multilabel counter. As a control, the same amount of Wt ASA was assayed using the free assay method (section 2.2.1.8). The results showed that, on average, the percentage of enzyme captured by the anti-ASA polyclonal antibody was 90%.

4.4.3. Effect of pH on the immune-capture activity assay

To determine the effect of pH during the capture step, immune-capture activity assays were carried out using (i) 0.1 M sodium acetate/acetic acid buffer, heat-treated 0.1% BSA at pH 5.5, and (ii) 0.1 M Tris/HCl, 0.25 M NaCl buffer with 0.1% BSA at pH 7.2 as diluent for Wt ASA (4.0 ng/well to 2.0 pg/well), followed by incubation (4°C, overnight). The strip incubated at pH 5.5 was washed (6x) with 20 mM sodium acetate/acetic acid buffer, pH 5.5, while the strip incubated at pH 7.2 was washed (6x) with 20 mM Tris/HCl, 0.25 M NaCl buffer at pH 7.2. Activity was determined by the addition of 100 µL of 10 mM 4-MUS prepared in 20 mM sodium acetate/acetic acid buffer, heat-treated 0.1% BSA, pH 5.0, using the protocol described in section 4.3.3.3.

Figure 4.15 shows the difference in ASA activity using the capture step at pH 5.0 and pH 7.2, respectively: the activity obtained by capturing the protein at pH 5.0 was approximately 20% higher than that at pH 7.2.

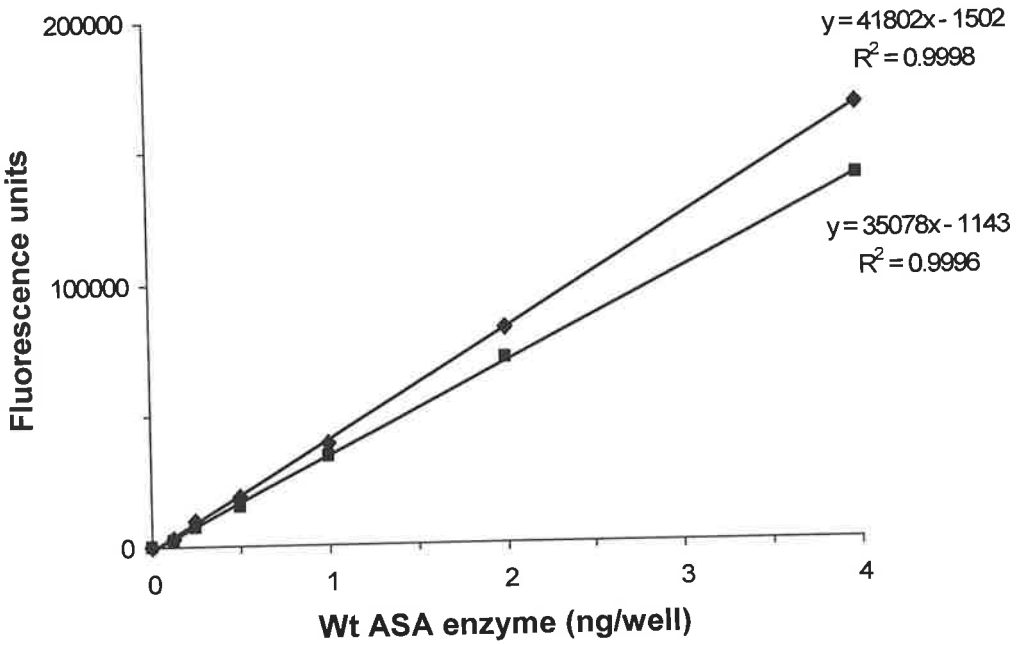

Figure 4.15 Effect of pH on the capture step in the immune-capture activity assay

Wt ASA (4.0 ng/well to 2.0 pg/well) was diluted and captured in 0.1 M sodium acetate/acetic acid buffer, heat-treated 0.1% BSA, pH 5.5 (◆), and 0.1 M Tris/HCl, 0.25 M NaCl buffer, heat-treated 0.1% BSA, pH 7.2 (■). The strip incubated at pH 5.5 was washed (6x) with 20 mM sodium acetate/acetic acid buffer, pH 5.5, and the strip incubated at pH 7.2 was washed (6x) with 20 mM Tris/HCl, 0.25 M NaCl buffer, pH 7.2. Activity was determined by the addition of 100 µL of 10 mM 4-MUS prepared in 20 mM sodium acetate/acetic acid buffer, heat-treated 0.1% BSA, pH 5.0, using the protocol described in section 4.3.3.3.

4.4.4. Effect of BSA on the immune-capture activity assay

To determine the effect of BSA on the background reading of the assay, 10 mM 4-MUS substrate was prepared using 20 mM acetate/acetic acid buffer, pH 5.8, with heat-treated (60°C, 40 min) and non-heat-treated BSA (1.0 g/L), respectively. Each substrate was then dispensed (100 µL/well) into two Immunlon® 4HBX Removawell® strips (12 wells/strip); four control strips using 10 mM 4-MUS substrate prepared without BSA were also included. One strip of each substrate was incubated at 37°C for 2 hrs; 100 µL of 0.2 M glycine/NaOH buffer, pH 10.7, was added to the remaining strips (zero hr incubation). The fluorescence was measured immediately on a Perkin-Elmer 1420 multilabel counter. The reactions on the incubated strips were stopped after the incubation period by the addition of 100 µL of 0.2 M glycine/NaOH buffer, pH 10.7, and fluorescence measured on a Perkin-Elmer 1420 multilabel counter.

The results showed that the fluorescence units obtained from the control, untreated BSA substrate and the heat-treated BSA substrate were almost identical at zero hr incubation; no increase was observed in the activity of the heat-treated BSA substrate after a 2 hr incubation, however a 12% increase in activity was observed in the untreated BSA substrate after a 2 hr incubation.

4.5. Determination of ASA in dried blood spots

The two immune-based assays developed in this study (sections 4.3.3 and 4.3.4) were evaluated for their ability to measure ASA activity and protein in dried blood spots from unaffected controls, ASA-PD individuals and MLD patients.

4.5.1. Immune-capture activity of ASA in dried blood spots

ASA activity in dried blood spots was determined using the immune-capture assay described in section 2.2.10.1. Two blood spots (equivalent to 6 µL whole blood) from 20 unaffected controls, four ASA-PD individuals and five MLD patients were assayed in duplicate. Figure 4.16 shows that ASA activity in unaffected individuals was between 1.48 and 7.72 pmol/h/µL whole blood (median=4.16 pmol/h/µL), while no detectable activity was observed in either ASA-PD or MLD individuals. Results shown are the mean of the duplicate samples.

4.5.2. Immune-quantification of ASA protein in dried blood spots

ASA protein in dried blood spots was determined using the immune-quantification assay described in section 2.2.10.2. One blood spot (equivalent to 3 µL whole blood) from 20 unaffected controls, four ASA-PD individuals and five MLD patients was assayed in duplicate. Figure 4.17 shows that the median amount of ASA protein in unaffected and ASA-PD individuals was 31.9 pg/µL (range = 21.0 to 46.3 pg/µL) and 13.0 pg/µL (range = 8.3 to 17.0 pg/µL) whole blood, respectively; no detectable ASA protein was observed in MLD individuals. Results shown are the mean of the duplicate samples.

4.5.3. Stability of ASA in dried blood spots stored at room temperature

To assess the stability of ASA protein and activity, dried blood spots from an unaffected control were stored at RT: six 3 mm spots were subsequently punched out at days 0, 1, 2, 3, 4, 5, 6, 7, 10, 14, 18, 22, 26 and 30. The dried blood spots were immediately placed in a sealed plastic bag, placed in a desiccator and stored at -20°C until analysis on day 30. Two spots (duplicate) were used for the immune-capture activity assay (section 2.2.10.1) and one spot was used for the immune-quantification protein assay (section 2.2.10.2). Figure 4.18 shows that ASA protein was stable over the 30-day period but ASA activity had decreased significantly, with only 39% of activity remaining at the 30-day time-point. Results shown are the mean of the duplicate samples.

To confirm this result, blood from an unaffected control was spiked with Wt ASA and N350S ASA (400 ng/mL), then spotted onto filter paper, dried and subjected to the same experiment. The results showed that the amount of ASA protein was stable, with no significant change observed over the 30-day period; Wt ASA and N350S ASA activity had, however, decreased to 28% and 30% of the activity measured on day zero, respectively.

4.5.4. Effect of anti-coagulant on ASA activity in dried blood spots

To determine the effect of anti-coagulant on ASA activity in dried blood spots, blood samples from three unaffected controls were collected in plain, lithium heparin and EDTA tubes. The blood samples were spotted onto dried blood spot cards (50 μL/spot) and air-dried. These dried blood spots were assayed in duplicate and the immune-capture activity assay performed on the same day using the protocol described in section 2.2.10.1. No difference in activity was observed in blood samples collected in plain, lithium heparin or EDTA tubes, indicating that lithium heparin and EDTA do not inhibit ASA activity.

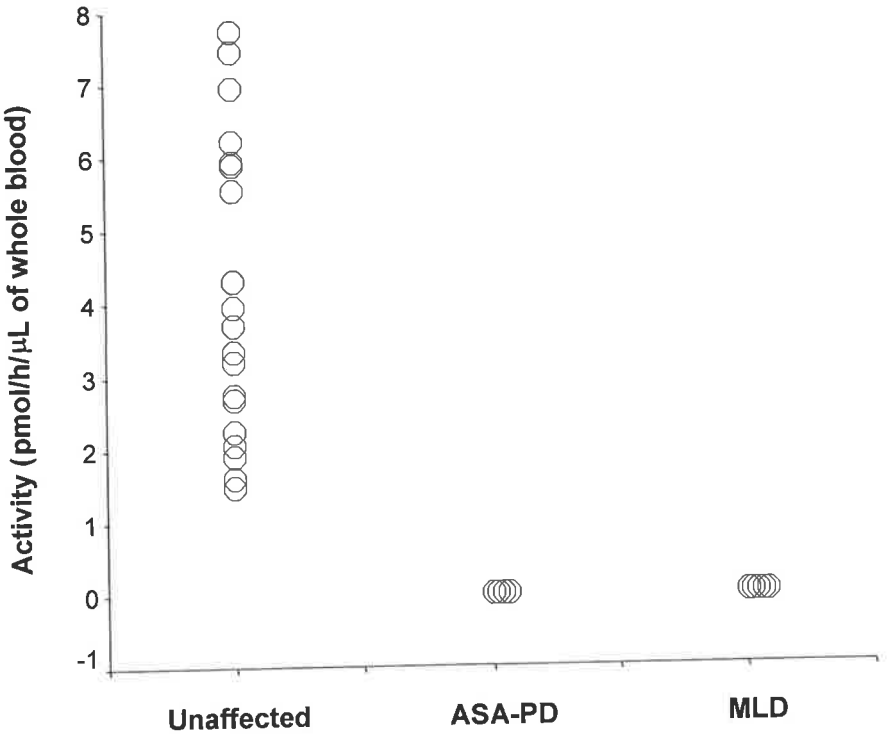

Figure 4.16 Immune-capture activity of ASA in dried blood spots

Two dried blood spots each were collected from unaffected controls (n=20), ASA-PD individuals (n=4) and MLD patients (n=5). Assays were run in duplicate using the immune-capture activity assay described in section 2.2.10.1. Results shown are the mean of the duplicate samples.

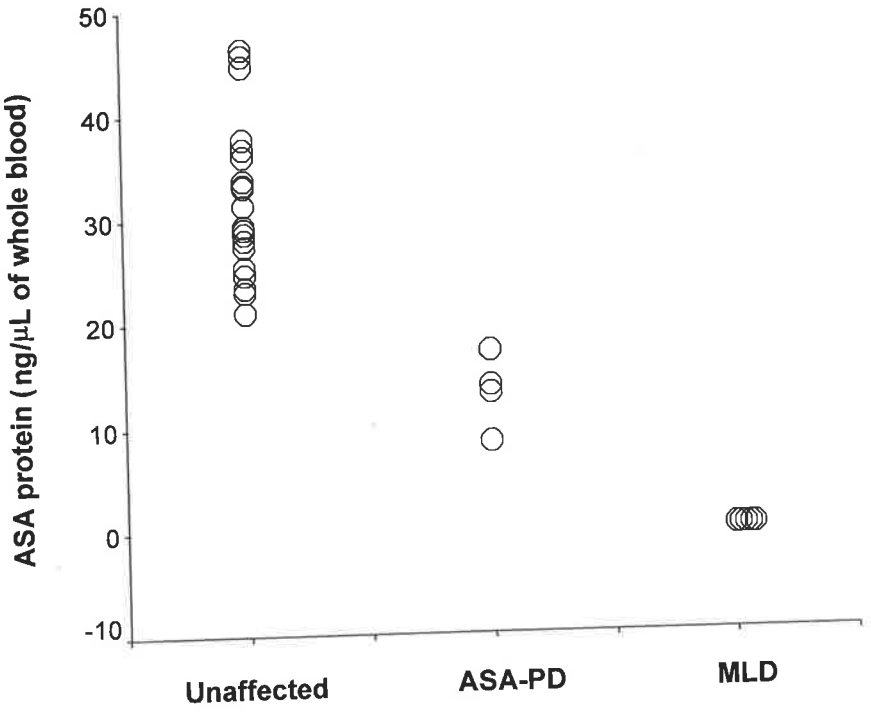

Figure 4.17 Immune-quantification of ASA protein in dried blood spots

Dried blood spots from unaffected controls (n=20), ASA-PD individuals (n=4) and MLD patients (n=5) were assayed in duplicate using the immune-quantification assay described in section 2.2.10.2. Results shown are the mean of the duplicate samples.

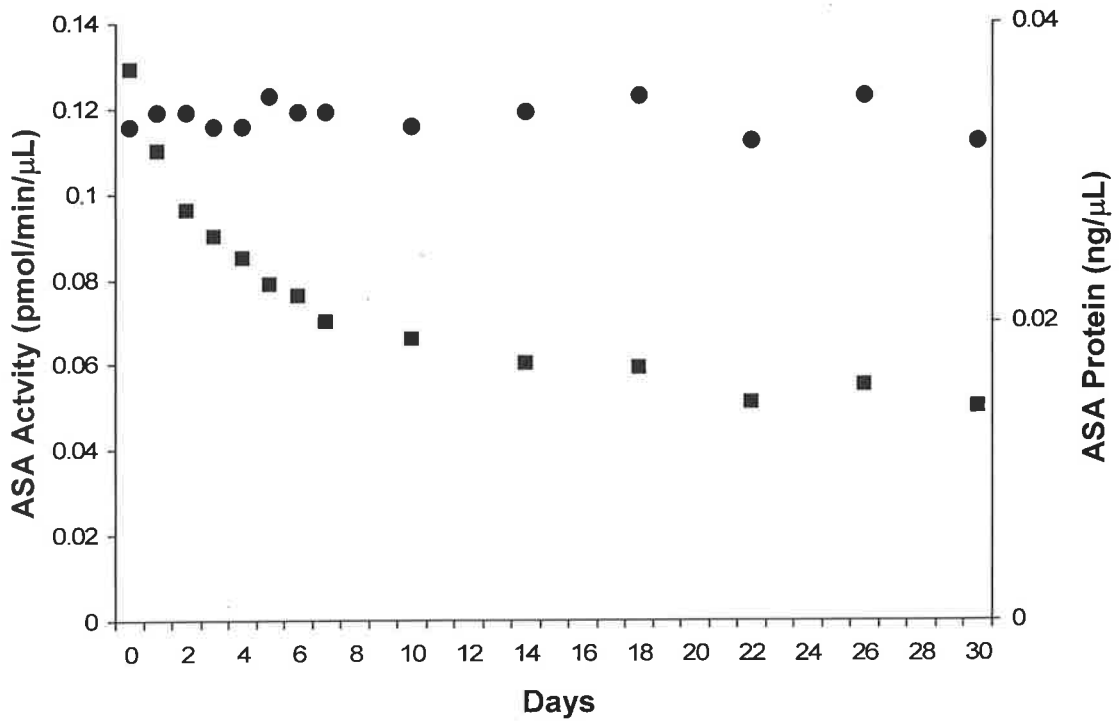

Figure 4.18 ASA stability in dried blood spots stored at room temperature

A dried blood spot was collected from an unaffected control. Six 3 mm punches were taken from this blood spot at days 1, 2, 3, 4, 5, 6, 7, 10, 14, 18, 22, 26 and 30 post-collection. The punches were immediately placed in a sealed plastic bag in desiccant and stored at -20°C until analysis on day 30. Two spots were used for the immune-capture activity assay (in duplicate) using the protocol described in section 2.2.10.1; one spot was used in the immune-quantification assay (in duplicate) using the protocol described in section 2.2.10.2. ● = ASA protein; ■ = ASA activity.

4.6. Discussion

A major aim of this study was to improve the diagnostic protocol for the detection of MLD. From the literature, it is known that the major weakness in current biochemical diagnostic methods is the inability to unambiguously diagnose a MLD patient by enzyme assay of ASA activity alone: the repertoire of assays required to confirm a diagnosis is cumbersome, time-consuming and only available in specialised laboratories. In consequence, relatively few laboratories offer such testing. Furthermore, collection and transport of samples such as whole blood and skin biopsies present logistical problems, particularly from remote locations. To overcome these difficulties, it was proposed to develop immune-based assays for the measurement of ASA enzyme activity and protein from dried blood spots, which are easily collected and transported.

There is also a requirement to overcome the diagnostic dilemma posed by the existence of ASA-PD individuals. The approach taken in this study was to develop antibody-based methodology that could distinguish ASA-PD individuals from unaffected controls and MLD patients by detection of the enzyme with the N350S mutation. The N350S mutation substitutes an asparagine with a serine, thereby removing a glycosylation site on the surface of the protein. The 3-D structure of the ASA protein (drawn with Mol script based on human cDNA sequence by Stein *et al.*, 1989) shows that the amino acid sequence surrounding the N350S mutation is on the surface of the protein. Consequently, the absence of the glycosylation site due to the substitution of the asparagine will expose the surrounding amino acids. An antibody generated to recognise those peptides would therefore be expected to differentiate N350S ASA from Wt ASA. However, the sheep polyclonal antibody raised against the peptide conjugate across the N350 sequence failed to capture the N350S protein in this study, despite showing specific cross-reactivity to N350S ASA by Western blotting. This failure could be due to the surface being folded (buried) consequent to a conformational change resulting from the missing carbohydrate residue, as N-linked oligosaccharides are known to be associated with the folding, function and stability of glycoproteins (Hammond *et al.*, 1994).

The carbohydrate residue in the ASA enzyme could also act as a buoy due to its hydrophilic nature, thus maintaining the surface structure seen in the 3-D structure of the protein. This hypothesis is further supported by the results obtained from epitope mapping of the sheep and mice sera immunised against N350S ASA: no reactivity was observed on the 12 amino acid sequence across the N350 site (section 4.2.2) in all sera tested. Attempts to expose the surface through heating and the addition of a reducing agent (1% β-mercaptoethanol) were

also unsuccessful (results not shown), suggesting that the level of denaturation was insufficient to expose the N350S epitope or the protein. However, the failure to establish an immune assay system to detect ASA-PD did not hamper the aim to improve the detection system for MLD. This initial impediment to the detection of ASA-PD was overcome by the development of two immune-based assays with the necessary specificity and sensitivity required to discriminate between ASA-PD and MLD.

Monoclonal antibody production was a challenging aspect of this study. Despite a number of attempts, no useful monoclonal antibodies were generated. While strong titres were obtained using Freund's complete adjuvant, immunisation using the ImmuneEasy™ mouse adjuvant produced almost no immunological response. The manufacturer of the ImmuneEasy™ mouse adjuvant claimed that it had the ability to invoke antibody titres that were at least equal to or higher than that induced by Freund's complete adjuvant, using less antigen and in less time, however, the resultant titre of 1:4 000 indicated otherwise. There was no plausible explanation for the failure, as the titre level did not increase subsequent to the administration of an extra booster dose.

Epitope mapping has aided our understanding of the epitope reactivity of polyclonal antibodies produced against native enzymes obtained from sheep and mouse sera towards the linear sequence of the ASA enzyme. The result showed that the polyclonal antibodies generated against Wt ASA and N350S ASA produced a very low percentage of high-affinity reactivity epitopes to the ASA enzyme. On average, the sheep polyclonal antibody raised against N350S ASA produced slightly more than 20% of high-affinity epitopes, while the sera from mice immunised against Wt ASA produced only 5% of high-affinity reactivity epitopes. Comparatively, the high-affinity epitopes were far less than those obtained with iduronate-2-sulphatase, which was reported to produce approximately 60% of high-affinity epitopes (Parkinson-Lawrence *et al.*, 2005). This suggests that the ASA enzyme is not antigenic to mice and could be due to the high degree of homology (86%) between the mouse and human ASA amino acid sequence (Kresying *et al.*, 1994).

Despite the low percentage of high affinity epitopes observed, three peptide conjugates were designed based on the results of epitope mapping. It was anticipated that the peptide conjugates would be more antigenic than the native enzymes since they were specifically designed to represent the surface of the native protein. However, test-bleed samples from mice immunised with these peptide conjugates showed that the antibody titre against Wt ASA was very low (1:4 000), even though an overall increase in titre level (>1:1 000 000)

was obtained in most mice. These results indicated that the epitope on the ASA enzyme was not recognised by antibody produced against these peptide conjugates. Due to time constraints and the fact that the anti-ASA polyclonal antibody was working well in the immune-based assays, the task of producing a monoclonal antibody was discontinued.

A number of problems encountered in the immune-based assay optimisation process were resolved. It is noteworthy that the concentration and pH of the 4-MUS used in the study ranged from 5 mM to 40 mM, and the pH ranged from pH 5.0 to pH 5.8. The concentration of 4-MUS substrate used in the earlier part of the study was either from the existing protocol used in the Department of Genetic Medicine or obtained from the literature. However, the final concentration and pH used was determined through characterisation of the enzymes and optimisation of the immune-based assays.

High background readings were evident in both the immune-capture and immune-quantification assays. It was found that the background reading in the immune-capture activity assay was inherent to the 4-MUS substrate and, to a lesser extent, to the 0.1% BSA, which was used as a stabiliser in the assay buffer. This finding led to the use of 4-MUS substrate at a concentration of 5 mM rather than 10 mM. Although results of the substrate concentration experiment showed that 10 mM 4-MUS gave a higher signal at the higher end of the calibration curve, the background reading was almost two-fold higher, which would have significantly reduced assay sensitivity. The contribution of BSA to the problem of background reading was overcome by heat-treating the BSA at 60°C for 40 min before use. The higher background reading may have been due to the presence of catalytically active bovine ASA acting on the 4-MUS. High background reading was overcome in the immune-quantification protein assay through the use of detection antibody at a lower concentration (0.2 μg/mL) than was optimal (section 4.3.4.2).

An additional factor affecting assay background was the pH of the buffer used as diluent in the immune-capture activity assay in SF lysates: it was found that at pH 5.0, the background was almost two-fold higher when compared to the capture step carried out at pH 7.2. The reason for this is unknown but from observations made during the assay, SF lysates diluted in buffer at pH 5.0 became turbid, which may have been due to the protein aggregations present in SF, hence contributing to the higher background reading due to unspecific protein binding. For this reason, the immune-capture activity assay for SF lysates used 0.1 M Tris/HCl, 0.25 M NaCl, pH 7.2, as opposed to the sodium acetate/acetic acid buffer, pH 5.0, used in the dried blood spot assay.

A 20% increase in activity was observed in the immune-capture activity assay in dried blood spots when the capturing step was carried out at pH 5.0 (Figure 4.15) compared with pH 7.2. This increase could be due to the nature of the ASA enzyme captured at pH 5.0 (octamer form), thus binding more tightly to the antibody-coated wells and having more accessible active sites for substrate cleavage. It was also demonstrated that the immune-capture activity assay was capturing >90% of the ASA enzyme using the Wt ASA calibrator (40 ng/mL), however, the activity of the captured enzyme was only about 47% of the level obtained in the free assay. The reduced activity could be due to the steric restriction of the captured enzyme, thus reducing its accessibility to the substrate. Another possible reason is the inhibitory effect on the enzyme arising from the capturing polyclonal antibody. However, the lower activity was corrected by the use of an activity calibration curve with each assay.

The absence of ASA activity in the dried blood spots collected from ASA-PD individuals led to studies of enzyme stability (section 4.5.3). It was expected that these individuals would retain some residual enzyme activity since a reasonable amount of ASA protein was detected in the immune-quantification assay. The results of the experiment carried out in section 4.5.3 showed that ASA in dried blood spots stored at RT was unstable, with significant loss of activity over time. One explanation that may account for this is the change in pH that occurs in dried blood. However, this particular problem was overcome by storing the dried blood spots at -20°C: ASA enzyme in dried blood spots stored at this temperature was stable for up to three-months.

The effect of anti-coagulant on blood collected in heparin and EDTA was also investigated. Anti-coagulants that act by chelating (such as EDTA) are known to have inhibitory effects on the activity of some lysosomal enzymes (personal communication, Prof. J. Hopwood). The results of these experiments showed that neither EDTA nor heparin had such an effect on the ASA enzyme.

In conclusion, the two immune-based assays developed in this study were shown to be highly specific, with the immune-quantification ASA protein assay having the ability to clearly distinguish between unaffected controls, ASA-PD individuals and MLD patients (section 4.5.2) using a 3 mm blood spot sample. This is one of the most important achievements of this project. The ability of these assays to measure ASA protein and activity in dried blood spots and unequivocally identify MLD patients will simplify the

procedures for sample collection, handling and storage for MLD testing. This will be particularly important for countries where sample collection and transport services are not well established or where transport overseas is required. The development of these assays will provide a more rapid and definitive diagnostic procedure for MLD.

CHAPTER FIVE

Establishment of a Sulphatide Quantification Method using Electrospray Ionisation–Tandem Mass Spectrometry and Development of a Sulphatide Loading Protocol

5. Introduction and aims

With the detection of asymptomatic MLD patients via NBS programmes, it will be essential to ascertain the clinical phenotype of these individuals. The ability to accurately predict clinical phenotype in an asymptomatic newborn will help the physician reach a decision about the most appropriate form of therapy and when it should commence. In addition, careful assessment of the benefit or otherwise of therapy in these patients will require new biochemical monitoring strategies. As discussed in section 1.4.7, genotype-to-phenotype and genotype-to-enzyme (1.4.7.1) correlations have limited application for the prediction of clinical severity for MLD.

In the case of MPS I (Bunge *et al.*, 1998) and Gaucher disease (Whitfield *et al.*, 2002), biochemical prediction of clinical severity utilises multiple parameters such as enzyme activity and protein, accumulated substrate and genotyping in SF, thus making SF a suitable model for the measurement of these parameters in MLD. However, because sulphatide does not accumulate in the SF of MLD patients (Dawson *et al.*, 1972), the only way to determine the substrate in SF is by induced accumulation through sulphatide-loading in cultured cells using either a radio-labelled substrate (Leinekugel *et al.*, 1992) or a fluorescent substrate (Bach *et al.*, 1987). In this study, ESI-MS/MS methodology was established and employed to measure the rate of sulphatide accumulation as well as secondary storage of other lipids in SF that had been subjected to sulphatide-loading. The use of ESI-MS/MS for the direct quantification of sulphatide in SF extracts was expected to simplify the loading protocol by avoiding the use of radio-labelled sulphatide. Furthermore, the method is amenable to the measurement of urinary sulphatide as a means by which to predict clinical severity as well as monitor therapy.

An ESI-MS/MS sulphatide quantification method was previously established in this Department, which enables the measurement of 13 species of monohexosyl sulphatide and one species of dihexosyl sulphatide in MLD urine (Whitfield *et al.*, 2001a). This study seeks to improve that methodology by characterising and identifying additional sulphatide species.

Hence, the two main aims of this chapter were, firstly, to establish an ESI-MS/MS method to accurately quantify sulphatide, and, secondly, to develop a functional SF assay to enable the quantification of stored substrate. In addition, an established glycosphingolipid quantification method (Fuller *et al.*, 2005a) was employed to quantify secondarily stored lipids resulting from sulphatide accumulation.

5.1. Sulphatide quantification using ESI-MS/MS

Sulphatides show strong ionisation in negative ion mode and produce a characteristic daughter ion at *m/z* 97 during collisionally activated dissociation (CAD) (Hsu *et al.*, 1998 and Whitfield *et al.*, 2001a). Hsu *et al.* (1998) also characterised the sulphatide species based on their fatty acid substituents using CAD MS/MS. CAD-MS/MS can also be used to resolve ambiguities associated with some sulphatide species where *m/z* values correspond to either a sulphatide with a non-hydroxylated fatty acid substituent or a hydroxylated fatty acid substituent with one additional double bond in the fatty acid; an example of a *m/z* value that demonstrates this ambiguity is 890.8, which can be either sulphatide 24:0 or sulphatide h23:1.

According to Hsu *et al.* (1998), sulphatide species with an α-hydroxy fatty acid (hFA) substituent will yield a characteristic ion cluster consisting of *m/z* 522, *m/z* 540 and *m/z* 568: the product ion at *m/z* 568 originates from the α-hydroxy-direct cleavage of the fatty acid side-chain from the parent ion; the subsequent loss of CO produces *m/z* 540, and the loss of H_2O forms *m/z* 522. This ion cluster is either absent or less abundant in the non-hydroxylated fatty acid substituent. These characteristics, together with the common ions at *m/z* 97 and *m/z* 241 and the ions resulting from the fatty acid amides (FA-amide), allow the identification of each sulphatide species.

5.1.1. Identification of sulphatide species

The identification of sulphatide species in this study was carried out using urine from a known MLD patient and sulphatide from bovine brain (Sigma Chemical Co., St. Louis, MO, USA). Lipids were extracted from urine (1.0 mL) according to the method of Bligh and Dyer (section 2.2.17.1); a sulphatide preparation from bovine brain was dissolved in chloroform/methanol (1:4) (50 μmol/L). Both samples were analysed by the infusion method described in section 2.2.18.5 using the instrument settings described in section 2.2.18. Figure 5.1 shows the Q1 scan in negative ion mode for both the MLD urine extract (A) and bovine brain sulphatide (B).

CAD MS/MS identified both the hydroxylated and non-hydroxylated sulphatide species in MLD urine and bovine brain. Each ion corresponding to a theoretical $[M-H]^{-1}$ of a sulphatide species identified in the Q1 scan was subjected to CAD MS/MS analysis. CAD was performed by scanning the CE value, starting at -130V and finishing at -5.0V. Using the method of identification employed by Hsu *et al.* (1998), a total of 18 sulphatide species were identified in MLD urine: nine species each of the hydroxylated and non-hydroxylated species were found in significant amounts, including two dihexosyl species (Table 5.1). Table 5.2 summarises the sulphatide species identified in the bovine brain sulphatide: 18 sulphatide species were identified, 10 of which were found to be hydroxylated; the remainder consisted of the non-hydroxylated species.

CAD-MS/MS was used to resolve the ambiguity of sulphatide species at *m/z* 890 and *m/z* 904. The tandem mass spectra in Figure 5.2 show the daughter ions obtained after CAD-MS/MS on the parent ions at *m/z* 890 (Panel A) and at *m/z* 904 (Panel B). CAD-MS/MS of the parent ion at *m/z* 890 produced an FA-amide ion at *m/z* 392 and the common ions at *m/z* 241 and *m/z* 97; the common ion at *m/z* 241 is known to be a dehydration product of the galactose-sulphate moiety, while the latter is known to be HSO_4^- (Hsu *et al.*, 1998). This identified the sulphatide as a non-hydroxylated species with a fatty acyl chain of 24:0. CAD-MS/MS of the parent ion at *m/z* 904 produced the cluster ions of *m/z* 568, *m/z* 540 and *m/z* 522, and a FA-amide ion at *m/z* 406. This fragmentation pattern identified the sulphatide species as a hSulp24:1 rather than Sulp25:0.

(A)

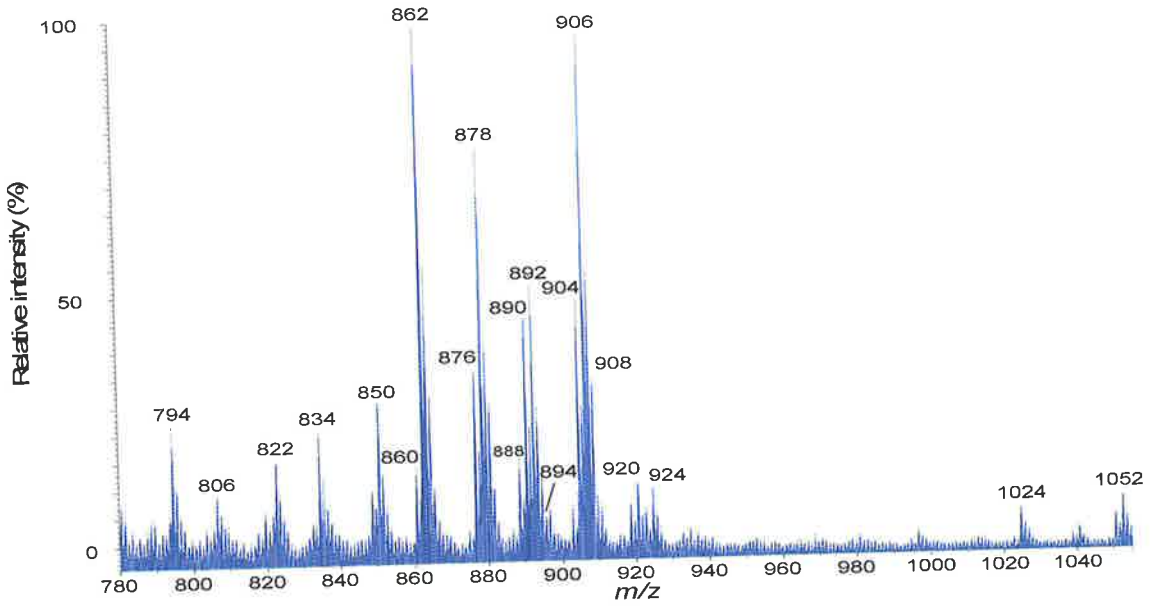

(B)

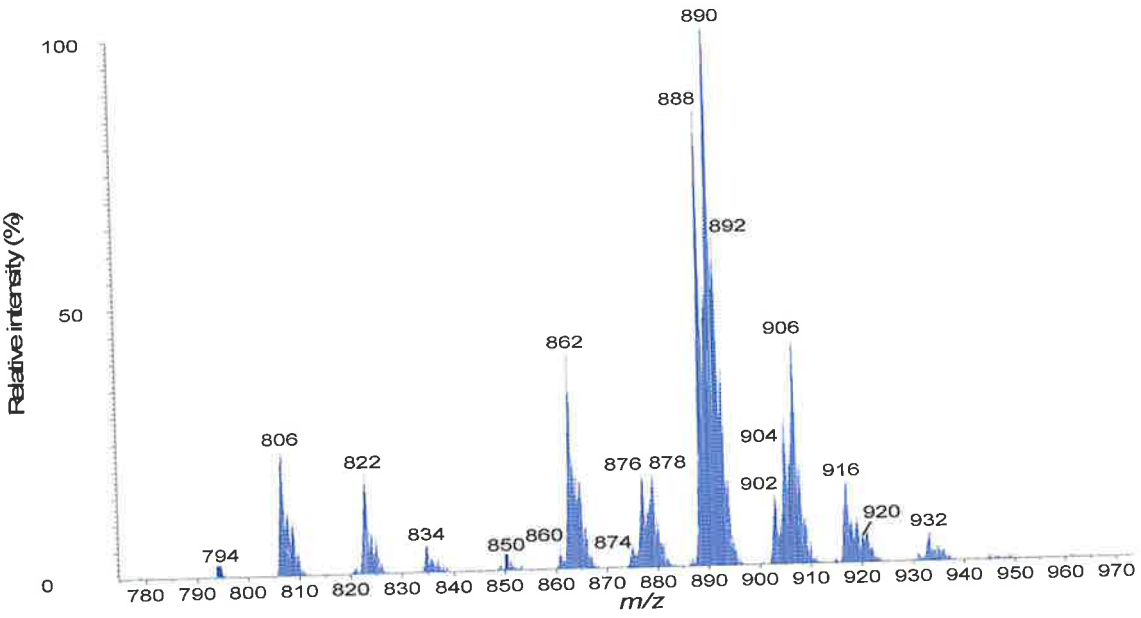

Figure 5.1 Mass spectra of sulphatide from MLD urine and bovine brain obtained from Q1 scan.

A lipid extract from MLD urine (section 2.2.17.1) and bovine brain sulphatide (50 µmol/L in chloroform/methanol [1:4]) was analysed by the infusion method described in section 2.2.18.5. Sulphatide species were detected in negative ion mode. Panel A shows the sulphatide profile obtained from MLD urine and Panel B shows the sulphatide profile obtained from bovine brain sulphatide using a Q1 scan.

Table 5.1 Sulphatide species identified in MLD urine

$[M-H]^-$ (*m/z*)	Fatty acyl chain[a]	FA-amide ion (*m/z*)	hFA ion cluster[b]
794	hSulp16:0	280	+
806	Sulp18:0	308	-
822	hSulp18:0	324	+
834	Sulp20:0	336	-
848	Sulp21:0	350	-
850	hSulp20:0	352	+
862	Sulp22:0	364	-
876	Sulp23:0	378	-
878	hSulp22:0	380	+
888	Sulp24:1	390	-
890	Sulp24:0	392	-
892	hSulp23:0	394	+
904	hSulp24:1	406	+
906	hSulp24:0	408	+
918	hSulp25:1	420	+
920	hSulp25:0	422	+
1024[b]	dhSulp22:0	364	-
1052[b]	dhSulp24:0	392	-

[a] Sulp = sulphatide; hSulp = hydroxy sulphatide; dhSulp = dihexosyl sulphatide;

[b] – indicates the absence or low abundance of the ions associated with hFA (*m/z* 522, *m/z* 540 and *m/z* 568); + indicates the presence of the hFA cluster ions.

Table 5.2 Sulphatide species identified in bovine brain

$[M-H]^-$ (*m/z*)	Fatty acyl chain[a]	FA-amide ion (*m/z*)	hFA cluster[b]
794	hSulp16:0	280	+
806	Sulp18:0	308	-
822	hSulp18:0	324	+
834	Sulp20:0	336	-
850	hSulp20:0	352	+
862	Sulp22:0	364	-
876	Sulp23:0	378	-
878	hSulp22:0	380	+
888	Sulp24:1	390	-
890	Sulp24:0	392	-
892	hSulp23:0	394	+
902	Sulp25:0	404	-
904	hSulp24:1	406	+
906	hSulp24:0	408	+
916	Sulp26:1	418	-
918	hSulp25:1	420	+
920	hSulp25:0	422	+
932	hSulp26:1	434	+

[a] Sulp = sulphatide; hSulp = hydroxy sulphatide; dhSulp = dihexosyl sulphatide;

[b] – indicates the absence or low abundance of the ions associated with hFA (*m/z* 522, *m/z* 540 and *m/z* 568);

+ indicates the presence of the hFA cluster ions.

(A)

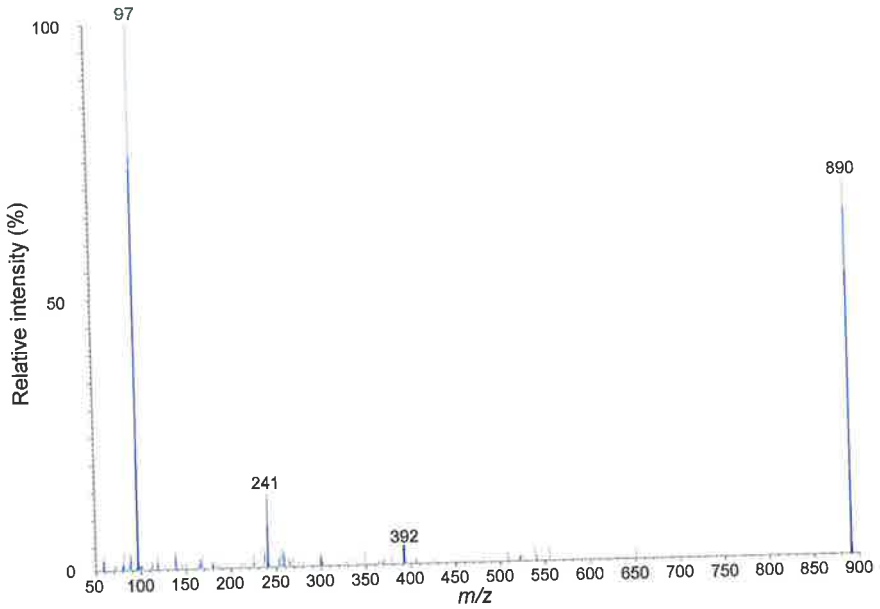

(B)

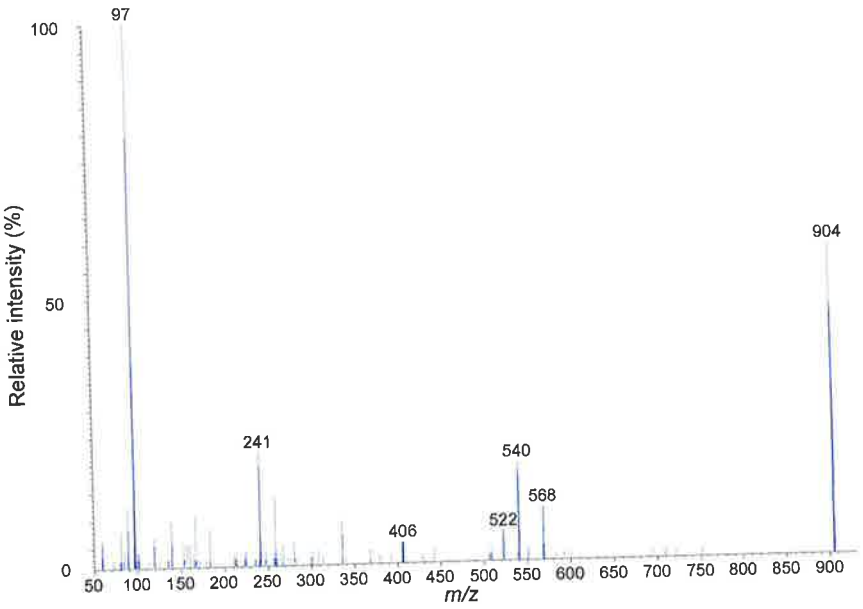

Figure 5.2 Tandem mass spectra of CAD-MS/MS on parent ions of *m/z* 890 and *m/z* 904

Parent ions were identified using ESI-MS/MS with Q1 scan before being subjected to CAD-MS/MS with CE scanned from -130V to -5.0V. Panel A: tandem mass spectrum of parent ion *m/z* 890 producing daughter ions of *m/z* 97, *m/z* 241 (common ions) and *m/z* 392 (FA-amide ion) in the absence of hFA cluster ions; Panel B: tandem mass spectrum of parent ion *m/z* 904 producing daughter ions of *m/z* 97, *m/z* 241 (common ions) and *m/z* 406 (FA-amide ion) in the presence of hFA cluster ions (*m/z* 522, *m/z* 540 and *m/z* 568).

5.1.2. Establishing multiple reaction monitoring mode for sulphatide quantification

Quantification of individual sulphatide species was performed using MRM mode where the ions monitored represented the parent $[M-H]^{-1}$ ion and the most abundant daughter ion (*m/z* 97) resulting from the release of HSO_4^-. Based on the results obtained from the characterisation and identification of individual sulphatide species in MLD urine and bovine brain, a total of 19 MRM pairs, including *m/z* 778.8/97.0 (16:0-sulphatide, which was added as ISTD), were selected based on their relative abundance in both sample types. The MRM ion pairs used to quantify sulphatide are listed in section 2.2.18.1, Table 2.1. The coefficient of variation (inter-assay) of the assay in the Department of Genetic Medicine at the Women's and Children's Hospital, Adelaide, SA, Australia, has previously been reported as 8.1% (Whitfield *et al.* 2002); in the present study the coefficient of variation (intra-assay), determined in triplicate assays from 22 cultured SF in the presence of sulphatide, was 2-26%.

5.2. Development of a sulphatide-loading protocol

The development of a sulphatide-loading protocol for SF cell cultures was essential since sulphatide does not accumulate in the SF of MLD patients. All loading protocols reported to date utilise either ^{35}S-labelled (Porter *et al.*, 1971; Fluharty *et al.*, 1978; Kihara *et al.*, 1980) or ^{14}C-stearic acid-labelled sulphatide (Kudoh *et al.*, 1981); various fluorescence derivatives of sulphatide have also been employed (Viani *et al.*, 1989; Monti *et al.*, 1992). The use of ESI-MS/MS to quantify accumulated sulphatide was expected to simplify the loading protocol by avoiding the use of radio-labelled substrate and replacing it with crude bovine brain sulphatide that is directly incorporated into the culture media.

5.2.1. Optimisation of sulphatide concentration in culture media for sulphatide loading

To determine the optimum concentration of sulphatide to be incorporated into the cell culture media for loading, SF from late-infantile MLD and unaffected controls were cultured to seven-days post-confluence using the conditions described in section 2.2.12. The cells were washed with PBS (3 x 5.0 mL) before the addition to each flask of BME (8.0 mL) containing 5% HIFCS, 1% penicillin/streptomycin and bovine brain sulphatide in concentrations of 0, 2, 4, 8, 16, 32 and 64 μM. The cells were then incubated (5% CO_2, 37°C) for a further three-days.

After the incubation period, all SF were harvested (section 2.2.13), sonicated (section 2.2.16), and total protein quantified (section 2.2.5). Cell lysates (100 μL) were extracted for lipid analysis using the method of Folch (section 2.2.17.2). Sulphatide was quantified in each cell extract as described in section 2.2.18.1

Figure 5.4 shows the amount of accumulated sulphatide in SF from late-infantile MLD and unaffected controls cultured in BME with different concentrations of sulphatide over a period of three-days: sulphatide accumulation was highest in late-infantile MLD SF cultured in media containing 64 μM sulphatide; the control cell lines showed only a slight increase in sulphatide accumulation, with the highest amount in the cell line cultured in 64 μM sulphatide. At 64 μM sulphatide, control cells accumulated sulphatide to slightly less than 10% of that observed in the late-infantile MLD cell line. In view of this, it was determined that the optimum concentration of sulphatide to be used for loading was 64 μM.

5.2.2. Optimisation of the incubation period for sulphatide-loading

To determine the optimum period for incubation, SF from late-infantile MLD patients and unaffected controls were cultured to seven-days post-confluence using the conditions described in section 2.2.12. The cell lines were washed with PBS (3 x 5.0 mL) before the addition to each flask of BME (8.0 mL) containing 5% HIFCS, 1% penicillin/streptomycin and bovine brain sulphatide (64 μM). The cells were then incubated (5% CO_2, 37°C) for 1, 2, 4, 6, 8 and 10 days.

On reaching each incubation time point, one flask of each of the designated cell lines was harvested (section 2.2.13) and the cell pellet stored at -20°C. Upon harvesting at the last time-point (day 10), all SF were sonicated (section 2.2.16) and protein determined (section 2.2.5). Using the method of Folch (section 2.2.17.2) each cell lysate (100 μL) was extracted for lipid analysis. Sulphatide quantification was performed using ESI-MS/MS, as described in section 2.2.18.1.

Figure 5.5 shows the amount of accumulated sulphatide in late-infantile MLD and control SF cultured in media with 64 μM sulphatide at different incubation times. Sulphatide accumulation in late-infantile MLD SF was highest on day 10, but the rate of increase had started to taper-off from day 8. It was determined that an incubation period of eight-days in BME containing 5% HIFCS, 1% penicillin/streptomycin with 64 μM bovine brain

sulphatide was required for the optimum accumulation of sulphatide in late-infantile MLD SF cell lines.

5.2.2.1. Determination of secondary lipid accumulation

The effect of sulphatide accumulation on other lipids in the unaffected control and late-infantile MLD SF cell lines over the incubation period was also investigated. The samples utilised in section 5.2.2 were subjected to lipid profiling using ESI-MS/MS, as described in sections 2.2.18.2, 2.2.18.3 and 2.2.18.4. Figure 5.5 shows the changes recorded in the level of PG/LBPA18:1/18:1, which was measured at each time point and plotted over 10-days.

These observations, together with the results obtained in sections 5.1 and 5.2, led to the conclusion that the optimal conditions for maximum sulphatide accumulation can be achieved by culturing SF in BME containing 5% HIFCS, 1% penicillin/streptomycin with 64 μM bovine brain sulphatide over eight-days.

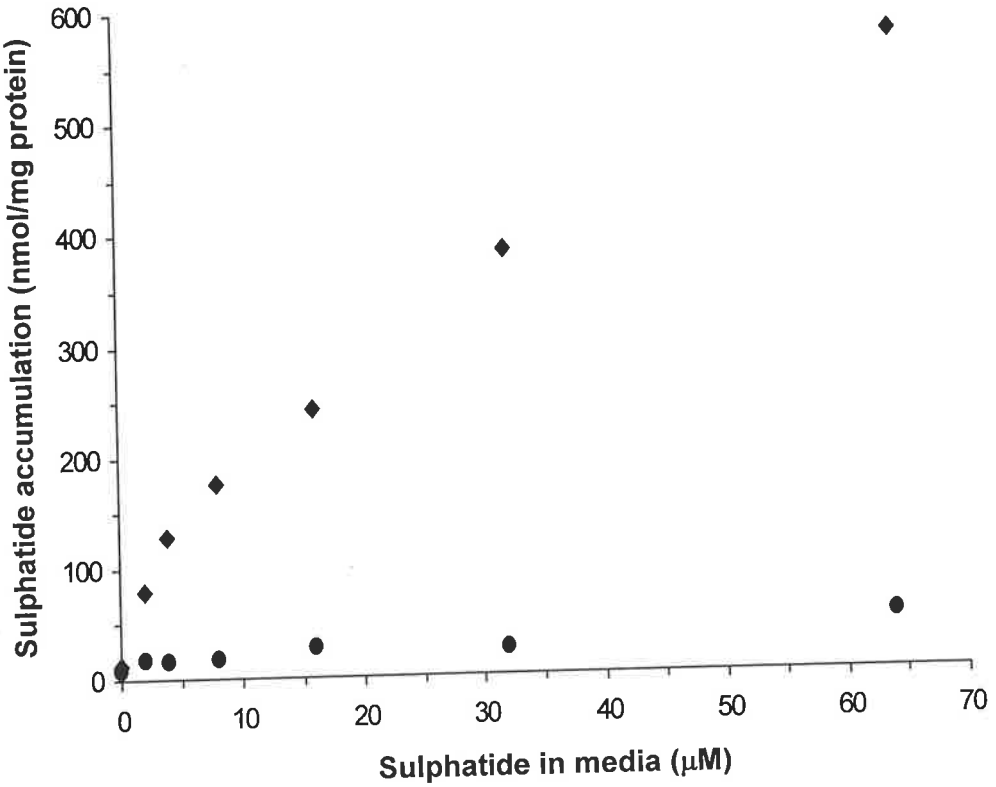

Figure 5.3 Effect of sulphatide concentration in unaffected and MLD skin fibroblasts
SF from late-infantile MLD (♦) and unaffected controls (●) were cultured in 75 cm^2 flasks to seven-days post-confluence in BME (10 mL) containing 10% FCS. The cell lines were washed with PBS (3 x 5.0 mL) before the addition of BME (8.0 mL) containing 5% HIFCS, 1% penicillin/streptomycin and bovine brain sulphatide. The cell lines were then incubated (5% CO_2, 37°C) for a further three-days. After the incubation period, all SF were harvested and sonicated, and total cell protein measured using the protocol described in section 2.2.5. The cell lysates (100 μL) were extracted using the method of Folch and sulphatide quantification was performed by ESI-MS/MS, as described in section 2.2.18.1.

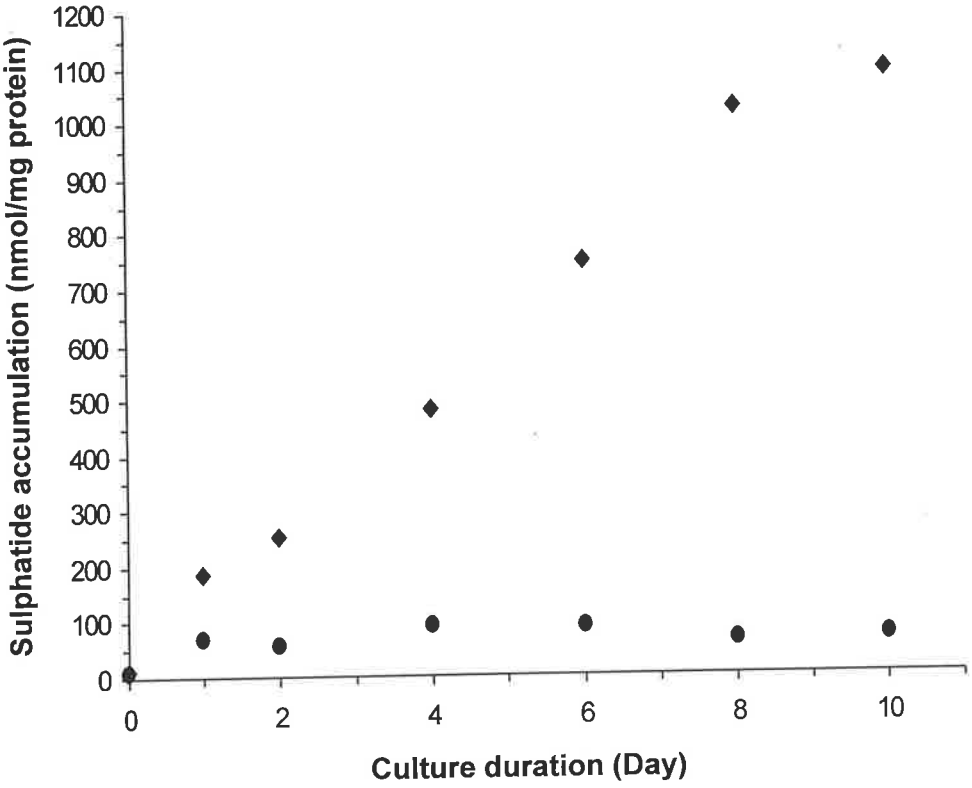

Figure 5.4 Effect of incubation time in unaffected and MLD skin fibroblast cultures

SF from late-infantile MLD (♦) and unaffected controls (●) were cultured in 75 cm^2 flasks to seven-days post-confluence in BME (10 mL) containing 10% FCS and incubated (5% CO_2, 37°C). The cell lines were washed with PBS (3 x 5.0 mL) before the addition of BME (8.0 mL) containing 5% HIFCS, 1% penicillin/streptomycin and bovine brain sulphatide (64 μM). The cell lines were then incubated (5% CO_2, 37°C). On the days indicated, one SF cell line each from MLD and unaffected controls was harvested and kept at -20°C; all SF were sonicated on day 10. Extraction of cell lipids (100 μL/each cell line) was carried out using the method of Folch before sulphatide quantification was performed by ESI-MS/MS, as described in section 2.2.18.1.

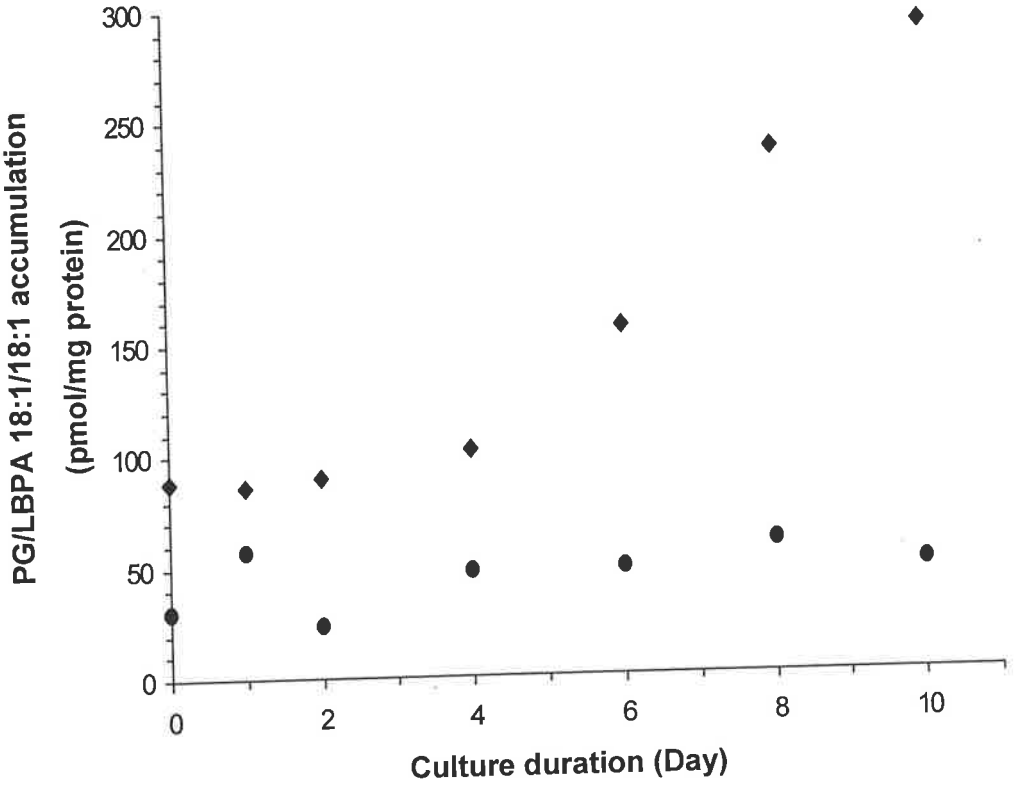

Figure 5.5 Effect of incubation time on secondary lipid accumulation in unaffected and MLD skin fibroblast cultures

SF from late-infantile MLD (♦) and unaffected controls (●) were cultured in 75 cm^2 flasks to seven-days post-confluence in BME (10 mL) containing 10% FCS and incubated (5% CO_2, 37°C). The cell lines were washed with PBS (3 x 5.0 mL) before the addition of BME (8.0 mL) containing 5% HIFCS, 1% penicillin/streptomycin and bovine brain sulphatide (64 μM). The cell lines were then incubated (5% CO_2, 37°C). On the days indicated, one SF cell line each from MLD and unaffected controls was harvested and kept at -20°C; all SF were sonicated on day 10. Extraction of cell lipids (100 μL/each cell line) was carried out using the method of Folch before the quantification of phospholipids was performed by ESI-MS/MS, as described in section 2.2.18.2.

5.3. Discussion

The need to accurately predict clinical phenotype in asymptomatic newborns and monitor the effectiveness of therapy prompted the establishment of an ESI-MS/MS sulphatide quantification method in this study. An existing method (Whitfield *et al.*, 2001a) was extended and adapted to a MS/MS instrument that had higher sensitivity and allowed the quantification of more sulphatide species.

In this study, pure 16:0-sulphatide was used as the ISTD for quantification purposes, consistent with that used by Whitfield *et al.* (2001a). The effect of endogenous 16:0-sulphatide in urine on the quantification of sulphatide species was minimised by the addition of an excess amount of ISTD (2.5 nmol). The endogenous contribution from this species in bovine brain was less than 0.5% of the total sulphatide and was therefore not a major source of error in the loading experiment.

The characterisation and identification of prominent sulphatide species in MLD urine and bovine brain sulphatide was made possible with the use of the CAD ESI-MS/MS method employed by Hsu *et al.* (1998). The sulphatide species in MLD urine and bovine brain were similar, with the exception of dihexosyl sulphatide species, which were absent in the bovine brain sulphatide. Two dihexosyl sulphatide species were found in the MLD urine, which were identified as having fatty acyl chains of 22:0 (*m/z* 1024) and 24:0 (*m/z* 1052), respectively. Overall, the assignment of MLD urine sulphatide species based on the parent and daughter ion analyses are consistent with those assigned by Whitfield *et al.* (2001a). In addition to those species reported by Whitfield *et al.* (2001a), four additional sulphatide species with *m/z* 848, 918, 920 and 1052 were identified in this study as sulphatides with fatty acyl chains of 21:0, h25:1, h25:0 and 24:0 dihexosyl, respectively.

The assignment of each sulphatide species in the bovine brain is consistent with those reported by Hsu *et al.* (1998). Five additional sulphatide species with *m/z* 794, 822, 850, 892 and 920 were identified in this study as sulphatides with fatty acyl chains of h16:0, h18:0, h20:0, h23:0 and h25:0, respectively. The major difference between sulphatide species in MLD urine and bovine brain was relative abundance: the most abundant individual species found in MLD urine was the non-hydroxylated species with a fatty acyl chain of 22:0 (behenic acid), while the non-hydroxylated species with a fatty acyl chain of 24:0 (lignoceric acid) was the most abundant species found in the bovine brain.

The second aim of this chapter was to develop a functional assay to measure the metabolism of sulphatide in SF, which was essential because sulphatide does not naturally accumulate in SF of MLD patients. Previous reports have indicated that the methods used to disperse exogenous lipids in media for loading studies can influence both the rate of uptake (Viani *et al.*, 1989; Rousseau and Gatt, 1990) and the distribution of lipids within the cells (Sutrina and Chen, 1982; Lipsky and Pagano, 1985; Inui *et al.* 1988). In this study, bovine brain sulphatide was incorporated into BME containing 5% HIFCS and 1% penicillin/streptomycin. Bovine brain sulphatide stock solution (20 mM) was prepared in chloroform/methanol (2:1 [v/v]) prior to its incorporation into the media, with a final concentration of less than 0.5% (v/v). The direct incorporation of this stock solution into the media was achieved by adding it to pre-warmed media (37°C) with gentle mixing (at least 10 min). The media containing the dissolved sulphatide was kept at 37°C until use. The addition of 5% HIFCS to the culture media was essential since FCS has been reported as being necessary for the correct targeting of sulphatide to the lysosome (Inui *et al.* 1988). The FCS was heat-inactivated to prevent the endogenous ASA in the FCS from digesting the sulphatide.

To achieve maximum sulphatide accumulation in SF, two conditions thought to have an effect on the rate of accumulation were optimised: 1) sulphatide concentration; and 2) incubation period. The results of the sulphatide-loading experiment using different sulphatide concentrations showed that sulphatide accumulation in SF from late-infantile MLD patients was linear with sulphatide concentration up to 8.0 μM; thereafter, each 2-fold increase in sulphatide concentration resulted in an increase in sulphatide accumulation in these cells of approximately 30%. This result was comparable to the cell uptake rate reported by Kudoh *et al.* (1981) who used ^{14}C-stearic acid-labelled sulphatide as the substrate in their study. The amount of sulphatide hydrolysed by the control cell line at the end of the three-day incubation period was also comparable to the result reported by Kihara *et al.* (1980), who used a 24 nmol/mL ^{35}S-labelled rat brain sulphatide/unlabelled beef brain sulphatide mixture in their study. Kihara *et al.* (1980) reported that the control cells hydrolysed between 82% to 92% of the incorporated sulphatide by day 5, while the initial results from the loading experiments carried out in this study showed that the unaffected control cells hydrolysed approximately 90% (average) compared to the amount accumulated in the late-infantile MLD cell line.

The difference in sulphatide accumulation observed between late-infantile MLD and control SF indicated that the loading protocol was delivering sulphatide to the lysosome,

and that degradation was occurring in the control cell line but not in the MLD cell line. The use of crude sulphatide as the sole substrate in the loading experiment has not been previously reported. The results obtained in this study compare favourably with those reported by others, despite differences in the substrates, loading protocols and quantification methods that were employed.

Previous reports suggest that altered lipid composition as a result of sulphatide accumulation might play a role in defining the pathogenesis of MLD, as discussed in sections 1.4.3.2.2 and 1.4.3.2.3. In this study, additional lipids were measured in the cell after sulphatide-loading, since secondary changes in lipid levels may be useful markers of clinical severity in MLD. The initial results of lipid analysis showed relatively few changes as a consequence of sulphatide accumulation, however, one significant observation was the increase in the PG/LBPA species: eight out of the 13 species were found to be elevated in the MLD SF when compared to the unaffected controls. Even though LBPA has been reported to be elevated in Niemann-Pick disease (Huterer *et al.*, 1983), the increase observed in this study could be attributed to either PG or LBPA or both (section 2.2.18.2), as the MRM mode used in this study does not differentiate between the two.

The successful use of unlabelled sulphatide as a substrate for loading has circumvented the substrate preparation step; prior to this the radio-labelled substrate analogue required preparation 'in-house' before loading could be performed, which restricted the use of this technique to specialist laboratories only. This study has demonstrated that, with the quantification of sulphatide by ESI-MS/MS, crude sulphatide can be directly incorporated into culture media for loading studies.

In conclusion, the first aim of this chapter was achieved with the establishment a sulphatide quantification method using ESI-MS/MS on a API 3000 tandem mass spectrometer. A total of 19 MRM ion pairs were used for quantification, based on the prominent sulphatide species found in MLD urine and bovine brain.

The second aim of this chapter was met through the development of the loading protocol for the SF functional assay. The initial results showed that the direct incorporation of sulphatide into cell culture media was functional and comparable with other reported sulphatide-loading methods. The application of these methods as prognostic indicators of clinical severity will be reported and discussed in Chapter 6.

CHAPTER SIX

Prediction of Clinical Severity in Metachromatic Leukodystrophy

6. Introduction and aims

The accurate prediction of clinical severity for MLD patients will become a laboratory responsibility once presymptomatic detection of affected individuals is achieved. The genetic and clinical heterogeneity observed in MLD makes accurate prediction of clinical severity based on genotype-to-phenotype and genotype-to-enzyme activity correlations unreliable (sections 1.4.7 and 1.4.7.1). Sulphatide is the primary storage substrate in MLD: the measurement of this compound in urine as a means by which to differentiate ASA-PD individuals from MLD patients has had some success but it does not, on its own, unequivocally identify each of the MLD clinical phenotypes (section 1.4.8.1.1). The experimental aim of this section of the project was therefore to establish new analytical techniques to improve the prediction of clinical severity for MLD.

To overcome existing limitations, two separate approaches were evaluated in this study. The first approach was the measurement of sulphatide and other lipids by ESI-MS/MS in urine collected from unaffected controls, ASA-PD individuals, and juvenile and late-infantile MLD patients. The underlying hypothesis for this approach was that mass spectrometric analysis of a wide range of lipid types would identify useful additional diagnostic markers, since sulphatide accumulation is known to have an effect on lipid homeostasis in the cell (sections 1.4.3.2.2 and 1.4.3.2.3); ESI-MS/MS would also provide the necessary sensitivity and accuracy to detect the minute changes not otherwise measurable by conventional methods.

The second approach was to perform biochemical profiling in SF collected from unaffected controls, ASA-PD and ASA-PD/MLD individuals, and patients affected by the three major forms of MLD. ASA protein and activity were determined using the immune-based assays developed in this study and these were used to calculate the specific activity of ASA, which provided additional information on the functional aspect of the mutant enzyme. The SF were then subjected to quantification of stored substrates and lipid profiling. This was achieved through induced accumulation of sulphatide with the sulphatide-loading protocol developed in this study (section 5.2). The results obtained from these experiments were then correlated to both the patient phenotype and other biochemical data to validate the markers for their usefulness as predictors of clinical phenotype.

6.1. Sulphatide quantification and lipid profiling of urine samples

Urine samples from 11 MLD patients, six ASA-PD individuals and 18 unaffected controls were used in this study; the cohort of unaffected controls consisted of six samples each from adults (>18 years), juveniles (10-16 years) and infantiles (1-4 years). The biochemical data for all patients whose urine was analysed in this study are shown in Table 6.1. Genotyping and measurement of ASA activity in blood leucocytes and SF was carried out in the National Referral Laboratory for the Diagnosis of Lysosomal, Peroxisomal and Related Genetic Disorders, Department of Genetic Medicine, Women's and Children's Hospital, Adelaide, SA, Australia.

6.1.1. Normalisation of urinary analytes

Earlier reports have shown that normalisation of urinary sulphatide against urinary phosphatidylcholine (PC) enables better differentiation between ASA-PD and MLD patients than urinary sulphatide normalised against volume or creatinine (CR). This is thought to result from urinary volume and CR being related to glomerular filtration, while PC originates from the same renal cells as sulphatide and can thus effectively correct for the amount of urinary sediment in each individual (Whitfield *et al.*, 2001a); furthermore, PC is known to be unrelated to the MLD disease process (Whitfield *et al.*, 2001a). In this study, statistical analysis was performed on the lipid analytes normalised to urinary volume, CR and PC to assess the suitability of each method of normalisation (expressed as nmol/L, nmol/mmol/CR and nmol/nmol PC): as reported by Whitfield *et al.* (2001a) normalisation to urinary PC was most informative, thus all urinary lipid data are presented as nmol/nmol PC.

6.1.2. ESI-MS/MS determination of urinary sulphatide

Using the method of Bligh and Dyer (section 2.2.17.1), sulphatide was extracted from SF lysates collected from the patient cohort described in section 6.1 and measured using ESI-MS/MS (section 2.2.18.1). Table 6.2 summarises the value of each sulphatide species and total sulphatide, which was expressed as nmol/nmol PC.

Table 6.1 Biochemical data of individuals providing urine samples in this study

Sample[a]	Sex	Age at sampling (years)	Type	ASA activity[b] (nmol/min/mg protein)	Urinary creatinine (mmol/L)	Genotype
UA1-UA6 (n=6)		1-4	Normal			
UJ1-UJ6 (n=6)		10-16	Normal			
UI1-UI6 (n=6)		27-51	Normal			
U1	M	23	ASA-PD	0.34	5.9	ASA-PD/?
U2	F	27	ASA-PD	0.66	8.8	ASA-PD/ASA-PD
U3	M	31	ASA-PD	0.66	3.0	ASA-PD/ASA-PD
U4	M	9	ASA-PD	0.45	1.2	ASA-PD/T391S
U5	M	29	ASA-PD	0.63	12.0	ASA-PD/ASA-PD
U6	M	26	ASA-PD	0.60[c]	8.1	ASA-PD/ASA-PD+Y39C
U7	F	5	Late-infantile	0.30	1.6	T274M/T274M
U8	M	4	Late-infantile	0.04	2.4	A212V/Y39C
U9	F	9	Late-infantile	0.30	6.6	Not done
U10	F	2	Late-infantile	0.15	4.7	Not done
U11	M	2	Late-infantile	0.11	1.4	R84Q/R114X
U12	M	2	Late-infantile	0.14	3.7	SDEx2/1027delC
U13	F	12	Juvenile	0.12	4.7	SDEx2/P426L
U14	F	10	Juvenile	0.38	9.4	Not done
U15	M	11	Juvenile	NA[d]	10.7	Y306H/1622G>A(IVS5)
U16	F	4	Juvenile	0.20	0.9	insG97-99/P426L
U17	M	13	Juvenile	NA[d]	11.3	Y306H/1622G>A(IVS5)

[a] Urine samples from: UA1 to UA6 = unaffected adults; UJ1 to UJ6 = unaffected juveniles; UI1 to UI6 = unaffected infantiles; U1 to U6 = ASA-PD individuals; U7 to U12 = late-infantile MLD; and U13 to U17 = juvenile MLD;

[b] blood leucocyte ASA activity measured using artificial substrate (control range 1-5 nmol/min/mg protein);

[c] ASA activity measured in SF using artificial substrate (control range 6-50 nmol/min/mg protein);

[d] NA = not available.

Table 6.2 Urinary sulphatide (nmol/nmol PC)[a] in unaffected controls, ASA-PD individuals and MLD patients

		Sulphatide species[b]																	
Sample	Type	hSulp 16:0	Sulp 18:0	hSulp 18:0	Sulp 20:0	Sulp 21:0	hSulp 20:0	Sulp 22:0	Sulp 23:0	hSulp 22:0	Sulp 24:1	Sulp 24:0	hSulp 23:0	hSulp 24:1	hSulp 24:0	hSulp 25:1	hSulp 25:0	dhSulp 22:0	dhSulp 24:0	Total[c]
UA1-UA6 (n=6)	Normal	0.04-0.17	0.06-0.30	0.02-0.08	0.04-0.08	0.03-0.06	0.03-0.07	0.08-0.26	0.05-0.15	0.05-0.16	0.05-0.14	0.07-0.19	0.06-0.18	0.06-0.18	0.11-0.38	0.02-0.10	0.03-0.07	0.02-0.07	0.03-0.07	0.85-2.71
UJ1-UJ6 (n=6)	Normal	0.02-0.15	0.03-0.29	0.01-0.07	0.02-0.09	0.01-0.07	0.01-0.08	0.06-0.22	0.03-0.12	0.04-0.15	0.02-0.13	0.05-0.18	0.04-0.16	0.04-0.15	0.09-0.30	0.01-0.06	0.01-0.07	0.01-0.07	0.01-0.06	0.51-2.42
UI1-UI6 (n=6)	Normal	0.08-0.32	0.16-0.88	0.03-0.10	0.07-0.12	0.03-0.08	0.04-0.11	0.22-0.37	0.11-0.21	0.11-0.24	0.09-0.25	0.18-0.33	0.12-0.27	0.11-0.23	0.25-0.55	0.02-0.09	0.02-0.09	0.02-0.09	0.02-0.09	1.68-4.42
U1	ASA-PD	0.24	0.38	0.10	0.10	0.09	0.13	0.36	0.19	0.28	0.18	0.37	0.34	0.25	0.75	0.20	0.14	0.07	0.11	4.28
U2	ASA-PD	0.07	0.10	0.03	0.05	0.04	0.04	0.23	0.12	0.12	0.07	0.17	0.15	0.12	0.29	0.05	0.06	0.02	0.02	1.76
U3	ASA-PD	0.20	0.46	0.06	0.07	0.04	0.08	0.21	0.12	0.15	0.16	0.23	0.20	0.17	0.36	0.07	0.09	0.05	0.07	2.80
U4	ASA-PD	0.39	0.93	0.14	0.19	0.10	0.21	0.70	0.34	0.48	0.30	0.66	0.57	0.41	1.25	0.11	0.14	0.11	0.11	7.15
U5	ASA-PD	0.08	0.13	0.04	0.07	0.04	0.07	0.33	0.17	0.21	0.13	0.32	0.25	0.17	0.57	0.03	0.05	0.06	0.07	2.76
U6	ASA-PD	0.24	0.32	0.14	0.15	0.10	0.20	0.62	0.32	0.56	0.18	0.51	0.69	0.45	1.58	0.12	0.18	0.16	0.22	6.73
U7	Late-infantile	0.68	0.56	0.43	1.00	0.43	0.74	5.07	1.55	2.23	1.31	3.48	1.60	2.68	4.94	0.30	0.35	0.44	0.53	28.3
U8	Late-infantile	1.38	1.06	0.96	1.58	0.61	1.33	8.79	2.15	4.05	1.82	5.28	2.43	4.67	9.16	0.40	0.50	1.23	1.72	49.1
U9	Late-infantile	1.45	0.92	1.34	1.92	1.02	2.10	10.72	3.02	5.25	1.54	4.75	3.22	5.43	10.66	0.56	0.88	0.63	0.84	56.2
U10	Late-infantile	1.11	0.81	0.91	1.62	0.65	1.40	7.68	1.88	3.85	1.73	4.21	2.16	4.00	7.79	0.35	0.44	1.00	1.44	43.0
U11	Late-infantile	1.38	1.46	1.09	2.50	1.04	1.55	11.99	3.18	4.06	3.55	7.39	2.73	4.98	8.15	0.50	0.47	1.09	1.39	58.4
U12	Late-infantile	0.78	0.68	0.64	1.28	0.48	0.98	5.87	1.54	2.76	1.37	3.45	1.65	2.83	5.52	0.26	0.33	0.86	1.20	32.4
U13	Juvenile	0.79	0.27	0.34	0.75	0.25	0.70	4.65	1.08	2.35	1.03	3.26	1.50	2.68	6.77	0.19	0.20	0.78	1.33	28.9
U14	Juvenile	0.60	0.33	0.41	0.65	0.35	0.69	4.19	1.19	2.14	0.74	2.24	1.34	2.24	4.67	0.21	0.26	0.27	0.41	22.9
U15	Juvenile	1.95	0.81	0.98	1.91	0.66	1.90	11.99	3.51	6.67	3.61	11.74	4.66	9.89	22.84	0.87	0.81	1.19	2.08	88.0
U16	Juvenile	1.33	1.28	1.06	1.98	0.76	1.75	9.14	2.26	5.25	1.93	5.18	2.96	5.17	11.36	0.47	0.58	1.55	2.22	56.2
U17	Juvenile	1.02	0.42	0.49	0.91	0.35	1.02	5.57	1.75	3.24	1.33	4.64	2.38	4.50	10.27	0.41	0.39	0.54	1.00	40.2

[a] sulphatide species were determined by ESI-MS/MS using MRM mode (section 2.2.18.1);

[b] Sulp = sulphatide; hSulp = hydroxy sulphatide; dhSulp = dihexosyl sulphatide;

[c] Total = the sum of the 18 individual sulphatide species.

6.1.3. ESI-MS/MS determination of urinary phospholipids, glycolipids and gangliosides

The lipid extracts used to determine urinary sulphatide (section 2.2.18.1) were also used to measure urinary phospholipids in negative ion mode using the protocol described in section 2.2.18.2, and urinary glycolipids, sphingomyelin and PC in positive ion mode using the protocol described in section 2.2.18.3. Gangliosides were extracted from the aqueous phase using the Bligh and Dyer extraction procedure (section 2.2.17.3), and analysed by ESI-MS/MS using the protocol described in section 2.2.18.4.

Sixty-one individual analytes were determined using MRM mode, which comprised: seven ceramide (Cer) species; six each of glucosylceramide (GC), lactosylceramide (LC), ceramide trihexoside (CTH) species; seven phosphatidylcholine (PC) species; three sphingomyelin (SM) species; 13 PG/LBPA species; nine phosphatidylinositol (PI) species, and four monosialoganglioside (G_{M3}) species. The value of each urinary lipid species and the total of each species was expressed as nmol/nmol PC and summarised in Table 6.3.

6.1.4. Fragmentation of sulphatide species in positive ion mode using ESI-MS/MS

Sulphatide can undergo a loss of sulphate in the electrospray source (Naggar *et al.*, 2004), thereby producing galactosylceramide or dihexosylceramide that will subsequently fragment under positive ion mode MS/MS conditions to produce a major product ion at *m/z* 264 and a minor product ion at *m/z* 282 (Whitfield *et al.*, 2001a). This suggests the possibility that the sulphatide species were contributing to the signal of GC and LC measured in positive ion mode (section 2.2.18.3). To investigate the extent of this contribution, bovine brain sulphatide standard (0.64 μM) prepared in chloroform/methanol was analysed for glycolipid content in positive ion mode (section 2.2.18.3). The results are summarised in Table 6.4.

6.1.5. Statistical analysis

The Mann-Whitney U (M-W U) test was used to evaluate the ability of each analyte to differentiate between: (i) MLD and unaffected controls; (ii) ASA-PD and unaffected controls; and (iii) ASA-PD and MLD patients. Table 6.5 summarises the M-W U values and the significance (p) values for each analyte in each comparison. The values of a number of analytes showed significant differences between the unaffected control and MLD groups: six of the seven Cer species (the exception being Cer23:1); GC24:1, LC24:1 and CTH18:0; two of the seven PC species, PC32:0 and PC36:4; five PG/LBPA species, PG/LBPA18:1/18:0, 18:1/18:1, 18:1/18:2, 18:1/22:5 and 18:1/22:6; all 18 sulp species; and

total Cer, CTH, PG and Sulp. Although significantly different values were observed in many analytes in the control and MLD patient groups, most did not completely differentiate either group but rather tended to overlap (a M-W U value greater than 0). The exceptions to this were the urinary sulphatide species, minus Sulp18:0 (M-W U value of 17). CTH 18:0, which had a M-W U value of 0, was thought to be the signal from dhSulph24:0 and will be further discussed in section 6.3.

A comparison of the values between ASA-PD individuals and unaffected controls showed significant differences in 19 analytes: Cer23:0, Cer24:0, CTH18:0, CTH20:0, SM16:0, PG/LBPA20:4/22:6, PG/LBPA22:6/22:6, PI18:0/22:5, and 11 of the 18 Sulp species; the values for total Cer, SM and Sulp were also found to be significantly different. However, no analyte unequivocally distinguished either group.

A comparison of the analyte values between ASA-PD individuals and MLD patients showed significant differences in 22 analytes: CTH18:0, PG/LBPA18:1/18:0, 18:1/18:1, 18:1/18:2, 18:1/20:4, and 17 out of 18 sulp species; the values for total PG/LBPA and Sulp were also found to be significantly different; and CTH18:0 and 17 sulphatide species found in the MLD patients were elevated in comparison to ASA-PD individuals.

Clear discrimination between the different MLD phenotypes could not be achieved using total urinary sulphatide alone, as shown in Figure 6.1: statistically, no significant differences were observed in the amount of sulphatide detected between the juvenile and late-infantile forms. Despite significant differences in the values of most sulphatide species, not all ASA-PD individuals had urinary sulphatide levels above the unaffected control range (Figure 6.1).

The values for five out of 13 PG/LBPA species were significantly different between the MLD and unaffected control groups, and four were significantly different between the ASA-PD and MLD groups. This prompted further assessment of their usefulness as markers of clinical severity. A scatter plot of hSulp24:0 against PG/LBPA18:1/18:1 is shown in Figure 6.2, which shows that four out of five juvenile MLD patients had lower PG/LBPA values compared to those with late-infantile MLD, thus enabling some discrimination between the two MLD groups.

To determine whether a relationship could be drawn between lipid markers and disease severity, correlation coefficients (Spearman's rho) between the age at diagnosis and each

lipid analyte were calculated for MLD patients. Age at diagnosis was used as a measure of severity. The same analysis was performed on the control group to identify those lipids that showed a correlation with age in the unaffected population. Table 6.6 shows the Spearman's rho values obtained from unaffected controls aged less than 18-years old (n=12) and MLD patients aged two- to 13-years (n=11); values that represent a significant correlation ($p \leq 0.05$) are bolded. No correlation was established between age and any sulphatide species in the MLD group although a significant correlation was observed in the control group, suggesting that urinary sulphatide is unlikely to be a useful marker of disease severity in MLD. In contrast, a strong correlation was observed between PG/LBPA18:1/18:1 or 18:1/18:2 and age in the MLD group that was not apparent in the control group, which suggests that the concentration of these lipids in MLD may vary with disease severity. Panel A in Figure 6.3 shows the graph of hSulp24:0 plotted against age (no correlation), and Panel B shows the graph of PG/LBPA18:1/18:1 plotted against age (strong correlation).

Table 6.3 **Ranges for urinary glycolipids, phosphatidylcholine, sphingomyelin, phospholipids and gangliosides (nmoL/nmol PC)[a] in unaffected controls, ASA-PD individuals and MLD patients**

Analyte[b]	Adult controls (n=6)		Juvenile controls (n=6)		Infantile controls (n=6)		ASA/PD (n=6)		MLD late- Infantile (n=6)		MLD Juvenile (n=5)	
	Min	max	min	Max	min	max	min	max	min	max	min	max
Age (years)	27	51	7	16	0.5	4	9	31	2	9	4	13
Cer16:0	0.01	0.02	0.00	0.05	0.01	0.03	0.01	0.04	0.01	0.07	0.03	0.22
Ce20:0	0.00	0.01	0.00	0.00	0.00	0.00	0.00	0.01	0.00	0.01	0.00	0.01
Cer20:1	0.00	0.01	0.00	0.00	0.00	0.00	0.00	0.01	0.00	0.01	0.00	0.01
Cer23:0	0.00	0.02	0.00	0.01	0.00	0.01	0.00	0.01	0.00	0.02	0.00	0.02
Cer23:1	0.00	0.01	0.00	0.00	0.00	0.01	0.00	0.01	0.00	0.01	0.00	0.01
Cer24:0	0.01	0.02	0.00	0.02	0.01	0.02	0.01	0.03	0.01	0.11	0.02	0.10
Cer24:1	0.00	0.01	0.00	0.01	0.00	0.01	0.00	0.02	0.01	0.03	0.01	0.11
GC16:0	0.06	0.39	0.04	0.30	0.11	1.41	0.10	0.85	0.10	0.37	0.09	0.53
GC18:0	0.01	0.06	0.00	0.03	0.01	0.08	0.01	0.34	0.02	0.05	0.01	0.05
GC20:0	0.01	0.06	0.01	0.06	0.02	0.07	0.01	0.05	0.02	0.05	0.01	0.04
GC22:0	0.03	0.12	0.02	0.10	0.05	0.16	0.06	0.11	0.07	0.15	0.06	0.14
GC24:0	0.03	0.08	0.02	0.08	0.04	0.13	0.04	0.10	0.05	0.11	0.04	0.13
GC24:1	0.01	0.04	0.01	0.02	0.02	0.04	0.01	0.06	0.02	0.05	0.02	0.05
LC16:0	0.08	0.20	0.03	0.19	0.10	0.29	0.06	0.42	0.08	1.27	0.08	2.37
LC20:0	0.06	0.26	0.03	0.18	0.10	0.40	0.06	0.59	0.06	0.22	0.05	0.36
LC22:0	0.13	0.76	0.08	0.83	0.28	2.01	0.24	3.24	0.17	0.67	0.13	1.66
LC22:0-OH	0.13	0.35	0.06	0.31	0.20	0.53	0.20	0.51	0.18	0.30	0.13	0.41
LC24:0	0.06	0.27	0.03	0.15	0.10	0.30	0.09	0.40	0.09	0.35	0.10	0.65
LC24:1	0.04	0.17	0.02	0.14	0.07	0.19	0.06	0.31	0.07	0.71	0.06	1.45

Table 6.3 Continued

Analyte[b]	Adult controls (n=6)		Juvenile controls (n=6)		Infantile controls (n=6)		ASA/PD (n=6)		MLD late-Infantile (n=6)		MLD Juvenile (n=5)	
	min	max	min	Max	min	max	min	max	min	max	min	max
CTH16:0	0.04	0.18	0.03	0.23	0.10	1.03	0.08	0.27	0.07	0.17	0.08	0.63
CTH18:0	0.03	0.10	0.01	0.08	0.04	0.14	0.07	0.16	0.21	1.17	0.19	0.99
CTH20:0	0.04	0.12	0.02	0.10	0.06	0.26	0.08	0.27	0.05	0.19	0.04	0.25
CTH22:0	0.05	0.17	0.02	0.12	0.07	0.24	0.08	0.21	0.05	0.15	0.07	0.36
CTH24:0	0.04	0.10	0.02	0.10	0.07	0.17	0.07	0.19	0.05	0.11	0.05	0.33
CTH24:1	0.02	0.12	0.01	0.07	0.04	0.19	0.05	0.12	0.03	0.11	0.03	0.18
PC32:0	0.04	0.06	0.02	0.06	0.05	0.06	0.04	0.09	0.05	0.13	0.06	0.17
PC32:1	0.05	0.08	0.02	0.05	0.05	0.08	0.05	0.07	0.04	0.07	0.05	0.08
PC34:1	0.38	0.42	0.23	0.51	0.41	0.51	0.37	0.45	0.43	0.51	0.36	0.48
PC34:2	0.19	0.25	0.17	0.38	0.17	0.22	0.17	0.25	0.11	0.21	0.11	0.25
PC36:2	0.14	0.22	0.13	0.24	0.14	0.18	0.14	0.19	0.14	0.18	0.14	0.21
PC36:4	0.04	0.09	0.05	0.08	0.04	0.07	0.05	0.07	0.02	0.07	0.02	0.06
PC38:4	0.02	0.03	0.02	0.04	0.02	0.03	0.02	0.03	0.02	0.03	0.02	0.03
SM16:0	0.15	0.25	0.06	0.24	0.16	0.32	0.20	0.36	0.14	0.28	0.20	0.32
SM22:0	0.18	0.30	0.13	0.32	0.29	0.57	0.29	0.42	0.20	0.31	0.18	0.37
SM24:0	0.16	0.29	0.09	0.30	0.28	0.55	0.25	0.46	0.18	0.34	0.17	0.34

Table 6.3 Continued

Analyte[b] e	Adult controls (n=6)		Juvenile controls (n=6)		Infantile controls (n=6)		ASA/PD (n=6)		MLD late-Infantile (n=6)		MLD Juvenile (n=5)	
	min	max	min	Max	min	max	min	max	min	max	min	max
PG/LBPA16:0/22:6	0.00	0.01	0.00	0.00	0.00	0.01	0.00	0.00	0.00	0.01	0.00	0.01
PG/LBPA16:1/20:4	0.00	0.00	0.00	0.00	0.00	0.00	0.00	0.00	0.00	0.00	0.00	0.00
PG/LBPA18:1/18:0	0.00	0.02	0.00	0.01	0.01	0.03	0.01	0.01	0.04	0.07	0.01	0.05
PG/LBPA18:1/18:1	0.01	0.07	0.00	0.03	0.01	0.02	0.01	0.08	0.09	0.18	0.03	0.10
PG/LBPA18:1/18:2	0.00	0.01	0.00	0.01	0.00	0.01	0.01	0.02	0.02	0.03	0.01	0.03
PG/LBPA18:1/20:4	0.00	0.00	0.00	0.00	0.00	0.01	0.00	0.00	0.00	0.01	0.00	0.01
PG/LBPA18:1/22:5	0.00	0.01	0.00	0.00	0.00	0.01	0.00	0.01	0.00	0.01	0.00	0.01
PG/LBPA18:1/22:6	0.01	0.03	0.00	0.02	0.00	0.01	0.01	0.04	0.01	0.05	0.00	0.02
PG/LBPA18:2/22:6	0.00	0.01	0.00	0.01	0.00	0.00	0.00	0.01	0.00	0.01	0.00	0.01
PG/LBPA20:4/22:6	0.00	0.00	0.00	0.00	0.00	0.00	0.00	0.00	0.00	0.00	0.00	0.00
PG/LBPA22:5/22:5	0.00	0.00	0.00	0.00	0.00	0.00	0.00	0.00	0.00	0.00	0.00	0.00
PG/LBPA22:6/22:5	0.00	0.00	0.00	0.00	0.00	0.00	0.00	0.00	0.00	0.00	0.00	0.00
PG/LBPA22:6/22:6	0.00	0.01	0.00	0.01	0.00	0.00	0.00	0.01	0.00	0.01	0.00	0.01
PI16:0/18:0	0.01	0.01	0.00	0.02	0.01	0.65	0.01	0.02	0.01	0.03	0.01	0.03
PI16:0/20:4	0.00	0.01	0.00	0.01	0.01	0.01	0.00	0.01	0.00	0.01	0.00	0.01
PI18:0/18:1	0.01	0.02	0.00	0.01	0.01	0.02	0.01	0.02	0.01	0.01	0.01	0.04
PI18:0/18:1	0.00	0.02	0.00	0.02	0.00	0.01	0.00	0.02	0.00	0.02	0.00	0.02
PI18:0/20:3	0.01	0.02	0.01	0.03	0.01	0.02	0.01	0.02	0.01	0.01	0.01	0.06
PI18:0/20:4	0.02	0.06	0.01	0.05	0.03	0.06	0.03	0.06	0.03	0.05	0.03	0.10
PI18:0/22:5	0.00	0.00	0.00	0.00	0.00	0.00	0.00	0.00	0.00	0.00	0.00	0.00

Table 6.3 Continued

Analyte[b]	Adult controls (n=6)		Juvenile controls (n=6)		Infantile controls (n=6)		ASA/PD (n=6)		MLD late- Infantile (n=6)		MLD Juvenile (n=5)	
	min	max	min	Max	min	max	min	max	min	max	min	max
PI18:1/18:1	0.00	0.01	0.00	0.01	0.00	0.01	0.01	0.01	0.01	0.02	0.00	0.01
PI18:1/20:4	0.00	0.01	0.00	0.00	0.00	0.01	0.00	0.01	0.00	0.00	0.00	0.01
G_{M3} 16:0	0.01	0.13	0.01	0.06	0.08	0.27	0.02	0.07	0.03	0.18	0.06	0.30
G_{M3} 22:0	0.00	0.02	0.00	0.02	0.02	0.13	0.00	0.02	0.00	0.08	0.00	0.07
G_{M3} 24:0	0.01	0.08	0.01	0.04	0.07	0.20	0.01	0.05	0.02	0.14	0.02	0.17
G_{M3} 24:1	0.01	0.06	0.01	0.04	0.05	0.24	0.01	0.04	0.02	0.15	0.02	0.24
Cer total	0.03	0.09	0.01	0.09	0.03	0.08	0.04	0.11	0.04	0.22	0.07	0.46
GC total	0.16	0.70	0.10	0.46	0.28	1.79	0.25	1.24	0.28	0.70	0.25	0.86
LC total	0.52	1.99	0.27	1.60	0.94	3.64	0.71	5.47	0.66	2.99	0.57	5.39
CTH total	0.23	0.74	0.12	0.66	0.41	1.69	0.45	1.17	0.46	1.84	0.47	2.60
PC total	1.00	1.00	1.00	1.00	1.00	1.00	1.00	1.00	1.00	1.00	1.00	1.00
SM total	0.49	0.83	0.28	0.85	0.73	1.45	0.73	1.24	0.52	0.91	0.56	0.95
PG total	0.04	0.16	0.02	0.09	0.04	0.09	0.05	0.20	0.17	0.35	0.08	0.22
PI total	0.07	0.14	0.03	0.13	0.09	0.76	0.09	0.15	0.08	0.13	0.08	0.25
G_{M3} total	0.03	0.28	0.03	0.14	0.23	0.84	0.04	0.16	0.07	0.54	0.11	0.75

[a] glycolipids, phosphatidylcholine, sphingomyelin species were determined by ESI-MS/MS using MRM mode (section 2.2.18.3), phospholipids species were determined by ESI-MS/MS using MRM mode (section 2.2.18.2) and gangliosides species were determined by ESI-MS/MS using MRM mode (section 2.2.18.4)

[b] Cer = ceramide; GC = glucosylceramide; LC = lactosylceramide; CTH = ceramide trihexoside, PC = phosphatidylcholine; SM = sphingomyelin, PG/LBPA = phosphatidylglycerol/lysobisphosphatidic acid, PI = phosphatidylinositol, G_{M3} = Monosialogangliosides.

Table 6.4 Concentration of glycolipids measured from sulphatide (bovine brain) using positive ion mode by ESI-MS/MS[a]

Analytes[b]	Ion pair[c]	Concentration (nmoL)
Cer16:0	538.7/264.4	0.49
Cer20:0	592.7/264.4	0.02
Cer20:1	590.7/264.4	0.01
Cer23:0	636.7/264.4	0.11
Cer23:1	634.8/264.4	0.06
Cer24:0	650.7/264.4	1.46
Cer24:1	648.7/264.4	0.13
GC16:0	700.6/264.4	0.60
GC18:0	728.6/264.4	0.43
GC20:0	756.8/264.4	0.11
GC22:0	784.7/264.4	0.52
GC24:0	812.7/264.4	2.19
GC24:1	810.8/264.4	5.13
LC16:0	862.4/264.4	8.14
LC20:0	918.7/264.4	11.06
LC22:0	946.7/264.4	1.07
LC24:0	974.8/264.4	1.05
LC24:1	972.8/264.4	2.00

[a] The concentrations of these glycolipids were obtained by ESI-MS/MS analysis of bovine brain sulphatide (0.64 μM) using the protocol described in section 2.2.18.3, with concentrations expressed as nmol/L;

[b] Cer = ceramide; GC = glucosylceramide; LC = lactosylceramide; CTH = ceramide trihexoside;

[c] ion pairs indicate Q1/Q3 setting.

Table 6.5 **Discrimination between unaffected controls, ASA-PD and MLD patients with urinary sulphatide, glycolipid, phospholipid and ganglioside species[a]**

Analyte[b]	MLD vs Unaffected		ASA-PD vs Unaffected		ASA-PD vs MLD	
	M-W U	p value	M-W U	p value	M-W U	p value
Cer16:0	**16**	**0.002**	30	0.110	20	0.191
Cer20:0	**26**	**0.014**	25	0.053	33	1.000
Cer20:1	**23**	**0.008**	31	0.125	32	0.920
Cer23:0	**28**	**0.019**	**23**	**0.039**	21	0.228
Cer23:1	38	0.085	33	0.162	32	0.920
Cer24:0	**16**	**0.002**	**16**	**0.011**	25	0.421
Cer24:1	**22**	**0.007**	28	0.083	21	0.228
GC16:0	58	0.622	41	0.386	21	0.228
GC18:0	52	0.389	33	0.162	25	0.421
GC20:0	52	0.389	45	0.549	29	0.688
GC22:0	35	0.056	37	0.257	16	0.088
GC24:0	36	0.065	36	0.230	26	0.482
GC24:1	**20**	**0.005**	44	0.505	20	0.191
LC16:0	44	0.176	32	0.142	32	0.920
LC20:0	58	0.622	34	0.182	27	0.546
LC22:0	57	0.580	35	0.205	20	0.191
LC22:0-OH	55	0.498	36	0.230	16	0.088
LC24:0	43	0.157	28	0.083	31	0.841
LC24:1	**32**	**0.036**	27	0.072	29	0.688
CTH16:0	64	0.902	35	0.205	23	0.315
CTH18:0	**0**	**0.000**	**18**	**0.016**	**0**	**0.001**
CTH20:0	57	0.580	**19**	**0.020**	16	0.088
CTH22:0	52	0.389	29	0.096	29	0.688
CTH24:0	58	0.622	30	0.110	27	0.546
CTH24:1	64	0.902	34	0.182	25	0.421
PC32:0	**25**	**0.012**	41	0.386	20	0.191
PC32:1	51	0.356	40	0.351	22	0.269
PC34:1	49	0.295	49	0.739	16	0.088
PC34:2	35	0.056	51	0.841	17	0.108
PC36:2	63	0.854	53	0.947	29	0.688
PC36:4	**28**	**0.019**	37	0.257	17	0.108
PC38:4	51	0.356	42	0.424	20	0.191
SM16:0	51	0.356	**14**	**0.008**	14	0.056
SM22:0	56	0.538	30	0.110	17	0.108
SM24:0	63	0.854	28	0.083	18	0.132
PG/LBPA16:0/22:6	35	0.056	36	0.230	27	0.546
PG/LBPA16:1/20:4	38	0.085	43	0.463	31	0.841
PG/LBPA18:1/18:0	**5**	**0.000**	40	0.351	**1**	**0.001**
PG/LBPA18:1/18:1	**2**	**0.000**	42	0.424	**7**	**0.009**
PG/LBPA18:1/18:2	**2**	**0.000**	40	0.351	**4**	**0.004**
PG/LBPA18:1/20:4	44	0.176	52	0.894	**13**	**0.044**
PG/LBPA18:1/22:5	**13**	**0.001**	37	0.257	20	0.191
PG/LBPA18:1/22:6	**34**	**0.049**	34	0.182	32	0.920
PG/LBPA18:2/22:6	37	0.074	28	0.083	29	0.688
PG/LBPA20:4/22:6	39	0.097	**22**	**0.033**	28	0.615
PG/LBPA22:5/22:5	39	0.097	33	0.162	32	0.920
PG/LBPA22:6/22:5	40	0.110	26	0.062	30	0.763
PG/LBPA22:6/22:6	50	0.325	**24**	**0.046**	22	0.269

Table 6.5 Continued

Analyte[b]	MLD vs Unaffected		ASA-PD vs Unaffected		ASA-PD vs MLD	
	M-W U	p value	M-W U	p value	M-W U	p value
PI16:0/18:0	56	0.538	39	0.317	25	0.421
PI16:0/20:4	48	0.268	49	0.739	29	0.688
PI18:0/18:1	52	0.389	36	0.230	24	0.366
PI18:0/18:1	61	0.758	29	0.096	21	0.228
PI18:0/20:3	49	0.295	44	0.505	18	0.132
PI18:0/20:4	58	0.622	39	0.317	21	0.228
PI18:0/22:5	47	0.242	**20**	**0.023**	21	0.228
PI18:1/18:1	43	0.157	26	0.062	32	0.920
PI18:1/20:4	52	0.389	40	0.351	14	0.056
G_{M3}16:0	53	0.424	41	0.386	15	0.070
G_{M3} 22:0	63	0.854	44	0.505	18	0.132
G_{M3} 24:0	60	0.712	50	0.790	21	0.228
G_{M3} 24:1	62	0.806	49	0.739	21	0.228
hSulp16:0	**0**	**0.000**	29	0.096	**0**	**0.001**
Sulp18:0	**17**	**0.003**	34	0.182	14	0.056
hSulp18:0	**0**	**0.000**	27	0.072	**0**	**0.001**
Sulp20:0	**0**	**0.000**	32	0.142	**0**	**0.001**
Sulp21:0	**0**	**0.000**	26	0.062	**0**	**0.001**
hSulp20:0	**0**	**0.000**	**23**	**0.039**	**0**	**0.001**
Sulp22:0	**0**	**0.000**	**18**	**0.016**	**0**	**0.001**
Sulp23:0	**0**	**0.000**	**19**	**0.020**	**0**	**0.001**
hSulp22:0	**0**	**0.000**	**15**	**0.009**	**0**	**0.001**
Sulp24:1	**0**	**0.000**	27	0.072	**0**	**0.001**
Sulp24:0	**0**	**0.000**	**17**	**0.014**	**0**	**0.001**
hSulp23:0	**0**	**0.000**	**12**	**0.005**	**0**	**0.001**
hSulp24:1	**0**	**0.000**	**16**	**0.011**	**0**	**0.001**
hSulp24:0	**0**	**0.000**	**14**	**0.008**	**0**	**0.001**
hSulp25:1	**0**	**0.000**	**21**	**0.028**	**1**	**0.001**
hSulp25:0	**0**	**0.000**	**19**	**0.020**	**0**	**0.001**
dhSulp22:0	**0**	**0.000**	27	0.072	**0**	**0.001**
dhSulp 24:0	**0**	**0.000**	**18**	**0.016**	**0**	**0.001**
Cer total	**14**	**0.001**	**19**	**0.020**	22	0.269
GC total	63	0.854	36	0.230	24	0.366
LC total	55	0.498	32	0.142	27	0.546
CTH total	**25**	**0.012**	28	0.083	21	0.228
SM total	63	0.854	**23**	**0.039**	14	0.056
PG/LBPA total	**6**	**0.000**	33	0.162	**10**	**0.021**
PI total	55	0.498	45	0.549	24	0.366
G_{M3} total	60	0.712	50	0.790	19	0.159
Sulp total	**0**	**0.000**	**20**	**0.023**	**0**	**0.001**

[a] The relative amount of each analyte was determined by ESI-MS/MS using the MRM mode described in sections 2.2.18.1, 2.2.18.2, 2.2.18.3 and 2.2.18.4. The M-W U and p values (≤0.05 bolded) are reported for all sulphatide, glycolipid, phospholipid and ganglioside species to enable comparison between MLD patients (n=11), unaffected controls (n=18) and ASA-PD individuals (n=6).

[b] Cer = ceramide; GC = glucosylceramide; LC = lactosylceramide; CTH = ceramide trihexoside; PC = phosphatidylcholine; SM = sphingomyelin; PG/LBPA = phosphatidylglycerol/lysobisphosphatidic acid; PI = phosphatidylinositol; G_{M3} = monosialogangliosides GM3; Sulp= sulphatide; dhSulp = dihexosyl sulphatide.

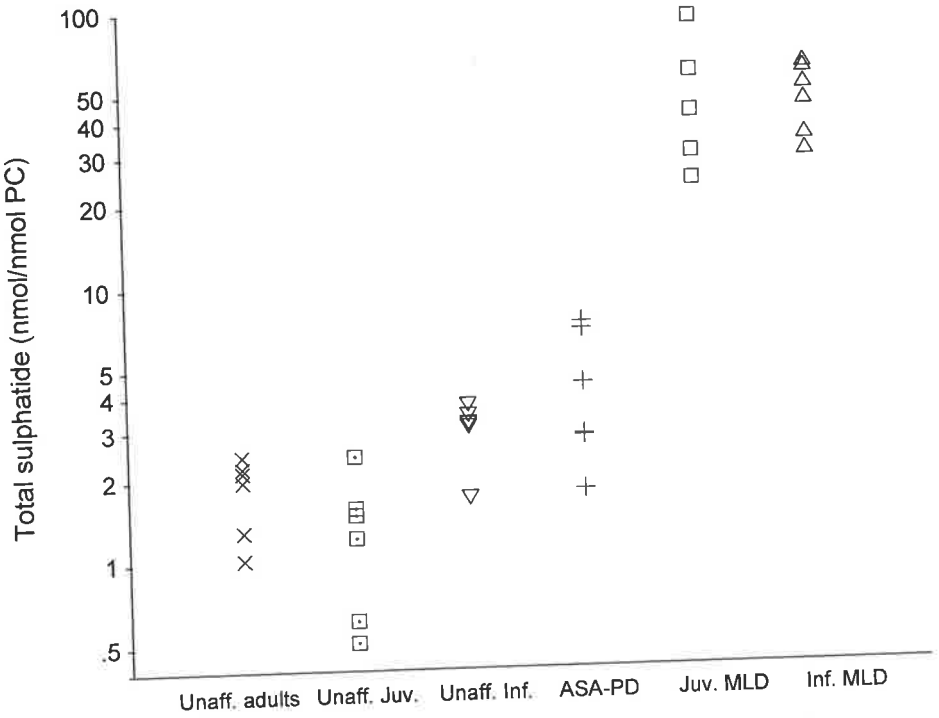

Figure 6.1 Total urinary sulphatide measured in MLD, ASA-PD and unaffected controls

Using the method of Bligh and Dyer (section 2.2.17.1), lipid extracts were prepared from urine (1.5 mL) collected from unaffected adults (unaff. Adults), unaffected juvenile (Unaff. Juv.), unaffected late-infantile (Unaff. Inf.), ASA-PD individuals (ASA-PD), late-infantile MLD (Inf. MLD) and juvenile MLD (Juv. MLD). Urinary sulphatide was measured by ESI-MS/MS (section 2.2.18.1). Total urinary sulphatide is the sum of 18 sulphatide species and expressed as nmol/nmol PC.

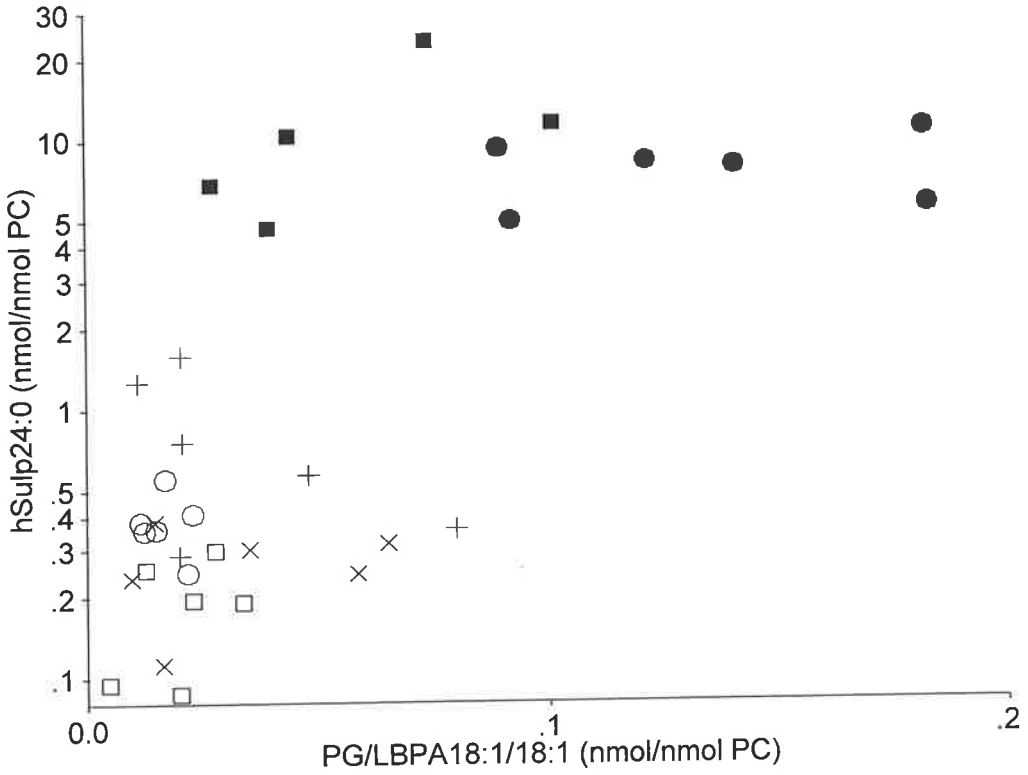

Figure 6.2 Ratios of hSulp24:0 and PG/LBPA18:1/18:1 in urine from unaffected controls, ASA PD individuals and MLD patients

Using the method of Bligh and Dyer (section 2.2.17.1), lipid extracts were prepared from urine (1.5 mL) collected from unaffected adults (×), unaffected juvenile (□), unaffected late-infantile (○), ASA-PD individuals (+), juvenile MLD (■) and late-infantile MLD (●). hSulp24:0 and PG/LBPA18:1/18:1 were measured by ESI-MS/MS (sections 2.2.18.1 and 2.2.18.2, respectively) and expressed as nmol/nmol PC.

Table 6.6 **Correlation analysis between unaffected controls and MLD patients with age[a]**

Analyte[b]	Unaffected		MLD	
	Spearman's rho	p value	Spearman's rho	p value
Cer16:0	-0.088	0.787	**0.658**	**0.028**
Cer20:0	**-0.767**	**0.004**	-0.032	0.925
Cer20:1	-0.574	0.051	-0.271	0.420
Cer23:0	**-0.627**	**0.029**	-0.037	0.914
Cer23:1	**-0.795**	**0.002**	-0.184	0.588
Cer24:0	-0.273	0.390	0.294	0.380
Cer24:1	-0.151	0.640	0.372	0.259
GC16:0	**-0.592**	**0.043**	-0.299	0.372
GC18:0	-0.536	0.073	-0.308	0.357
GC20:0	-0.473	0.121	-0.303	0.364
GC22:0	**-0.595**	**0.041**	-0.331	0.320
GC24:0	-0.546	0.066	-0.313	0.349
GC24:1	**-0.637**	**0.026**	-0.069	0.840
LC16:0	-0.529	0.077	0.234	0.488
LC20:0	-0.480	0.114	-0.018	0.957
LC22:0	-0.515	0.087	0.097	0.778
LC22:0-OH	-0.483	0.111	-0.363	0.272
LC24:0	**-0.641**	**0.025**	0.124	0.716
LC24:1	-0.557	0.060	0.267	0.428
CTH16:0	-0.564	0.056	-0.202	0.551
CTH18:0	-0.574	0.051	-0.046	0.893
CTH20:0	**-0.662**	**0.019**	-0.143	0.676
CTH22:0	-0.529	0.077	-0.005	0.989
CTH24:0	**-0.680**	**0.015**	0.115	0.736
CTH24:1	**-0.585**	**0.046**	-0.189	0.579
PC32:0	-0.284	0.372	**0.726**	**0.011**
PC32:1	**-0.602**	**0.038**	0.418	0.200
PC34:1	-0.483	0.111	-0.492	0.124
PC34:2	0.571	0.053	0.253	0.453
PC36:2	0.322	0.307	-0.129	0.706
PC36:4	**0.620**	**0.032**	-0.271	0.420
PC38:4	0.473	0.121	-0.552	0.078
SM16:0	-0.518	0.084	0.308	0.357
SM22:0	**-0.785**	**0.003**	-0.409	0.211
SM24:0	**-0.792**	**0.002**	-0.046	0.893
PG/LBPA16:0/22:6	-0.291	0.359	-0.087	0.798
PG/LBPA16:1/20:4	-0.252	0.429	**0.602**	**0.050**
PG/LBPA18:1/18:0	**-0.739**	**0.006**	**-0.731**	**0.011**
PG/LBPA18:1/18:1	0.200	0.534	**-0.782**	***0.004***
PG/LBPA18:1/18:2	-0.091	0.778	**-0.731**	**0.011**
PG/LBPA18:1/20:4	**-0.606**	**0.037**	**-0.639**	**0.034**
PG/LBPA18:1/22:5	-0.193	0.549	-0.395	0.229
PG/LBPA18:1/22:6	0.263	0.409	-0.216	0.523
PG/LBPA18:2/22:6	0.228	0.477	-0.372	0.259
PG/LBPA20:4/22:6	-0.070	0.829	-0.041	0.904
PG/LBPA22:5/22:5	0.095	0.770	-0.529	0.094
PG/LBPA22:6/22:5	0.207	0.519	-0.372	0.259
PG/LBPA22:6/22:6	0.147	0.648	-0.161	0.636

Table 6.6 continued

Analyte[b]	Unaffected		MLD	
	Spearman's Rho	significant	Spearman's Rho	significant
PI16:0/18:0	-0.550	0.064	0.083	0.809
PI16:0/20:4	**-0.708**	**0.010**	-0.510	0.109
PI18:0/18:1	**-0.655**	**0.021**	0.064	0.851
PI18:0/18:1	0.035	0.914	-0.244	0.470
PI18:0/20:3	-0.123	0.704	-0.166	0.627
PI18:0/20:4	-0.466	0.127	-0.120	0.726
PI18:0/22:5	-0.480	0.114	-0.060	0.861
PI18:1/18:1	-0.473	0.121	-0.326	0.327
PI18:1/20:4	**-0.736**	**0.006**	-0.244	0.470
G_{M3}16:0	**-0.690**	**0.013**	0.212	0.532
G_{M3} 22:0	**-0.781**	**0.003**	-0.009	0.979
G_{M3} 24:0	**-0.690**	**0.013**	0.005	0.989
G_{M3} 24:1	**-0.760**	**0.004**	0.147	0.666
hSulp16:0	**-0.774**	**0.003**	-0.055	0.872
Sulp18:0	**-0.676**	**0.016**	-0.593	0.054
hSulp18:0	**-0.795**	**0.002**	-0.414	0.206
Sulp20:0	**-0.837**	**0.001**	-0.533	0.091
Sulp21:0	**-0.771**	**0.003**	-0.556	0.075
hSulp20:0	**-0.802**	**0.002**	-0.207	0.542
Sulp22:0	**-0.851**	**0.000**	-0.317	0.342
Sulp23:0	**-0.851**	**0.000**	-0.216	0.523
hSulp22:0	**-0.858**	**0.000**	-0.129	0.706
Sulp24:1	**-0.806**	**0.002**	-0.409	0.211
Sulp24:0	**-0.865**	**0.000**	-0.161	0.636
hSulp23:0	**-0.858**	**0.000**	-0.083	0.809
hSulp24:1	**-0.858**	**0.000**	-0.046	0.893
hSulp24:0	**-0.844**	**0.001**	0.170	0.617
hSulp25:1	**-0.764**	**0.004**	-0.028	0.936
hSulp25:0	**-0.662**	**0.019**	-0.143	0.676
dhSulp22:0	**-0.620**	**0.032**	-0.437	0.179
dhSulp 24:0	**-0.697**	**0.012**	-0.285	0.395
Cer total	-0.284	0.372	0.354	0.285
GC total	-0.550	0.064	-0.354	0.285
LC total	-0.546	0.066	0.179	0.598
CTH total	**-0.578**	**0.049**	0.074	0.830
SM total	**-0.809**	**0.001**	0.009	0.979
PG/LBPA total	-0.091	0.778	**-0.768**	**0.006**
PI total	**-0.630**	**0.028**	-0.175	0.607
G_{M3} total	**-0.729**	**0.007**	0.133	0.696
Sulp total	**-0.897**	**0.000**	-0.198	0.560

[a] The relative amount of each analyte was determined by ESI-MS/MS using the MRM mode (sections 2.2.18.1, 2.2.18.2, 2.2.18.3 and 2.2.18.4). The Spearman's rho and p values (≤0.05 bolded) are reported for all sulphatide, glycolipid, phospholipid and ganglioside species in unaffected controls aged less than 18-years old (n=12) and MLD patients aged two- to 13-years old (n=11).

[b] Cer = ceramide; GC = glucosylceramide; LC = lactosylceramide; CTH = ceramide trihexoside; PC = phosphatidylcholine; SM = sphingomyelin; PG/LBPA = phosphatidylglycerol/lysobisphosphatidic acid, PI = phosphatidylinositol; G_{M3} = monosialogangliosides; Sulp = sulphatide; hSulp = hydroxy sulphatide; dhSulph = dihexosyl sulphatide

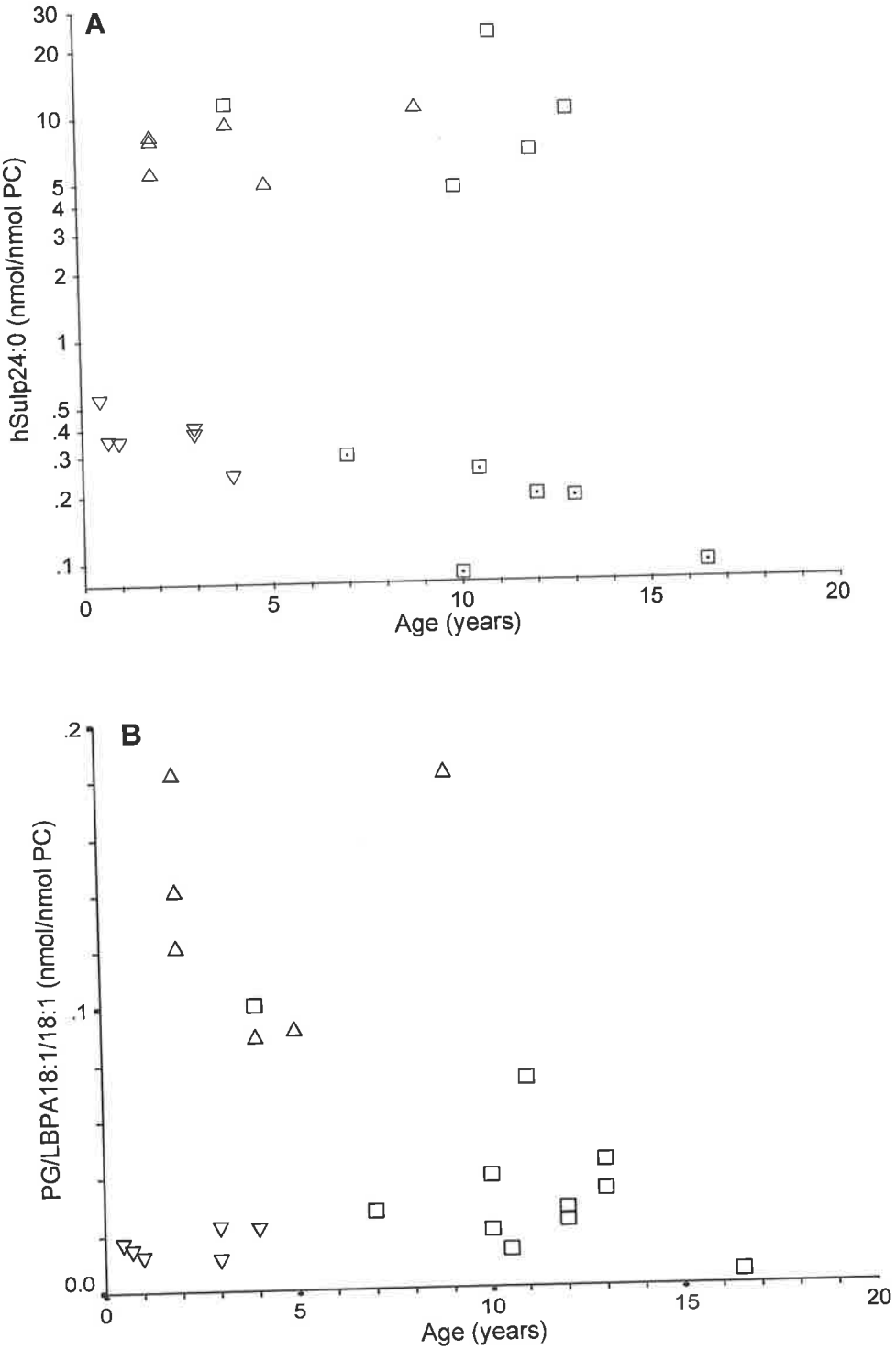

Figure 6.3 Correlation between age and hSulp24:0 (A), and age and PG/LBPA18:1/18:1 (B)

Using the method of Bligh and Dyer (section 2.2.17.1), lipid extracts were prepared from urine (1.5 mL) collected from unaffected juveniles (⊡), unaffected late-infantiles (▽), juvenile MLD (□) and late-infantile MLD (△) patients. hSulp24:0 (section 2.2.18.1) and PG/LBPA18:1/18:1 (section 2.2.18.2) were measured using ESI-MS/MS and expressed as nmol/nmol PC.

6.2. Biochemical profiling of SF samples

To evaluate the utility of using multiple biochemical parameters to predict clinical severity in MLD, SF from 13 MLD patients, two ASA-PD, two ASA-PD/MLD individuals and five unaffected controls were subjected to biochemical profiling. In this context, biochemical profiling refers to the characterisation of residual ASA protein and activity, as well as the response of intracellular lipids to sulphatide-loading. Genotype data for all patients whose SF were used in this study are shown in Table 6.7. Genotyping was carried out in the National Referral Laboratory for the Diagnosis of Lysosomal, Peroxisomal and Related Genetic Disorders, Department of Genetic Medicine, Women's and Children's Hospital, Adelaide, SA, Australia.

6.2.1. Determination of ASA

To determine ASA activity and protein in SF, cells were cultured (section 2.2.12) to seven-days post-confluence before being harvested (section 2.2.13) and lysed by sonication (section 2.2.16). The total protein in each SF lysate was determined using the BCA method (section 2.2.5). ASA activity and protein are expressed as pmol/min/mg cell protein and ng/mg cell protein, respectively.

6.2.1.1. Immune-quantification of ASA protein

ASA protein in SF lysates was determined using the immune-quantification assay and the protocol described in section 2.2.10.2; the results are summarised in Table 6.8. The amount of ASA protein detected was approximately: (i) 10% and 5% of normal in ASA-PD and ASA-PD/MLD SF, respectively; (ii) 2% and 3.5% of normal in adult and juvenile MLD SF, respectively. The higher percentage of ASA protein detected in the juvenile group was due to patient S15 (29.1 ng/mg cell protein); and (iii) less than 2% of normal in late-infantile MLD SF. Patients S20 and S21 had no detectable ASA protein (below the assay detection limit of 95 pg/mg cell protein).

6.2.1.2. Immune-capture of ASA activity

ASA activity in SF lysates was determined using the immune-capture activity assay and protocol developed in this study (section 2.2.10.1); the results are summarised in Table 6.8. The amount of ASA activity detected was approximately: (i) 18% and 8.5% of normal in ASA-PD and ASA/MLD SF, respectively; (ii) 3% and 1.5% of normal in adult and juvenile MLD SF, respectively; and (iii) less than 1% of normal in late-infantile MLD SF. Patients S19, S20 and S21 had no detectable ASA activity (below the assay detection limit of 0.6 pmol/min/mg cell protein).

Using a combination of ASA protein and activity, unaffected controls, ASA-PD and ASA-PD/MLD compound heterozygotes could be distinguished from each other (Figure 6.4). However, with the exception of three of the five late-infantile MLD patients who had a severe phenotype (S19, S20 and S21) and two whose ASA activity and protein (S20 and S21 only) were below the limit of detection, these two parameters did not clearly discriminate between the different phenotypes of MLD.

6.2.1.3. Specific activity of ASA

The specific activity of ASA was calculated for all of the SF samples analysed and is shown in Table 6.8. Specific activity was: (i) higher than the control range in ASA-PD and ASA-PD/MLD individuals; (ii) within or above the control range in adult MLD patients; and (iii) below the control in late-infantile MLD patients. Specific activity in juvenile MLD patients showed no consistent trend, with values that were either below or above the normal range.

Table 6.7 **SF cell lines used to evaluate multiple parameters for the prediction of clinical severity in MLD**

SF	Age at sampling[a] (years)	Type	Genotype[b]
S1	NA	Normal	
S2	NA	Normal	
S3	NA	Normal	
S4	NA	Normal	
S5	NA	Normal	
S6	NA	ASA-PD	ASA-PD/ASA-PD
S7	NA	ASA-PD	ASA-PD/ASA-PD
S8	NA	ASA-PD/MLD	ASA-PD/T274M
S9	NA	ASA-PD/MLD	ASA-PD/D169N
S10	31	Adult	SDEX2/I179S
S11	19	Adult	P426L/unknown
S12	17	Adult	SDEX2/unknown
S13	8	Juvenile	SDEX2/P426L
S14	7	Juvenile	G345C/T274M
S15	11	Juvenile	R244C/ R288C
S16	8	Juvenile	SDEX2/unknown
S17	6	Juvenile	SDEX2/P426L, Y429S
S18	1	Late-infantile	T274M/T274M
S19	3	Late-infantile	DelCCT(EX7)/DelCCT(EX7)
S20	2	Late-infantile	SDEX2/SDEX2
S21	3	Late-infantile	SDEX2/SDEX2
S22	4	Late-infantile	D335V/P377L

[a] NA = age not available;

[b] SDEX2 = single deletion at exon 2; delCCT(EX7) = deletion of CCT at exon 7.

Table 6.8 ASA activity and protein in cultured SF

SF	Type	ASA protein[a] (ng/mg)	ASA activity[b] (pmol/min/mg)	Specific activity[c] (pmol/min/ng ASA)
S1	Normal	204	1395.	6.8
S2	Normal	200	1223	6.1
S3	Normal	215	1171	5.5
S4	Normal	263.	1714	6.5
S5	Normal	218	1017	4.7
S6	ASA-PD	27.5	241	8.8
S7	ASA-PD	25.2	222	8.8
S8	ASA-PD/MLD	11.4	118	10.4
S9	ASA-PD/MLD	9.2	106	12.2
S10	Adult	5.3	60.4	11.4
S11	Adult	4.7	26.1	5.6
S12	Adult	3.2	26.5	8.3
S13	Juvenile	2.6	9.3	3.6
S14	Juvenile	0.5	7.6	15.3
S15	Juvenile	29.1	32.0	1.1
S16	Juvenile	0.3	4.5	15.0
S17	Juvenile	6.1	50.7	8.3
S18	Late-infantile	1.8	1.3	0.7
S19	Late-infantile	0.9	nd[d]	nc[e]
S20	Late-infantile	nd[d]	nd[d]	nc[e]
S21	Late-infantile	nd[d]	nd[d]	nc[e]
S22	Late-infantile	4.3	10.5	2.5

[a] SF ASA protein was determined using the immune-quantification assay described in section 2.2.10.2;

[b] SF ASA activity was determined using the immune-capture activity assay described in section 2.2.10.1;

[c] Specific activity was calculated by dividing ASA activity by ASA protein;

[d] nd = not detectable;

[e] nc = not calculated.

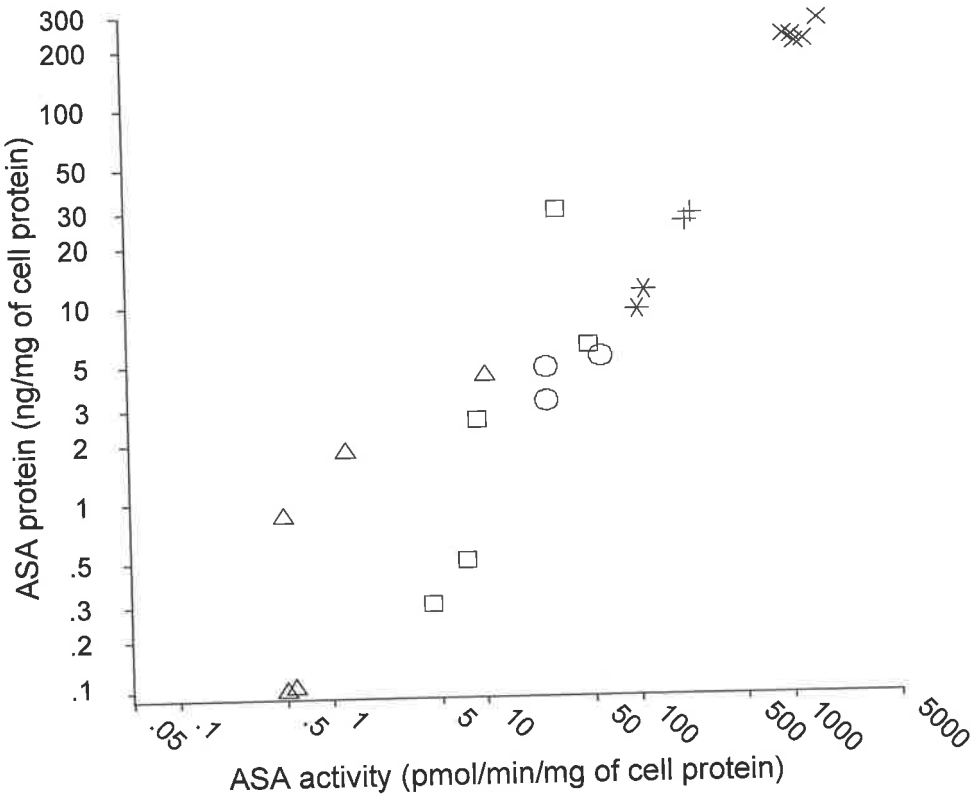

Figure 6.4 Correlations between ASA protein and activity

SF lysates from unaffected controls (×), ASA-PD individuals (+), ASA-PD/MLD compound heterozygotes (⁎), adult MLD patients (○), juvenile MLD patients (□) and late-infantile MLD patients (△) were assayed for total cell protein (section 2.2.5). ASA protein was measured using the immune-quantification assay (section 2.2.10.2), and ASA activity was measured using the immune-capture activity assay (section 2.2.10.1). ASA protein in patients S19 and S20 was assigned the lower assay limit of detection (0.095 ng/mg cell protein). ASA activity in patients S19, 20 and 21 was assigned the lower assay limit of detection (0.6 pmol/min/mg cell protein).

6.2.2. Lipid profiling

The 22 SF cell lines were cultured (in triplicate, 75 cm^2 flasks) in BME with 10% FCS to seven-days post-confluence, as described in section 2.2.12. The cell lines were washed with PBS (3 x 5.0 mL) and cultured with BME (8.0 mL) containing 5% HIFCS, 1% penicillin/streptomycin and bovine brain sulphatide (64 μM). The cell lines were incubated (5% CO_2, 37°C) for a further eight-days (section 2.2.15), harvested (section 2.2.13) and cell lysates prepared by sonication (section 2.2.16). Total protein was estimated for all cell lysates (section 2.2.5). Using the method of Folch (section 2.2.17.2), lipids were extracted from each SF lysate for ESI-MS/MS analysis.

6.2.2.1. ESI-MS/MS determination of accumulated sulphatide

Sulphatide was determined in the SF cell lysates by ESI-MS/MS (section 2.2.18.1). Table 6.9 summarises the mean value (n=3) of sulphatide accumulation in each cell line, which is expressed as nmol/mg protein. A response similar to that observed for urinary sulphatide was noted (discussed in section 6.1.5) for almost all of the sulphatide species that were monitored and this was reflected in the amount of total sulphatide: MLD patients accumulated more sulphatide than unaffected controls, with ASA-PD and ASA-PD/MLD individuals generally situated between the two groups.

The rate of total sulphatide accumulation in cultured SF following sulphatide-loading clearly distinguished unaffected controls from MLD patients, as well as unaffected controls and three of four ASA-PD or ASA-PD/MLD individuals (Figure 6.5). However, it was not useful in differentiating each of the MLD phenotypes.

When residual enzyme activity was combined with the rate of sulphatide accumulation, an inverse relationship was observed that enabled discrimination between unaffected controls, ASA-PD, ASA-PD/MLD and all MLD patients (Figure 6.6). In addition, four of five infantile MLD patients could be distinguished from the juvenile and adult forms of the disease. ASA activity in patient S22 (late-infantile MLD) was consistent with that expected in juvenile MLD but total sulphatide was higher and in the range suggestive of a severe phenotype. Some separation was possible between the juvenile and adult MLD patient groups, however Sulp24:1 and ASA activity in patients S15 and S17 were in the adult MLD range despite a clinical diagnosis of juvenile MLD.

Table 6.9 Sulphatide accumulation[a] in cultured SF (nmol/mg cell protein)

Cell line	Type	Sulphatide species[b]																		
		hSulp 16:0	Sulp 18:0	hSulp 18:0	Sulp 20:0	Sulp 21:0	hSulp 20:0	Sulp 22:0	Sulp 23:0	hSulp 22:0	Sulp 24:1	Sulp 24:0	hSulp 23:0	hSulp 24:1	hSulp 24:0	hSulp 25:1	hSulp 25:0	dhSulp 22:0	dhSulp 24:0	Total
S1	Normal	0.11 (0.01)	0.67 (0.16)	0.53 (0.04)	0.14 (0.03)	0.04 (0.01)	0.06 (0.01)	1.32 (0.24)	0.53 (0.12)	0.37 (0.07)	3.86 (1.00)	4.37 (0.84)	1.10 (0.20)	1.04 (0.24)	1.44 (0.24)	0.34 (0.06)	0.19 (0.03)	0.00 (0.00)	0.01 (0.01)	16.2
S2	Normal	0.14 (0.02)	0.58 (0.15)	0.42 (0.03)	0.15 (0.03)	0.00 (0.01)	0.02 (0.00)	1.51 (0.27)	0.61 (0.09)	0.37 (0.05)	5.41 (0.98)	5.09 (0.87)	1.19 (0.19)	1.26 (0.17)	1.51 (0.18)	0.40 (0.07)	0.19 (0.01)	0.00 (0.00)	0.01 (0.00)	18.7
S3	Normal	0.18 (0.02)	0.50 (0.10)	0.48 (0.06)	0.18 (0.03)	0.04 (0.02)	0.05 (0.01)	1.50 (0.16)	0.60 (0.06)	0.34 (0.01)	5.13 (0.95)	4.94 (0.64)	1.14 (0.03)	1.18 (0.14)	1.34 (0.03)	0.39 (0.03)	0.00 (0.00)	0.01 (0.00)	0.01 (0.00)	18.0
S4	Normal	0.00 (0.01)	0.73 (0.13)	0.37 (0.05)	0.11 (0.03)	0.03 (0.01)	0.03 (0.01)	0.75 (0.10)	0.29 (0.03)	0.19 (0.03)	2.15 (0.25)	2.30 (0.16)	0.59 (0.07)	0.59 (0.07)	0.75 (0.11)	0.20 (0.03)	0.11 (0.02)	0.00 (0.00)	0.00 (0.00)	9.2
S5	Normal	0.00 (0.02)	0.70 (0.12)	0.26 (0.05)	0.08 (0.01)	0.00 (0.00)	0.02 (0.01)	0.97 (0.10)	0.41 (0.05)	0.23 (0.03)	3.23 (0.28)	3.31 (0.29)	0.81 (0.07)	0.75 (0.12)	0.95 (0.13)	0.00 (0.02)	0.02 (0.02)	0.00 (0.01)	0.02 (0.00)	11.8
S6	ASA-PD	0.06 (0.01)	0.66 (0.12)	0.34 (0.05)	0.12 (0.02)	0.01 (0.01)	0.02 (0.01)	1.20 (0.12)	0.46 (0.05)	0.25 (0.03)	3.92 (0.77)	3.77 (0.36)	0.87 (0.06)	0.85 (0.11)	0.93 (0.07)	0.00 (0.03)	0.12 (0.01)	0.00 (0.00)	0.06 (0.00)	13.6
S7	ASA-PD	0.17 (0.05)	1.02 (0.29)	0.69 (0.19)	0.32 (0.07)	0.04 (0.03)	0.06 (0.03)	2.81 (0.17)	1.14 (0.08)	0.69 (0.07)	9.34 (0.80)	9.34 (0.53)	2.34 (0.11)	2.20 (0.11)	2.76 (0.18)	0.73 (0.06)	0.00 (0.00)	0.02 (0.01)	0.01 (0.01)	33.7
S8	ASA-PD/MLD	0.13 (0.01)	2.62 (0.62)	1.48 (0.38)	0.69 (0.19)	0.08 (0.03)	0.16 (0.05)	6.33 (1.70)	2.61 (0.78)	1.71 (0.52)	17.21 (3.32)	21.02 (5.76)	5.69 (1.68)	4.90 (1.38)	6.88 (2.06)	1.82 (0.57)	0.95 (0.29)	0.04 (0.00)	0.04 (0.00)	74.0
S9	ASA-PD/MLD	0.37 (0.04)	1.86 (0.15)	1.08 (0.13)	0.66 (0.03)	0.08 (0.00)	0.13 (0.01)	6.08 (0.33)	2.40 (0.03)	1.30 (0.02)	22.35 (1.41)	19.67 (0.70)	4.36 (0.12)	4.49 (0.20)	4.70 (0.37)	1.50 (0.06)	0.62 (0.03)	0.04 (0.01)	0.03 (0.01)	70.8

Table 6.9 Continued

Cell line	Type	Sulphatide species																		Total
		hSulp 16:0	Sulp 18:0	hSulp 18:0	Sulp 20:0	Sulp 21:0	hSulp 20:0	Sulp 22:0	Sulp 23:0	hSulp 22:0	Sulp 24:1	Sulp 24:0	hSulp 23:0	hSulp 24:1	hSulp 24:0	hSulp 25:1	hSulp 25:0	dhSulp 22:0	dhSulp 24:0	
S10	Adult	0.15 (0.01)	5.31 (0.52)	2.26 (0.20)	1.25 (0.17)	0.17 (0.02)	0.25 (0.03)	10.53 (1.42)	4.06 (0.48)	2.24 (0.26)	38.57 (5.17)	33.71 (4.77)	7.41 (0.98)	8.17 (0.94)	8.07 (0.84)	2.55 (0.32)	1.10 (0.15)	0.04 (0.00)	0.03 (0.00)	125
S11	Adult	0.09 (0.03)	4.50 (0.59)	1.83 (0.29)	1.10 (0.16)	0.16 (0.02)	0.24 (0.05)	9.69 (1.15)	3.91 (0.70)	2.14 (0.36)	34.88 (4.48)	31.90 (4.25)	7.21 (0.99)	7.21 (1.24)	7.63 (1.36)	2.46 (0.34)	1.05 (0.17)	0.04 (0.00)	0.02 (0.00)	115
S12	Adult	0.04 (0.02)	4.66 (0.36)	2.19 (0.24)	1.09 (0.08)	0.18 (0.01)	0.27 (0.02)	9.52 (0.75)	3.83 (0.30)	2.19 (0.19)	30.30 (2.59)	30.74 (2.48)	7.07 (0.48)	7.25 (0.65)	7.83 (0.94)	2.41 (0.19)	1.09 (0.10)	0.02 (0.00)	0.02 (0.00)	110
S13	Juvenile	0.18 (0.02)	5.70 (0.22)	2.88 (0.22)	1.38 (0.10)	0.19 (0.02)	0.31 (0.02)	11.55 (0.54)	4.63 (0.31)	2.66 (0.25)	39.47 (1.40)	37.56 (1.81)	8.39 (0.72)	9.08 (0.41)	9.98 (1.01)	2.86 (0.22)	1.29 (0.13)	0.03 (0.00)	0.03 (0.00)	137
S14	Juvenile	0.01 (0.01)	6.17 (0.28)	2.30 (0.08)	1.41 (0.03)	0.22 (0.01)	0.30 (0.01)	11.54 (0.49)	4.57 (0.16)	2.38 (0.12)	45.52 (2.03)	37.64 (1.41)	7.81 (0.32)	8.60 (0.32)	7.95 (0.21)	2.72 (0.15)	1.12 (0.05)	0.02 (0.00)	0.01 (0.00)	140
S15	Juvenile	0.03 (0.01)	4.91 (0.68)	2.08 (0.22)	1.11 (0.16)	0.16 (0.03)	0.24 (0.03)	9.35 (1.52)	3.75 (0.57)	2.10 (0.29)	31.90 (5.37)	30.21 (4.64)	6.77 (1.04)	7.12 (1.01)	7.46 (0.88)	2.29 (0.34)	1.03 (0.13)	0.01 (0.00)	0.00 (0.00)	110
S16	Juvenile	0.04 (0.00)	4.99 (0.07)	1.87 (0.02)	1.15 (0.03)	0.19 (0.00)	0.24 (0.01)	9.29 (0.15)	3.62 (0.07)	1.87 (0.05)	37.41 (0.46)	29.87 (0.39)	6.22 (0.07)	6.85 (0.17)	6.36 (0.31)	2.23 (0.05)	0.88 (0.05)	0.01 (0.00)	0.01 (0.00)	113
S17	Juvenile	0.04 (0.02)	4.58 (0.37)	1.69 (0.20)	1.03 (0.08)	0.17 (0.01)	0.21 (0.02)	8.52 (0.25)	3.27 (0.16)	1.66 (0.09)	34.61 (2.05)	27.43 (1.28)	5.52 (0.31)	6.19 (0.47)	5.64 (0.43)	1.96 (0.13)	0.77 (0.05)	0.02 (0.01)	0.02 (0.00)	103
S18	Late-infantile	0.00 (0.01)	5.60 (0.34)	2.11 (0.13)	1.24 (0.06)	0.21 (0.01)	0.27 (0.02)	9.99 (0.59)	3.92 (0.13)	2.09 (0.18)	41.18 (3.03)	32.58 (2.11)	6.61 (0.50)	7.55 (0.50)	6.92 (0.32)	2.32 (0.15)	0.95 (0.05)	0.01 (0.00)	0.00 (0.00)	123
S19	Late-infantile	0.39 (0.04)	12.62 (0.23)	5.62 (0.07)	2.76 (0.06)	0.45 (0.01)	0.72 (0.02)	23.10 (0.31)	9.46 (0.05)	5.57 (0.02)	83.91 (1.66)	74.71 (1.46)	16.65 (0.30)	19.46 (0.60)	21.79 (0.38)	6.25 (0.09)	2.90 (0.13)	0.02 (0.01)	0.03 (0.01)	286
S20	Late-infantile	0.04 (0.03)	9.07 (0.53)	3.98 (0.34)	2.07 (0.17)	0.32 (0.04)	0.48 (0.05)	17.14 (1.75)	6.61 (0.51)	3.75 (0.37)	69.95 (3.68)	55.51 (4.01)	11.23 (0.82)	13.71 (1.34)	13.78 (1.74)	3.95 (0.36)	1.75 (0.14)	0.02 (0.00)	0.01 (0.00)	213
S21	Late-infantile	0.08 (0.01)	9.62 (0.43)	3.79 (0.17)	2.15 (0.10)	0.34 (0.02)	0.47 (0.02)	17.58 (0.76)	6.78 (0.33)	3.61 (0.17)	69.66 (2.73)	55.39 (1.66)	11.56 (0.33)	13.48 (0.69)	12.98 (0.55)	4.17 (0.23)	1.74 (0.11)	0.02 (0.00)	0.01 (0.000	213
S22	Late-infantile	0.04 (0.01)	6.80 (0.20)	2.55 (0.16)	1.44 (0.07)	0.21 (0.00)	0.32 (0.01)	11.92 (0.56)	4.64 (0.21)	2.43 (0.16)	50.43 (3.81)	38.32 (1.98)	7.83 (0.51)	9.41 (1.03)	8.87 (0.99)	2.89 (0.26)	1.21 (0.11)	0.01 (0.00)	0.00 (0.00)	149

Table 6.9 Continued

[a] SF cell lines were cultured as described in section 6.2 2 (in triplicate). Lipid extracts were determined by ESI-MS/MS for sulphatide species (section 2.2.18.1). Results shown are the average and (standard deviation) of triplicate experiments for sulphatide species and expressed as nmol/mg cell protein;
[b] Sulp =sulphatide; hSulp = hydroxy sulphatide; dhSulp = dihexosyl sulphatide.

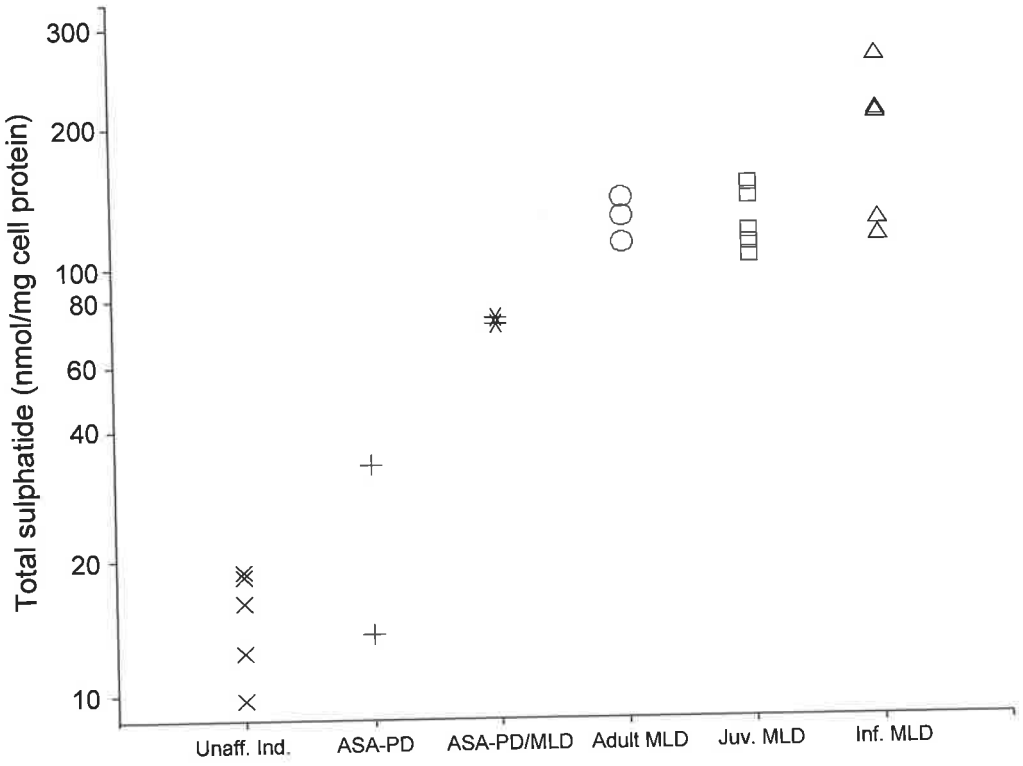

Figure 6.5 Sulphatide accumulation in cultured SF

SF were cultured using the conditions described in section 6.2.2. The amount of sulphatide was determined in cultured SF from five unaffected controls (unaff. Ind.), two ASA-PD individuals (ASA-PD), two ASA-PD/MLD individuals (ASA-PD/MLD), three adult MLD patients (adult MLD), five juvenile MLD (Juv. MLD) and five late-infantile MLD (Inf. MLD) patients. SF lysates were analysed for sulphatide using the ESI-MS/MS method described in section 2.2.18.1. Each point in the graph represents the average of triplicate samples.

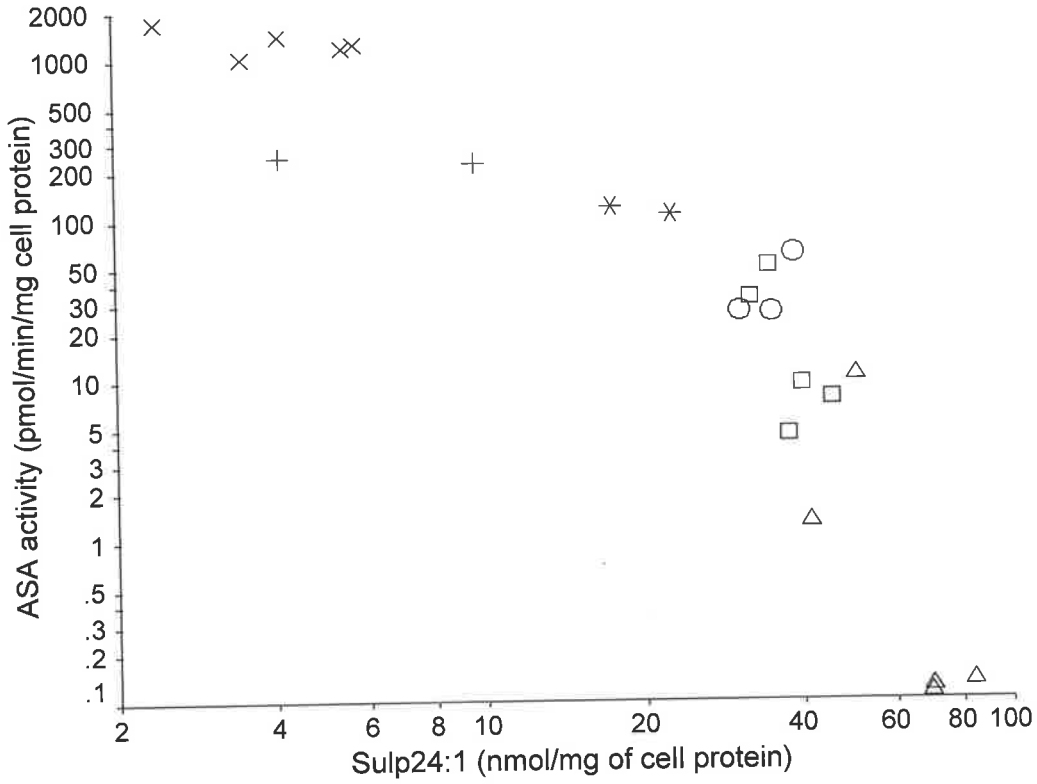

Figure 6.6 Relationship between ASA activity and Sulp24:1 accumulation in cultured SF

SF were cultured using the culture conditions described in section 6.2.2. The amount of Sulp24:1 was determined in cultured SF from five unaffected individuals (×), two ASA-PD individuals (+), two ASA-MLD compound heterozygotes (⁎) three adult MLD patients (○), five juvenile MLD patients (□) and five late-infantile MLD patients (△). ASA activity was determined on cell lysates prepared from cultured SF collected from the patient cohort described in section 6.2.1.2. The level of Sulp24:1 in the graph represents the average of triplicate samples.

6.2.2.2. ESI-MS/MS determination of phospholipids, glycolipids, phophatidylcholine, sphingomyelin and gangliosides

Phospholipid measurement in SF lysates was performed using the protocol described in section 2.2.18.2; glycolipids were measured using the protocol described in section 2.2.18.3; and G_{M3} gangliosides were measured using the protocol described in section 2.2.18.4. Table 6.10 summarises the results, which are expressed as nmol/mg cell protein. Values shown are the minimum and maximum obtained for each group studied.

6.2.3. Statistical analyses

The M-W U test was used to evaluate the ability of each analyte to differentiate between: (i) MLD and unaffected controls; (ii) ASA-PD (together with ASA-PD/MLD) and unaffected controls; and (iii) ASA-PD (together with ASA-PD/MLD) and MLD patients. Table 6.11 summarises the M-W U values and the significance (p) values for each analyte in each comparison.

The values of 41 analytes were significantly different between the unaffected control and MLD groups: Cer16:0, 20:0, 20:1 and 23:1; four out of six GC species; CTH16:0; PC32:0, 32:1 and 36:4; eight out of 13 PG/LBPA species; PI18:0/18:1, PI18:1/18:1 and PI18:1/20:4; G_{M3}24:0 and G_{M3}24:1; and 16 of 18 sulphatide species; the values of total PG/LBPA and sulphatide were also found to be significantly different. Most of these analytes did not, however, unambiguously differentiate unaffected controls from MLD patients but rather showed some overlap (a M-W U value greater than 0); the exceptions to this were the urinary sulphatide species, minus dhSulp22:0 (M-W U value of 10).

The LC, GC and Cer species, which appeared to discriminate between unaffected controls and MLD patients (particularly LC20:0 and GC24:1; M-W U values of 0), were excluded as potential markers for the prediction of severity. The values obtained for these glycolipids were attributed to sulphatide, as a result of the loss of the sulphate moiety in the electrospray source that leads to the formation of these glycolipid species, as demonstrated in section 6.1.4.

No significant differences were observed in the lipid values between ASA-PD and the unaffected control group.

A comparison of the ASA-PD and MLD groups revealed a total of 27 analytes with significantly different values: Cer20:0; GC24:1; LC20:0; PC32:1; five PG/LBPA species

(PG/LBPA18:1/18/1, 18;1/20/4, 18:1/22:5, 18:1/22:6 and 22:5/22:5); PI 16:0/20:4; G_{M3}24:0 and G_{M3}24:1; and 15 of 18 sulphatide species; the values of total PG/LBPA and total sulphatide were also found to be significantly different. With the exception of the sulphatide species that had a M-W U value of 0, most analytes did not completely differentiate these groups but showed some overlap.

The finding of eight and five out of 13 PG/LBPA species with significantly different values between the unaffected and MLD groups, and the ASA-PD and MLD groups, respectively, prompted further assessment of their utility as markers of disease severity. A scatter plot of Sulp24:1 plotted against PG/LBPA18:1/22:6 is shown in Figure 6.7: PG/LBPA is higher in all of the five late-infantile MLD SF than the other groups, facilitating the discrimination of this group of MLD patients from the others.

Table 6.10 Phospholipid, glycolipid, phophatidylcholine, sphingomyelin and ganglioside accumulation in cultured SF[a] (nmol/mg cell protein)

Analyte[b]	Controls (n=5)		ASA-PD (n=2)		ASA-PD/MLD (n=2)		Adult MLD (n=3)		Juvenile MLD (n=5)		Late-Infantile MLD (n=5)		
	Min	Max	Min	Max	Min	Max	Min	Max	Min	Max	Min	Max	CV (%)[c]
Cer16:0	0.45	1.56	0.79	1.32	0.89	0.99	1	1.81	0.68	3.78	0.66	3.5	12
Cer20:0	0	0.01	0	0	0	0	0	0.01	0	0.01	0	0.01	18
Cer20:1	0	0	0	0	0	0	0	0.01	0	0.01	0	0.01	20
Cer23:0	0.06	0.21	0.11	0.19	0.15	0.21	0.11	0.16	0.07	0.43	0.04	0.29	13
Cer23:1	0.02	0.09	0.04	0.06	0.05	0.07	0.07	0.08	0.04	0.18	0.03	0.21	13
Cer24:0	0.24	1.59	0.61	1.16	0.83	0.97	1.03	1.27	0.57	3.45	0.36	2.38	13
Cer24:1	0.21	1.04	0.55	0.79	0.79	0.79	0.76	0.93	0.47	1.94	0.31	1.91	17
GC16:0	2.24	3.61	1.17	3.59	1.97	2.91	2.25	3.71	1.06	5.66	0.95	3.86	24
GC18:0	0.2	0.4	0.1	0.34	0.33	0.41	0.41	0.55	0.34	0.85	0.27	0.65	26
GC20:0	0.03	0.07	0.02	0.06	0.04	0.06	0.06	0.11	0.05	0.14	0.04	0.09	18
GC22:0	0.34	0.48	0.16	0.57	0.43	0.6	0.56	0.83	0.44	1.11	0.3	0.94	19
GC24:0	1	1.14	0.4	1.81	1.07	1.72	1.28	2.21	1.18	2.8	0.7	2.31	19
GC24:1	0.59	0.79	0.33	1.02	0.93	1.15	1.42	2	1.43	3	1.05	2.52	18
LC16:0	0.55	0.79	0.5	0.68	0.71	0.73	0.59	0.78	0.48	1.1	0.64	1	16
LC20:0	0.29	0.5	0.33	0.88	1.25	1.43	1.74	2.7	1.87	5.52	1.32	3.28	11
LC22:0	0.4	1.07	0.45	0.73	0.57	0.79	0.65	0.82	0.46	1.11	0.56	0.93	15
LC22:0-OH	0.08	0.18	0.1	0.14	0.13	0.15	0.13	0.15	0.08	0.28	0.08	0.15	12
LC24:0	0.97	1.92	0.96	1.65	1.08	1.77	0.98	1.52	0.76	1.76	0.89	1.59	12
LC24:1	0.69	0.87	0.44	1.03	0.76	0.92	0.41	1.03	0.41	0.99	0.6	1.22	11

Table 6.10 Continued

Analyte[b]	Controls (n=5)		ASA-PD (n=2)		ASA-PD/MLD (n=2)		Adult MLD (n=3)		Juvenile MLD (n=5)		Late-Infantile MLD (n=5)		
	Min	Max	Min	Max	Min	Max	Min	Max	Min	Max	Min	Max	CV (%)
CTH16:0	1.88	2.38	2.12	2.14	1.19	2.21	1.46	2.23	0.57	2.23	0.88	2.28	14
CTH18:0	0.66	1.19	0.67	0.82	0.64	0.83	0.86	0.94	0.47	1.38	0.38	1.35	12
CTH20:0	0.12	0.42	0.18	0.22	0.13	0.22	0.22	0.29	0.15	0.49	0.08	0.34	15
CTH22:0	0.7	1.99	1.18	1.24	0.9	1.29	1.45	1.9	0.52	1.4	0.53	1.57	23
CTH24:0	2.33	4.25	3.17	3.98	2.28	3.33	3.47	4.64	1.32	2.93	1.33	3.26	15
CTH24:1	1.5	2.34	1.93	2.06	1.27	2.32	1.57	3.09	0.74	2.32	0.78	2.32	14
PC32:0	2.84	5.41	3.23	6.33	4.52	9.48	2.8	6.59	5.24	7.47	4.27	7.53	13
PC32:1	3.76	6.69	3.35	6.78	5.18	5.38	3.84	8.04	5.8	8.98	6.38	9.12	10
PC34:1	17.81	20.62	16.37	19.1	20.35	21.3	17.56	22.91	16.09	19.57	15.87	26.65	9
PC34:2	2.95	4.78	2.26	5.33	3.35	4.29	2.31	4.9	3.24	5.89	5.13	7.7	11
PC36:2	5.53	8.35	4.24	8.16	5.18	9.23	4.96	7.31	5.77	8.65	6.86	12.96	10
PC36:4	2.21	4.16	1.93	4.09	2.97	4.83	2.51	3.3	1.64	3.33	1.72	3.14	15
PC38:4	4.03	8.31	4.27	6.02	5.61	6.29	4.52	7.7	4.42	7	4.31	7.33	13
SM16:0	4.49	6.44	4.64	6.42	3.37	6.29	5.26	6.79	3.98	5.68	3.12	5.64	9
SM22:0	2.9	4.04	2.66	3.7	3.05	4.06	3.48	5.07	3.6	3.92	2.86	5.44	9
SM24:0	1.8	3.97	3.4	3.85	3.45	3.5	3.05	6.3	2.42	5.14	1.78	3.05	12
PG/LBPA 16:0/22:6	0.01	0.02	0.01	0.04	0.01	0.01	0.01	0.01	0.01	0.05	0.02	0.05	25
PG/LBPA 16:1/20:4	0.01	0.02	0	0.01	0.01	0.01	0	0.01	0.01	0.01	0.01	0.03	28
PG/LBPA 18:1/18:0	0.07	0.15	0.1	0.1	0.07	0.19	0.09	0.13	0.07	0.12	0.09	0.28	12

Table 6.10 Continued

Analyte[b]	Controls (n=5)		ASA-PD (n=2)		ASA-PD/MLD (n=2)		Adult MLD (n=3)		Juvenile MLD (n=5)		Late-Infantile MLD (n=5)		
	Min	Max	Min	Max	Min	Max	Min	Max	Min	Max	Min	Max	CV (%)
PG/LBPA 18:1/18:1	0.08	0.25	0.06	0.2	0.14	0.19	0.23	0.49	0.19	0.49	0.3	1.63	12
PG/LBPA 18:1/18:2	0.02	0.04	0.01	0.02	0.02	0.03	0.02	0.03	0.01	0.03	0.03	0.13	26
PG/LBPA 18:1/20:4	0.03	0.05	0.01	0.05	0.04	0.05	0.05	0.05	0.03	0.07	0.05	0.09	21
PG/LBPA 18:1/22:5	0.05	0.17	0.04	0.07	0.07	0.07	0.06	0.1	0.06	0.14	0.11	0.14	20
PG/LBPA 18:1/22:6	0.03	0.1	0.06	0.06	0.06	0.07	0.07	0.11	0.06	0.12	0.13	0.23	25
PG/LBPA 18:2/22:6	0	0.01	0.01	0.01	0.01	0.01	0.01	0.01	0	0.01	0.01	0.03	28
PG/LBPA 20:4/22:6	0.01	0.02	0.02	0.02	0.02	0.02	0.01	0.03	0.01	0.02	0.01	0.04	23
PG/LBPA 22:5/22:5	0.01	0.01	0.01	0.01	0.01	0.01	0.01	0.02	0.01	0.05	0.01	0.04	24
PG/LBPA 22:6/22:5	0.01	0.03	0.01	0.02	0.02	0.03	0.02	0.05	0.02	0.06	0.02	0.06	26
PG/LBPA 22:6/22:6	0	0.01	0.01	0.01	0.01	0.02	0.01	0.03	0.01	0.01	0.01	0.03	22
PI16:0/18:0	0.19	0.26	0.32	0.54	0.17	0.2	0.18	0.24	0.18	0.28	0.19	0.39	18
PI16:0/20:4	0.09	0.14	0.12	0.13	0.1	0.19	0.08	0.12	0.06	0.1	0.07	0.22	13
PI18:0/18:1	0.01	0.05	0.04	0.08	0.05	0.05	0.03	0.1	0.03	0.05	0.03	0.09	25
PI18:0/18:1	0.12	0.28	0.15	0.29	0.14	0.22	0.18	0.23	0.22	0.29	0.22	0.38	9
PI18:0/20:3	0.25	0.51	0.29	0.3	0.3	0.51	0.32	0.41	0.31	0.38	0.33	0.54	12
PI18:0/20:4	3.53	5.02	3.67	3.72	4.57	5.98	4.45	4.93	3.92	4.33	3.99	6.66	21
PI18:0/22:5	0.07	0.14	0.11	0.12	0.06	0.17	0.08	0.09	0.08	0.13	0.08	0.17	17
PI18:1/18:1	0.12	0.23	0.17	0.39	0.13	0.16	0.1	0.28	0.22	0.46	0.29	0.56	11
PI18:1/20:4	0.27	0.36	0.23	0.54	0.35	0.36	0.2	0.41	0.27	0.48	0.44	0.62	16

Table 6.10 Continued

Analyte[b]	Controls (n=5)		ASA-PD (n=2)		ASA-PD/MLD (n=2)		Adult MLD (n=3)		Juvenile MLD (n=5)		Late-Infantile MLD (n=5)		
	Min	Max	Min	Max	Min	Max	Min	Max	Min	Max	Min	Max	CV (%)
G_{M3}16:0	1.22	1.68	0.93	1.22	1.31	1.78	1	1.46	0.23	1.4	1.08	1.82	16
G_{M3} 22:0	0	0.01	0	0	0	0.01	0	0.01	0	0.01	0	0.01	38
G_{M3} 24:0	0.57	1.34	0.98	1.09	0.89	1.26	1.26	1.62	0.36	1.4	1.48	2.32	18
G_{M3} 24:1	0.62	1.42	0.86	1.07	0.95	1.1	1.06	1.68	0.31	1.25	1.43	2.18	19
Cer total	0.97	4.5	2.09	3.52	2.78	2.98	2.97	4.17	1.88	9.81	1.43	8.31	
GC total	4.6	6.36	2.17	7.39	4.77	6.85	5.99	8.6	4.55	13.56	3.33	10.35	
LC total	3.22	5.25	3.36	4.52	4.71	5.59	5.46	6.05	4.05	10.18	4.87	7.11	
CTH total	7.47	12.3	9.3	10.39	6.41	10.2	9.26	11.84	3.99	10.44	4.09	11.12	
SM total	9.46	13.66	11.74	12.93	10.93	12.79	11.79	17.19	10.24	14.75	8.62	14.13	
PG/LBPA total	0.39	0.97	0.4	0.64	0.55	0.72	0.65	1.04	0.54	1.1	1.12	2.58	
PI total	4.93	6.89	5.39	5.83	6	7.71	5.95	6.67	5.55	6.11	5.87	9.42	
G_{M3} total	2.83	4.12	2.77	3.39	3.62	3.67	3.33	4.77	0.9	3.98	4.25	5.59	

[a] SF were cultured (in triplicate) as described in section 6.2 2. The amount of each lipid analyte was determined by ESI-MS/MS using the MRM mode described in sections 2.2.18.1, 2.2.18.2, 2.2.18.3 and 2.2.18.4. The average of each triplicate was calculated and the minimum and maximum average values in each group studied are shown;

[b] Cer = ceramide; GC = glucosylceramide; LC = lactosylceramide; CTH = ceramide trihexoside; PC = phosphatidylcholine; SM = sphingomyelin; PG/LBPA = phosphatidylglycerol/lysobisphosphatidic acid, PI = phosphatidylinositol; G_{M3} = monosialogangliosides; Sulp = sulphatide; hSulp = hydroxy sulphatide; dhSulph = dihexosyl sulphatide;

[c] the CV values were calculated for each triplicate sample and results shown are average CV values from 22 samples.

Table 6.11 Discrimination between unaffected controls, ASA-PD and MLD patients with sulphatide, glycolipid, phospholipid and ganglioside species in cultured SF[a]

	MLD and unaffected		ASA-PD and unaffected		ASA-PD and MLD	
Analyte[b]	M-W U	p value	M-W U	p value	M-W U	p value
Cer16:0	**13**	**0.05**	7	0.46	14	0.17
Cer20:0	**12**	**0.04**	7	0.46	**9**	**0.05**
Cer20:1	**11**	**0.03**	7	0.46	15	0.21
Cer23:0	31	0.88	7	0.46	23	0.73
Cer23:1	**13**	**0.05**	5	0.22	14	0.17
Cer24:0	17	0.13	5	0.22	16	0.26
Cer24:1	16	0.10	5	0.22	19	0.43
GC16:0	19	0.18	7	0.46	22	0.65
GC18:0	**8**	**0.02**	7	0.46	15	0.21
GC20:0	**8**	**0.02**	8	0.62	12	0.11
GC22:0	**10**	**0.03**	6	0.33	18	0.37
GC24:0	15	0.08	8	0.62	21	0.57
GC24:1	**0**	**0.00**	5	0.22	**3**	**0.01**
LC16:0	24	0.40	7	0.46	18	0.37
LC20:0	**0**	**0.00**	3	0.09	**1**	**0.00**
LC22:0	16	0.10	7	0.46	12	0.11
LC22:0-OH	29	0.73	7	0.46	26	1.00
LC24:0	32	0.96	9	0.81	22	0.65
LC24:1	32	0.96	8	0.62	26	1.00
CTH16:0	**10**	**0.03**	9	0.81	17	0.31
CTH18:0	32	0.96	7	0.46	18	0.37
CTH20:0	21	0.26	6	0.33	21	0.57
CTH22:0	30	0.81	10	1.00	23	0.73
CTH24:0	17	0.13	7	0.46	15	0.21
CTH24:1	16	0.10	7	0.46	15	0.21
PC32:0	**10**	**0.03**	6	0.33	25	0.91
PC32:1	**13**	**0.05**	7	0.46	**8**	**0.04**
PC34:1	19	0.18	9	0.81	20	0.50
PC34:2	14	0.07	8	0.62	12	0.11
PC36:2	22	0.30	9	0.81	20	0.50
PC36:4	**10**	**0.03**	10	1.00	17	0.31
PC38:4	23	0.35	6	0.33	23	0.73
SM16:0	25	0.46	10	1.00	22	0.65
SM22:0	14	0.07	10	1.00	17	0.31
SM24:0	31	0.88	10	1.00	20	0.50
PG/LBPA16:0/22:6	14	0.07	5	0.22	20	0.50
PG/LBPA16:1/20:4	27	0.59	5	0.22	17	0.31
PG/LBPA18:1/18:0	30	0.81	9	0.81	26	1.00
PG/LBPA18:1/18:1	**4**	**0.00**	9	0.81	**1**	**0.00**
PG/LBPA18:1/18:2	23	0.35	8	0.62	14	0.17
PG/LBPA18:1/20:4	**3**	**0.00**	8	0.62	**7**	**0.03**
PG/LBPA18:1/22:5	21	0.26	9	0.81	**6**	**0.02**
PG/LBPA18:1/22:6	**4**	**0.00**	4	0.14	**2**	**0.01**
PG/LBPA18:2/22:6	**11**	**0.03**	4	0.14	17	0.31
PG/LBPA20:4/22:6	**10**	**0.03**	2	0.06	25	0.91
PG/LBPA22:5/22:5	**8**	**0.02**	9	0.81	**6**	**0.02**
PG/LBPA22:6/22:5	**6**	**0.01**	5	0.22	10	0.07
PG/LBPA22:6/22:6	**8**	**0.02**	3	0.09	21	0.57

Table 6.11 Continued

Analyte[b]	MLD and unaffected		ASA-PD and unaffected		ASA-PD and MLD	
	M-W U	p value	M-W U	p value	M-W U	p value
PI16:0/18:0	28	0.66	9	0.81	25	0.91
PI16:0/20:4	19	0.18	6	0.33	**9**	**0.05**
PI18:0/18:1	**8**	**0.02**	2	0.06	16	0.26
PI18:0/18:1	17	0.13	9	0.81	11	0.09
PI18:0/20:3	22	0.30	8	0.62	11	0.09
PI18:0/20:4	26	0.52	9	0.81	22	0.65
PI18:0/22:5	20	0.22	7	0.46	18	0.37
PI18:1/18:1	**9**	**0.02**	10	1.00	12	0.11
PI18:1/20:4	**12**	**0.04**	7	0.46	18	0.37
G_{M3}16:0	17	0.13	7	0.46	22	0.65
G_{M3}22:0	17	0.13	9	0.81	16	0.26
G_{M3}24:0	**9**	**0.02**	7	0.46	**5**	**0.02**
G_{M3}24:1	**11**	**0.03**	6	0.33	**6**	**0.02**
hSulp16:0	24	0.40	7	0.46	14	0.17
Sulp18:0	**0**	**0.00**	5	0.22	**0**	**0.00**
hSulp18:0	**0**	**0.00**	4	0.14	**0**	**0.00**
Sulp20:0	**0**	**0.00**	3	0.09	**0**	**0.00**
Sulp21:0	**0**	**0.00**	3	0.09	**0**	**0.00**
hSulp20:0	**0**	**0.00**	3	0.09	**0**	**0.00**
Sulp22:0	**0**	**0.00**	3	0.09	**0**	**0.00**
Sulp23:0	**0**	**0.00**	3	0.09	**0**	**0.00**
hSulp22:0	**0**	**0.00**	4	0.14	**1**	**0.00**
Sulp24:1	**0**	**0.00**	3	0.09	**0**	**0.00**
Sulp24:0	**0**	**0.00**	3	0.09	**0**	**0.00**
hSulp23:0	**0**	**0.00**	3	0.09	**1**	**0.00**
hSulp24:1	**0**	**0.00**	3	0.09	**0**	**0.00**
hSulp24:0	**0**	**0.00**	4	0.14	**3**	**0.01**
hSulp25:1	**0**	**0.00**	3	0.09	**0**	**0.00**
hSulp25:0	**0**	**0.00**	4	0.14	**3**	**0.01**
dhSulp22:0	**10**	**0.03**	5	0.22	19	0.43
dhSulp 24:0	22	0.30	9	0.81	26	1.00
Cer total	14	0.07	5	0.22	17	0.31
GC total	27	0.59	9	0.81	20	0.50
LC total	**4**	**0.00**	6	0.33	**7**	**0.03**
CTH total	19	0.18	9	0.81	21	0.57
SM total	32	0.96	9	0.81	24	0.82
PG/LBPA total	**6**	**0.01**	7	0.46	**4**	**0.01**
PI total	16	0.10	6	0.33	18	0.37
G_{M3} total	**13**	**0.05**	8	0.62	12	0.11
Sulp total	**0**	**0.00**	3	0.09	**0**	**0.00**

[a] The M-W U and p values (≤0.05 bolded) are shown;

[b] Cer = ceramide; GC = glucosylceramide; LC = lactosylceramide; CTH = ceramide trihexoside; PC = phosphatidylcholine; SM = sphingomyelin; PG/LBPA = phosphatidylglycerol/lysobisphosphatidic acid; PI = phosphatidylinositol; G_{M3} = monosialogangliosides; Sulp = sulphatide; hSulp = hydroxy sulphatide; dhSulph = dihexosyl sulphatide

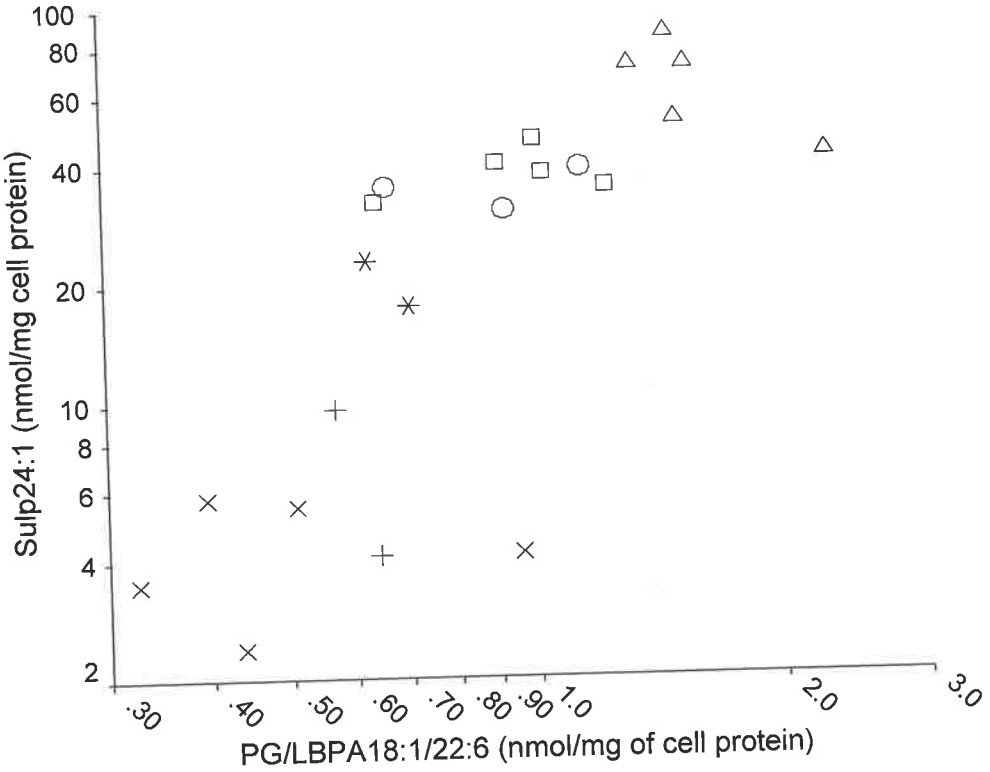

Figure 6.7 Sulp24:1 and PG/LBPA18:1/22:6 in cultured SF following sulphatide-loading

SF from five unaffected individuals (×), two ASA-PD individuals (+), two ASA-MLD compound heterozygotes (⁎), three adult MLD patients (○), five juvenile MLD patients (□) and five late-infantile MLD patients (△) were cultured in BME containing 5% HIFCS, 1% penicillin/streptomycin and bovine brain sulphatide (64 μM). Cells were harvested and lipids extracted using the method of Folch (section 2.2.17.2). Quantification of Sulp24:1 (section 2.2.18.1) and PG/LBPA18:1/22:6 (section 2.2.18.2) was performed by ESI-MS/MS. Each point in the graph represents the average of triplicate samples.

6.3. Discussion

The major aim of the experiments in this chapter was to develop methods that would enable the prediction of clinical severity of MLD. ESI-MS/MS, which is known to have high sensitivity and specificity in the determination of biological compounds, was used to measure sulphatide in urine and cultured SF from MLD patients; other lipids were also measured in view of the previous finding of altered lipid trafficking and composition in LSD cells, particularly GSL and cholesterol (sections 1.4.3.2.2 and 1.4.3.2.3; Pagano *et al.*, 2000).

Historically, the measurement of total urinary sulphatide has been used as an auxiliary parameter to differentiate unaffected and ASA-PD individuals from MLD patients. The amount of sulphatide in urine is usually normalised against urinary creatinine or urinary volume. Initial statistical analyses performed in this study using three methods of normalisation (urinary volume, urinary CR and urinary PC) showed that normalisation against urinary PC resulted in less variation in the control population and greater separation of unaffected controls and MLD patients, supporting the earlier reports by Whitfield *et al.* (2001a) and Fuller *et al.* (2005a).

Statistical analysis was also performed to identify and evaluate those analytes that correlated to disease severity. In this study, patient age at the time of sampling was used as a measure of severity; the same correlation was performed on unaffected control samples to determine whether the effect was due to disease severity or simply to variations in urinary lipids associated with patient age. Thus, markers that showed a significant correlation with age in the MLD patient group but no correlation in the control group were considered as potential markers of disease severity. Despite the significantly different values observed in many urinary lipid species in the unaffected control and MLD patient groups, most of these analytes did not correlate with age at disease onset and were unable to discriminate between the different MLD phenotypes. However, the most interesting finding in this work was the increase in some PG/LBPA species found in the urine of MLD patients: PG/LBPA species such as 18:1/18:0, 18:1/18:1 and 18:1/18:18:2 showed a correlation with age at disease onset and could be utilised to further discriminate between the juvenile and late-infantile forms of MLD; this finding also identified these PG/LBPA species as potential biomarkers for further studies using cultured SF cells to predict phenotype.

The finding of elevated CTH18:0 in the urine of MLD patients was almost certainly the result of the loss of sulphate in the source from dihexosyl sulphatide 24:0, which has the

same molecular mass of 1051, resulting in a *m/z* of 1052 in positive ion mode; the resulting dihexosylceramide then fragments to produce the product ion at *m/z* 264, characteristic of the sphingolipids. Although the measurement of bovine brain sulphatide in positive ion mode (section 6.1.4) produced a relatively small signal at *m/z* 1052, bovine brain sulphatide is known to have no or little dihexosyl sulphatide species (*m/z* 1052, dhSulp24:0). In addition, the relatively low concentration of CTH18:0 in urine means that a small increase resulting from dihexosyl sulphatide 24:0 producing a signal with the ion pair 1052/264 will correlate well to the presence of MLD. Further studies involving product ion analysis will help resolve this issue but were outside the scope of this study.

Metabolic profiling of SF samples also produced some interesting results that can assist in the prediction of clinical severity. The SF used in this study covered a broad genotypic and phenotypic spectrum. Enzyme profiling showed good correlation between the amount of protein and activity in unaffected, ASA-PD and ASA-PD/MLD individuals. However, there was overlap in the range of enzyme activity and protein between the MLD patient groups, thus making interpretation difficult; this overlap was not observed in the late-infantile MLD patients with a severe phenotype.

In these studies, the determination of both residual ASA protein and activity provided an extra diagnostic parameter (specific activity) that could be used to indicate the presence of either: (i) normal amounts of enzyme with reduced/no activity; (ii) reduced enzyme with normal activity; or (iii) reduced enzyme with reduced activity. The calculation of specific activity provided additional insight into the intracellular processing and trafficking of ASA in these patients. Specific activity of ASA in the unaffected group (including normal, ASA-PD and ASA-PD/MLD) was between 5.5 and 12.2 pmol/min/ng. Interestingly, specific activity in ASA-PD and ASA-PD/MLD individuals appeared to be higher than that observed in the unaffected control group (Table 6.8), which contrasts with the apparently similar kinetic properties of recombinant N350S ASA and Wt ASA (discussed in Chapter 3) and may indicate greater stability of ASA-PD in the hydrolytic environment of the lysosome.

Specific activity was in the normal range in all adult MLD patients but no consistent trend was observed in patients with the juvenile form of the disorder. Specific activity in the SF of patient S15 was 1.1 pmol/min/ng ASA, indicating relatively high ASA protein with low activity. Patient S15 is a R244C/R288C compound heterozygote: R244C is associated with the severe form of MLD (Draghia *et al.*, 1997) and R288C is known to produce some

residual activity (19% of normal) using the 4-MUS assay (unpublished data; Harvey, PhD Thesis, Adelaide University, Australia, 1996), which suggests that the R288C mutation is likely to produce enzyme with a low specific activity, thus explaining this patient's result.

Specific activity in all of the late-infantile MLD patients tested was below the control range and enabled clear separation of these patients from the other groups: the value in four out of five patients was below 1.0, and one patient (S22) had a specific activity of 2.5. Patient S22 is a compound heterozygote for the D335V (Hess *et al.*, 1996) and P377L mutations (Zlotogora *et al.*, 1995), both of which are known to lead to the retention of mutant enzyme in the ER and its subsequent inability to act on lysosomal sulphatide, which may explain the higher than expected amount of residual enzyme found in this patient who otherwise has a severe clinical phenotype.

The logic behind the use of sulphatide-loading in SF was to analyse the catalytic capacity of the ASA enzyme *in-vivo* to resolve the anomalies that arose in those patients whose protein or activity was higher than expected after analysis with the immune-based assays. Further, the novel approach of using lipid profiling in cultured SF provided additional diagnostic markers that could be evaluated as predictors of clinical severity.

The amount of accumulated sulphatide in SF showed an inverse relationship to residual enzyme activity. The two exceptions to this were patients S15 and S22: in these cases higher than expected levels of accumulation relative to enzyme activity were confirmed to be due to either altered trafficking of ASA (not reaching the lysosome) or to intra-lysosomal instability of the mutated enzyme, as discussed earlier. However, sulphatide accumulation on its own was a poor indicator of MLD phenotype in cultured SF. The higher than expected level of sulphatide accumulation in the two ASA-PD/MLD heterozygotes should certainly provoke more effort towards the study of this group of individuals, as there is speculation about the potential for neurological involvement for these patients later in life (Propping *et al.*, 1986; Kappler *et al.*, 1991).

Although the values of many lipid analytes differed between the control and MLD patient groups, the only analyte to show potential as a marker of clinical severity was the PG/LBPA species: by plotting the values of the significantly different PG/LBPA species against the sulphatide species a clear separation of late-infantile MLD patients was achieved. This finding allows the unambiguous identification of the most severe group of

MLD patients and will be very important to the clinician in patient management and initiating early treatment.

In summary, prediction of phenotype from cultured SF involves the initial measurement of ASA protein and activity: the absence of both indicates a severe phenotype (late-infantile form), as does the presence of a measurable amount of protein but no activity. Specific activity can be calculated by dividing ASA activity by ASA protein: a specific activity below the normal range is likely to result in a juvenile or late-infantile phenotype (see Figure 6.4 and Table 6.8), although these phenotypes may also display normal specific activity. To further differentiate individuals who have significant ASA protein and activity, which may include both juvenile- and adult-onset phenotypes, the sulphatide-loading experiment is required: severe phenotypes can be identified by a high amount of accumulated sulphatide as well as a significant increase in PG/LBPA (see Figure 6.7). The remaining patients can be stratified according to enzyme activity to identify likely juvenile patients who have lower ASA activity (Figure 6.6).

In conclusion, the most useful approach to the prediction of clinical severity for MLD is a combination of genotype, residual ASA protein and activity, and sulphatide-loading, as no single method is an accurate indicator of severity on its own. This study provides evidence for the suitability of the methods that were utilised and an approach for a more comprehensive study to be performed in a larger cohort of samples. Ideally, urine, SF and blood spots should be obtained from each patient, together with full clinical details, to enable the accurate prediction of clinical phenotype.

CHAPTER SEVEN

Concluding Remarks

7.1. Outcomes of the Study

As therapeutic options are further developed for LSD, it will become increasingly important to identify asymptomatic patients early in the disease process to ensure optimal therapeutic efficacy. In anticipation of these developments, this study was undertaken to improve the diagnosis and prognosis for MLD.

In this study, recombinant Wt ASA and N350S ASA were expressed, purified and biochemically characterised. N350S ASA was used to produce a sheep polyclonal antibody, which was subsequently used to develop both the immune-capture activity and the immune-quantification protein assays; together, these assays enable the diagnosis of MLD patients from dried blood spots. A sulphatide-loading protocol for SF was established and used to study the accumulation of sulphatide and secondarily stored lipids in SF from controls, ASA-PD individuals and MLD patients. This protocol, in combination with the measurement of ASA activity and protein, has been demonstrated to be useful for the prediction of disease severity in MLD.

7.2. Concluding Remarks

The study of LSD has gained prominence over the last few years. Collectively, LSD have a reported incidence of 1:7 700 births in Australia (Meikle *et al.*, 1999); two-thirds of LSD patients will develop progressive pathological CNS disease. To maximise the efficacy of therapies, it is therefore important that patients are detected early, preferably before the appearance of clinical signs and symptoms. The only practical way to achieve early detection is through a NBS programme. MLD, with a reported incidence 1:92 000 live births in Australia (Meikle *et al.*, 1999), is one of the more common LSD and results in severe neurological pathology in all patients. The appearance of clinical symptoms can occur from the first year to the seventh decade of life (von Figura *et al.*, 2001). Given the wide range in the age of onset, early detection, combined with accurate identification of phenotype and the initiation of BMT before the onset of pathology, is likely to provide the best outcome for patients.

At present, MLD is biochemically diagnosed by analysis of ASA activity in peripheral blood leucocytes and cultured SF. The conventional enzymatic assay, which has been in

use now for more than 40 years, utilises artificial substrate to measure ASA activity (Baum *et al.*, 1959); whilst assay specificity has improved over the years, the assay's inability to differentiate between ASA-PD and MLD remains unresolved. To overcome this problem, the approach taken by most laboratories is to use auxiliary tests such as sulphatide-loading, electrophoresis and PCR, but this only results in a diagnostic process that is more complicated and time-consuming (Gieselmann, 1991).

To simplify the diagnosis of MLD, this study developed two immune-based assays that are highly specific and eliminate the problems caused by the presence of other sulphatases that catabolise 4-MUS in the free assay; with the measurement of ASA activity and protein in dried blood spots, these assays can also discriminate between unaffected controls, ASA-PD and MLD patients. The immune-quantification of ASA protein can be combined with similar assays developed for the detection of other LSD such as α-glucosidase for Pompe disease (Umapathysivam *et al.*, 2000), N-acetylgalactosamine-4-sulphatase for MPS VI (Hein *et. al.*, 2005) and β-glucosidase for Gaucher disease (Fuller *et al.*, 2005b), into a single assay using currently available multiplex technology.

At the time of writing, a multiplexed immuno-quantification assay consisting of an 11-plex assay, including ASA, has been established using the antibodies produced in this study. This has placed us one step closer to the implementation of NBS for LSD. Meikle *et al.* (2005) reported that more than 95% of patients were identified from the control populations based on individual markers or combinations of markers using dried blood spots. This finding concurs with the results obtained in this study, whereby all MLD patients were positively identified using the dried blood spot immune-quantification protein assay. Importantly, in this study, the stability of ASA activity in dried blood spots was shown to reduce with storage at RT but the amount of ASA protein remained constant. These findings support the need for caution if measurement of ASA activity is used as the sole means of identifying MLD patients and ASA-PD individuals.

In view of the latest developments in the field of diagnosis and therapy for LSD, it will be imperative to accurately predict clinical severity in asymptomatic patients using biochemical means. The results presented in Chapter 6 suggest that multiple parameters are required for the accurate prediction of clinical severity, since parameters such as ASA activity, protein and ASA specific activity showed only limited discriminatory capacity if measured individually (sections 6.2.1.1, 6.2.1.2 and 6.2.1.3). This finding concurs with

earlier reports for other LSD such as MPS I (Fuller *et al.*, 2005c), suggesting that correlation of enzyme activity to phenotype alone is insufficient to enable accurate prediction of severity.

The accumulation of substrates leading to an increase in the number and size of lysosomes is a common feature of all LSD (Hopwood and Brooks, 1997). Consequently, measurement of the accumulating primary metabolites and secondarily-stored lipids and proteins, combined with the measurement of residual enzyme activity and protein, has provided a powerful approach to the prediction of clinical severity for several LSD. Whitfield *et al.* (2002) reported a relationship between phenotype and several lipid and protein markers that was successfully used to differentiate Gaucher disease phenotypes.

In this study, metabolite profiling, which analyses both primary substrates and secondarily stored metabolites by ESI-MS/MS, was used in combination with the ASA protein/activity assays to predict clinical severity. This demonstrated that, although total sulphatide is a useful marker by which to differentiate unaffected controls from MLD patients, it failed to discriminate between the different MLD phenotypes. However, when this substrate was plotted against another lipid biomarker (PG/LBPA), which was also significantly increased in both urine and cultured SF loaded with sulphatide, improved discrimination was possible between juvenile and late-infantile MLD in urine, and late-infantile MLD was clearly separated from the other forms of MLD in the sulphatide-loaded SF. This finding demonstrates that secondary lipid accumulation might have a role to play in the definition of clinical severity in MLD.

In asymptomatic patients, a strategy will be required to biochemically monitor the benefit or otherwise of therapy. In MLD, the most effective therapy currently available is BMT (section 1.4.9), however a recent trial of high-dose ERT in mice has shown delivery of ASA enzyme to the brain and signs of improved pathology (Matzner *et al.*, 2005); initial results from a bone marrow stem cell gene therapy trial in mice have also been promising (Matzner *et al.*, 2001). The common aim of these therapies is to deliver ASA to the most critically affected tissue, i.e. cells within the CNS. Irrespective of the therapeutic strategy used, methods to monitor efficacy will be required. Methods that monitor the development of clinical symptoms or techniques that provide images of the extent of demyelination in the CNS are currently available but have limitations. The measurement of enzyme activity in circulation can be monitored using the sensitive and specific immune-assays described here, but the amount of enzyme in circulation will not necessarily reflect the amount of

enzyme in the CNS due to the presence of the protective BBB. Similarly, the measurement of urinary sulphatide represents the sulphatide that originates from renal cells (von Figura *et al.*, 2001) rather than sulphatide from the brain. Measurement of residual enzyme and sulphatide in cerebrospinal fluid would be useful, but, because of the invasive nature of the sampling, it is unlikely to be adopted as a long term monitoring strategy. Nevertheless, future studies in animal models such as mice may enable correlations to be drawn between enzyme in circulation or urinary sulphatide and CNS pathology that are useful for future therapeutic monitoring strategies.

Alternatively, measurement of secondarily accumulated metabolites such as PG/LBPA might be useful if the accumulation of this lipid is linked to disease pathology. It has been suggested that the heterogeneity seen in LSD is due to the effect of cellular accumulation of secondary substrates in the cells (Raas-Rothschild *et al.*, 2004). Thus, the finding of increased PG/LBPA should be further investigated. Furthermore, smaller sulphated glycolipids such as GC have been found in increased amounts in the kidneys of double knock-out mice that are unable to produce ASA and galactosyl ceramide (Lullmann-Rauch *et al.*, 2001), suggesting that smaller sulphated oligosaccharides that are able to traverse the BBB should also be evaluated as potential biochemical markers for predicting severity or monitoring therapy.

7.3. Future Work and Direction

This thesis presents a model for improved diagnosis and prognosis for MLD in particular and LSD in general. With the development of highly sensitive and specific immune-based assays for measuring ASA activity and protein, further studies can now focus on the implementation of a NBS programme for LSD. Furthermore, the sulphatide-loading protocol developed in this study for the prediction of clinical severity may be adapted to other LSD where storage in SF is minimal, such as Krabbe disease or some of the MPSs. Appropriate substrates can be used to load the cultured SF for a specific period before the measurement of primary and secondary metabolites.

The finding of significant increases in some PG/LBPA species in urine and sulphatide-loaded SF raises the possibility of a connection between secondary accumulation and disease pathogenesis, hence providing a further avenue of investigation into the molecular mechanisms of pathogenesis. LBPA was also found to be increased in Niemann-Pick disease some 20-years ago (Huterer *et al.*, 1983) and so may represent a general marker for lysosomal dysfunction. In addition, ASA is known to cleave a variety of sulphated

substrates other than sulphatide (von Figura *et al.*, 2001), so it may therefore be possible to identify additional markers, such as sulphated carbohydrates or lipids for example, for use as predictors of clinical severity.

Small patient sample numbers are a continual limitation when dealing with rare disorders and this makes validation of new assays difficult and time-consuming. This may be overcome to some extent by the establishment of national testing centres and by collaboration between centres to share samples and data. Ideally, such centres would link to provide a global bank/registry of patient samples and data. A positive development towards this end was observed in a recent multi-centre study on the prevalence of certain MLD mutations in Europe (Lugowska *et al.*, 2005). Similarly, collection of samples, particularly those required for ongoing therapeutic monitoring, could be better coordinated and, with patient consent, the samples could be made available to researchers for further validation of diagnostic, prognostic and monitoring strategies. Such developments and cooperation between laboratories and countries will be essential for the continued development and validation of diagnostics prognostics and monitoring for MLD and other LSD.

References

Ahn VE, Faull KF, Whitelegge JP, Fluharty AL, Prive GG. (2003) Crystal structure of saposin B reveals a dimeric shell for lipid binding. Proc Natl Acad Sci USA. **100**(1):38-43.

Arbour LT, Silver K, Hechtman P, Treacy EP, Coulter-Mackie MB. (2000) Variable onset of metachromatic leukodystrophy in a Vietnamese family. Pediatr Neurol. **23**(2):173-6.

Ashton LJ, Brooks DA, McCourt PA, Muller VJ, Clements PR, Hopwood JJ. (1992) Immunoquantification and enzyme kinetics of alpha-L-iduronidase in cultured fibroblasts from normal controls and mucopolysaccharidosis type I patients. Am J Hum Genet. **50**(4):787-94.

Austin J. (1973) Metachromatic leukodystrophy (sulfatide lipidosis), in Hers HG, van Hoof F. (eds): Lysosomes and Lysosomal Storage Diseases. Academic Press, New York, pp 411.

Bach G, Dagan A, Herz B, Gatt S. (1987) Diagnosis of arylsulfatase A deficiency in intact cultured cells using a fluorescent derivative of cerebroside sulfate. Clin Genet. **31**(4):211-7.

Baldinger S, Pierpont ME, Wenger DA. (1987) Pseudodeficiency of arylsulfatase A: a counseling dilemma. Clin Genet. **31**(2):70-6.

Baquis GD, Kelly JJ Jr, Lieberman A, Wolpert SM. (1991) Adult metachromatic leukodystrophy and pes cavus foot deformity. Muscle Nerve. **14**(8):784-5.

Barriocanal JG, Bonifacino JS, Yuan L, Sandoval IV. (1986) Biosynthesis, glycosylation, movement through the Golgi system, and transport to lysosomes by an N-linked carbohydrate-independent mechanism of three lysosomal integral membrane proteins. J Biol Chem. **261**(35):16755-63.

Barth ML, Fensom A, Harris A. (1993) Prevalence of common mutations in the arylsulphatase A gene in metachromatic leukodystrophy patients diagnosed in Britain. Hum Genet. **91**(1):73-7.

Barth ML, Ward C, Harris A, Saad A, Fensom A. (1994) Frequency of arylsulphatase A pseudodeficiency associated mutations in a healthy population. J Med Genet. **31**(9):667-71.

Baum H, Dodgson KS, Spencer B. (1959) The assay of arylsulphatase A and B in human urine. Clin Chim Acta. **4**:453-5.

Baumann N, Turpin JC, Lefevre M, Colsch B. (2002) Motor and psycho-cognitive clinical types in adult metachromatic leukodystrophy: genotype/phenotype relationships? J Physiol Paris. **96**(3-4):301-6.

Bayever E, Ladisch S, Philippart M, Brill N, Nuwer M, Sparkes RS, Feig SA. (1985) Bone-marrow transplantation for metachromatic leucodystrophy. Lancet. **2**(8453):471-3.

Berg T, King B, Meikle PJ, Nilssen O, Tollersrud OK, Hopwood JJ. (2001) Purification and characterization of recombinant human lysosomal alpha-mannosidase. Mol Genet Metab. **73**(1):18-29.

Berger J, Loschl B, Bernheimer H, Lugowska A, Tylki-Szymanska A, Gieselmann V, Molzer B. (1997) Occurrence, distribution, and phenotype of arylsulfatase A mutations in patients with metachromatic leukodystrophy. Am J Med Genet. **69**(3):335-40.

Beron W, Alvarez-Dominguez C, Mayorga L, Stahl PD. (1995) Membrane trafficking along the phagocytic pathway. Trends Cell Biol. **5**(3):100-4.

Beutler E, Grabowski GA. (1995) Glucosylceramide lipidoses: Gaucher disease, in Scriver CR, Beaudet AL, Sly WS, Valle D. (eds): The Metabolic Basis of Inherited Disease. 7th ed. McGraw-Hill. New York, pp 2641-70.

Bielicki J, Hopwood JJ, Melville EL, Anson DS. (1998) Recombinant human sulphamidase: expression, amplification, purification and characterization. Biochem J. **329**(Pt 1):145-50.

Bligh EG, Dyer WJ. (1959) A rapid method of total lipid extraction and purification. Can J Biochem Physiol. **37**(8):911-7.

Bond CS, Clements PR, Ashby SJ, Collyer CA, Harrop SJ, Hopwood JJ, Guss JM. (1997) Structure of a human lysosomal sulfatase. Structure. **5**(2):277-89.

Bosio A, Binczek E, Stoffel W. (1996) Functional breakdown of the lipid bilayer of the myelin membrane in central and peripheral nervous system by disrupted galactocerebroside synthesis. Proc Natl Acad Sci USA. **93**(23):13280-5.

Bunge S, Clements PR, Byers S, Kleijer WJ, Brooks DA, Hopwood JJ. (1998) Genotype-phenotype correlations in mucopolysaccharidosis type I using enzyme kinetics, immunoquantification and in vitro turnover studies. Biochim Biophys Acta. **1407**(3):249-56.

Burgess JH, Kalfayan B, Slungaard RK, Gilbert E. (1985) Papillomatosis of the gallbladder associated with metachromatic leukodystrophy. Arch Pathol Lab Med. **109**(1):79-81.

Chang MH, Bindloss CA, Grabowski GA, Qi X, Winchester B, Hopwood JJ, Meikle PJ (2000). Saposins A, B, C, and D in plasma of patients with lysosomal storage disorders. Clin Chem. **46**(2):167-74.

Chang PL, Davidson RG. (1983) Pseudo arylsulfatase-A deficiency in healthy individuals: genetic and biochemical relationship to metachromatic leukodystrophy. Proc Natl Acad Sci USA. **80**(23):7323-7.

Chang PL, Rosa NE, Varey PA, Kihara H, Kolodny EH, Davidson RG. (1984) Diagnosis of pseudo-arylsulfatase A deficiency with electrophoresis techniques. Pediatr Res. **18**:1042-5.

Chataway TK, Barritt GJ. (1994) Studies on the iodination of a ras protein and the detection of ras polymers. Mol Cell Biochem. **137**(1):75-83.

Chen CS, Patterson MC, Wheatley CL, O'Brien JF, Pagano RE. (1999) Broad screening test for sphingolipid-storage diseases. Lancet. **354**(9182):901-5.

Christomanou H, Aignesberger A, Linke P. (1986) Immunochemical characterization of two activator proteins stimulating enzymic sphingomyelin degradation in vitro. Absence of one of them in a human Gaucher disease variant. Biol Chem Hoppe Seyler. **367**(9):879-90.

Christomanou H, Sandhoff K. (1977) A sensitive fluorescence assay for the simultaneous and separate determination of arylsulphatases A and B. Clin Chim Acta. **79**(3):527-31.

Chruszcz M, Laidler P, Monkiewicz M, Ortlund E, Lebioda L, Lewinski K. (2003) Crystal structure of a covalent intermediate of endogenous human arylsulfatase A. J Inorg Biochem. **96**(2-3):386-92.

Clarke JT, Skomorowski MA, Chang PL. (1989) Marked clinical difference between two sibs affected with juvenile metachromatic leukodystrophy. Am J Med Genet. **33**(1):10-3.

Clarke LA. (1997) Clinical diagnosis of lysosomal storage disease, in Applegarth DA, Dimmick JE and Hall JG. (eds): Organelle Diseases. Chapman and Hall, London, pp 37-71.

Clements PR, Brooks DA, Saccone GT, Hopwood JJ. (1985) Human alpha-L-iduronidase. 1. Purification, monoclonal antibody production, native and subunit molecular mass. Eur J Biochem. **152**(1):21-8.

Conzelmann E, Sandhoff K. (1979) Purification and characterization of an activator protein for the degradation of glycolipids GM2 and GA2 by hexosaminidase A. Hoppe Seylers Z Physiol Chem. **360**(12):1837-49.

Cooper MJ, Anders MW. (1975) High pressure liquid chromatography of fatty acids and lipids. J Chromatogr Sci. **13**(9):407-11.

Cosma MP, Pepe S, Annunziata I, Newbold RF, Grompe M, Parenti G, Ballabio A. (2003) The multiple sulfatase deficiency gene encodes an essential and limiting factor for the activity of sulfatases. Cell. **113**(4):445-56.

Dawson G, Matalon R, Dorfman A. (1972) Glycosphingolipids in cultured human skin fibroblasts. II. Characterization and metabolism in fibroblasts from patients with inborn errors of glycosphingolipid and mucopolysaccharide metabolism. J Biol Chem **247**(18): 5951-58.

De Duve C, Pressman BC, Gianetto R, Wattiaux R, Applemans F. (1955) Tissue fractionation studies. 6. Intracellular distribution patterns of enzymes in rat-liver tissue. Biochem J. **60**(4):604-17.

Desnick RJ, Wasserstein MP, Banikazemi M. (2001) Fabry disease (alpha-galactosidase A deficiency): renal involvement and enzyme replacement therapy. Contrib Nephrol. (136):174-92.

Diamandis EP, Bhayana V, Conway K, Reichstein E, Papanastasiou-Diamandis A. (1988) Time-resolved fluoroimmunoassay of cortisol in serum with a europium chelate as label. Clin Biochem. **21**(5):291-6.

Dierks T, Schmidt B, Borissenko LV, Peng J, Preusser A, Mariappan M, von Figura K. (2003) Multiple sulfatase deficiency is caused by mutations in the gene encoding the human C(alpha)-formylglycine generating enzyme. Cell. **113**(4):435-44.

Dole M, Mack LL, Hines RL, Mobley RC, Ferguson LD, Alice MB. (1968) Molecular beams of macroions. J Chem Phys. **49**:2240-49.

Draghia R, Letourneur F, Drugan C, Manicom J, Blanchot C, Kahn A, Poenaru L, Caillaud C. (1997) Metachromatic leukodystrophy: identification of the first deletion in exon 1 and of nine novel point mutations in the arylsulfatase A gene. Hum Mutat. **9**(3):234-42.

Dubois G, Turpin JC, Baumann N. (1975) Arylsulfatases isoenzymes in metachromatic leucodystrophy/detection of a new variant by electrophoresis improvement of quantitative assay. Biomedicine. **23**(3):116-9.

Duncan JR, Kornfeld S. (1988) Intracellular movement of two mannose 6-phosphate receptors: return to the Golgi apparatus. J Cell Biol. **106**(3):617-28.

Duyff RF, Weinstein HC. (1996) Late-presenting metachromatic leukodystrophy. Lancet. **348**(9038):1382-3.

Eng B, Nakamura LN, O'Reilly N, Schokman N, Nowaczyk MM, Krivit W, Waye JS. (2003) Identification of nine novel arylsulfatase A (ARSA) gene mutations in patients with metachromatic leukodystrophy (MLD). Hum Mutat. **22**(5):418-9.

Farrell PM, Aronson RA, Hoffman G, Laessig RH. (1994) Newborn screening for cystic fibrosis in Wisconsin: first application of population-based molecular genetics testing. Wis Med J. **93**(8):415-21.

Finean JB, Gunn TK, Hutchinson A, Mills D. (1984) An X-ray diffraction and electron microscopy study of the extraction of erythrocyte membranes with the bile salt, cholate. Biochim Biophys Acta. **777**(1):140-6.

Fischer G, Jatzkewitz H. (1977) The activator of cerebroside sulphatase. Binding studies with enzyme and substrate demonstrating the detergent function of the activator protein. Biochim Biophys Acta. **481**(2):561-72.

Fluharty AL, Meek WE, Kihara H. (1983) Pseudo arylsulfatase A deficiency: evidence for a structurally altered enzyme. Biochem Biophys Res Commun. **112**(1):191-7.

Fluharty AL, Stevens RL, Kihara H. (1978) Cerebroside sulfate hydrolysis by fibroblasts from a parent with metachromatic leukodystrophy. J Pediatr. **92**(5):782-4.

Folch J, Lees M, Sloane Stanley GH. (1957) A simple method for the isolation and purification of total lipids from animal tissues. J Biol Chem. **226**(1):497-509.

Franco B, Meroni G, Parenti G, Levilliers J, Bernard L, Gebbia M, Cox L, Maroteaux P, Sheffield L, Rappold GA, et al. (1995) A cluster of sulfatase genes on Xp22.3: mutations in chondrodysplasia punctata (CDPX) and implications for warfarin embryopathy. Cell. **81**(1):15-25.

Fuller M, Brooks DA, Evangelista M, Hein LK, Hopwood JJ, Meikle PJ. (2005c) Prediction of neuropathology in mucopolysaccharidosis I patients. Mol Genet Metab. **84**(1):18-24.

Fuller M, Lovejoy M, Hopwood JJ, Meikle PJ. (2005b) Immunoquantification of beta-glucosidase: diagnosis and prediction of severity in Gaucher disease. Clin Chem. **51**(11):2200-2.

Fuller M, Sharp PC, Rozaklis T, Whitfield PD, Blacklock D, Hopwood JJ, Meikle PJ. (2005a) Urinary lipid profiling for the identification of Fabry hemizygotes and heterozygotes. Clin Chem. **51**(4):688-94.

Fuller M, van der Ploeg A, Reuser AJ, Anson DS, Hopwood JJ. (1995) Isolation and characterisation of a recombinant, precursor form of lysosomal acid alpha-glucosidase. Eur J Biochem. **234**(3):903-9.

Gelb BD, Moissoglu K, Zhang J, Martignetti JA, Bromme D, Desnick RJ. (1996) Cathepsin K: isolation and characterization of the murine cDNA and genomic sequence, the homologue of the human pycnodysostosis gene. Biochem Mol Med. **59**(2):200-6.

Gieselmann V. (1991) An assay for the rapid detection of the arylsulfatase A pseudodeficiency allele facilitates diagnosis and genetic counseling for metachromatic leukodystrophy. Hum Genet. **86**(3):251-5.

Gieselmann V, Fluharty AL, Tonnesen T, von Figura K. (1991) Mutations in the arylsulfatase A pseudodeficiency allele causing metachromatic leukodystrophy. Am J Hum Genet. **49**(2):407-13

Gieselmann V, Matzner U, Hess B, Lullmann-Rauch R, Coenen R, Hartmann D, D'Hooge R, DeDeyn P, Nagels G. (1998) Metachromatic leukodystrophy: molecular genetics and an animal model. J Inherit Metab Dis. **21**(5):564-74.

Gieselmann V, Polten A, Kreysing J, von Figura K. (1989) Arylsulfatase A pseudodeficiency: loss of a polyadenylylation signal and N-glycosylation site. Proc Natl Acad Sci USA. **86**(23):9436-40.

Ginsberg L, Gershfeld NL. (1991) Membrane bilayer instability and the pathogenesis of disorders of myelin. Neurosci Lett. **130**(1):133-6.

Gniot J, Dzialoszynski LM. (1964) Arylsulfatases of human placenta. Clin Chim Acta. **9**:334-8.

Granger BL, Green SA, Gabel CA, Howe CL, Mellman I, Helenius A. (1990) Characterization and cloning of lgp110, a lysosomal membrane glycoprotein from mouse and rat cells. J Biol Chem. **265**(20):12036-43.

Grivell LA. (1988) Protein import into mitochondria. Int Rev Cytol. **111**:107-41.

Gu M, Kerwin JL, Watts JD, Aebersold R. (1997) Ceramide profiling of complex lipid mixtures by electrospray ionization mass spectrometry. Anal Biochem. **244**(2):347-56.

Guarnieri FG, Arterburn LM, Penno MB, Cha Y, August JT (1993). The motif Tyr-X-X-hydrophobic residue mediates lysosomal membrane targeting of lysosome-associated membrane protein 1. J Biol Chem. **268** (3):1941-6.

Gustavson KH, Hagberg B. (1971) The incidence and genetics of metachromatic leukodystrophy in northern Sweden. Acta Ped Scand. **60**:585-90.

Hagberg B. (1963) Clinical symptoms, signs and tests in metachromatic leukodystrophy, in Folch-Pi J, Bauer H. (eds): Brain Lipids and Lipoproteins and the Leukodystrophies. Elsevier, Amsterdam, pp 134.

Hageman AT, Gabreels FJ, de Jong JG, Gabreels-Festen AA, van den Berg CJ, van Oost BA, Wevers RA. (1995) Clinical symptoms of adult metachromatic leukodystrophy and arylsulfatase A pseudodeficiency. Arch Neurol. **52**(4):408-13.

Hammond C, Braakman I, Helenius A. (1994) Role of N-linked oligosaccharide recognition, glucose trimming, and calnexin in glycoprotein folding and quality control. Proc Natl Acad Sci USA. **91**(3):913-7.

Han X. (2002) Characterization and direct quantitation of ceramide molecular species from lipid extracts of biological samples by electrospray ionization tandem mass spectrometry. Anal Biochem. **302**(2):199-212.

Han X, Gross RW. (2003) Global analyses of cellular lipidomes directly from crude extracts of biological samples by ESI mass spectrometry: a bridge to lipidomics. J Lipid Res. **44**(6):1071-9.

Han X, Gross RW. (2005) Shotgun lipidomics: electrospray ionization mass spectrometric analysis and quantitation of cellular lipidomes directly from crude extracts of biological samples. Mass Spectrom Rev. **24**(3):367-412.

Harlow E, Lane D. (1988) Antibodies: A laboratory manual. Laboratory Press, Cold Spring Harbor, New York.

Harvey JS. (1996) Metachromatic leukodystrophy: the role of non-pathogenic sequence variants in the causation of disease. PhD Thesis, Adelaide University, Adelaide, Australia.

Harvey JS, Carey WF, Morris CP. (1998) Importance of the glycosylation and polyadenylation variants in metachromatic leukodystrophy pseudodeficiency phenotypes. Hum Mol Genet. **7**:1215-9.

Harvey JS, Nelson PV, Carey WF, Robertson EF, Morris CP. (1993) An arylsulfatase A (ARSA) missense mutation (T274M) causing late-infantile metachromatic leukodystrophy. Hum Mutat. **2**(4):261-7.

Hauser G. (1964) Labeling of cerebrosides and sulfatides in rat brain. Biochim Biophys Acta. **84**:212-5.

Heier L, Daneman A, Lowden JA, Cutz E, Craw S, Martin DJ. (1983) Biliary disease in metachromatic leukodystrophy. Pediatr Radiol. **13**(6):313-8.

Heim P, Claussen M, Hoffmann B, Conzelmann E, Gartner J, Harzer K, Hunneman DH, Kohler W, Kurlemann G, Kohlschutter A. (1997) Leukodystrophy incidence in Germany. Am J Med Genet. **71**(4):475-8.

Hein LK, Meikle PJ, Dean CJ, Bockmann MR, Auclair D, Hopwood JJ, Brooks DA. (2005) Development of an assay for the detection of mucopolysaccharidosis type VI patients using dried blood-spots. Clin Chim Acta. **353**(1-2):67-74.

Heinisch U, Zlotogora J, Kafert S, Gieselmann V. (1995) Multiple mutations are responsible for the high frequency of metachromatic leukodystrophy in a small geographic area. Am J Hum Genet. **56**:51.

Hemmila I, Dakubu S, Mukkala VM, Siitari H, Lovgren T. (1984) Europium as a label in time-resolved immunofluorometric assays. Anal Biochem. **137**(2):335-43.

Hers, HG. (1963) Alpha-glucosidase deficiency in generalised glycogen-storage disease. Biochem. J. **86**:11.

Herz B, Bach G. (1984) Arylsulfatase A in pseudodeficiency. Hum Genet. **66**:147-50.

Hess B, Kafert S, Heinisch U, Wenger DA, Zlotogora J, Gieselmann V. (1996) Characterization of two arylsulfatase A missense mutations D335V and T274M causing late infantile metachromatic leukodystrophy. Hum Mutat. **7**(4):311-7.

Hohenschutz C, Friedl W, Schlor KH, Waheed A, Conzelmann E, Sandhoff K, Propping P. (1988) Probable metachromatic leukodystrophy/pseudodeficiency compound heterozygote at the arylsulfatase A locus with neurological and psychiatric symptomatology. Am J Med Genet. **31**(1):169-75.

Honing S, Sandoval IV, von Figura K. (1998) A di-leucine-based motif in the cytoplasmic tail of LIMP-II and tyrosinase mediates selective binding of AP-3. Embo J. **17** (5):1304-14.

Hopwood JJ and Ballabio A. (2001) Multiple sulfatase deficiency and the nature of the sulfatase family, in Scriver CR, Beaudet AL, Sly WS, Valle D (eds): The Metabolic and Molecular Bases of Inherited Disease. 8th Ed. McGraw-Hill, New York, pp 3725-32.

Hopwood JJ, Brooks DA. (1997) An introduction to the basic science and biology of the lysosome and storage diseases, in: Applegarth DA, Dimmick JE, Hall JG. (eds) Organelle Diseases. Chapman & Hall. New York, pp 7-35.

Hsu FF, Bohrer A, Turk J. (1998) Electrospray ionization tandem mass spectrometric analysis of sulfatide. Determination of fragmentation patterns and characterization of molecular species expressed in brain and in pancreatic islets. Biochim Biophys Acta. **1392**(2-3):202-16.

Hua CT, Hopwood JJ, Carlsson SR, Harris RJ, Meikle PJ. (1998) Evaluation of the lysosome-associated membrane protein LAMP-2 as a marker for lysosomal storage disorders. Clin Chem. **44**(10):2094-102.

Hunziker W, Geuze HJ (1996). Intracellular trafficking of lysosomal membrane proteins. Bioessays. **18**(5):379-89.

Huterer S, Wherrett JR, Poulos A, Callahan JW. (1983) Deficiency of phospholipase C acting on phosphatidylglycerol in Niemann-Pick disease. Neurology. **33**(1):67-73.

Inui K, Furukawa M, Okada S, Yabuuchi H. (1988) Metabolism of cerebroside sulfate and subcellular distribution of its metabolites in cultured skin fibroblasts from controls, metachromatic leukodystrophy, and globoid cell leukodystrophy. J Clin Invest. **81**(2):310-7.

Isshiki M, Anderson RG. (1999) Calcium signal transduction from caveolae. Cell Calcium. **26**(5):201-8.

James GT, Austin JH. (1979) Studies in metachromatic leukodystrophy. XIV. Purification and subunit structure of human liver arylsulfatase A. Clin Chim Acta. **98**(1-2):103-11.

Kapaun P, Dittmann RW, Granitzny B, Eickhoff W, Wulbrand H, Neumaier-Probst E, Zander A, Kohlschuetter A. (1999) Slow progression of juvenile metachromatic leukodystrophy 6 years after bone marrow transplantation. J Child Neurol. **14**(4):222-8.

Kappler J, Leinekugel P, Conzelmann E, Kleijer WJ, Kohlschutter A, Tonnesen T, Rochel M, Freycon F, Propping P. (1991) Genotype-phenotype relationship in various degrees of arylsulfatase A deficiency. Hum Genet. **86**(5):463-70.

Kappler J, Sommerlade HJ, von Figura K, Gieselmann V. (1994) Complex arylsulfatase A alleles causing metachromatic leukodystrophy. Hum Mutat. **4**(2):119-27.

Kerwin JL, Tuininga AR, Ericsson LH. (1994) Identification of molecular species of glycerophospholipids and sphingomyelin using electrospray mass spectrometry. J Lipid Res. **35**(6):1102-14.

Kidd D, Nelson J, Jones F, Dusoir H, Wallace I, McKinstry S, Patterson V. (1998) Long-term stabilization after bone marrow transplantation in juvenile metachromatic leukodystrophy. Arch Neurol. **55**(1):98-9.

Kihara H, Ho CK, Fluharty AL, Tsay KK, Hartlage DL. (1980) Prenatal diagnosis of metachromatic leukodystrophy in a family with pseudo-arylsulfatase A deficiency by cerebroside sulfate loading test. Pediatr Res. **14**:224-27.

Kihara H, Meek WE, Fluharty AL. (1986) Attenuated activities and structural alterations of arylsulfatase A in tissues from subjects with pseudo arylsulfatase A deficiency. Hum Genet. **74**(1):59-62.

Kishimoto Y, Hiraiwa M, O'Brien JS. (1992) Saposins: structure, function, distribution, and molecular genetics. J Lipid Res. **33**(9):1255-67.

Knowles SE, Ballard FJ. (1976) Selective control of the degradation of normal and aberrant proteins in Reuber H35 hepatoma cells. Biochem J. **156**(3):609-17.

Kolodny EH, Fluharty AL. (1995) Metachromatic leukodystrophy and multiple sulfatase deficiency: sulfatide lipidosis, in Scriver CR, Beaudet AL, Sly WS, Valle D (eds): The Metabolic and Molecular Bases of Inherited Disease. 7th Ed. McGraw-Hill, New York, pp 2693-2739.

Kolodny EH, Mumford RA. (1976) Arylsulfatases A and B in metachromatic leukodystrophy and Maroteaux-Lamy syndrome: studies with 4-methylumelliferyl sulfate. Adv Exp Med Biol. **68**:239-51.

Kornfeld S. (1986) Trafficking of lysosomal enzymes in normal and disease states. J Clin Invest. **77**(1):1-6.

Kretz KA, Carson GS, Morimoto S, Kishimoto Y, Fluharty AL, O'Brien JS. (1990) Characterization of a mutation in a family with saposin B deficiency: a glycosylation site defect. Proc Natl Acad Sci USA. **87**(7):2541-4.

Kreysing J, Bohne W, Bosenberg C, Marchesini S, Turpin JC, Baumann N, von Figura K, Gieselmann V. (1993) High residual arylsulfatase A (ARSA) activity in a patient with late-infantile metachromatic leukodystrophy. Am J Hum Genet. **53**(2):339-46.

Kreysing J, von Figura K, Gieselmann V. (1990) Structure of the arylsulfatase A gene. Eur J Biochem. **191**(3):627-31.

Kreysing J, Polten A, Hess B, von Figura K, Menz K, Steiner F, Gieselmann V. (1994) Structure of the mouse arylsulfatase A gene and cDNA. Genomics. **19**(2):249-56.

Krivit W, Aubourg P, Shapiro E, Peters C. (1999) Bone marrow transplant for globoid cell leukodystrophy, adrenoleukodystrophy, metachromatic leukodystrophy, and Hurler syndrome. Curr Opin Hematol. **6**(6):377-82.

Krivit W, Shapiro E, Kennedy W, Lipton M, Lockman L, Smith S, Summers CG, Wenger DA, Tsai MY, Ramsay NK, *et al.* (1990) Treatment of late infantile metachromatic leukodystrophy by bone marrow transplantation. N Engl J Med. **322**(1):28-32.

Krivit W. (2004) Allogeneic stem cell transplantation for the treatment of lysosomal and peroxisomal metabolic diseases. Springer Semin Immunopathol. **26**(1-2):119-32.

Kudoh T, Sattler M, Malmstrom J, Bitter MA, Wenger DA. (1981) Metabolism of fatty acid-labeled cerebroside sulfate in cultured cells from controls and metachromatic leukodystrophy patients. Use in the prenatal identification of a false positive fetus. J Lab Clin Med. **98**(5):704-14.

Laemmli UK. (1970) Cleavage of structural proteins during the assembly of the head of bacteriophage T4. Nature. **227**(5259):680-5.

Laidler PM. (1991) Arylsulfatase A-physico-chemical properties and the use of enzyme radioimmunoassay in medical diagnosis. Folia Med Cracov. **32**(3-4):149-68.

Laidler PM, Ryder KW, Glick MR, Oei TO, Van Etten RL. (1985a) Radioimmunoassay for arylsulfatase A in urine. Clin Chem. **31**(3):391-6.

Laidler PM, Waheed A, Van Etten RL. (1985b) Structural and immunochemical characterization of human urine arylsulfatase A purified by affinity chromatography. Biochim Biophys Acta. **827**(1):73-83.

Langenbeck U, Dunker P, Heipertz R, Pilz H. (1977) Inheritance of metachromatic leukodystrophy. Am J Hum Genet. **29**:639-40.

Lee-Vaupel M, Conzelmann E. (1987) A simple chromogenic assay for arylsulfatase A. Clin Chim Acta. **164**(2):171-80.

Leinekugel P, Michel S, Conzelmann E, Sandhoff K. (1992) Quantitative correlation between the residual activity of beta-hexosaminidase A and arylsulfatase A and the severity of the resulting lysosomal storage disease. Hum Genet. **88**(5):513-23.

Liebisch G, Drobnik W, Reil M, Trumbach B, Arnecke R, Olgemoller B, Roscher A, Schmitz G. (1999) Quantitative measurement of different ceramide species from crude cellular extracts by electrospray ionization tandem mass spectrometry (ESI-MS/MS). J Lipid Res. **40**(8):1539-46.

Lipsky NG, Pagano RE. (1985) Intracellular translocation of fluorescent sphingolipids in cultured fibroblasts: endogenously synthesized sphingomyelin and glucocerebroside analogues pass through the Golgi apparatus en route to the plasma membrane. J Cell Biol. **100**(1):27-34.

Li ZG, Waye JS, Chang PL. (1992) Diagnosis of arylsulfatase A deficiency. Am J Med Genet. **43**(6):976-82.

Lugowska A, Amaral O, Berger J, Berna L, Bosshard NU, Chabas A, Fensom A, Gieselmann V, Gorovenko NG, Lissens W, Mansson JE, Marcao A, Michelakakis H, Bernheimer H, Ol'khovych NV, Regis S, Sinke R, Tylki-Szymanska A, Czartoryska B. (2005) Mutations c.459+1G>A and p.P426L in the ARSA gene: prevalence in metachromatic leukodystrophy patients from European countries. Mol Genet Metab. **86**(3):353-9.

Lugowska A, Berger J, Tylki-Szymanska A, Czartoryska B, Loschl B, Molzer B. (2002) High prevalence of I179S mutation in patients with late-onset metachromatic leukodystrophy. Clin Genet. **61**(5):389-90.

Lugowska A, Tylki-Szymanska A, Berger J, Molzer B. (1997) Elevated sulfatide excretion in compound heterozygotes of metachromatic leukodystrophy and ASA-pseudodeficiency allele. Clin Biochem. **30**(4):325-31.

Lukatela G, Krauss N, Theis K, Selmer T, Gieselmann V, Figura VK, Saenger W. (1998) Crystal structure of human arylsulfatase A: the aldehyde function and the metal ion at the active site suggest a novel mechanism for the sulfate ester hydrolysis. Biochemistry. **37**:3654-64.

Lullmann-Rauch R, Matzner U, Franken S, Hartmann D, Gieselmann V. (2001) Lysosomal sulfoglycolipid storage in the kidneys of mice deficient for arylsulfatase A (ASA) and of double-knockout mice deficient for ASA and galactosylceramide synthase. Histochem Cell Biol. **116**(2):161-9.

Malone MJ, Stoffyn P, Moser H. (1966) Structural studies on sulphatides in metachromatic leucodystrophy. J Neurochem. **13**(11):1033-6.

Manowitz P, Kling A, Kohn H. (1978) Clinical course of adult metachromatic leukodystrophy presenting as schizophrenia. A report of two living cases in siblings. J Nerv Ment Dis. **166**(7):500-6.

Marcao A, Azevedo JE, Gieselmann V, Sa Miranda MC. (2003) Oligomerization capacity of two arylsulfatase A mutants: C300F and P425T.Biochem Biophys Res Commun. **306**(1):293-7.

Matzner U, Herbst E, Hedayati KK, Lullmann-Rauch R, Wessig C, Schroder S, Eistrup C, Moller C, Fogh J, Gieselmann V. (2005) Enzyme replacement improves nervous system pathology and function in a mouse model for metachromatic leukodystrophy. Hum Mol Genet. **14**(9):1139-52.

Matzner U, Schestag F, Hartmann D, Lullmann-Rauch R, D'Hooge R, De Deyn PP, Gieselmann V. (2001) Bone marrow stem cell gene therapy of arylsulfatase A-deficient mice, using an arylsulfatase A mutant that is hypersecreted from retrovirally transduced donor-type cells. Hum Gene Ther. **12**(9):1021-33.

Matsuzawa Y, Hostetler KY. (1979) Degradation of bis(monoacylglycero)phosphate by an acid phosphodiesterase in rat liver lysosomes. J Biol Chem. **254**(13): 5997-6001.

Mehl E, Jatzkewitz H. (1964) A cerebrosidesulfatase from swine kidney. Hoppe Seylers Z Physiol Chem. **339**(1):260-76.

Meikle PJ, Brooks DA, Ravenscroft EM, Yan M, Williams RE, Jaunzems AE, Chataway TK, Karageorgos LE, Davey RC, Boulter CD, Carlsson SR, Hopwood JJ. (1997) Diagnosis

of lysosomal storage disorders: evaluation of lysosome-associated membrane protein LAMP-1 as a diagnostic marker. Clin Chem. **43**(8 Pt 1):1325-35.

Meikle PJ, Dean CJ, Grasby D Bockmann MR, Whittle AM, Lang DL, Fuller M, Brooks DA, Hopwood JJ. (2005) Newborn screening for lysosomal storage disorders: evaluation of protein profiling. J Inherit Metab. **28**:21–33.

Meikle PJ, Fietz MJ, Hopwood JJ. (2004a) Diagnosis of lysosomal storage disorders: current techniques and future directions. Expert Rev Mol Diag. **4**(5):677-91.

Meikle PJ, Hopwood JJ, Clague AE, Carey WF. (1999) Prevalence of lysosomal storage disorders. JAMA. **281**(3):249-54.

Meikle PJ, Ranieri E, Simonsen H, Rozaklis T, Ramsay SL, Whitfield PD, Fuller M, Christensen E, Skovby F, Hopwood JJ. (2004b) Newborn screening for lysosomal storage disorders: clinical evaluation of a two-tier strategy. Pediatrics. **114**(4):909-16.

Meng CK, Mann M, Fenn JB. (1988) Of protons or proteins. Z Phys D. **10**:361-8.

Menjivar M, Ortiz G, Cardenas M, Garza-Flores J. (1993) Comparison of the DELFIA and RIA methods for measuring luteinizing and follicle stimulating hormones in serum. Rev Invest Clin. **45**(6):579-84.

Molzer B, Sundt-Heller R, Kainz-Korschinsky M, Zobel M. (1992) Elevated sulfatide excretion in heterozygotes of metachromatic leukodystrophy: dependence on reduction of arylsulfatase A activity. Am J Med Genet. **44**(4):523-6.

Monti E, Preti A, Novati A, Aleo MF, Clemente ML, Marchesini S. (1992) Uptake and metabolism of a fluorescent sulfatide analogue in cultured skin fibroblasts. Biochim Biophys Acta. **1124**(1):80-7.

Mortimore GE, Schworer CM. (1977) Induction of autophagy by amino-acid deprivation in perfused rat liver. Nature. **270**(5633):174-6.

Moser HW, Moser AB, McKhann GM. (1967) The dynamics of a lipidosis. Turnover of sulfatide, steroid sulfate, and polysaccharide sulfate in metachromatic leukodystrophy. Arch Neurol. **17**(5):494-511.

Muenzer J, Lamsa JC, Garcia A, Dacosta J, Garcia J, Treco DA. (2002) Enzyme replacement therapy in mucopolysaccharidosis type II (Hunter syndrome): a preliminary report. Acta Paediatr Suppl. **91**(439):98-9.

Munro S. (2003) Lipid rafts: elusive or illusive? Cell. **115**(4):377-88.

Naggar EF, Costello CE, Zaia J. (2004) Competing fragmentation processes in tandem mass spectra of heparin-like glycosaminoglycans. J Am Soc Mass Spectrom. **15**(11):1534-44.

Natowicz MR, Prence EM, Chaturvedi P, Newburg DS. (1996) Urine sulfatides and the diagnosis of metachromatic leukodystrophy. Clin Chem. **42**(2):232-8.

Navarro C, Fernandez JM, Dominguez C, Fachal C, Alvarez M. (1996) Late juvenile metachromatic leukodystrophy treated with bone marrow transplantation; a 4-year follow-up study. Neurology. **46**(1):254-6.

Nelson PV, Carey WF, Morris CP. (1991) Population frequency of the arylsulphatase A pseudo-deficiency allele. Hum Genet. **87**(1):87-8.

Neufeld EF. (1991) Lysosomal storage disease. Annual Review of Biochemistry. **60**:257-80.

Neuwelt E, Stumpf D, Austin J, Kohler P. (1971) A monospecific antibody to human sulfatase A. Preparation, characterization and significance. Biochim Biophys Acta. **236**(1):333-46.

Newborn Screening Policy. (2004) Human Genetics Society of Australasia–Royal Australasian College of Physicians.

Nicholls RG, Roy AB. (1971) The sulphatase of ox liver. XV. Changes in the properties of sulphatase A in the presence of substrate. Biochim Biophys Acta. **242**(1):141-51.

Nishino I, Fu J, Tanji K, Yamada T, Shimojo S, Koori T, Mora M, Riggs JE, Oh SJ, Koga Y, Sue CM, Yamamoto A, Murakami N, Shanske S, Byrne E, Bonilla E, Nonaka I, DiMauro S, Hirano M. (2000) Primary LAMP-2 deficiency causes X-linked vacuolar cardiomyopathy and myopathy (Danon disease). Nature. **406**(6798):906-10.

Niwa T. (1995) Procedures for MS analysis of clinically relevant compounds. Clin Chim Acta. **241-242**:75-152.

Norton WT, Poduslo SE. (1982) Biochemical studies of metachromatic leukodystrophy in three siblings. Acta Neuropathol (Berl). **57**(2-3):188-96.

O'Brien JS, Kishimoto Y. (1991) Saposin proteins: structure, function, and role in human lysosomal storage disorders. FASEB J. **5**(3):301-8.

O'Brien JS, Kretz KA, Dewji N, Wenger DA, Esch F, Fluharty AL. (1988) Coding of two sphingolipid activator proteins (SAP-1 and SAP-2) by same genetic locus. Science. **241**(4869):1098-101.

Ogata S, Fukuda M. (1994) Lysosomal targeting of Limp II membrane glycoprotein requires a novel Leu-Ile motif at a particular position in its cytoplasmic tail. J Biol Chem. **269**(7):5210-7

Oram JF, Yokoyama S. (1996) Apolipoprotein-mediated removal of cellular cholesterol and phospholipids. J Lipid Res. **37**(12):2473-91.

Ozkara HA, Topcu M. (2004) Sphingolipidoses in Turkey. Brain Dev. **26**(6):363-6.

Pagano RE, Puri V, Dominguez M, Marks DL. (2000) Membrane traffic in sphingolipid storage diseases. Traffic. **1**(11):807-15.

Parenti G, Meroni G, Ballabio A. (1997) The sulfatase gene family. Curr Opin Genet Dev. **7**(3):386-91.

Parkinson-Lawrence E, Turner C, Hopwood J, Brooks D. (2005) Analysis of normal and mutant iduronate-2-sulphatase conformation. Biochem J. **386**(Pt 2):395-400.

Parpal S, Gustavsson J, Stralfors P. (1995) Isolation of phosphooligosaccharide /phosphoinositol glycan from caveolae and cytosol of insulin-stimulated cells. J Cell Biol. **131**(1):125-35.

Pastor-Soler NM, Schertz EM, Rafi MA, de Gala G, Wenger DA. (1995) Metachromatic leukodystrophy among southern Alaskan Eskimos: molecular and genetic studies. J Inher Metab Dis. **18**(3):326-32.

Penzien JM, Kappler J, Herschkowitz N, Schuknecht B, Leinekugel P, Propping P, Tonnesen T, Lou H, Moser H, Zierz S, et al. (1993) Compound heterozygosity for metachromatic leukodystrophy and arylsulfatase A pseudodeficiency alleles is not associated with progressive neurological disease. Am J Hum Genet. **52**(3):557-64.

Perkins KJ, Byers S, Yogalingam G, Weber B, Hopwood JJ. (1999) Expression and characterization of wild type and mutant recombinant human sulfamidase. Implications for Sanfilippo (Mucopolysaccharidosis IIIA) syndrome. J Biol Chem. **274**(52):37193-9.

Peters C, von Figura K. (1994) Biogenesis of lysosomal membranes. FEBS Lett. **346**(1):108-14.

Peters CW, Kruse U, Pollwein R, Grzeschik KH, Sippel AE. (1989) The human lysozyme gene. Sequence organization and chromosomal localization. Eur J Biochem. **182**(3):507-16.

Phelan MC, Thomas GR, Saul RA, Rogers RC, Taylor HA, Wenger DA, McDermid HE. (1992) Cytogenetic, biochemical, and molecular analyses of a 22q13 deletion. Am J Med Genet. **43**(5):872-6.

Pinto R, Caseiro C, Lemos M, Lopes L, Fontes A, Ribeiro H, Pinto E, Silva E, Rocha S, Marcao A, Ribeiro I, Lacerda L, Ribeiro G, Amaral O, Sa Miranda MC. (2004) Prevalence of lysosomal storage diseases in Portugal. Eur J Hum Genet. **12**(2):87-92.

Polten A, Fluharty AL, Fluharty CB, Kappler J, von Figura K, Gieselmann V. (1991) Molecular basis of different forms of metachromatic leukodystrophy. N Engl J Med. **324**(1):18-22.

Poorthuis BJ, Wevers RA, Kleijer WJ, Groener JE, de Jong JG, van Weely S, Niezen-Koning KE, van Diggelen OP. (1999) The frequency of lysosomal storage diseases in The Netherlands. Hum Genet. **105**(1-2):151-6.

Porter MT, Fluharty AL, Trammell J, Kihara H. (1971) A correlation of intracellular cerebroside sulfatase activity in fibroblasts with latency in metachromatic leukodystrophy. Biochem Biophys Res Commun. **44**(3):660-6.

Propping P, Friedl W, Huschka M, Schlor KH, Reimer F, Lee-Vaupel M, Conzelmann E, Sandhoff K. (1986) The influence of low arylsulfatase A activity on neuropsychiatric morbidity: a large-scale screening in patients. Hum Genet. **74**(3):244-8.

Puri V, Watanabe R, Dominguez M, Sun X, Wheatley CL, Marks DL, Pagano RE. (1999) Cholesterol modulates membrane traffic along the endocytic pathway in sphingolipid-storage diseases. Nat Cell Biol. **1**(6):386-8.

Qu Y, Miller JB, Desnick RJ, Shapira E. (1997/98) Arylsulfatase A pseudodeficiency: altered kinetic and heat-inactivation properties. Genet Test. **1**(4):283-7.

Raas-Rothschild A, Pankova-Kholmyansky I, Kacher Y, Futerman AH. (2004) Glycosphingolipidoses: beyond the enzymatic defect. Glycoconj J. **21**(6):295-304.

Rafi MA, Zhang XL, DeGala G, Wenger DA. (1990) Detection of a point mutation in sphingolipid activator protein-1 mRNA in patients with a variant form of metachromatic leukodystrophy. Biochem Biophys Res Commun. **166**(2):1017-23.

Regis S, Filocamo M, Corsolini F, Caroli F, Keulemans JL, van Diggelen OP, Gatti R. (1999) An Asn > Lys substitution in saposin B involving a conserved amino acidic residue and leading to the loss of the single N-glycosylation site in a patient with metachromatic leukodystrophy and normal arylsulphatase A activity. Eur J Hum Genet. **7**(2):125-30.

Ricketts MH, Amsterdam JD, Park DS, Yang RS, Poretz RD, Zhang X, Fanale M, Baddoo A, Manowitz P. (1996) A novel arylsulfatase A protein variant and genotype in two patients with major depression. J Affect Disord. **40**(3):137-47.

Robledo R, Melis P, Schillinger E, Casciano I, Balazs I, Rinaldi A, Siniscalco M, Filippi G. (1995) X-linked ichthyosis without STS deficiency: clinical, genetical, and molecular studies. Am J Med Genet. **59**(2):143-8.

Rodda SJ, Tribbick G. (1996) Antibody-defined epitope mapping using the multipin method of peptide synthesis. Methods. **9**(3):473-81.

Rousseau A, Gatt S. (1990) Uptake and degradation of virus-associated fluorescent sulfatide by skin fibroblasts. FEBS Lett. **261**(2):271-3.

Roy AB. (1976) Sulphatases, lysosomes and disease. Aust J Exp Biol Med Sci. **54**(2):111-35.

Ryall RG, Gjerde EM, Gerace RL, Ranieri E. (1993) Modifying an enzyme immunoassay of immunoreactive trypsinogen to use time-resolved fluorescence. Clin Chem. **39**(2):224-8.

Sambrook J, Fritsch EF, Maniatis T. (1989) Molecular cloning: a laboratory manual. 2nd Ed. Cold Spring Harbor Laboratory Press, New York.

Saravanan K, Schaeren-Wiemers N, Klein D, Sandhoff R, Schwarz A, Yaghootfam A, Gieselmann V, Franken S. (2004) Specific downregulation and mistargeting of the lipid raft-associated protein MAL in a glycolipid storage disorder. Neurobiol Dis. **16**(2):396-406.

Schierau A, Dietz F, Lange H, Schestag F, Parastar A, Gieselmann V. (1999) Interaction of arylsulfatase A with UDP-N-acetylglucosamine:lysosomal enzyme-N-acetylglucosamine-1-phosphotransferase. J Biol Chem. **274**(6):3651-8.

Schmidt B, Selmer T, Ingendoh A, von Figura K. (1995) A novel amino acid modification in sulfatases that is defective in multiple sulfatase deficiency. Cell **82**:271-8.

Shapira E, Nadler HL. (1975) Purification and some properties of soluble human liver arylsulfatases. Arch Biochem Biophys. **170**(1):179-87.

Shen N, Li ZG, Waye JS, Francis G, Chang PL. (1993) Complications in the genotypic molecular diagnosis of pseudo arylsulfatase A deficiency. Am J Med Genet. **45**(5):631-7.

Simanovsky N, Ackerman Z, Kiderman A, Fields S. (1998) Unusual gallbladder findings in two brothers with metachromatic leukodystrophy. Pediatr Radiol. **28**(9):706-8.

Simons K, Gruenberg J. (2000) Jamming the endosomal system: lipid rafts and lysosomal storage diseases. Trends Cell Biol. **10**(11):459-62.

Simons K, Ikonen E. (1997) Functional rafts in cell membranes. Nature. **387**(6633):569-72.

Sleat DE, Donnelly RJ, Lackland H, Liu CG, Sohar I, Pullarkat RK, Lobel P. (1997) Association of mutations in a lysosomal protein with classical late-infantile neuronal ceroid lipofuscinosis. Science. **277**(5333):1802-5.

Smart EJ, Ying Y, Donzell WC, Anderson RG. (1996) A role for caveolin in transport of cholesterol from endoplasmic reticulum to plasma membrane. J Biol Chem. **271**(46):29427-35.

Smith DR, Rossi CA, Kijek TM, Henchal EA, Ludwig GV. (2001) Comparison of dissociation-enhanced lanthanide fluorescent immunoassays to enzyme-linked immunosorbent assays for detection of staphylococcal enterotoxin B, Yersinia pestis-specific F1 antigen, and Venezuelan equine encephalitis virus. Clin Diag Lab Immunol. **8**(6):1070-5.

Smith PK, Krohn RI, Hermanson GT, Mallia AK, Gartner FH, Provenzano MD, Fujimoto EK, Goeke NM, Olson BJ, Klenk DC. (1985) Measurement of protein using bicinchoninic acid. Anal Biochem. **150**(1):76-85.

Sommerlade HJ, Selmer T, Ingendoh A, Gieselmann V, von Figura K, Neifer K, Schmidt B. (1994) Glycosylation and phosphorylation of arylsulfatase A. J Biol Chem. **269**(33):20977-81.

Stein C, Gieselmann V, Kreysing J, Schmidt B, Pohlmann R, Waheed A, Meyer HE, O'Brien JS, von Figura K. (1989) Cloning and expression of human arylsulfatase A. J Biol Chem. **264**(2):1252-9.

Stevens RL. (1974) Minor anionic arylsulfatases in cultured human fibroblasts. Biochim Biophys Acta. **370**(1):249-56.

Stevens RL, Fluharty AL, Skokut MH, Kihara H. (1975) Purification and properties of arylsulfatase A from human urine. J Biol Chem. **250**(7):2495-501.

Storrie, B. (1988) Assembly of lysosomes: perspectives from comparative molecular cell biology. Int Rev Cytol. **111**:53-105.

Strasberg PM, Warren I, Skomorowski MA, Lowden JA. (1985) HPLC analysis of urinary sulfatide: an aid in the diagnosis of metachromatic leukodystrophy. Clin Biochem. **18**(2):92-7.

Stumpf D, Austin J. (1971) Metachromatic leukodystrophy (MLD). IX. Qualitative and quantitative differences in urinary arylsulfatase A in different forms of MLD. Arch Neurol. **24**(2):117-24.

Sutrina SL, Chen WW. (1982) Metabolism of ceramide-containing endocytotic vesicles in human diploid fibroblasts. J Biol Chem. **257**(6):3039-44.

Suzuki K, Chen GC. (1967) Isolation and chemical characterization of metachromatic granules from a brain with metachromatic leukodystrophy. J Neuropathol Exp Neurol. **26**(4):537-50.

Svennerholm E, Svennerholm L. (1962) Isolation of blood serum glycolipids. Acta Chem Scand. **16**:1282.

Toda K, Kobayashi T, Goto I, Ohno K, Eto Y, Inui K, Okada S. (1990) Lysosulfatide (sulfogalactosylsphingosine) accumulation in tissues from patients with metachromatic leukodystrophy. J Neurochem. **55**(5):1585-91.

Umapathysivam K, Hopwood JJ, Meikle PJ. (2001) Determination of acid alpha-glucosidase activity in blood spots as a diagnostic test for Pompe disease. Clin Chem. **47**(8):1378-83.

Umapathysivam K, Whittle AM, Ranieri E, Bindloss C, Ravenscroft EM, van Diggelen OP, Hopwood JJ, Meikle PJ. (2000) Determination of acid alpha-glucosidase protein:

evaluation as a screening marker for Pompe disease and other lysosomal storage disorders. Clin Chem. **46**(9):1318-25.

van Dyke RW. (1996) Acidification of lysosomes and endosomes. Subcell Biochem. **27**:331-60.

van Kerkhof P, Alves dos Santos CM, Sachse M, Klumperman J, Bu G, Strous GJ. (2001) Proteasome inhibitors block a late step in lysosomal transport of selected membrane but not soluble proteins. Mol Biol Cell. **12**(8):2556-66.

Vesa J, Hellsten E, Verkruyse LA, Camp LA, Rapola J, Santavuori P, Hofmann SL, Peltonen L. (1995) Mutations in the palmitoyl protein thioesterase gene causing infantile neuronal ceroid lipofuscinosis. Nature. **376**(6541):584-7.

Viani P, Marchesini S, Cestaro B, Gatt S. (1989) Correlation of the dispersion state of pyrene cerebroside sulfate and its uptake and degradation by cultured cells. Biochim Biophys Acta. **1002**(1):20-7.

Vogel A, Schwarzmann G, Sandhoff K. (1991) Glycosphingolipid specificity of the human sulfatide activator protein. Eur J Biochem. **200**(2):591-7.

von Bulow R, Schmidt B, Dierks T, Schwabauer N, Schilling K, Weber E, Uson I, von Figura K. (2002) Defective oligomerization of arylsulfatase A as a cause of its instability in lysosomes and metachromatic leukodystrophy. J Biol Chem. **277**(11):9455-61.

von Figura K, Gieselmann V, Jaeken J. (2001) Metachromatic leukodystrophy, in Scriver CR, Beaudet AL, Sly WS, Valle D (eds): The Metabolic and Molecular Bases of Inherited Disease. 8th Ed. McGraw-Hill, New York, pp 3695-724.

von Figura K, Hasilik A. (1986) Lysosomal enzymes and their receptors. Ann Rev Biochem. **55**:167-93.

von Figura K, Rey M, Prinz R, Voss B, Ullrich K. (1979) Effect of tunicamycin on transport of lysosomal enzymes in cultured skin fibroblasts. Eur J Biochem. **101**(1):103-9.

von Figura K, Steckel F, Hasilik A. (1983) Juvenile and adult metachromatic leukodystrophy: partial restoration of arylsulfatase A (cerebroside sulfatase) activity by inhibitors of thiol proteinases. Proc Natl Acad Sci USA. **80**(19):6066-70.

Vos JP, Lopes-Cardozo M, Gadella BM. (1994) Metabolic and functional aspects of sulfogalactolipids. Biochim Biophys Acta. **1211**(2):125-49.

Waheed A, Steckel F, Hasilik A, von Figura K. (1983) Two allelic forms of human arylsulfatase A with different numbers of asparagine-linked oligosaccharides. Am J Hum Genet. **35**(2):228-33.

Waheed A, van Etten RL. (1980) The structural basis of anomalous kinetics of rabbit liver arylsulfatase A. Arch Biochem Biophys. **203**(1):11-24.

Waldow A, Schmidt B, Dierks T, von Bulow R, von Figura K. (1999) Amino acid residues forming the active site of arylsulfatase A. Role in catalytic activity and substrate binding. J Biol Chem. **274**(18):12284-8.

Warner JO. (1975) Juvenile onset metachromatic leucodystrophy. Failure of response on a low vitamin A diet. Arch Dis Child. **50**(9):735-7.

Wattiaux R, Jadot M, Dubois F, Misquith S, Wattiaux-De Coninck S. (1995) Uptake of exogenous DNA by rat liver: effect of cationic lipids. Biochem Biophys Res Commun. **213**(1):81-7.

Wattiaux R, Laurent N, Wattiaux-De Coninck S, Jadot M (2000). Endosomes, lysosomes: their implication in gene transfer. Adv Drug Deliv Rev. **41**(2):201-8.

Wegrzyn G, Wegrzyn A, Tylki-Szymanska A. (2004) A general model for genetic regulation of turnover of glycosaminoglycans suggests a possible procedure for prediction of severity and clinical progress of mucopolysaccharidoses. Med Hypotheses. **62**(6):986-92.

Weitzner MA, Lehninger F, Sullivan D, Fields KK. (1999) Borderline personality disorder and bone marrow transplantation: ethical considerations and review. Psychooncology. **8**(1):46-54.

Whitfield PD, Nelson P, Sharp PC, Bindloss CA, Dean C, Ravenscroft EM, Fong BA, Fietz MJ, Hopwood JJ, Meikle PJ. (2002) Correlation among genotype, phenotype, and biochemical markers in Gaucher disease: implications for the prediction of disease severity. Mol Genet Metab. **75**(1):46-55.

Whitfield PD, Sharp PC, Johnson DW, Nelson P, Meikle PJ. (2001a) Characterization of urinary sulfatides in metachromatic leukodystrophy using electrospray ionization-tandem mass spectrometry. Mol Genet Metab. **73**(1):30-7.

Whitfield PD, Sharp PC, Taylor R, Meikle P. (2001b) Quantification of galactosylsphingosine in the twitcher mouse using electrospray ionization-tandem mass spectrometry. J Lipid Res. **42**(12):2092-5.

Wilcken B. (2003) Ethical issues in newborn screening and the impact of new technologies. Eur J Ped **162** Suppl 1:S62-6.

Wilson S, Howell S. (2002) High-throughput screening in the diagnostics industry. Biochem Soc Trans. **30**(4):794-7.

Wrobe D, Henseler M, Huettler S, Pascual Pascual SI, Chabas A, Sandhoff K. (2000) A non-glycosylated and functionally deficient mutant (N215H) of the sphingolipid activator protein B (SAP-B) in a novel case of metachromatic leukodystrophy (MLD). J Inherit Metab Dis. **23**(1):63-76.

Zlotogora J, Bach G, Barak Y, Elian E. (1980) Metachromatic leukodystrophy in the Habbanite Jews: high frequency in a genetic isolate and screening for heterozygotes. Am J Hum Genet. **32**(5):663-9.

Zlotogora J, Bach G, Bosenberg C, Barak Y, von Figura K, Gieselmann V. (1995) Molecular basis of late infantile metachromatic leukodystrophy in the Habbanite Jews. Hum Mutat. 5(2):137-43.

Zola H, Brooks DA. (1982) Techniques for the production and characterization of monoclonal hybridoma antibodies, in Hurrell J (ed): Monoclonal Hybridoma Antibodies: Techniques and Applications. CRC Press, Boca Raton, Florida, pp 1-57.

ADDENDUM

List of amendments:

1. Page 8, Table 1.2 (B): Km (μ/M) should read Km (μM).

2. Page 28, Figure 1.5: structure of sulphatide should be

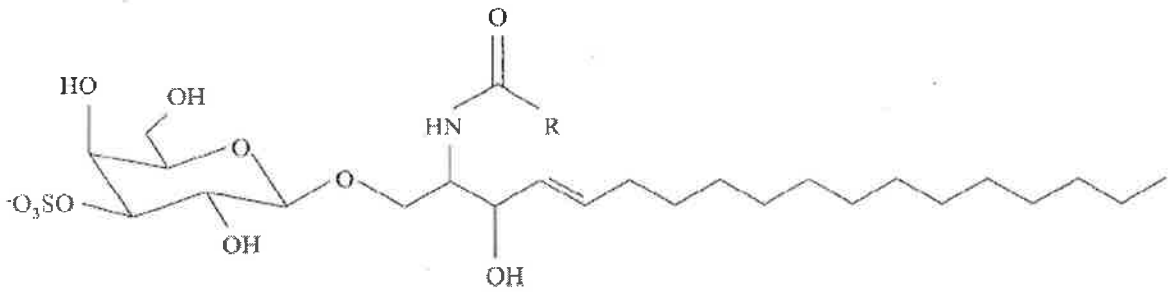

R = hydroxy and non-hydroxy fatty acyl chains of 15-23 carbons in length
(Figure reproduced from Whitfield *et al.*, 2001)

3. Page 44, line 9: section heading should read: 1.6 Electrospray ionisation-tandem mass spectrometry for the quantification of lipids

4. Page 44, line 16: the sentence should read: Electrospray ion (ESI) was developed by Dole and co-workers almost 40-years ago (Dole *et al.,* 1968), while further advances were achieved from the work of Fenn and colleagues who successfully used ESI-MS to analyse large biomolecules (Fenn *et al.* 1989).

5. Page 45, line 16: the sentence should read: MRM enables the simultaneous identification of multiple analytes in a single analysis. When this mode, which is highly specific, is utilised in a triple quadrupole tandem mass spectrometer, the first (Q1) and third (Q3) quadrupoles of the instrument are set to identify specific *m/z* values of the analytes.

6. Pages 78 to 84, sections 2.2.18.2 to 2.2.18.4, and Tables 2.2 to 2.5: the following product ions were used in the characterisation of:

   (i) anionic phospholipids (page 78, section 2.2.18.2, and Table 2.2): $[M-H]^-$ of the fatty acid ions corresponding to the *m/z* values as shown in Table 2.2;

   (ii) neutral glycolipids, sphingomyelin and phosphatidylcholine (page 79, section 2.2.18.3, and Table 2.3): for neutral glycolipids, $[M+H]^+$ of the dehydrated product of the sphingosine backbone corresponding to the *m/z* 264. While $[M+H]^+$ of the phosphocholine head group corresponding to the *m/z* 184 was used to characterise sphingomyelin and phosphatidylcholine.

   (iii) gangliosides (page 79, section 2.2.18.4, and Table 2.5): $[M-H]^-$ of the dehydrated sialic acid moiety corresponding to m/z 290.

7. Page 163, line 2: $[M-H]^{-1}$ should read $[M-H]^-$

8. Page 167, Figure 5.2: the amended figures are as follows:

(A)

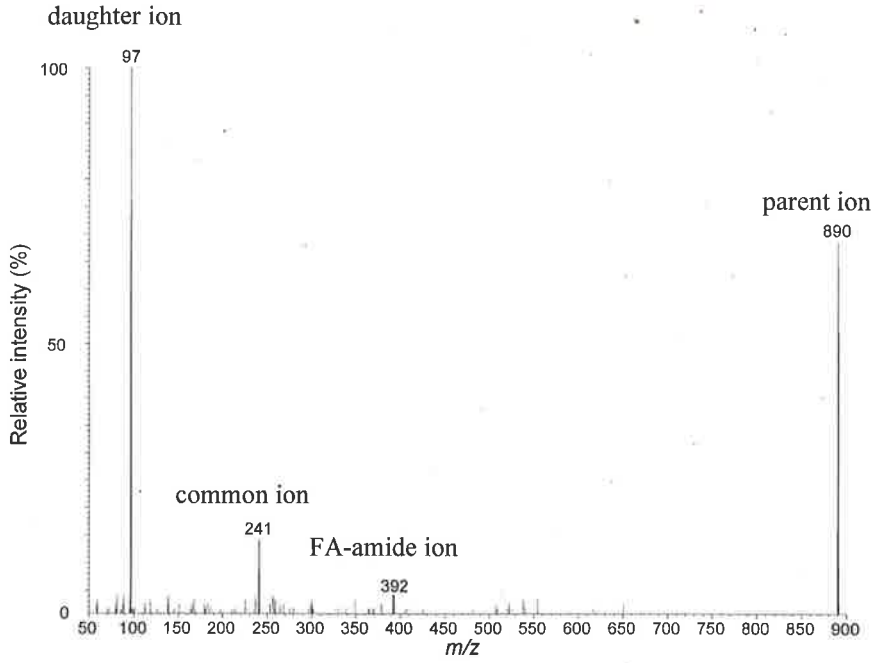

(B)

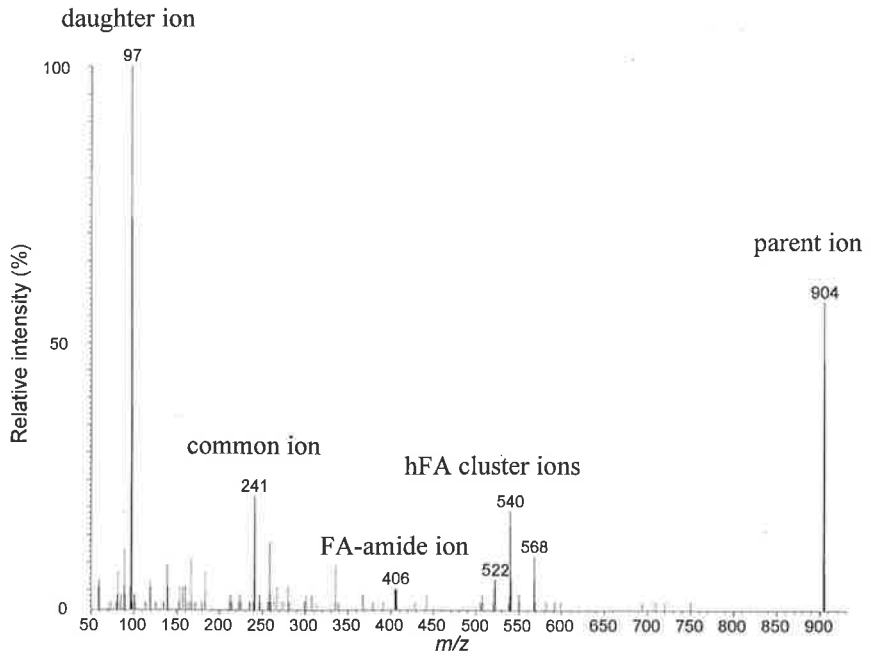

9. Page 168, line 4: $[M-H]^{-1}$ should read $[M-H]^{-}$

10. Page 169, line 5: Figure 5.4 should read Figure 5.3

11. Page 169, line 27: Figure 5.5 should read Figure 5.4

12. Page 178, line 24: '.....extracted from SF lysates.....' should read '.....extracted from urine.....'.